A Geochemical Investigation of a Suite of Central Arabian Crude Oils

by

Mohammad Radhi Al-Khadhrawi

A Thesis Presented to the

FACULTY OF THE COLLEGE OF GRADUATE STUDIES

KING FAHD UNIVERSITY OF PETROLEUM & MINERALS

DHAHRAN, SAUDI ARABIA

In Partial Fulfillment of the
Requirements for the Degree of

MASTER OF SCIENCE

In

CHEMISTRY

January, 1996

A GEOCHEMICAL INVESTIGATION OF A SUITE OF CENTRAL ARABIAN CRUDE OILS

BY

MOHAMMAD RADHI ALKHADHRAWI

A Thesis Presented to the

FACULTY OF THE COLLEGE OF GRADUATE STUDIES

KING FAHD UNIVERSITY OF PETROLEUM & MINERALS

DHAHRAN, SAUDI ARABIA

In Partial Fulfillment of the
Requirements for the Degree of

MASTER OF SCIENCE

In

CHEMISTRY

JANUARY, 1996

بسم الله الرحمن الرحيم

KING FAHD UNIVERSITY OF PETROLEUM AND MINERALS
DHAHRAN, SAUDI ARABIA

COLLEGE OF GRADUATE STUDIES

This thesis, written by Mr. Mohammad Radhi AlKhadhrawi under the direction of his Thesis Advisor and approved by his Thesis Committee, has been presented to and accepted by the Dean of the College of Graduate Studies, in partial fulfillment of the requirements for the degree of MASTER OF SCIENCE IN CHEMISTRY.

Thesis Committee

Thesis Advisor
(Prof. M. Farhat Ali)

Member (Dr. H. Perzanowski)

Member (Dr. H. I. Halpern)

Department Chairman
(Dr. Abdulrahman Al-Arfaj)

Dean, College of the Graduate Studies
(Dr. Ala H. Al-Rabeh)

This Thesis is dedicated to my parents, wife, brothers,

and sisters for all their moral support and encouragement.

ACKNOWLEDGMENTS

First and foremost many thanks are to ALLAH, The Almighty, for giving me the strength, patience, and ability to complete this work.

I greatly owe my success to my parents, family, and friends for their Dua'a and encouragement.

I would like to express my sincere gratitude and appreciation to Professor Mohammad Farhat Ali, Thesis committee chairman, for his guidance and encouragement. I would also like to thank Dr. Herman Perzanowski and Dr. Henry I. Halpern, Thesis committee members for all their help, support, and constructive suggestions which made the completion of this work possible.

My thanks are due to the chairman of the Chemistry Department Dr. Adulrahman Al-Arfaj, the coordinator of the graduate studies Dr. Abdullah Abdennabi, the faculty and staff members of the Chemistry Department for their support, guidance, and help. I wish to acknowledge KFUPM for utilizing its various facilities during the course of this study.

I would also like to thank the management of the Laboratory Research and Development Center of Saudi Aramco for giving me the chance to use Aramco facilities throughout the course of this study as well as providing the oil samples used for the Thesis project. Personnel of the Geochemistry Unit of the Laboratory Research and Development Center are thanked for their help. Mr. Walter Gwathney and Ms. Sabah Al-Tarah of the Advanced Instruments Unit of the Laboratory Research and Development Center are thanked for their help with the GCMS work. Dr. H. H. Chen of the Crude Evaluation Unit of the Laboratory Research and Development Center is thanked for his help with separation techniques.

My gratitude is to all of my colleagues and friends and to every person who helped me in this regard.

TABLE OF CONTENTS

LIST OF TABLES

LIST OF FIGURES

ABSTRACT

High quality (sulfur ≤ 0.1%, API gravity ≥ 40°) petroleum was discovered in Central Arabia in the mid-1980s. Ever since these discoveries, published studies have concentrated largely on identifying the source rock unit(s) from which these oils and condensates were generated. Previous research work conducted on these petroleums indicated that they are very lean in conventional biomarkers such as hopanes and steranes and that the biomarker compounds, where identified, are non-specific (*e.g.*, diasteranes and tricyclics).

The goal of the present Thesis is to investigate a suite of oils from Central Arabia and inspect them for the presence of conventional hopane and sterane biomarkers, as well as non-conventional markers such as phenanthrene and its methylated isomers.

Because it was not known whether useful biomarkers would be found in these light oils, additional analyses were performed on the oils for correlation purposes. These include light-hydrocarbon and mid-range micro-scale correlation techniques.

Paleozoic and Jurassic oils and condensates from several fields from Central Arabia as well as the Eastern Province (for comparison) were collected. Bulk properties, such as API gravity, percent sulfur, and nitrogen content of these oils were determined. The oils and condensates were then fractionated into their major compound classes: saturates, aromatics, polars, and asphaltenes. The saturate and aromatic fractions were analyzed by gas chromatography (GC) as well as by gas chromatography-mass spectrometry (GC/MS).

Bulk properties, pristane/phytane ratios, MPR, and $\%R_c$ values showed that Paleozoic oils from Central Arabia differ significantly from Jurassic oils from the Eastern Province.

Central Arabian Paleozoic oils and condensates are: high-API-gravity, exceedingly low sulfur, low nitrogen and low metals crude oils. They have pristane/phytane ratios that are greater than one indicating dysoxic conditions at the time of deposition of their source rocks. Their MPR and $\%R_c$ values are indicative of differences in timing of generation from the source rock as well as in maturity and, perhaps most significantly, indicative of post-generative alteration such as, water washing.

Eastern Province Jurassic oils are: medium-gravity, high sulfur, high nitrogen crude oils. They have pristane/phytane ratios that are less than one indicating highly reducing conditions at the time of source rock deposition. Their MPR and $\%R_c$ values are indicative of generation from a source rock that was at peak oil maturity (VRe ≈ 0.80 to 1.0%).

ملخـــص

اكتشف بترول بنوعية عالية الجودة (يحتوي على نسبة كبريت تقل عن أو تساوي ٠,١٪ وكثافة حسب درجات معهد البترول الامريكي تزيد على أو تساوي ٤٠) في المنطقة الوسطى من المملكة العربية السعودية في اواسط الثمانينات الميلادية. ومنذ ان تحققت تلك الاكتشافات ركزت الدراسات التي تم نشرها تركيزاً كبيراً على مسألة تحديد الوحدات الصخرية الاساسية التي استخرجت منها تلك الزيوت والمكثفات. وقد ظهر من البحوث السابقة التي اجريت على تلك الزيوت ان محتواها من المؤشرات الحيوية مثل مركبات الهوبينات والستيرينات العضوية قليل جداً وان تلك المركبات التي تم تحديدها غير محددة بعامل خاص (مثل الستيرينات المتغيرة وثلاثيات الحلقات).

ان الهدف من هذا البحث هو دراسة مجموعة من انواع الزيت المستخرجة من المنطقة الوسطى من المملكة العربية السعودية لمعرفة وجود أو عدم وجود المؤشرات الحيوية من الهوبينات والستيرينات العادية اضافة الى المؤشرات غير العادية مثل الفينانثرينات ومتشاكلاتها الممثيلة.

بما انه لم يكن من المعروف ما اذا كانت تلك الزيوت الخفيفة تحتوي على أية مؤشرات حيوية ذات فائدة فقد اجريت تحليلات اضافية عليها لأغراض المضاهاة بما في ذلك اساليب مضاهاة الهيدروكربونات الخفيفة وأساليب المضاهاة لمدى متوسط وبحجم دقيق.

تم جمع زيوت ومكثفات تعود الى العهد القديم والعصر الجيوراسي من عدة حقول في المنطقة الوسطى من المملكة العربية السعودية اضافة الى المنطقة الشرقية (لأغراض المقارنة). وجرى تحديد الخواص الحجمية مثل الكثافة حسب درجات معهد البترول الامريكي والنسبة المئوية للكبريت ومحتوى النتروجين في تلك الزيوت. ثم تمت تجزئة الزيوت والمكثفات الى اصناف المركبات الرئيسية مثل المركبات المشبعة والعطرية والقطبية والاسفلتية. وتم تحليل اصناف المركبات المشبعة والعطرية باستخدام طريقة الفصل الكروماتوغرافي بالغاز وطريقة الفصل الكروماتوغرافي بالغاز -قياس الطيف الكتلي.

وقد ظهر من الخواص الحجمية ومعدلات البريستينات / الفيتينات ومعدل فينانثرينات المثيل والنسبة المئوية للانعكاس المحسوب ان زيوت العهد القديم المستخرجة من المنطقة الوسطى من المملكة تختلف كثيراً عن زيوت العصر الجيوراسي المستخرجة من المنطقة الشرقية، حيث ان الزيوت والمكثفات الاولى ذات كثافة عالية ومحتوى منخفض جداً من الكبريت ومحتوى منخفض من النتروجين والمعادن، كما ان معدلات البريستينات/الفيتينات فيها اكبر من "واحد" مما يدل على توفر كمية قليلة من الاوكسجين في وقت ترسب صخورها المصدرية. وتدل معدلات الفينانثرينات المثيلية والنسبة المئوية للانعكاس المحسوب بها على اختلافات في وقت استخراجها من الصخر المصدر وفي نضجها وربما ان الاهم مما سبق هو دلالتها على التغير التالي للاستخراج بسبب الغسل بالماء مثلاً. أما زيوت العصر الجيوراسي في المنطقة الشرقية فهي ذات كثافة متوسطة ومحتوى عال من الكبريت ومحتوى عال من النتروجين. أما معدلات البريستينات/الفيتينات بها فتقل عن "واحد" مما يدل على ان ظروف الاختزال كانت عالية في وقت ترسب الصخور المصدرية الخاصة بها. وتدل معدلات الفينانثرينات المثيلية والنسبة المئوية للانعكاس المحسوب على استخراجها من صخور مصدرية تحتوي على زيوت في مرحلة قصوى من النضج (VRe ~ 0.80 to 1.0%).

CHAPTER 1

INTRODUCTION

1.1 BACKGROUND

Oil was discovered in Central Arabia in the mid-1980s. The Central Arabian oil fields have not yet been studied in great detail; particularly from a geochemical standpoint. Previous work centered mainly on oil to source rock correlation [1, 2, 3]. The oil in Central Arabian fields is believed to be sourced from the Paleozoic sequence of Arabia. The source rocks of the region were influenced by the transgressive cycles of the Paleo-Tethys ocean. The transgressive phase of the Early Silurian had the most important effect on source rock formation in this region. This is because the most likely source, the Qusaiba shale (and, in particular, the basal Qusaiba gamma-ray "hot" zone) of the Qalibah Formation, was deposited during this phase [1, 3, 4].

This transgressive phase resulted from advancement of polar glaciers during the Late Ordovician and Early Silurian, from the south pole in the central part of African Gondwana into Northern Africa and Western Arabia. The retreat of the glaciers during the Early Silurian caused the Paleo-Tethys Ocean level to

rise swiftly and flood northern Africa and the Middle East. These circumstances provided a good environment for source rock development [2, 4].

Principal components (source rocks, reservoirs, and seals) of the Paleozoic system of Saudi Arabia are shown in Figure 1.1. The figure also depicts the ages of the formations as well as their lithologies. The part of the figure that is most relevant to this study is the Qusaiba member of the Qalibah Formation which, most likely, generated, expelled, and charged the Unayzah and Khuff reservoirs.

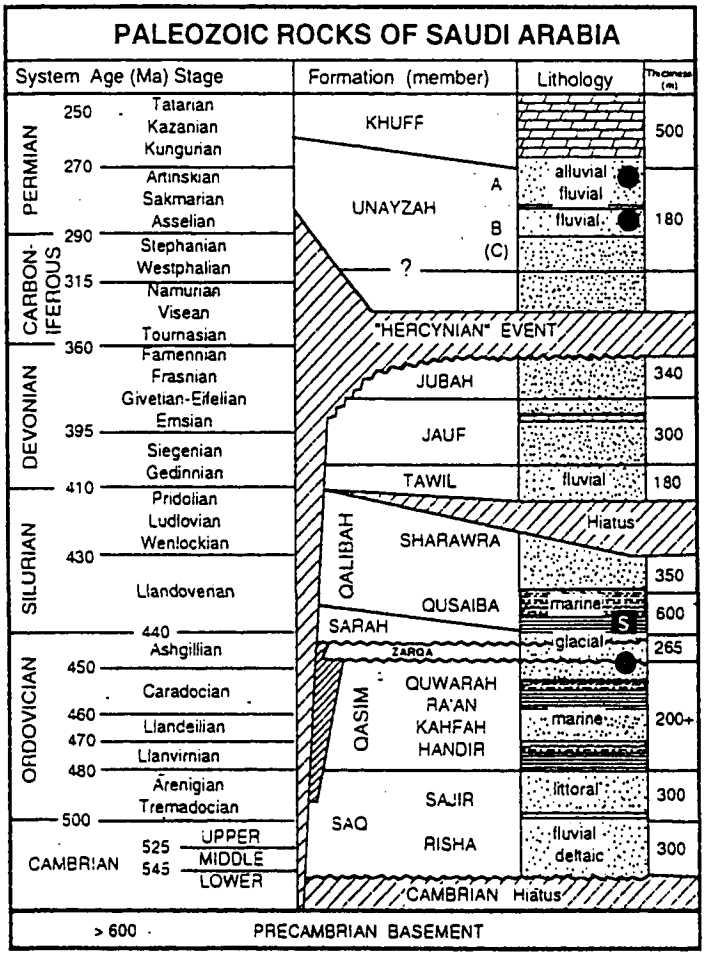

Figure 1.1. Generalized stratigraphic column for the Paleozoic sequence of Saudi Arabia (after Cole *et al.*, 1994).

1.2 OBJECTIVES

One of the objectives of this research is to examine a suite of Central Arabian oils so as to classify the types of biomarkers present. These include both conventional biomarkers (*e. g.*, steranes and hopanes) and non-conventional biomarkers (*e. g.*, bicyclics and aromatized compounds). Where possible, these biomarkers will be identified and characterized. The research work also entails development of ratios of compounds useful for maturity assessment, as well as finding individual compounds potentially useful for correlation.

Because of their high API gravity values (over 40°), the Central Arabian oils are very lean in biomarkers. It was possible that meaningful biomarkers (*i. e.*, non-routine) would not be found in these oils. In this case, detailed oil-oil correlation and data synthesis will be accomplished using modifications of Saudi Aramco in-house micro-scale correlation techniques employing both the light [5] and mid-range hydrocarbons [6].

1.3 PRESENT STATUS

Biomarker research has been on-going for several decades. Thousands of studies have been carried out characterizing biomarkers in oils from many

different regions of the world including the United States, Russia, China, and the Middle East (including Eastern Saudi Arabia). Based on the results of these numerous studies, certain biomarkers are now used in routine geochemical analyses. These standard biomarkers include hopanes, C_{27}-C_{30} steranes, pristane, and phytane [1, 7].

Biomarkers in Central Arabian oils, however, have not yet been fully investigated. Studies related to Central Arabian oils that have been undertaken to date have shown that the biomarkers were present in very low concentrations, and many of the compounds present are non-specific (*e. g.*, diasteranes and tricyclics). Furthermore, recent studies have shown that biomarkers in these Paleozoic fluids are different from biomarkers found in Paleozoic fluids of neighboring regions such as Oman. [1, 2, 3].

Gas chromatography coupled with mass spectrometry (GC/MS) is the technique most widely employed for the determination and characterization of biomarkers. It is generally referred to as GC/MS fingerprinting. This technique has been employed to determine the distribution of several biomarker classes in oils as well as source rocks. This technique has also been employed to identify individual biomarkers present in oils and source rock extracts. [1, 3, 4, 7, 8, 9, 10, 11].

1.4 Proposed Work Plan

1. Literature Review.
2. Collection of oil samples from different Central Arabian and selected Eastern Province fields.
3. Fractionation of Central Arabian crude oil samples to obtain concentrates of the fractions containing the biomarkers. The fractionation process will be carried out using SiO_2/Al_2O_3 column chromatography to obtain the saturate and aromatic fractions using a modified procedure based on the group-type fractionation method reported by [12].
4. Identification and characterization of the biomarkers in the saturate and aromatic fractions utilizing GC and GC/MS techniques.
5. Development of ratios of compounds that may be used for maturity assessment, as well as finding individual compounds and ratios that may be useful for correlation.
6. Where possible, correlation of the biomarkers with physical properties such as API gravity and sulfur content will be developed.

CHAPTER 2

Literature Review

2.1 Organic Geochemistry and Major Areas of Use

Organic geochemistry is "the study of the visual and chemical composition of organic matter[1] in sediments and rock, and of the changes induced in it by bacterial and thermal alteration with time" [13]. Hydrocarbons (oil and gas) generated from these source rocks are also studied under the realm of organic geochemistry. This discipline is often referred to as "petroleum geochemistry".

Petroleum geochemistry provides assistance to explorationists in their search for oil and gas reserves. One example of such assistance is in delineating drilling targets during exploration in a basin. Petroleum geochemistry helps in correlating a particular petroleum to the source rock from which it was generated [14, 15, 16]. This knowledge of the source rock, coupled with geological and geophysical information, is of major importance in identification of migration pathways, thus helping explorationists delineate drilling targets [17, 18, 19].

Petroleum geochemistry is used for evaluating the hydrocarbon generative potential of source rocks, as well as for determining the type and maturity of

[1] Organic matter here refers to the biogenic constituents of sedimentary rocks, also termed sedimentary organic matter. It is composed of insoluble kerogen and soluble bitumen or oil.

hydrocarbon generated *i. e.*, oil *vs.* gas [14; 18, 20]. Petroleum geochemistry can also provide insights for determining if an oil is weathered. It also aids in assessing the degree of weathering [21, 22].

A major portion of petroleum geochemistry is devoted to correlation studies. This type of work encompasses correlating oils to oils and/or oils to source rocks, and entails fingerprinting oils and source rock extracts. Fingerprinting of oils also plays an important role in tracing oil spills to their source(s). In addition, petroleum geochemistry also helps identify post-generation alteration phenomena that affect the properties of crude oils [14, 17, 23]. Examples of these alteration processes include:

1. Natural deasphaltening: a process that results in precipitating asphaltenes as a direct response to increasing concentration of light ends with time and depth of burial. This process is usually associated with decreasing API gravity of crude oils and increasing concentrations of sulfur, nitrogen, and metallic compounds such as nickel and vanadium [14, 17].
2. Water-washing: this refers to the preferential removal of water-soluble compounds. These include lower molecular weight hydrocarbons, especially aromatic compounds such as toluene and benzene. The zone most affected by water-washing is the oil-water contact [14, 17, 24].

3. Bacterial degradation: not only does moving water causes preferential removal of certain types of compounds as mentioned above, but it can also bring bacteria into contact with crude oils in reservoirs. Crude oil represents the food needed by the bacteria to survive. Classes of compounds within the composition of crude oils vary in their degree of susceptibility to bacterial attack. *n*-Paraffins are preferentially depleted by bacteria. The following series represent the varying degrees of susceptibility to bacterial attack amongst various constituents of crude oils (from most susceptible to least susceptible):

n-paraffins > aliphatic side chains > branched paraffins > cyclic paraffins > aromatics > sulfur compounds.

Since *n*-paraffins (high API) are the first and easiest to be consumed by bacteria, API gravity decreases as a result of bacterial activities. Biodegradation also results in increased sulfur and nitrogen contents because sulfur and nitrogen compounds are very resistant to bacterial degradation and the bacteria produce sulfur and nitrogen compounds as part of their natural biochemical and metabolic processes [14, 17, 25].

2.2 BIOMARKERS: VERSATILE GEOCHEMICAL TOOLS

The term biomarker is coined from two words: biological and markers. Biomarkers are also referred to as "geochemical fossils" or "molecular fossils" [8, 14].

Biomarkers are characteristic compounds found in petroleum and in extracts from source rocks. These compounds were synthesized by living organisms (*e. g.*, bacteria and plants). They became part of the sediments as they were buried with inorganic matter and subjected to higher temperatures and greater pressures during sedimentary processes. The carbon skeleton of any of these compounds is generally preserved throughout geologic time and is identical (or very closely related) to the skeletons of compounds known to be produced by living organisms. These compounds possess sufficient stability to survive long periods of time and sufficient structural complexity that render them very distinctive. Changes that sediments undergo may alter bonds and functional groups but not the carbon skeleton of these compounds.

Compounds that belong to this class include: a portion of the normal alkanes (these are derived from land plants waxes and fatty acids), isoalkanes, isoprenoids (such as pristane and phytane) and cyclized alkanes (such as hopanes and steranes). Figure 2.1 depicts the structures and diagnostic mass

spectrometric fragments of two biomarkers belonging to the most commonly studied biomarker classes: hopanes and steranes [8, 13, 26, 27, 28].

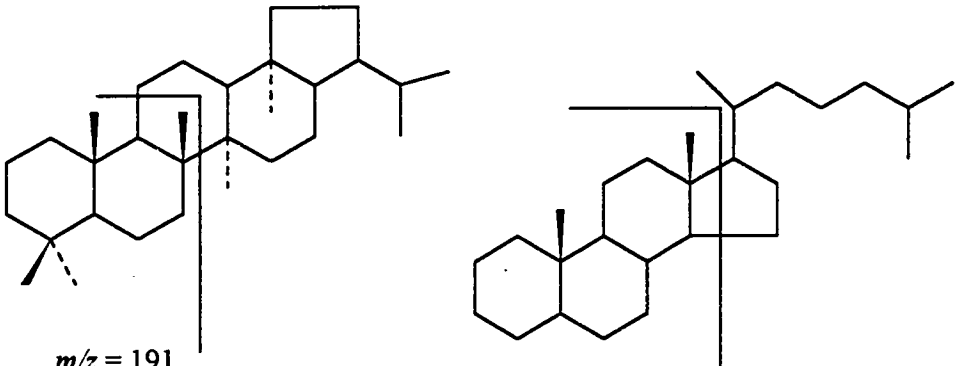

Figure 2.1. Structures and diagnostic mass spectrometric fragments of hopanes and steranes.

Thermal maturation can be inferred from biomarkers. The most commonly used parameters are steroid hydrocarbon isomer ratios. The biogenically produced steranes - 20R configuration - are converted into the geologically produced 20S configuration as a result of thermal maturation. The conversion of 20R to 20S ceases when the ratio (20S/20R) reaches equilibrium at about 0.54. This maturity parameter should be treated with caution since it may not be applicable to evaporite[2] or carbonate source rocks. Increasing maturity changes the stereochemistry at C_{14} and C_{17} from 14α(H), 17α(H) to 14β(H),

[2] Evaporite is a sedimentary deposit that results from the evaporation of seawater leaving the salts.

17β(H); this transformation is generally called the αα to ββ transformation [14, 17, 29, 30, 31].

A widely used biodegradation scale is the 20S/(20S+20R) ratio of the C_{29} steranes. Bacteria start consuming steranes with the naturally formed 20R configuration. Thus, severe biodegradation results in depletion of the 20R configuration and enrichment of the 20S configuration. An overall reduction in biomarker abundance typically means an increased maturity level [8, 11, 30, 32, 33, 34].

Hopanes also serve as a basis for maturity assessment. Increased maturity levels result in an increased ratio of 17α(H)-hopane/moretane. The ratio of C_{27} 18α(H)-22,29,30-trisnorneohopane (Ts, or C_{27} 18α(H)-trisnorhopane) to C_{27} 17α(H)-22,29,30-trisnorhopane (Tm, or C_{27} 17α(H)-trisnorhopane) is used as a maturity parameter. The abundance of Tm decreases, and that of Ts increases, with increasing thermal maturity. The structures of both Ts and Tm are depicted in Figure 2.2 [8, 31, 32].

The biologically produced C_{31} to C_{35} 17α(H)-hopanes possess the 22R configuration, while geologically produced C_{31} to C_{35} 17α(H)-hopanes possess 22S configuration.

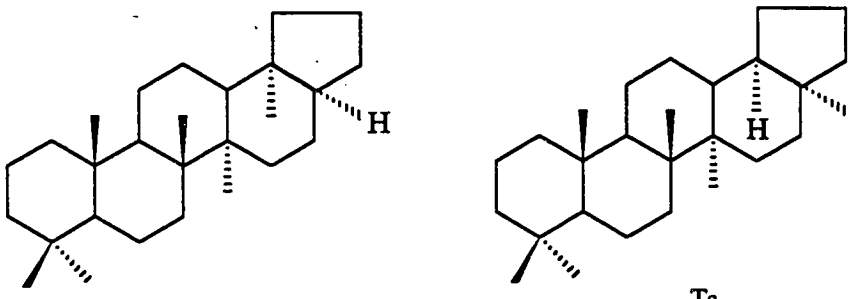

Tm Ts

Figure 2.2. Structures of Tm and Ts.

The 22R and 22S isomers in the range C_{31} to C_{35} 17α(H)-hopanes are called homohopanes. The ratio of 22S/(22S+22R) for any or all of the C_{31} to C_{35} 17α(H)-homohopanes can be used as maturity parameter. However, the most commonly used ratios are those of C_{31} or C_{32} 17α(H)-homohopanes. Throughout the gradual thermal maturation process, the 22S/(22S+22R) ratio increases from 0 to ≈ 0.6 at equilibrium (more specifically, 0.57-0.62) [8, 32, 35, 36, 37,38].

Biomarkers are also used for determining depositional environments of the source rock that generated petroleum. Highly reducing marine environments of deposition are associated with increased abundance of C_{35} homohopanes (22R + 22S) relative to the sum of C_{31} to C_{35} homohopanes. This is often referred to as the C_{35}-homohopane index [8, 17, 39, 40]. Presence of β-carotane or botryococcane is an indicator of brackish or lacustrine environments.

Gammacerane is a biomarker that is indicative of hypersaline environments. [8, 41, 42].

The oleanane index is defined as 18α(H)-oleanane/C_{30} hopane. This index is specific for tracking higher plant input to source rocks [8, 43].

2.3 AROMATIC BIOMARKERS

The aromatic fraction of petroleum contains a complex mixture of aromatic and alkyl-aromatic hydrocarbons. Among these compound there is a class known as polycyclic aromatic hydrocarbons (PAH). Microorganisms play an important role in the distribution patterns of PAH and the general idea is that PAH found in petroleum did not originate from aromatic precursors [44]. They are thought to have been produced in sediments through a process of consecutive aromatization of steranes and triterpanes during diagenesis [44, 45, 46].

A subgroup of PAH whose distribution is maturity-sensitive is phenanthrene and its methylated isomers [47, 48].

Alkylbenzenes and alkylnaphthalenes are readily susceptible to biodegradation. However, phenanthrene and its methylated isomers are more resistant to biodegradation than these other compounds in the aromatic fraction of crude oils [49]. Methylphenanthrene has five known isomers: 1-, 2-, 3-, 4-, and

9-methylphenanthrene (referred to hereafter as 1-MP, 2-MP, 3-MP, 4-MP, and 9-MP). Figure 2.3 shows the structure of phenanthrene.

4-MP, however, is not known to exist in crude oils [45]. The abundance of both 2-MP and 3-MP (ββ configuration) relative to the abundance of both 1-MP and 9-MP (αα configuration) increases with increasing maturity [50, 51, 52]. The methylphenanthrene ratio (MPR) has been suggested by Radke *et al.* [53] as a maturity parameter, and is defined as follows:

MPR= [2-MP]/[1-MP].

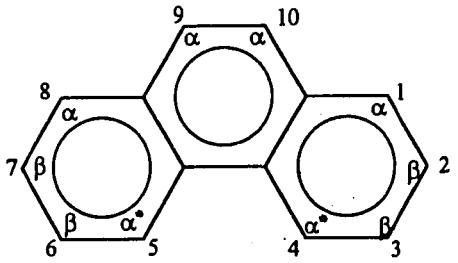

Figure 2.3. Structure of phenanthrene; an asterisk denotes a sterically crowded position.

Another maturity indicator based on phenanthrene and its four isomers that are known to exist in petroleum is the Methylphenanthrene Index (MPI 1).

MPI 1 has been shown to correlate with vitrinite reflectance [3] values in the

[3] Vitrinite is the maceral group derived from the lignified tissues of higher land plants that include trunks, branches, stems, leaves, and roots of trees and plants. Vitrinite reflectance is a maturation parameter based on the change in reflectance of polished vitrinite particles with increasing time of burial and temperature. Reflectance increases with increasing maturity.

range $\%R_m$ = 0.67-1.35%, *i. e.*, the oil generation window [44, 48]. MPI 1 is defined as follows:

MPI 1 = {1.5*[2-MP]+[3-MP]}/{[P]+[1-MP]+[9-MP]}.

MPI 1 was calibrated with R_m and this calibration resulted in the development of a new maturity parameter called "calculated vitrinite reflectance" ($\%R_C$). Figure 2.4 shows a plot of MPI 1 *vs.* $\%R_m$. The plot has a maximum at a $\%R_m$ of 1.35. Based on the relationship depicted in the Figure, R_C values have been calculated from MPI 1 [44] as follows:

$$R_c \text{ (for } 0.65\% \leq R_m \leq 1.35\%) = 0.60 \text{ MPI 1} + 0.40 \qquad (2.1)$$

$$R_c \text{ (for } 1.35\% < R_m \leq 2.00\%) = -0.60 \text{ MPI 1} + 2.30 \qquad (2.2).$$

When calculating R_C for oils, MPR helps to determine which of the above equations to use. Radke [54] found that a $\%R_m$ value of 1.35% corresponds to an MPR value of 2.24. Thus, when one is dealing with oil samples of unknown %Rm values, one should use the MPR values and then apply the proper equation (2.1 or 2.2) to determine R_C from MPI 1.

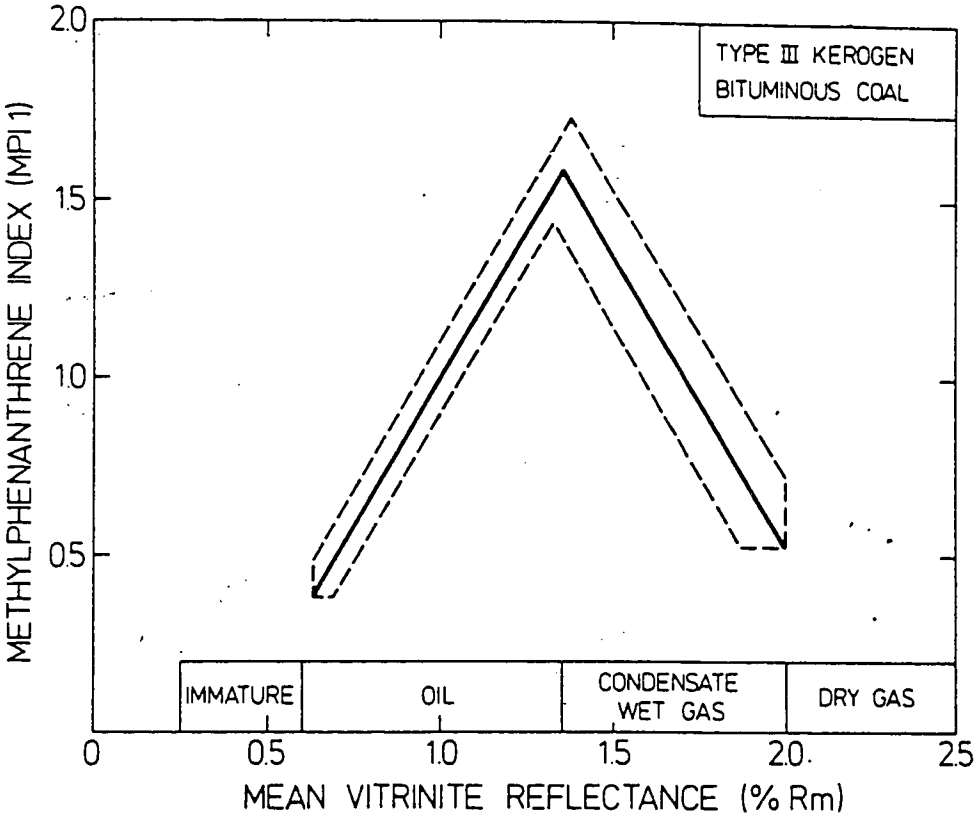

Figure 2.4. Relationship between Methylphenanthrene Index (MPI 1) and mean vitrinite reflectance (%R_m) as based on data from Type-III kerogen-bearing rock and bituminous coal samples (after Radke and Welte, 1981).

CHAPTER 3

EXPERIMENTAL

3. 1 CRUDE OILS

Thirteen crude oil and condensate samples were collected from seven different fields (A to G) in Central Saudi Arabia to be used in this study. Two more samples from an Eastern Arabian field ("H") were used for comparison. The samples are divided into the following sub-groups:

Area	Field I. D.	No. of Samples
Central Arabia	Field A	3
Central Arabia	Field B	3
Central Arabia	Field C	3
Central Arabia	Field D	1
Central Arabia	Field E	1
Central Arabia	Field F	1
Central Arabia	Field G	1
Eastern Province	Field H	2

The exact locations of the fields studied here and well identities were not disclodsed due to reasons of confidentiality on the part of Saudi Aramco. However, a general location map is presented in Figure 3.1.

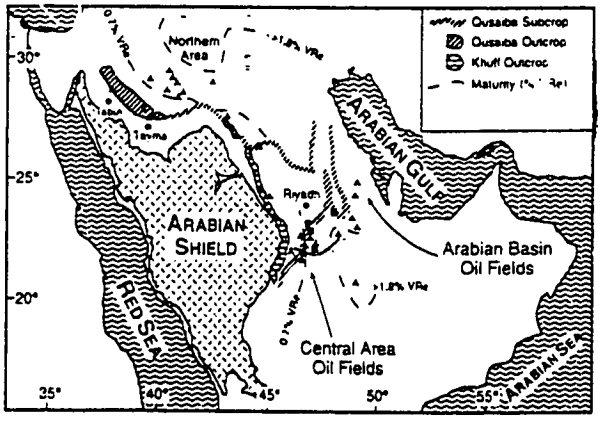

Figure 3.1. General location map of fields studied (after Cole *et al.*, 1994).

3.2 ANALYTICAL ASSAYS

3.2.1 CRUDE OIL CHARACTERIZATION

3.2.1.1 DETERMINATION OF API GRAVITY

3.2.1.1.1 INTRODUCTION

American Petroleum Institute (API) gravity is considered an important element for determining the quality of crude oils from an economic standpoint. API gravity is used for converting measured volumes to volumes at the standard temperature of 15 °C. This explains the need for API determination. API gravity was determined using ASTM standard method D 4052-91 employing a digital density meter.

3.2.1.1.2 REAGENTS AND MATERIALS

Reagent grade chemicals were used for determining API gravity. These reagents include acetone, *n*-nonane, *n*-tridecane, cyclohexane, and *n*-hexadecane. The water used was redistilled and boiled. These chemicals are used for calibration purposes.

3.2.1.1.3 APPARATUS

Digital density analyzer DMA 48 was the instrument used. It consists of a U-shaped tube, oscillating sample tube and a system for electronic excitation, frequency counting, and display. Circulating water was used to maintain the temperature of the U-shaped tube constant to within ± 0.05 °C of the test temperature, which was 60 °F. The syringes used for sample introduction were of 2-ml volume.

3.2.1.1.4 PROCEDURE

The instrument was calibrated using air and redistilled, freshly boiled and cooled water. This calibration was done by measuring periods of oscillation (T) when the sample tube contained air and when it contained redistilled water to determine constants A and B. The period of oscillation is sensitive to the density of the fluid filling the tube. Prior to the actual calibration, the sample tube was flushed with petroleum naphtha, followed by acetone, and finally, dry air. After the tube was dried, it was filled with air. The tube inlet and outlet were plugged, and the period of oscillation (T) was measured after the air inside the tube came to thermal equilibrium with the test temperature. This was then followed by the same sequence of flushes to prepare the tube for the water test. In this step,

about 0.7 ml of redistilled water was injected into the test tube. The output from the instrument is given either in the form of density or API readings.

When the calibration procedure was completed, about 0.7 ml of sample was introduced into the clean, dry, U-shaped tube. Two conditions were necessary before the sample was analyzed. These conditions were that the sample should be homogeneous and should not contain any air bubbles. The readings were taken after the sample reached thermal equilibrium with the compartment containing the U-shaped tube and instrument output stabilized.

3.2.1.2 DETERMINATION OF SULFUR CONTENT

3.2.1.2.1 INTRODUCTION

The presence of sulfur in crude oils lowers the quality of the crude. This is because sulfur is poisonous to catalysts used in petroleum refining processes even when it is present only in trace amounts. It also has environmental considerations. Sulfur content was determined using ANTEK 7000 Elemental Analyzer as per ASTM standard method D 5453-93.

3.2.1.2.2 REAGENTS AND MATERIALS

Chemicals used in the determination of sulfur contents of the oil samples used in this study include dibenzothiophene (99%) and toluene (HPLC grade).

Gases used were high-purity chromatography grade. These include: oxygen and argon or helium.

3.2.1.2.3 APPARATUS

The apparatus used for measuring sulfur content is composed of an electric furnace, combustion tube, flow controllers, drier tubes, UV fluorescence detector, microliter syringe, and a boat inlet system.

The electric furnace was held at 1100°C to pyrolyze the sample and convert sulfur to SO_2. The combustion tube is made of quartz. Flow controllers are used to maintain a constant supply of oxygen and carrier gas. Drier tubes are used to remove the water vapor produced during sample combustion. The UV fluorescence detector measures the light emitted from the fluorescence of the SO_2. The microliter syringe is used for sample introduction to the combustion tube *via* the boat inlet system. The sample inlet system is depicted in Figure 3.2.

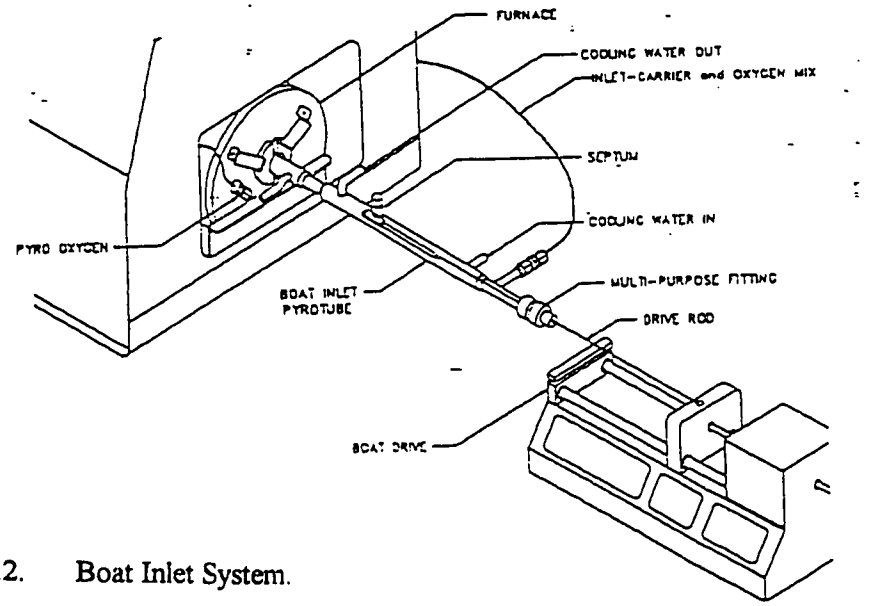

Figure 3.2. Boat Inlet System.

3.2.1.2.4 PROCEDURE

A stock solution of dibenzothiophene (99% from ACROS) in toluene was used for calibration purposes. Prior to carrying out actual sample analysis, the apparatus was checked for gas leaks, and the sample was also checked for the presence of air bubbles. If they were present, the sample was discarded, and a new sample was taken. The amount of sample used for each analysis was 5 μl. Instrument output is in parts per million (ppm).

3.2.1.3 DETERMINATION OF NITROGEN CONTENT

3.2.1.3.1 INTRODUCTION

Catalysts used in petroleum refining processes are poisoned by nitrogen-even at trace levels -rendering them ineffective. Thus, the presence of nitrogen in crude oil reduces its economic value due to the need for removing nitrogen prior to refining the crude. Nitrogen content was determined using ANTEK 7000 Elemental Analyzer using ASTM standard method D 4629-91.

3.2.1.3.2 REAGENTS AND MATERIALS

Chemicals used in the determination of nitrogen contents of the oil samples included aniline (ACS grade) and toluene (HPLC grade). Gases used

were of high-purity chromatography grade; these include: oxygen and argon or helium.

3.2.1.3.3 APPARATUS

The apparatus used for measuring nitrogen content is described earlier in section 3.2.2.

The electric furnace was held at 1100°C to pyrolyze the sample and oxidize nitrogen to nitric acid (HNO_3), which, in turn, was converted to excited nitric oxide (NO_2) by contact with ozone in the high temperature zone of the furnace. The combustion tube is made of quartz. Drier tubes are used to remove the water vapor produced during sample combustion. The light emitted as the excited NO_2 decays is measured by the detector, and the signal is a measure of the nitrogen content of the sample. A microliter syringe is used for sample introduction to the combustion tube *via* the boat inlet system. A typical block diagram of the instrument is depicted in Figure 3.3.

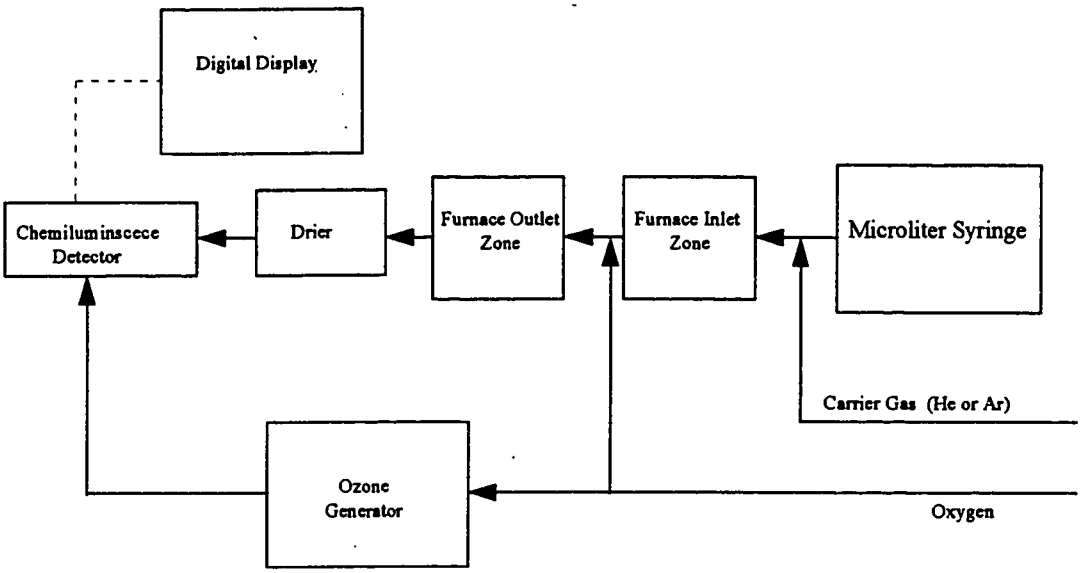

Figure 3.3. Block diagram for the ANTEK 7000 Elemental Analyzer

3.2.1.3.4 PROCEDURE

A stock solution of aniline in toluene was used for calibration purposes. Prior to carrying out actual sample analysis, the apparatus was checked for gas leaks and the sample was also checked for the presence of air bubbles. If they were present, the sample was discarded, and a new sample was taken. The amount of sample used for each analysis was 5 μl. Instrument output is in parts per million (ppm).

3.3 FRACTIONATION OF THE OILS

3.3.1 INTRODUCTION

Column chromatography was employed to fractionate the oils into their major compound classes, namely: saturate fraction (composed of normal, branched, and cyclic compounds), aromatic fraction (composed only of those compounds having aromatic rings), polar fraction (composed of polar compounds, usually containing nitrogen, sulfur, and/or oxygen), and asphaltenes [12].

3.3.2 MATERIALS

Solvents used were dichloromethane, n-pentane, n-hexane, toluene, and methanol. All solvents were of HPLC grade (except for toluene and methanol which were of ACS grade). Activated alumina and silica were used for column packing. The alumina used was 1077-6 EM SCIENCE, 70-230 Mesh ASTM with a size range of 0.063-0.200 mm. The silica used was 7734-3 SCIENCE, 70-230 Mesh ASTM with chloride and iron contents of 0.02% and 0.03%, respectively. The pH of the silica used was 7 in a 10% aqueous suspension. The column used was 4.4 cm internal diameter and 60 cm height.

3.3.3 PROCEDURE

Prior to fractionation, the crude oils were topped by evaporating light-end hydrocarbons under vacuum using a rotary evaporator. A minimum amount of dichloromethane (CH_2Cl_2, HPLC grade) was used to solvate the oils in preparation for topping. The oils were topped for thirty minutes at a temperature of 80°C.

The column packing materials (alumina and silica) were activated under vacuum for an average period of 45 hours at an average temperature of 170°C. Slurries were made using *n*-pentane (HPLC grade). The amount of oil used was about 5 g. The solvent (n-pentane) was used to facilitate the transfer of the oil to the column. The column was prepared by wet-packing using about 150 g of alumina (Al_2O_3) in the bottom and about 100 g of silica (SiO_2) gel at the top.

The saturate fraction was eluted using 800 ml of n-pentane at an average flow rate of 4-5 mls/min. The collected material was then rotavapped under vacuum at a temperature of 40 °C to evaporate the solvent.

The aromatic fraction was eluted using 500 ml of a 50:50 mixture of toluene : n-hexane followed by 300 ml of toluene. The average flow rate was the same as that used in eluting the saturate fraction (4-5 mls/min). The collected

material was then rotavapped under vacuum at a temperature of 65°C to remove the solvent.

The polar fraction was eluted using 200 ml of methanol followed by 100 ml of a (2:3) mixture of methanol : dichloromethane. The collected material was then rotavapped under vacuum at a temperature of 75°C to evaporate the solvent.

3.4 GAS CHROMATOGRAPHY - MASS SPECTROMETRY (GC-MS)

A *Hewlett-Packard* HP 5890 series II gas chromatograph (GC) was used to separate components before introduction in the *VG Autospec* mass spectrometer (MS). The column and temperature programming used depended on the analysis to be performed (see below).

Upon reaching the source chamber, samples were ionized by electron impact (EI) using a 70 eV electron beam. The ions were then accelerated into the mass analyzer at 8000 V.

Characteristic ions for the compounds of interest were obtained from the literature. Mass spectrometric monitoring of a specific mass/charge (m/z) ration or a limited number of ratios was the analysis method used. This method is called selected ion monitoring (SIM). Using SIM method of monitoring one or a few masses results in better sensitivity than can be obtained using full scan

method. Comparison of the fragmentograms obtained with fragmentograms from the literature [8, 10, 30, 44, 54] was used to identify compounds of interest.

3.4.1 THE SATURATE FRACTION

The column used for this analysis was 60 m, 0.25 mm ID, 0.25 μm film thickness DB-1 *J&W Scientific* product. The temperature program used was as follows:

Initial Temperature = 150°C

Initial Hold Time = 0 min (no hold)

Ramp = 2°C/min

Final Temperature = 320°C

Final Hold Time = 27 min

The compounds of interest in the saturate fraction (alkanes, hopanes, steranes, and tricyclics) were monitored by targeting the 183, 191, 217, and 218 ions. The m/z 183 fragmentogram shows the alkanes, the m/z 191 fragmentogram depicts the hopanes and tricyclics, and the m/z 217 and 218 fragmentograms show the steranes.

3.4.2 THE AROMATIC FRACTION

The column used was a 60 m long DB-5 *J&W Scientific* product with 0.25 mm ID and 0.25 μm film thickness. The experimental conditions used were as follows:

Initial Temperature = 100°C

Initial Hold Time = 0 min (no hold)

Ramp = 2°C/min

Final Temperature = 200°C

Final Hold Time = 10 min

The compounds of interest in the aromatic fraction, phenanthrene, methylphenanthrenes, dibenzothiophene, and methyldibenzothiophenes were monitored by targeting the m/z 178, 192, 206, and 220 ions for phenanthrenes and the m/z 184, 198, 212, and 226 ions for dibenzothiophenes.

3.5 GAS CHROMATOGRAPHY (GC)

Experimental procedures for the analyses of the saturate and aromatic fractions as well as whole-oil analysis are described separately below. Compound identification was done by comparisons with existing literature [10, 11, 30, 37, 38].

3.5.1 THE SATURATE FRACTION

The saturate fractions of all the samples were analyzed on a 5790 Hewlett-Packard GC equipped with a flame ionization detector (FID) and a *J & W Scientific* DB-1 capillary column. The column is 30 m long, has a 0.25 mm ID, and a film thickness of 0.25 microns. The injector temperature was set at 320°C, FID temperature at 350°C. Helium (He) was used as a carrier gas with a column pressure of 15 psig. The split ratio used was 50:1. The amount injected was 1μl. The temperature program used was as follows:

Initial Temperature = 80°C
Initial Hold Time = 2 min
Ramp = 4°C/min
Final Temperature = 320°C
Final Hold Time = 20 min

3.5.2 THE AROMATIC FRACTION

The aromatic fraction was analyzed on the same instrument used for the saturate GCs. The conditions used above were also used here with the exception of the temperature program which was as follows:

Initial Temperature = 35°C
Initial Hold Time = 2 min
Ramp = 3°C/min

Final Temperature = 315°C

Final Hold Time = 20 min

3.5.3 WHOLE-OIL GC

The oils were analyzed by whole-oil gas chromatography. The experimental conditions used here were identical to those used for the aromatic fraction GC analysis as described in the preceding section.

CHAPTER 4

RESULTS AND DISCUSSION

4.1 CLASSIFICATION OF OILS BASED ON THEIR BULK PROPERTIES

The results of the determinations of API gravity, sulfur, and nitrogen contents are presented in Table 4.1. The data show that oils from Central Arabia, fields A, B, C, and E, have high API gravity values that qualify them for the super light crude oil classification. The other two oils from Central Arabia, fields D and G may be classified as light crude oils on the basis of their API gravity values. Sample F1 is a Paleozoic condensates from Eastern Province. . .

API gravity may be lowered in response to alteration processes such as water-washing and/or biodegradation. Water-washing selectively removes the water-soluble compounds such as toluene and other light aromatics. As a consequence, the crude becomes enriched in heavier components. However, API gravity is not highly affected by water-washing. Bacteria remove the light end *n*-hydrocarbons, thus enriching the crude in heavier components and, in effect, decrease its API gravity.

The other two oils, which are from the Eastern Province (Jurassic), may be classified as medium gravity oils, based on their API gravity values. Higher sulfur

contents are related to the source rock from which these oils were generated. Carbonate source rocks generate oils with higher levels of sulfur [14]. Central Arabian oils have been shown to be generated from the Qusaiba Member (shale) of the Silurian (440-410 MYA[4]) Qalibah Formation and not from a carbonate source [3, 55].

Table 4.1: Bulk Properties of all Samples Used in the Study

Sample Code	Area	Sample Type	Sample Age	Gravity (°API)	Sulfur (Wt %)	Nitrogen (ppm)
A1	Central	Oil	Paleozoic	52.60	0.01	22
A2	Central	Oil	Paleozoic	51.00	0.01	21
A3	Central	Oil	Paleozoic	51.90	0.01	16
B1	Central	Oil	Paleozoic	46.80	0.02	80
B2	Central	Oil	Paleozoic	46.40	0.02	82
B3	Central	Oil	Paleozoic	46.20	0.02	81
C1	Central	Oil	Paleozoic	49.40	0.03	82
C2	Central	Oil	Paleozoic	46.10	0.03	87
C3	Central	Oil	Paleozoic	47.70	0.05	87
D1	Central	Oil	Paleozoic	37.10	0.07	350
E1	Central	Oil	Paleozoic	48.40	0.08	100
F1	Eastern	Condensate	Paleozoic	45.80	0.01	8
G1	Central	Oil	Paleozoic	39.90	0.04	210
H1	Eastern	Oil	Jurassic	31.30	2.35	1130
H2	Eastern	Oil	Jurassic	31.40	2.33	1110

The Central Arabia Paleozoic oils have sulfur contents that are, on average, 30 to 180 times less than the Eastern Province Jurassic oils.

These very low sulfur contents warrant the classification of these Central Arabian crude oils as very sweet oils.

[1]MYA: Million-Year-Ago

In most oil fields around the world, sulfur is the most abundant heteroatom (NSO) in crude oils. Sulfur is thought to occur naturally in early diagenesis in the form of H_2S, resulting from action of sulfate-reducing anaerobic bacteria. Sulfur can be found in low, medium, and high molecular weight fractions of crude oils [13, 14].

Sulfur is usually present in one of the following categories:

1. thiols (mercaptans), with general formula RSH, where R represents the hydrocarbon part; an example is 2-butanethiol,
2. sulfides, with general formula RSR; an example is 2-thiabutane,
3. disulfides, with general formula RSSR; an example is dithiabutane,
4. and thiophene derivatives; an example is methylbenzothiophene.

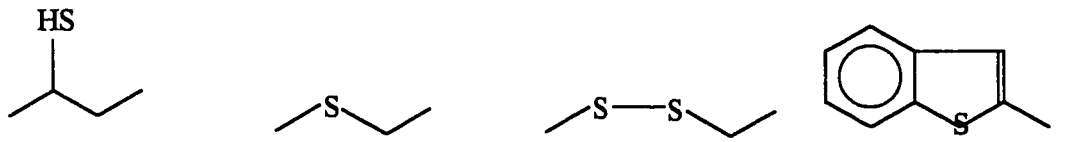

2-Butanethiol 2-Thiabutane Dithiabutane Methylbenzothiophene

Figure 4.1. Structures of some sulfur compounds found in crude oils

Nitrogen contents of the Central Arabian oils are also exceedingly low compared to the Eastern Province oils. Averages for A, B, and C fields are 20, 81, and 85 ppm, respectively. Oils from other Central Arabian fields have

nitrogen levels ranging between 8 and 350 ppm. Nitrogen levels of the Eastern Province Jurassic oils are noticeably higher: 1130 and 1110 ppm. The average value in Central Arabia is between three and 140 times less than the values of the oils from the Eastern Province.

Figure 4.2a is a plot of percent sulfur *vs.* API gravity for all oils in this study. The figure shows that oils from each field group tightly together, with those from the Eastern Province (Jurassic) being in the low-API-high-%S corner. The tight grouping of the Paleozoic fluids suggests a high degree of similarity for all these oils, except possibly those from fields D and G, which have relatively lower API gravity values. Figure 4.2b is a plot of the same parameters as in Figure 4.2a with the exclusion of the Jurassic fluids from the Eastern Province. These Figures show, more clearly than Figure 4.2a, the grouping of the Paleozoic fluids from fields A, B, C, D, E, F, and G.

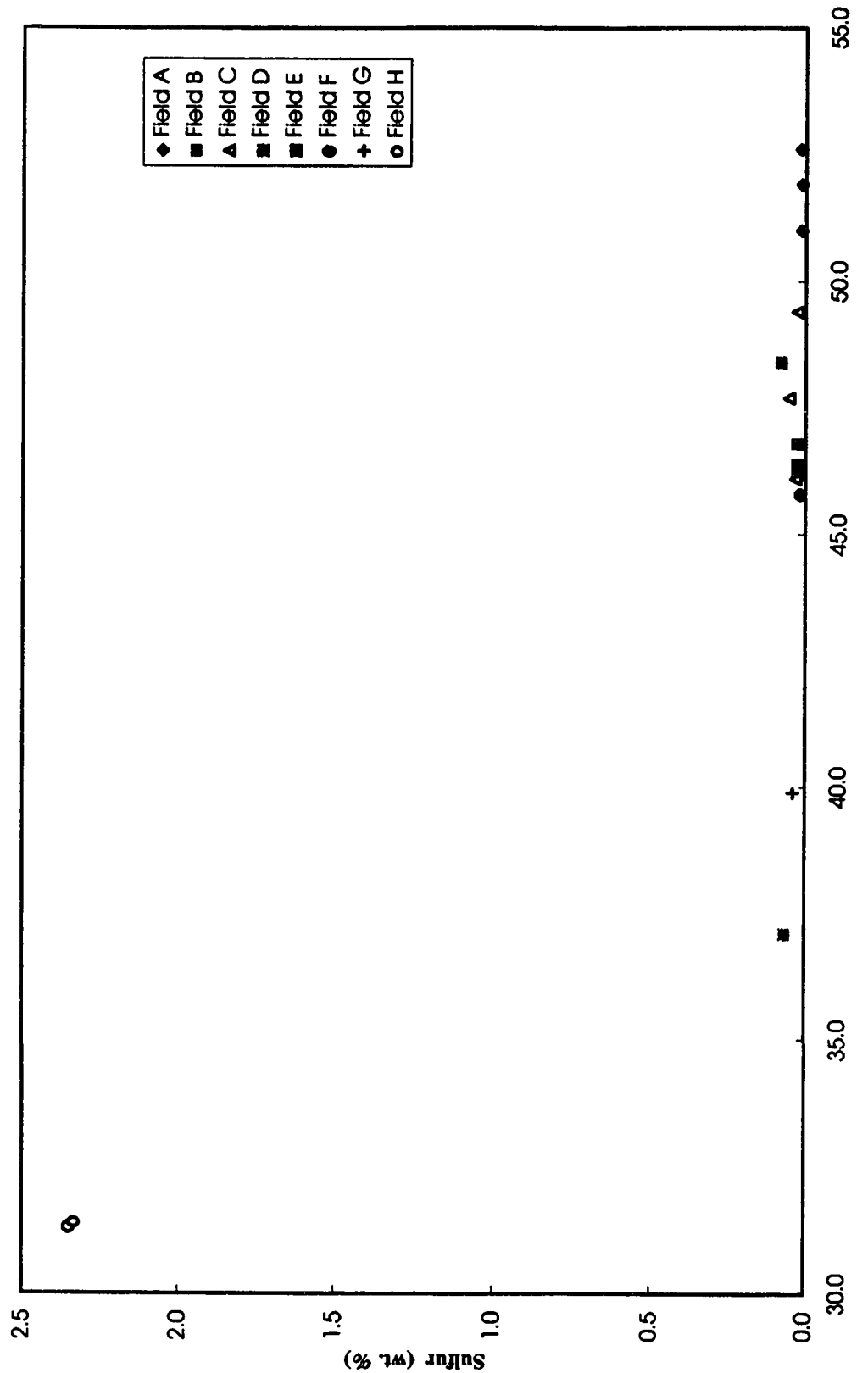

Figure 4.2a. Per cent sulfur *vs* . API gravity for all oils included in the study.

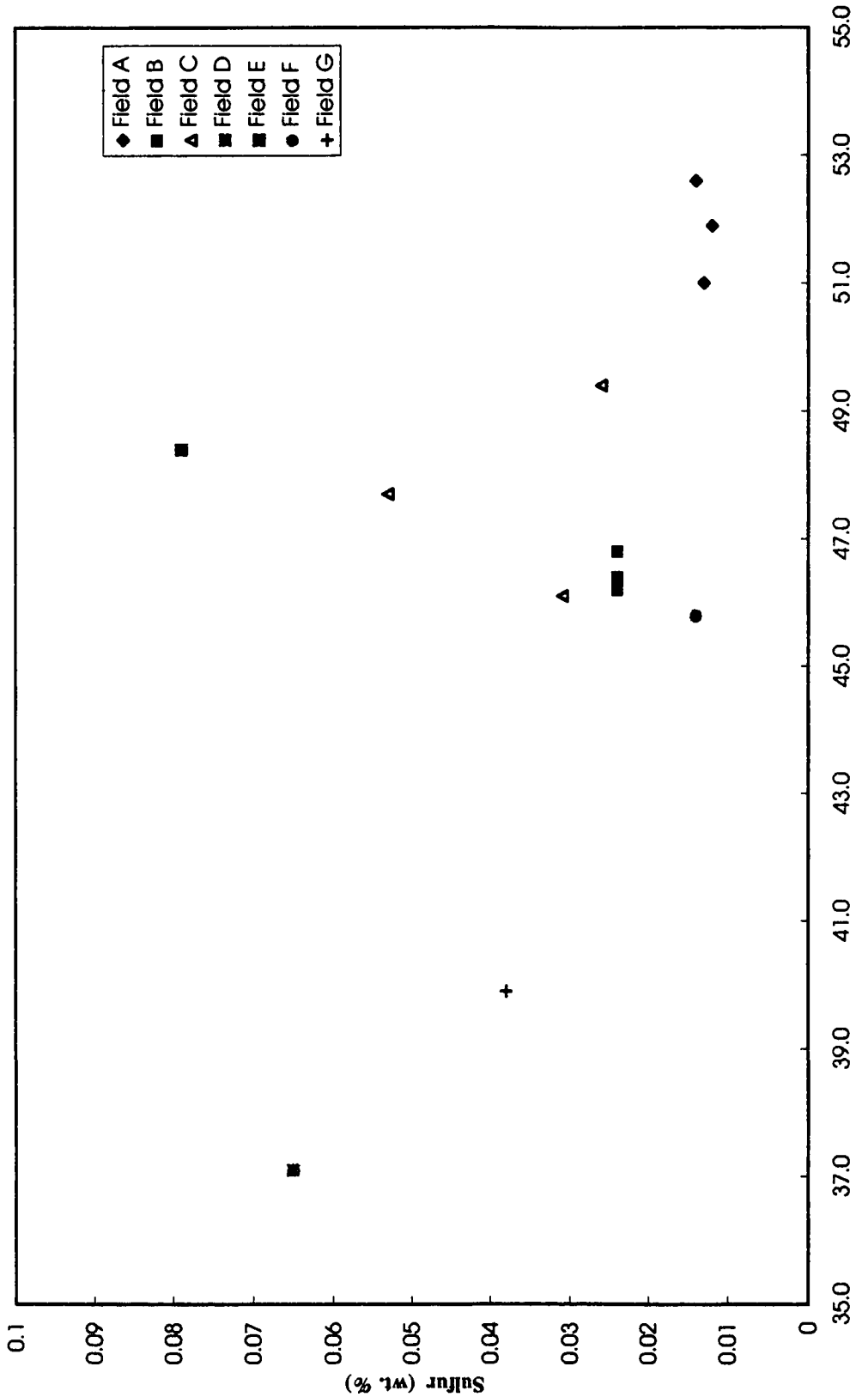

Figure 4.2b. Per cent sulfur *vs* . API gravity for Paleozioc fluids included in the Study.

Figure 4.3a is a plot of nitrogen content (in ppm) *vs.* API gravity for all oils included in the study. This plot also shows the tight grouping of the Paleozoic fluids. Once again, oils from fields D and G group closer to each other than to other oils from Central Arabia. Jurassic oils from the Eastern Province plot in the low-API-high-nitrogen corner. Figure 4.3b is a plot of the same parameters as in Figure 4.3a with the exclusion of the Jurassic fluids from the Eastern Province. These Figures show, more clearly than Figure 4.3a, the tight grouping of the Paleozoic fluids.

Figure 4.4a is a plot of nitrogen content *vs.* percent sulfur for all oils included in the study. Figure 4.4b is a plot of the same parameters as in Figure 4.4a with the exclusion of the Jurassic fluids from the Eastern Province. With the exception of oils from fields D and G, all Paleozoic fluids group together very tightly and at the opposite corner from Eastern Province (Jurassic) oils.

The three plots in Figures 4.2b, 4.3b, and 4.4b indicate that oils from fields D and G either have closer genetic relationship, or possibly a different source rock organic facies than other Central Arabian oils, or that they have undergone migration pathways that are similar to each other, but different from the others.

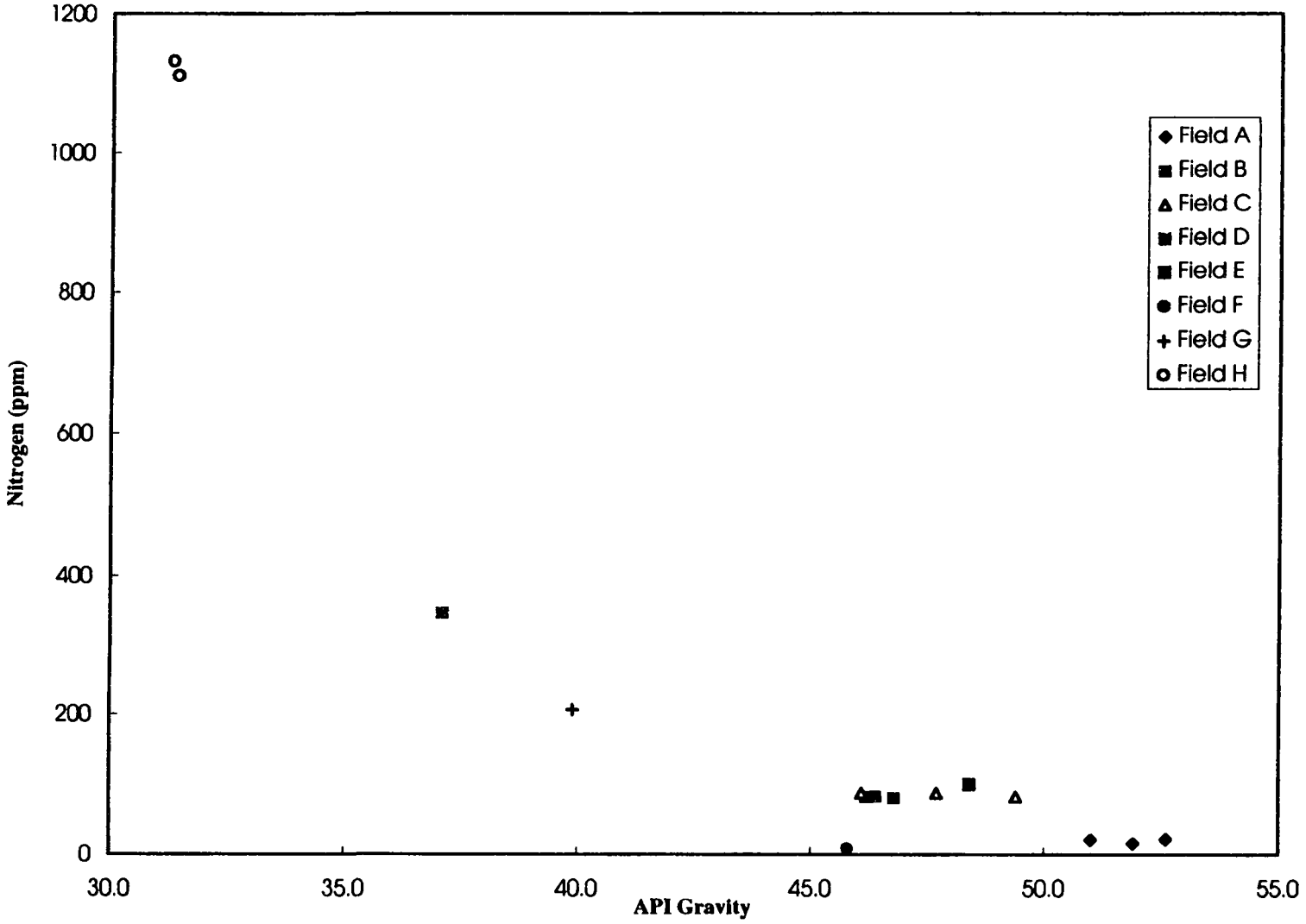

Figure 4.3a. Nitrogen content *vs*. API garvity for all oil included in the study.

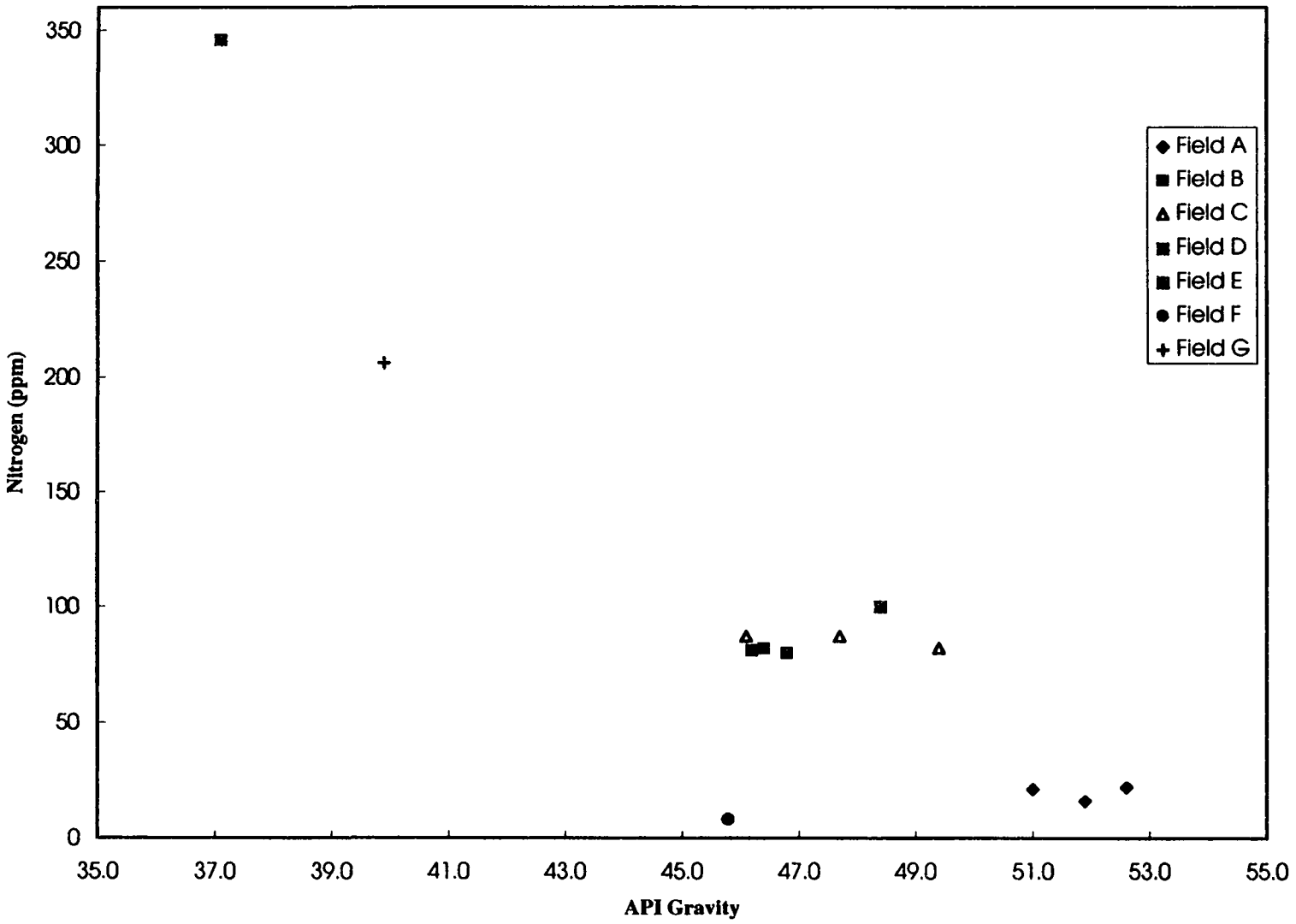

Figure 4.3b. Nitrogen content *vs* . API garvity for Paleozoic fluids included in the study.

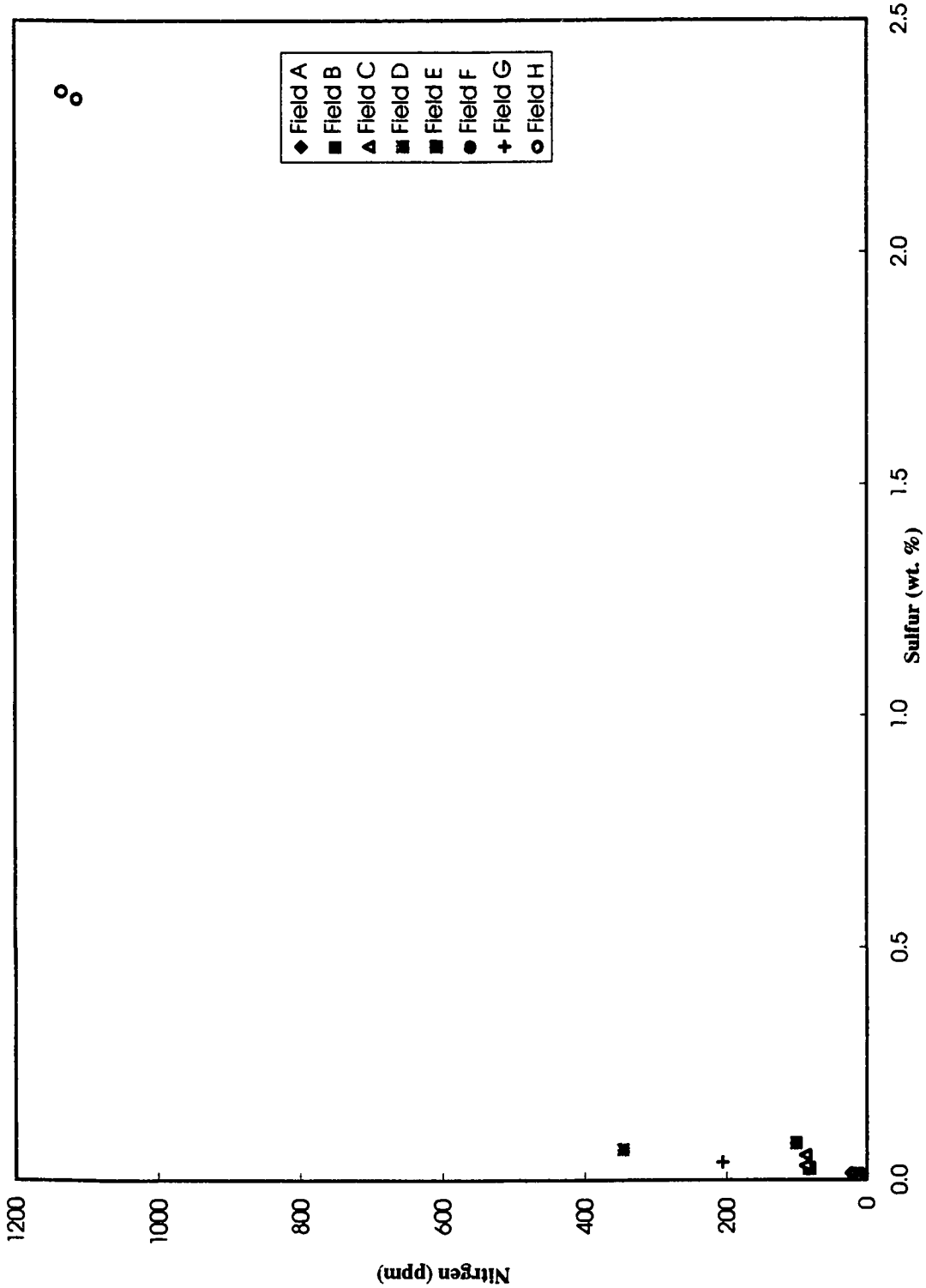

Figure 4.4a. Nitrgen content *vs.* per cent sulfur for all oils included in the study.

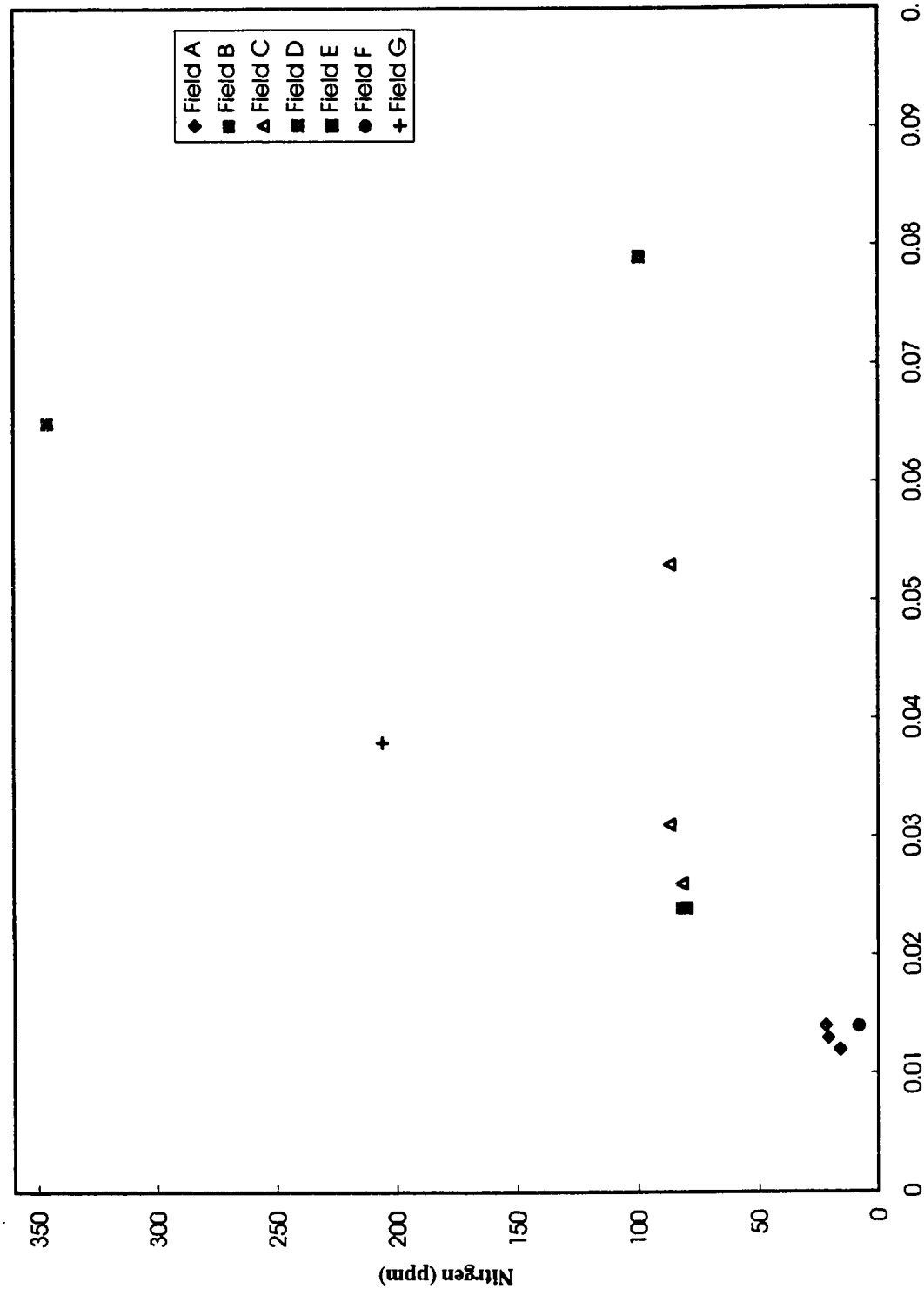

Figure 4.4b. Nitrgen content *vs.* per cent sulfur for Paleozoic fluids included in the study.

4.2 FRACTIONATION OF CRUDE OILS

Fifteen oil and condensate samples were fractionated into their compound class fractions which are the saturates, aromatics, and polar fractions using silica-alumina column chromatography. Table 4.2 shows the fractionation data of all fluids used in the study. Samples from field "A" (Paleozoic from Central Area) contain the highest average percentage (72%) of saturate compounds amongst all samples. Samples from fields "B" and "C" have average percentages of saturate compounds of 60% and 65%, respectively. Field "E" also has a high content of saturates. The API gravity of these Paleozoic oils follow the same trend as their saturate content while the sulfur and nitrogen contents follow a trend opposite to the saturate trend (*c.f.* Table 4.1) *i.e.* oils with highest API gravity have the lowest sulfur and nitrogen contents.

The two Jurassic oils from the Eastern Province have low saturate content and low API gravity; a trend similar but opposite in direction to that of the Paleozoic oils which have high saturate content and high API gravity. The sulfur and nitrogen contents of the Jurassic oils are very high when compared to those Paleozoic oils from Central Arabia. This represents another trend that is similar but opposite in direction to that of the Paleozoic oils which have low sulfur and nitrogen contents.

Table 4.2: Fractionation Data of all Samples Used in the Study

Sample Code	Area	Sample Type	Sample Age	%SATs	%AROs	%POLARs
A1	Central	Oil	Paleozoic	61.00	11.96	2.87
A2	Central	Oil	Paleozoic	75.18	14.60	4.01
A3	Central	Oil	Paleozoic	79.82	16.51	2.14
B1	Central	Oil	Paleozoic	56.42	18.51	29.85
B2	Central	Oil	Paleozoic	55.49	16.18	3.76
B3	Central	Oil	Paleozoic	68.51	19.83	2.92
C1	Central	Oil	Paleozoic	70.55	22.60	4.45
C2	Central	Oil	Paleozoic	58.26	19.13	3.77
C3	Central	Oil	Paleozoic	67.31	23.95	5.18
D1	Central	Oil	Paleozoic	55.47	28.52	3.52
E1	Central	Oil	Paleozoic	65.35	18.31	3.66
F1	Eastern	Condensate	Paleozoic	49.44	11.30	2.26
G1	Central	Oil	Paleozoic	43.22	21.47	3.11
H1	Eastern	Oil	Jurassic	34.04	44.58	7.23
H2	Eastern	Oil	Jurassic	35.77	42.82	10.70

4.3 GAS CHROMATOGRAPHY

Comparison with chromatograms available from the literature was the method used for peak identification for all chromatograms. Chromatograms obtained for fluids used in this study were obtained under the same chromatographic conditions as those in the literature used for comparisons, thus permitting peak identification by comparisons. [10, 11, 30, 37, 38]

Fractionation of crude oils prior to gas chromatographic analysis is typically carried out to simplify interpretation of results obtained from gas chromatographic analyses. Fractionation is especially important when gas

chromatography is coupled with mass spectrometry (GC/MS). This is due to the fact that if whole oil is used for GC/MS analysis, monitoring of ions of interest becomes very difficult as a result of the many possible fragments that come from the many compounds contained in crude oils.

4.3.1 GAS CHROMATOGRAPHIC ANALYSIS OF THE SATURATE FRACTION

Figures 4.5 is a typical GC chromatographic profile (5-80 min) for a saturate fraction of a Paleozoic crude oil (A-1) and Figure 4.18 is a typical GC chromatographic profile for a saturate fraction of a Jurassic crude oil (H-1). The GC chromatograms of the saturate fraction of all fluids covered in this study are presented in Appendix A in Figures 4.5 to 4.19.

A comparative study of these chromatograms led to the following observations:

No distinctive features, such as bimodality or odd-even predominance (suggesting early maturity) were noticed in these chromatograms. In fact, all Paleozoic fluids have chromatograms close enough to one another (in bulk) that they do not permit meaningful distinctions between them.

Bimodal distribution of the normal alkanes present in crude oils is an indication of mixed contributions to the organic matter from which the kerogen

that generated these crudes was formed. Mixed contributions come from marine and terrestrial sources. This feature is absent from the saturate GC chromatograms of all Central Arabian Paleozoic fluids covered in the present study (Figures 4.5 to 4.19 in Appendix A). The two Jurassic oils from the Eastern Province did not exhibit this feature also. Hence, no distinction could be made on the basis of such a feature.

Odd-even predominance refers to the dominant presence of odd-numbered normal alkanes relative to even-numbered normal alkanes. Odd-even predominance is an indication of early maturity. On the other hand, even-odd predominance indicates higher levels of maturity. Neither of these two phenomena was observed in either the Paleozoic Central Arabian fluids or the Jurassic oils from the Eastern Province. This is shown clearly in Figures 4.5 to 4.19 in Appendix A which depict the GC chromatograms of the saturate fractions of the all fluids included in the present study.

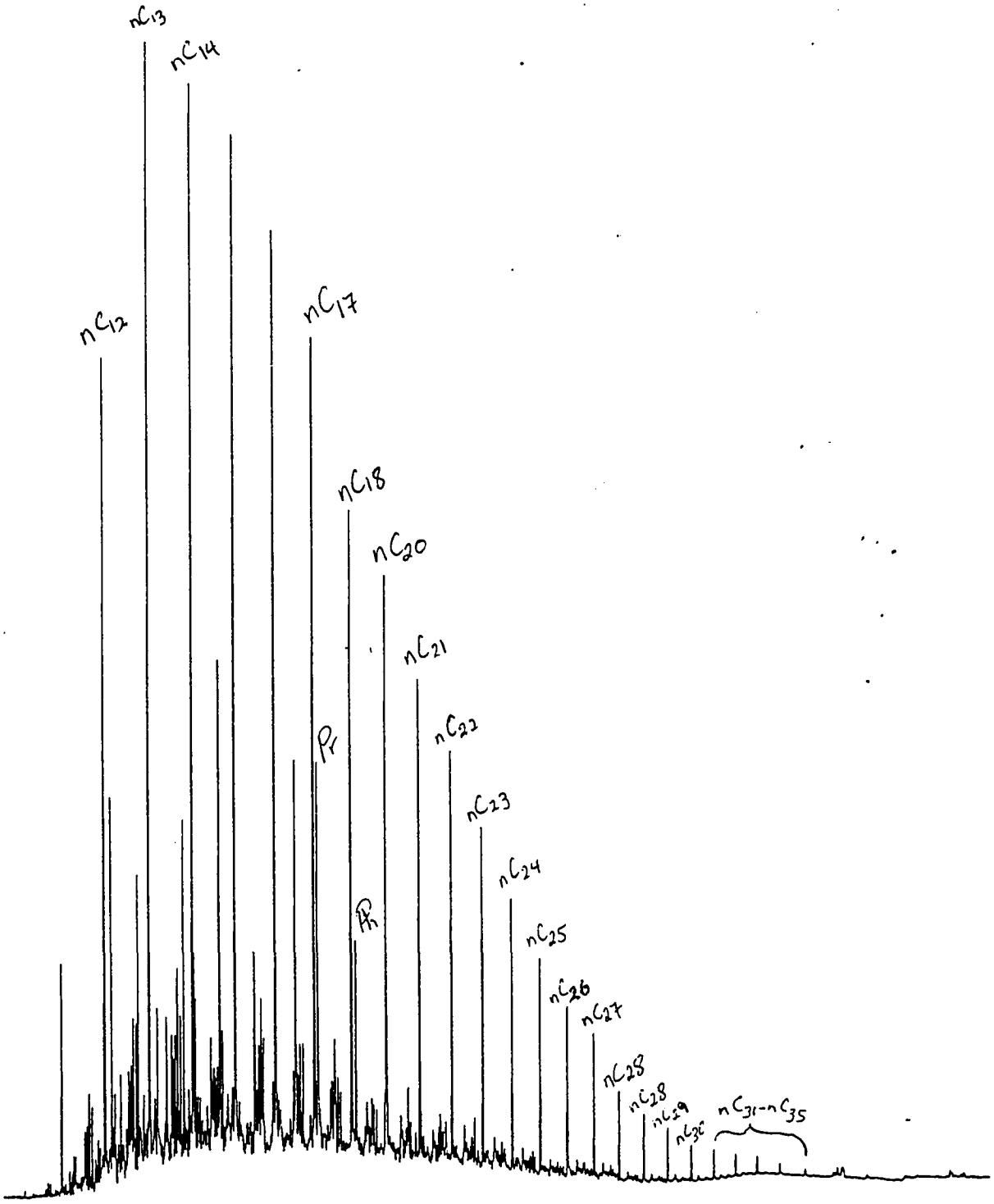

Figure 4.5. Gas chromatogram of the saturate fraction of oil A1.

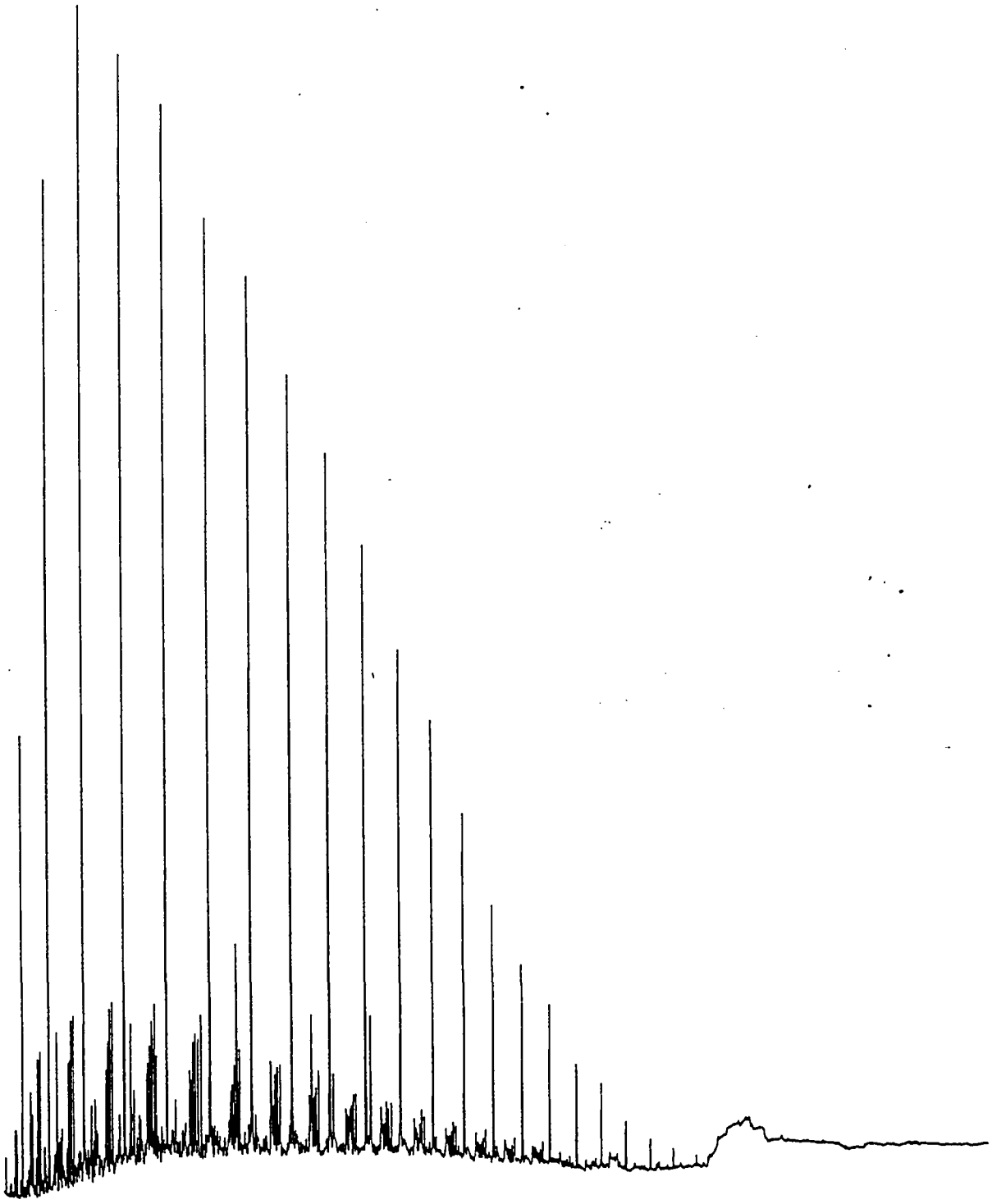

Figure 4.18. Gas chromatogram of the saturate fraction of oil H1.

4.3.2 GAS CHROMATOGRAPHIC ANALYSIS OF THE AROMATIC FRACTION

The aromatic fractions of all fluids covered in this study were analyzed by gas chromatography. Figure 4.20a shows a typical GC chromatographic profile (5-115 min) for an aromatic fraction of a Paleozoic crude oil (A-1). The full range chromatogram did not allow identification of aromatic compounds such as, naphthalenes, phenanthrenes, or benzothiophenes. A further attempt was made to identify these compounds by concentrating on the middle range of the chromatogram (10-78 min). This GC chromatographic profile is depicted in 4.20b for Paleozoic oil (A-1). However, the outcome of this attempt was not fruitful. High noise-to-signal ratio may be responsible for obstructing identification of compounds in some of the samples such as, the Jurassic oils H1 and H2 from the Eastern Province.

Sulfur-containing compounds may not be present in these samples in detectable amounts due to exceedingly low sulfur content of the Paleozoic fluids.

The GC chromatograms for all other samples are included in Appendix B (Figures 4.20-4.34; part (a) of each figure depicts the full range and part (b) depicts the middle range).

Comparing these chromatograms with chromatograms from the literature [44] did not yield identification of any aromatic compound classes, such as

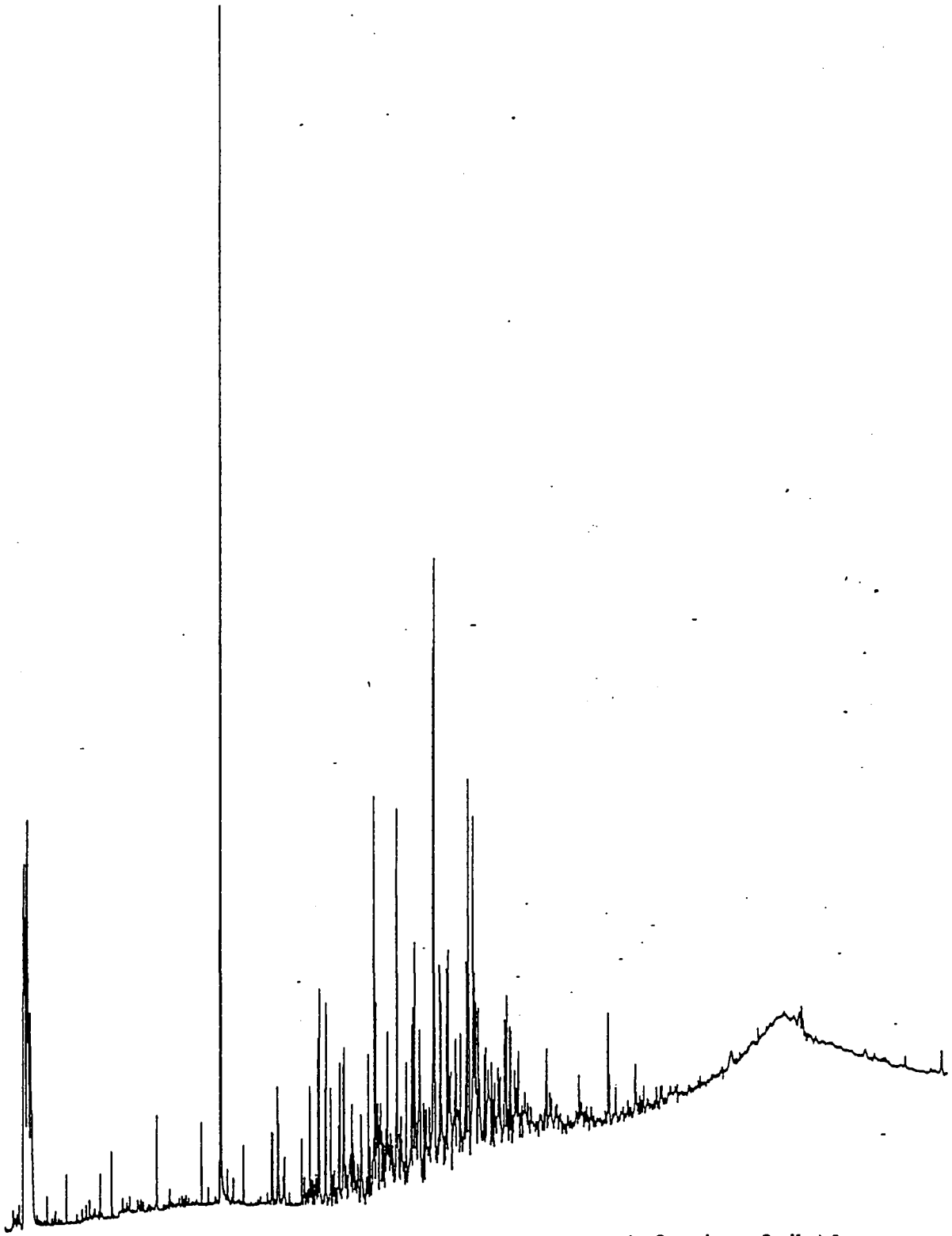

Figure 4.20 a. Gas chromatogram of the aromatic fraction of oil A1.

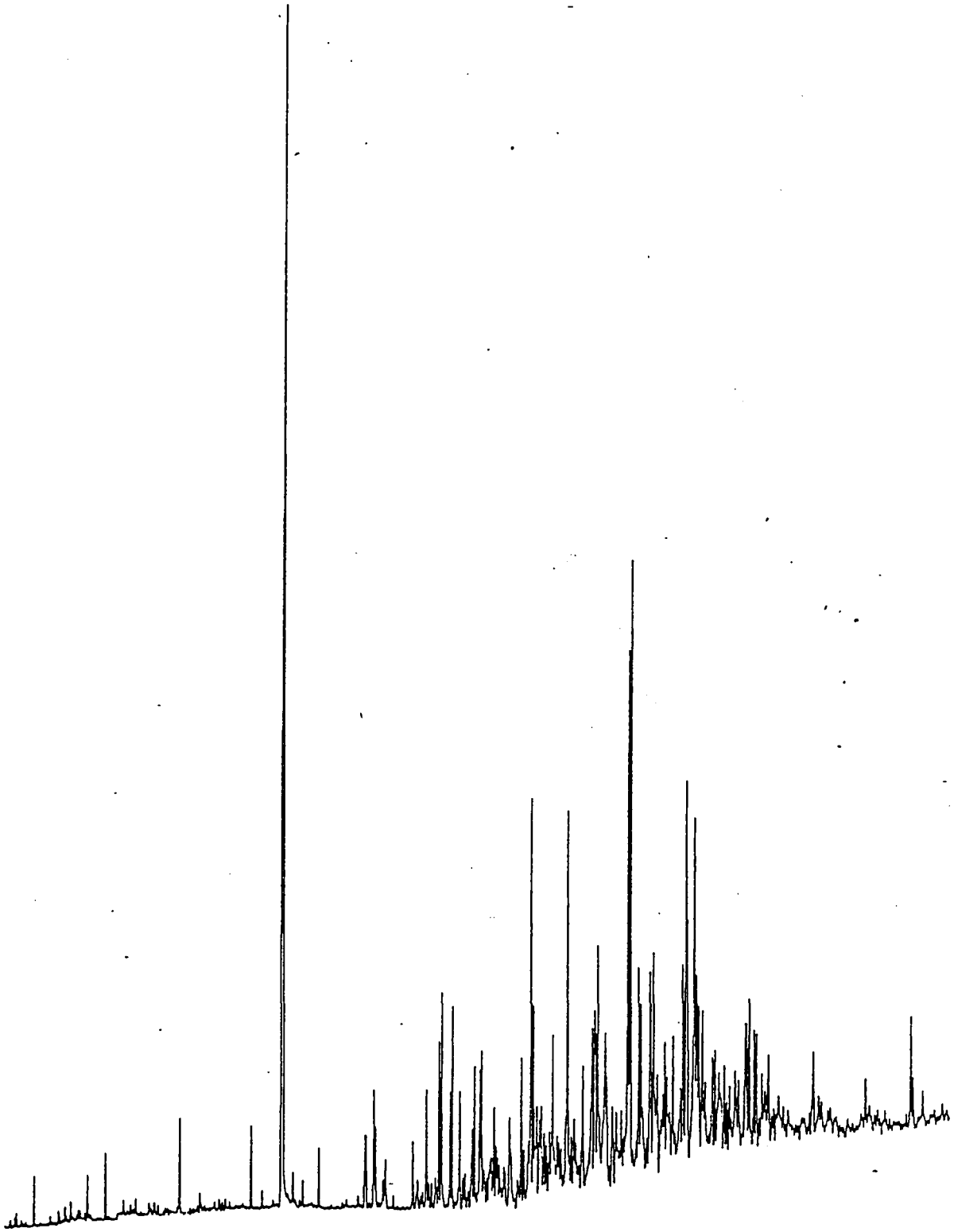

Figure 4.20 b. Gas chromatogram of the middle range (10-78 min.) of the aromatic fraction of oil A1.

naphthalenes, phenanthrenes, benzothiophenes in all samples covered in the present study.

Failure to come up with any useful correlation between the fluids under investigation by using gas chromatographic analyses of either the saturate or aromatic fractions led to the use of a technique known as micro-scale correlation using mid-range hydrocarbons. This technique will be discussed in greater detail in the following section.

4.3.3 WHOLE-OIL GAS CHROMATOGRAPHIC ANALYSIS

Micro-scale correlation technique depends on gas chromatographic analysis of whole oils rather than compound-class fractions of the crude such as, saturates and aromatics. The mid-range hydrocarbons used for micro-scale correlation purposes represent a random selection of compounds that elute in the time window between 38-67 minutes of the full range which is between 0-115 minutes. These compounds include normal alkanes (between n-C_{15} and n-C_{22}), branched saturated compounds, as well as a suite of unknown compounds that may not be seen in the GC chromatograms of either the saturate or aromatic fractions. Hence, the need for whole-oil gas chromatographic analyses. [5, 6]

Whole-oil gas chromatograms (0-115 min) of all oils covered in this study are depicted in Figures 4.35 through 4.49 (parts a and b) in Appendix C. The middle range of each chromatogram is depicted in part (b) of each figure. Part (b) of each figure was produced to simplify measurements of peak heights and make it more accurate since compounds selected for correlation purposes elute within this time window. Accurate measurement of peak heights is of major importance - as will be explained later - to the accuracy of mid-range hydrocarbons micro-scale correlation technique.

4.3.4 MID-RANGE HYDROCARBONS MICRO-SCALE CORRELATIONS

The basis for selection of compounds for this purpose is that these compounds should exhibits sample-to-sample variations that permit correlation and/or differentiation between fluids. All compounds selected between (n-C_{15} and n-C_{22}) elute within the time window between 38 and 67 minutes which is depicted in part (b) of Figures 4.35 to 4.49 in Appendix C.

These compounds are usually unknown minor components which meet the criteria for selection as cited above. Among the compounds selected are some known peaks such as, n-C_{17}, pristane (i-C_{19} with formula $C_{19}H_{40}$), n-C_{18}, and phytane (i-C_{20} with formula $C_{20}H_{42}$).

The main objective here is to correlate the fluids under investigation by comparing ratios of compounds. To put these comparisons in a pictorial form, multivariate plots (star diagrams) are used. These star diagrams make correlating and/or differentiating fluids easier. Star diagrams are multivariate plots in polar coordinates. Each star diagram can have as many axes as one needs to use. However, the more axes a star diagram has, the more complicated the picture becomes. Thus, for clarity, star diagrams that will be used in this study will have eight axes per plot *i.e.* the twenty four sequential ratios will be plotted on three star diagrams. These star diagrams will be referred to hereafter as mid-range star diagrams (MRSD).

Star diagrams have been used to represent chemical compositions of water and oil samples. Studies of oils that employ star diagrams include: evaluation of reservoir lateral and vertical continuity, assigning relative contributions in multizone producing reservoirs and monitoring contribution changes with time, and identification of production problems such as casing leakages. [6]

In the present study, twenty four compounds are selected for mid-range micro-scale correlation. These compounds are labeled "C" through "Z" as can be seen in part (b) of Figures 4.35 through 4.49. Sequential ratios of these twenty four compounds are used to construct mid-range star diagrams (MRSD).

The twenty-four sequential ratios are calculated based on peak heights of the compounds selected. The first ratio is calculated by dividing height of peak C by height of peak D; the second ratio is calculated by dividing height of peak D by height of peak E; the third ratio is calculated by dividing height of peak E by that of peak F, and so on till the last ratio which is the only non-sequential one. This ratio is calculated by dividing height of peak C by height of peak Z. The twenty-four ratios are normalized and then represented by twenty-four axes on the MRSDs. To simplify the matter of correlation, the twenty-four axes are divided into three groups each of which consists of eight axes. The first eight ratios, "C/D" through "J/K", constitute the eight axes for the first mid-range-star-diagram (MRSD-1). The second eight ratios, "K/L" through "R/S", constitute the eight axes for the second mid-range-star-diagram (MRSD-2). The third eight ratios, "S/T" through "C/Z", constitute the eight axes for the third mid-range-star-diagram (MRSD-3). The maxima of the axes of the MRSDs vary and are printed in parentheses next to the axis endpoints.

Table 4.3 lists peaks heights for "C" through "Z" for all fluids covered in the present study. Table 4.4 lists the ratios of the peaks before normalization, and Table 4.5 lists peak ratios after normalization.

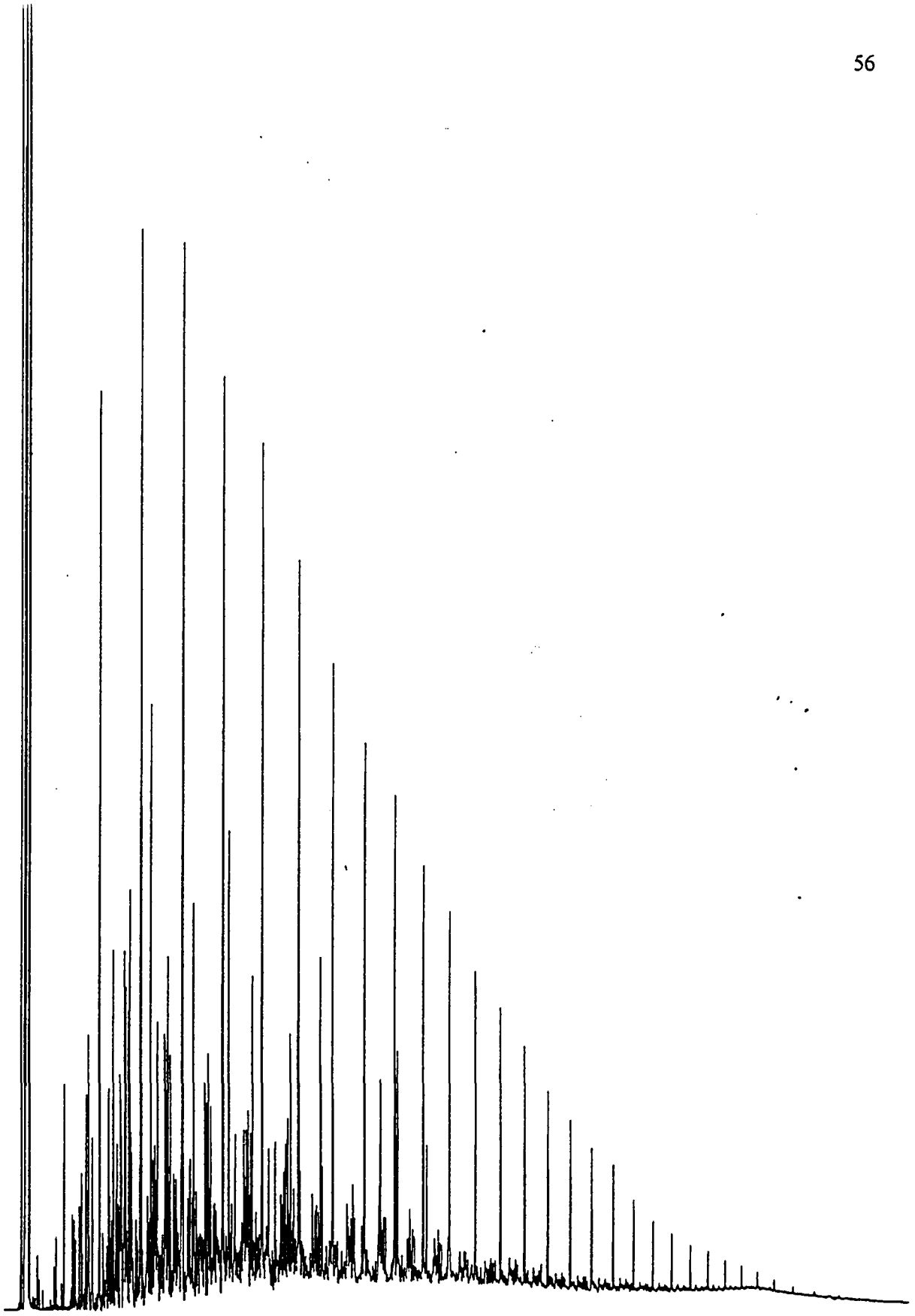

Figure 4.35 a. Whole-oil gas chromatogram of oil A1.

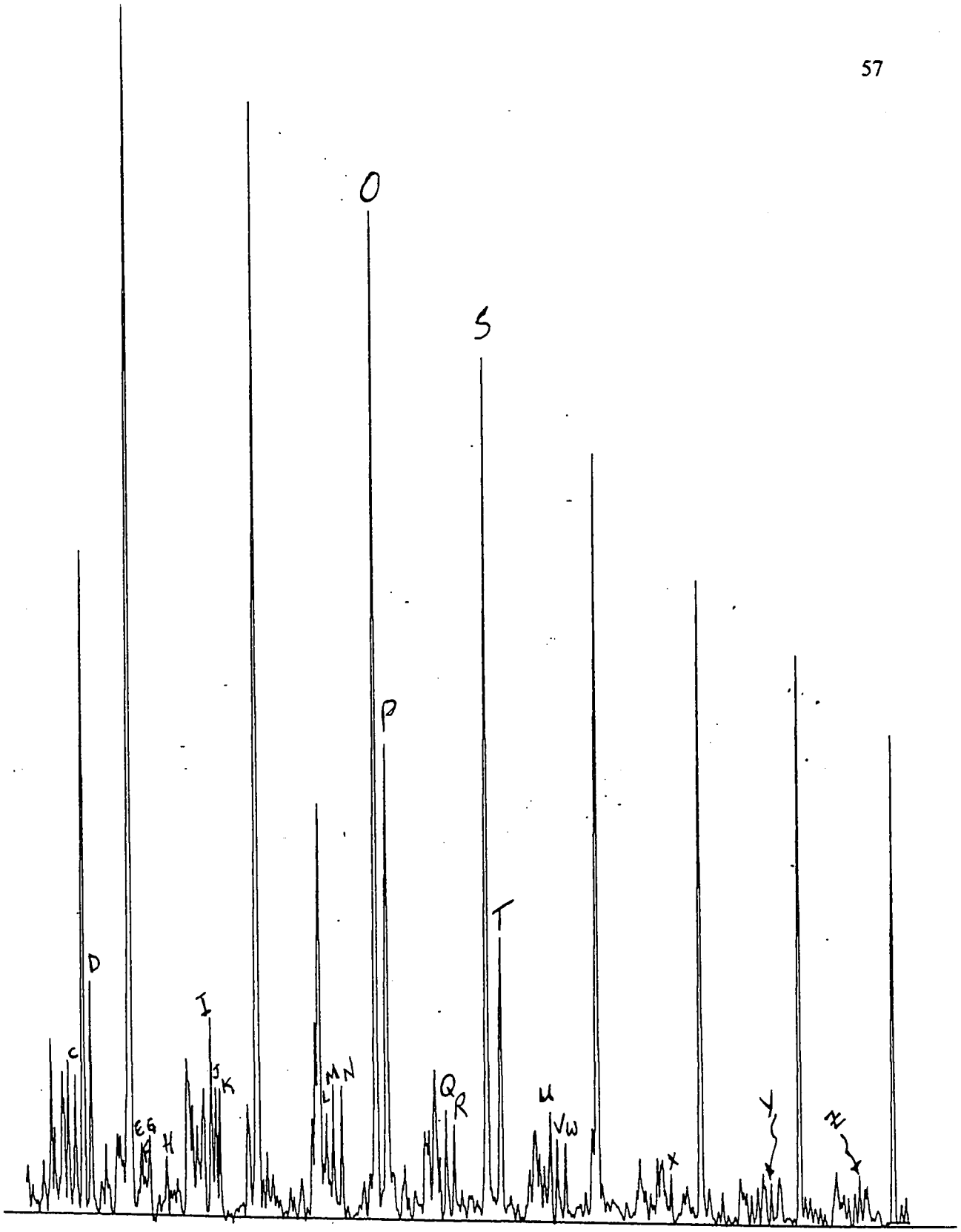

Figure 4.35 b. Whole-oil gas chromatogram of the middle range (38-67 min.) of oil A1.

Table 4.3: Peak-heights (cm); "C" through "Z" for all fluids used in the study

	Oil-A1	Oil-A2	Oil-A3	Oil-B1	Oil-B2	Oil-B3	Oil-C1	Oil-C2	Oil-C3	Oil-D1	Oil-E1	Oil-F1	Oil-G1	Oil-H1	Oil-H2
C	2.58	2.22	2.08	2.32	2.32	2.68	2.50	2.48	2.10	2.20	2.82	2.62	2.30	3.48	4.30
D	4.30	3.78	3.46	3.50	4.00	4.78	4.36	4.44	3.80	4.12	4.60	4.72	4.02	4.80	6.10
E	1.32	1.14	1.08	0.94	1.18	1.48	1.34	1.40	1.08	1.38	1.48	1.50	1.30	1.12	1.42
F	0.70	0.58	0.60	0.92	1.08	1.20	1.50	1.72	1.22	3.20	0.90	1.10	2.50	1.82	2.22
G	1.48	1.22	1.28	1.78	1.88	2.08	2.40	2.68	2.00	3.24	1.54	2.42	3.30	1.40	1.70
H	1.10	0.90	0.90	1.34	1.36	1.54	1.80	1.90	1.40	2.90	1.22	1.40	2.40	1.60	1.86
I	3.68	3.32	3.12	2.72	3.22	3.72	3.48	3.68	3.22	3.22	3.90	3.72	3.08	3.10	3.90
J	2.38	2.02	2.00	1.90	2.22	2.70	2.42	2.62	2.32	2.76	2.60	3.00	2.52	1.40	1.80
K	2.34	2.14	1.96	1.88	2.12	2.52	2.22	2.40	2.08	2.12	2.66	2.40	1.94	3.10	3.80
L	1.92	1.68	1.60	1.52	1.72	2.22	2.00	2.14	1.78	2.06	2.12	1.60	1.94	2.18	2.74
M	2.48	2.20	2.10	1.96	2.22	2.72	2.54	2.70	2.22	2.64	2.68	2.58	2.52	2.40	3.00
N	2.44	2.22	2.08	1.84	2.14	2.70	2.42	2.64	2.32	2.58	2.64	2.60	2.40	3.30	4.10
O (n17)	18.56	18.08	17.42	16.58	17.80	18.00	18.52	18.52	17.22	17.10	18.52	17.72	17.94	17.62	18.22
P (Pr)	8.78	7.76	7.30	7.18	8.02	9.52	9.02	9.00	8.08	9.20	8.62	8.52	8.38	3.00	3.80
Q	2.02	1.80	1.66	1.50	1.72	2.20	1.98	2.18	1.82	2.00	2.16	2.12	1.92	2.40	2.90
R	1.78	1.52	1.50	1.30	1.50	1.92	1.20	2.00	1.60	1.88	1.80	2.08	1.74	2.32	2.88
S (n18)	15.90	15.14	14.50	13.90	14.94	15.58	14.08	16.16	14.72	14.44	16.52	15.50	15.18	16.42	17.62
T (Ph)	5.22	4.44	4.20	4.14	4.72	5.88	4.98	5.80	5.00	5.84	5.42	5.38	5.20	4.70	5.60
U	2.02	1.76	1.66	1.48	1.74	2.30	1.92	2.30	1.90	2.08	2.10	2.28	2.02	1.70	1.96
V	1.52	1.34	1.28	1.22	1.40	1.80	1.58	1.74	1.52	1.60	1.74	1.68	1.60	1.90	2.20
W	1.46	1.20	1.20	1.12	1.36	1.78	1.62	1.98	1.56	2.00	1.60	1.90	2.00	2.20	2.60
X	0.92	0.82	0.80	0.82	0.90	1.10	1.10	1.14	1.06	1.02	1.08	1.18	1.00	1.58	1.74
Y	0.80	0.70	0.78	0.72	0.80	0.94	0.98	1.00	1.00	0.94	1.02	0.98	0.90	1.80	2.08
Z	0.98	0.78	0.72	0.70	0.72	1.00	1.00	1.10	1.00	0.92	1.00	1.08	0.92	1.22	1.54

Table 4.4: Ratios of the peaks "C" through "Z"; un-normalized

MAX (plot)	MAX (calculated)	Axis	Oil-A1	Oil-A2	Oil-A3	Oil-B1	Oil-B2	Oil-B3	Oil-C1	Oil-C2	Oil-C3	Oil-D1	Oil-E1	Oil-F1	Oil-G1	Oil-H1	Oil-H2
1.00	0.73	C/D	0.60	0.59	0.60	0.66	0.58	0.56	0.57	0.56	0.55	0.53	0.61	0.56	0.57	0.73	0.70
6.00	4.41	D/E	3.26	3.32	3.20	3.72	3.39	3.23	3.25	3.17	3.52	2.99	3.11	3.15	3.09	4.29	4.30
2.40	1.97	E/F	1.89	1.97	1.80	1.02	1.09	1.23	0.89	0.81	0.89	0.43	1.64	1.36	0.52	0.62	0.64
2.00	1.48	F/G	0.47	0.48	0.47	0.52	0.57	0.58	0.63	0.64	0.61	0.99	0.58	0.45	0.76	1.30	1.31
2.50	1.73	G/H	1.35	1.36	1.42	1.33	1.38	1.35	1.33	1.41	1.43	1.12	1.26	1.73	1.38	0.88	0.91
1.25	0.90	H/I	0.30	0.27	0.29	0.49	0.42	0.41	0.52	0.52	0.43	0.90	0.31	0.38	0.78	0.52	0.48
3.00	2.21	I/J	1.55	1.64	1.56	1.43	1.45	1.38	1.44	1.40	1.39	1.17	1.50	1.24	1.22	2.21	2.17
1.80	1.30	J/K	1.02	0.94	1.02	1.01	1.05	1.07	1.09	1.09	1.12	1.30	0.98	1.25	1.30	0.45	0.47

MAX (plot)	MAX (calculated)	Axis	Oil-A1	Oil-A2	Oil-A3	Oil-B1	Oil-B2	Oil-B3	Oil-C1	Oil-C2	Oil-C3	Oil-D1	Oil-E1	Oil-F1	Oil-G1	Oil-H1	Oil-H2
2.00	1.50	K/L	1.22	1.27	1.23	1.24	1.23	1.14	1.11	1.12	1.17	1.03	1.25	1.50	1.00	1.42	1.39
1.50	1.00	L/M	0.77	0.76	0.76	0.78	0.77	0.82	0.79	0.79	0.80	0.78	0.79	0.62	0.77	0.91	0.91
1.50	1.07	M/N	1.02	0.99	1.01	1.07	1.04	1.01	1.05	1.02	0.96	1.02	1.02	0.99	1.05	0.73	0.73
0.50	0.23	N/O	0.13	0.12	0.12	0.11	0.12	0.15	0.13	0.14	0.13	0.15	0.14	0.15	0.13	0.19	0.23
7.00	6.13	O/P	2.11	2.33	2.39	2.31	2.22	1.89	2.05	2.06	2.13	1.86	2.15	2.08	2.14	5.87	4.79
6.00	4.79	P/Q	4.35	4.31	4.40	4.79	4.66	4.33	4.56	4.13	4.44	4.60	3.99	4.02	4.36	1.25	1.31
2.00	1.65	Q/R	1.13	1.18	1.11	1.15	1.15	1.15	1.65	1.09	1.14	1.06	1.20	1.02	1.10	1.03	1.01
0.30	0.16	R/S	0.11	0.10	0.10	0.09	0.10	0.12	0.09	0.12	0.11	0.13	0.11	0.13	0.11	0.14	0.16

MAX (plot)	MAX (calculated)	Axis	Oil-A1	Oil-A2	Oil-A3	Oil-B1	Oil-B2	Oil-B3	Oil-C1	Oil-C2	Oil-C3	Oil-D1	Oil-E1	Oil-F1	Oil-G1	Oil-H1	Oil-H2
4.20	3.61	S/T	3.05	3.41	3.45	3.36	3.17	2.65	2.83	2.79	2.94	2.47	3.05	2.88	2.92	3.49	3.15
3.50	2.99	T/U	2.58	2.52	2.53	2.80	2.71	2.56	2.59	2.52	2.63	2.81	2.58	2.36	2.57	2.76	2.86
1.60	1.36	U/V	1.33	1.31	1.30	1.21	1.24	1.28	1.22	1.32	1.25	1.30	1.21	1.36	1.26	0.89	0.89
1.50	1.12	V/W	1.04	1.12	1.07	1.09	1.03	1.01	0.98	0.88	0.97	0.80	1.09	0.88	0.80	0.86	0.85
2.50	2.00	W/X	1.59	1.46	1.50	1.37	1.51	1.62	1.47	1.74	1.47	1.96	1.48	1.61	2.00	1.39	1.49
1.50	1.20	X/Y	1.15	1.17	1.03	1.14	1.13	1.17	1.12	1.14	1.06	1.09	1.06	1.20	1.11	0.88	0.84
2.00	1.48	Y/Z	0.82	0.90	1.08	1.03	1.11	0.94	0.98	0.91	1.00	1.02	1.02	0.91	0.98	1.48	1.35
4.00	3.31	C/Z	2.63	2.85	2.89	3.31	3.22	2.68	2.50	2.25	2.10	2.39	2.82	2.43	2.50	2.85	2.79

Table 4.5: Ratios of the peaks "C" through "Z"; normalized

MRSD-1	MAX	MIN	AVERAGE	Well	Oil-A1	Oil-A2	Oil-A3	Oil-B1	Oil-B2	Oil-B3	Oil-C1	Oil-C2	Oil-C3	Oil-D1	Oil-E1	Oil-F1	Oil-G1	Oil-H1	Oil-H2
E/F	0.82	0.18	0.43	E/F	0.79	0.82	0.75	0.43	0.46	0.51	0.37	0.34	0.37	0.18	0.69	0.57	0.22	0.26	0.27
D/E	0.73	0.50	0.59	D/E	0.54	0.55	0.53	0.62	0.56	0.54	0.54	0.53	0.59	0.50	0.52	0.52	0.52	0.71	0.72
C/D	0.73	0.53	0.61	C/D	0.60	0.59	0.60	0.66	0.58	0.56	0.57	0.56	0.55	0.53	0.61	0.56	0.57	0.73	0.70
J/K	0.72	0.25	0.52	J/K	0.57	0.52	0.57	0.56	0.58	0.60	0.61	0.61	0.62	0.72	0.54	0.69	0.72	0.25	0.26
I/J	0.74	0.39	0.53	I/J	0.52	0.55	0.52	0.48	0.48	0.46	0.48	0.47	0.46	0.39	0.50	0.41	0.41	0.74	0.72
H/I	0.72	0.22	0.37	H/I	0.24	0.22	0.23	0.39	0.34	0.33	0.41	0.41	0.35	0.72	0.25	0.30	0.62	0.41	0.38
G/H	0.69	0.35	0.50	G/H	0.54	0.54	0.57	0.53	0.55	0.54	0.53	0.56	0.57	0.45	0.50	0.69	0.55	0.35	0.37
F/G	0.74	0.23	0.41	F/G	0.24	0.24	0.23	0.26	0.29	0.29	0.31	0.32	0.31	0.49	0.29	0.23	0.38	0.65	0.65

MRSD-2	MAX	MIN	AVERAGE	Well	Oil-A1	Oil-A2	Oil-A3	Oil-B1	Oil-B2	Oil-B3	Oil-C1	Oil-C2	Oil-C3	Oil-D1	Oil-E1	Oil-F1	Oil-G1	Oil-H1	Oil-H2
M/N	0.71	0.48	0.63	M/N	0.68	0.66	0.67	0.71	0.69	0.67	0.70	0.68	0.64	0.68	0.68	0.66	0.70	0.48	0.49
L/M	0.67	0.41	0.55	L/M	0.52	0.51	0.51	0.52	0.52	0.54	0.52	0.53	0.53	0.52	0.53	0.41	0.51	0.61	0.61
K/L	0.75	0.50	0.62	K/L	0.61	0.64	0.61	0.62	0.62	0.57	0.56	0.56	0.58	0.51	0.63	0.75	0.50	0.71	0.69
R/S	0.54	0.28	0.41	R/S	0.37	0.33	0.34	0.31	0.33	0.41	0.28	0.41	0.36	0.43	0.36	0.45	0.38	0.47	0.54
Q/R	0.83	0.50	0.56	Q/R	0.57	0.59	0.55	0.58	0.57	0.57	0.83	0.55	0.57	0.53	0.60	0.51	0.55	0.52	0.50
P/Q	0.80	0.21	0.59	P/Q	0.72	0.72	0.73	0.80	0.78	0.72	0.76	0.69	0.74	0.77	0.67	0.67	0.73	0.21	0.22
O/P	0.88	0.27	0.44	O/P	0.30	0.33	0.34	0.33	0.32	0.27	0.29	0.29	0.30	0.27	0.31	0.30	0.31	0.84	0.68
N/O	0.45	0.22	0.30	N/O	0.26	0.25	0.24	0.22	0.24	0.30	0.26	0.29	0.27	0.30	0.29	0.29	0.27	0.37	0.45

MRSD-3	MAX	MIN	AVERAGE	Well	Oil-A1	Oil-A2	Oil-A3	Oil-B1	Oil-B2	Oil-B3	Oil-C1	Oil-C2	Oil-C3	Oil-D1	Oil-E1	Oil-F1	Oil-G1	Oil-H1	Oil-H2
U/V	0.85	0.56	0.74	U/V	0.83	0.82	0.81	0.76	0.78	0.80	0.76	0.83	0.78	0.81	0.75	0.85	0.79	0.56	0.56
T/U	0.85	0.67	0.76	T/U	0.74	0.72	0.72	0.80	0.78	0.73	0.74	0.72	0.75	0.80	0.74	0.67	0.74	0.79	0.82
S/T	0.86	0.59	0.74	S/T	0.73	0.81	0.82	0.80	0.75	0.63	0.67	0.66	0.70	0.59	0.73	0.69	0.70	0.83	0.75
C/Z	0.83	0.53	0.67	C/Z	0.66	0.71	0.72	0.83	0.81	0.67	0.63	0.56	0.53	0.60	0.71	0.61	0.63	0.71	0.70
Y/Z	0.74	0.41	0.55	Y/Z	0.41	0.45	0.54	0.51	0.56	0.47	0.49	0.45	0.50	0.51	0.51	0.45	0.49	0.74	0.68
X/Y	0.80	0.56	0.70	X/Y	0.77	0.78	0.68	0.76	0.75	0.78	0.75	0.76	0.71	0.72	0.71	0.80	0.74	0.59	0.56
W/X	0.80	0.52	0.62	W/X	0.63	0.59	0.60	0.55	0.60	0.65	0.59	0.69	0.59	0.78	0.59	0.64	0.80	0.56	0.60
V/W	0.74	0.53	0.63	V/W	0.69	0.74	0.71	0.73	0.69	0.67	0.65	0.59	0.65	0.53	0.73	0.59	0.53	0.58	0.56

Figures 4.50 a, b, and c depict MRSD-1, MRSD-2, and MRSD-3, respectively, for all oils. Since it is somewhat hard to distinguish individual oils in Figures 4.50 a, b, and c, the star diagrams are divided into four subgroups as follows:

1. Figures 4.51 a, b, and c depict MRSD-1, MRSD-2, and MRSD-3 of oils from field A contrasted with the two oils from field H.
2. Figures 4.52 a, b, and c depict MRSD-1, MRSD-2, and MRSD-3 of oils from field B contrasted with the two oils from field H.
3. Figures 4.53 a, b, and c depict MRSD-1, MRSD-2, and MRSD-3 of oils from field C contrasted with the two oils from field H.
4. Figures 4.54 a, b, and c depict MRSD-1, MRSD-2, and MRSD-3 of the Paleozoic oils from fields D, E, and G as well as the Paleozoic condensate from field F, contrasted with the two Jurassic oils from field H.

Figure 4.51a depicts MRSD-1 of field A oils and shows the close grouping among field A oils, and their extreme differences from field H oils. This differentiation is in line with the differences in source rock between the two fields (source rock of field "A" is Paleozoic shale while that of field "H" is Jurassic carbonate). Figure 4.51b depicts MRSD-2 of field A oils and also shows differences between these oils and field H oils. MRSD-3 of field A oils is

depicted in Figure 4.51c and shows that all three field A oils follow the same pattern except for a slight deviation by oil A3 at ratios "X/Y" and "Y/Z".

Figures 4.52a, b, and c depict MRSD-1, MRSD-2, and MRSD-3, respectively, of field B oils. These three figures show that these three oils also follow well-defined patterns on the star diagrams. However, oil B3 behaves somewhat differently on the "N/O", "O/P", and "R/S" axes of MRSD-2 and the "C/Z" axis of MRSD-3. These small differences in behavior are not considered significant in view of their overall similarity on the star diagrams.

Figures 4.53a, b, and c depict MRSD-1, MRSD-2, and MRSD-3 of oils from field C. The three oils fall in a very tight envelope on MRSD-1 and a somewhat looser envelope on MRSD-3. On MRSD-2, however, oil C1 shows a gross difference on the "Q/R" axis and a slightly less significant deviation on the "R/S" axis. These differences are probably due to slight intra-reservoir variations.

Of the remaining oils from fields D, E, F, and G, one can see that there are gross differences between these oils. However, oils D1 and G1 do follow similar paths on the three MRSDs suggesting a strong similarity between these two oils. Figures 4.54a, b, and c display the tightness of the envelope containing oils D1 and G1 and the difference between these two oils and oils E1 and F1.

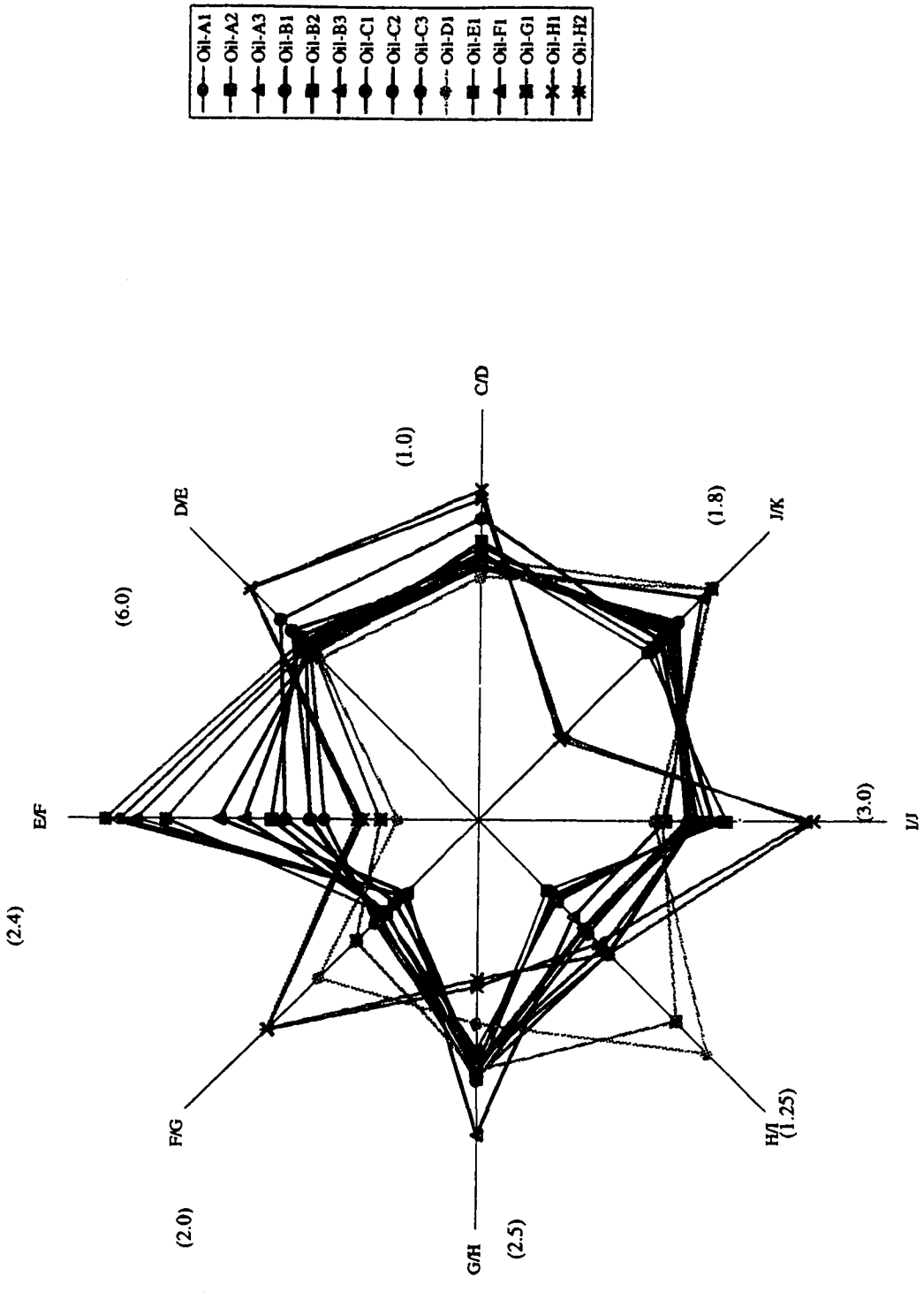

Figure 4.50 a. MRSD-1 of all oils included in the study.

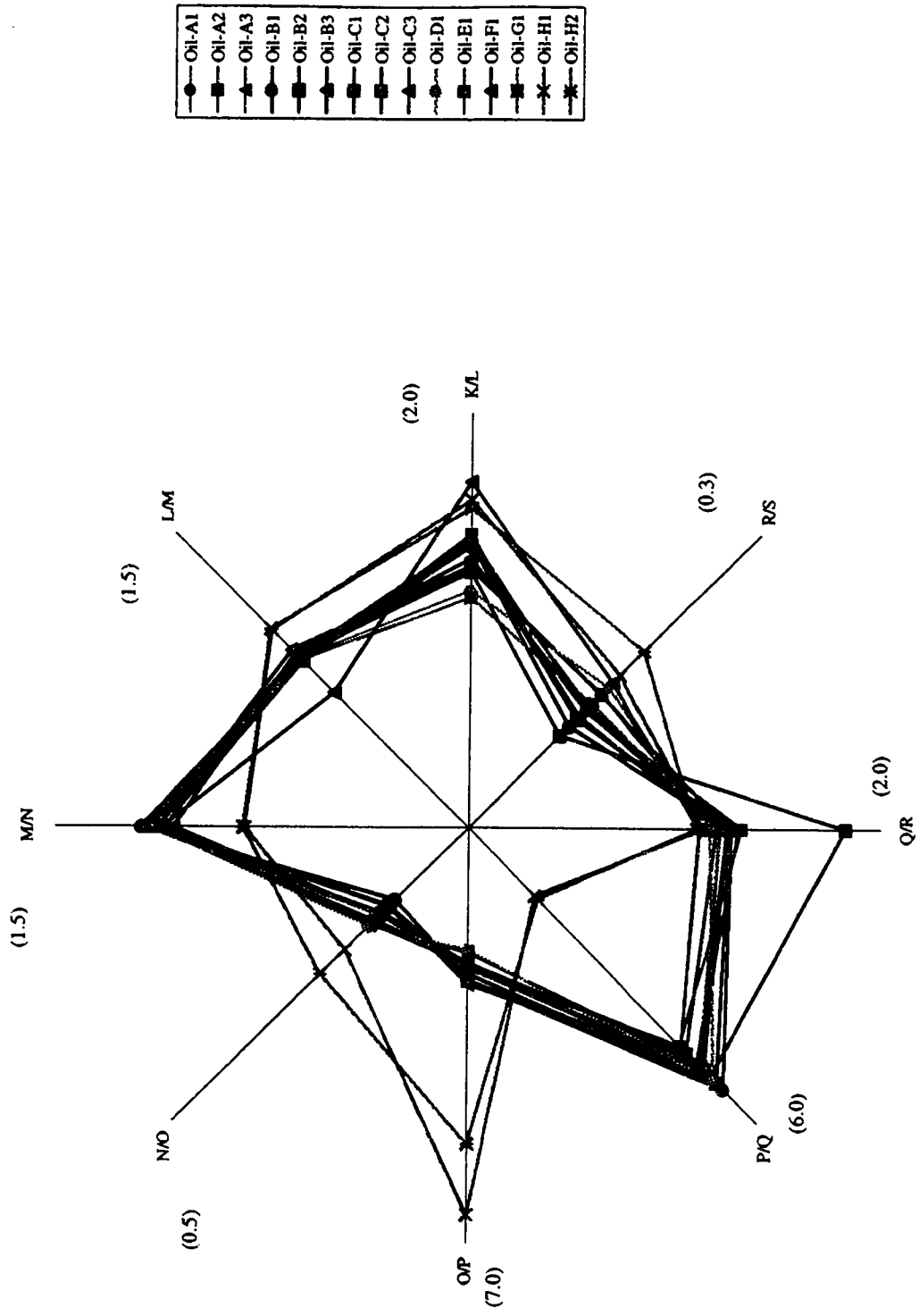

Figure 4.50 b. MRSD-2 of all oils included in the study.

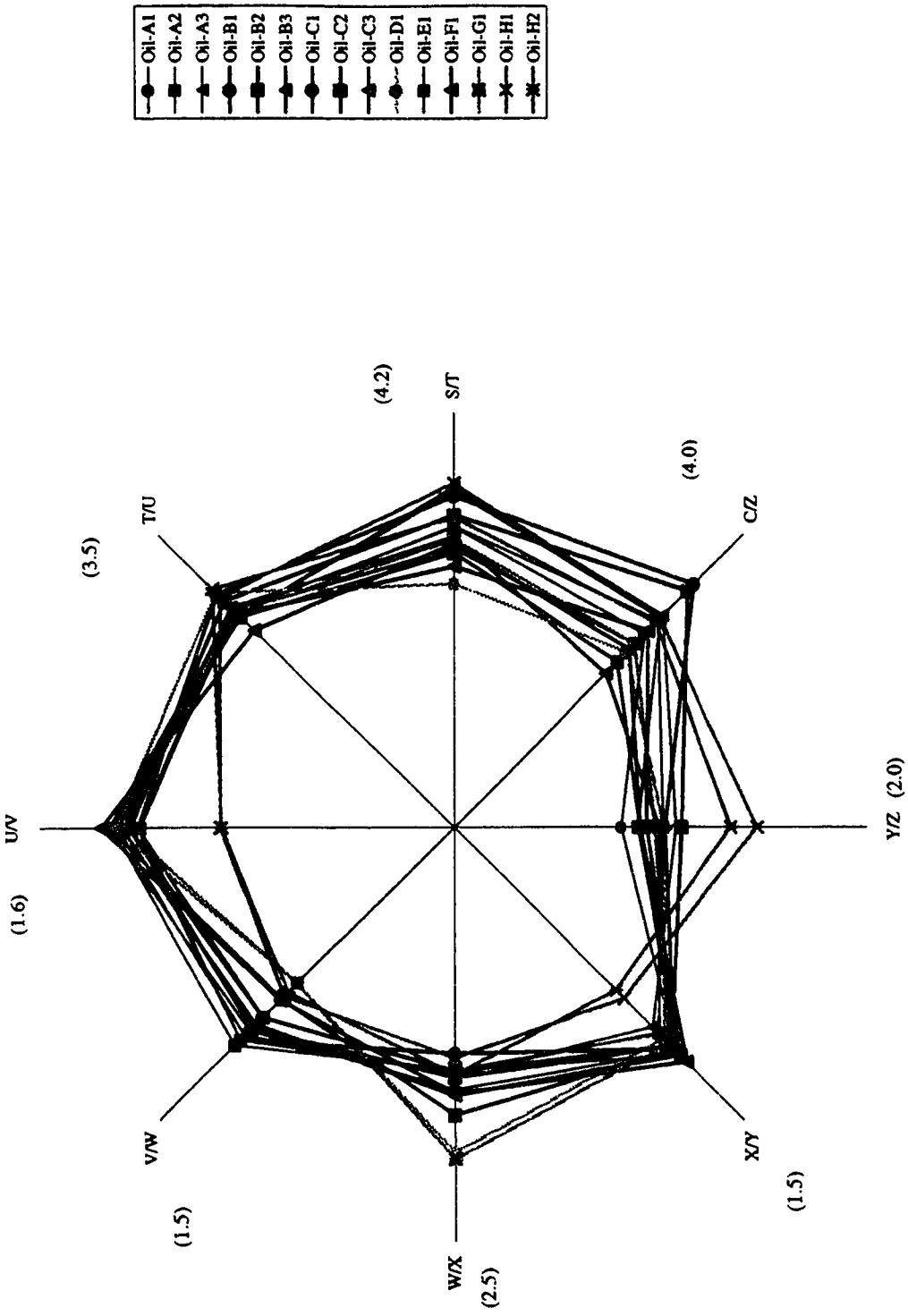

Figure 4.50 c. MRSD-3 of all oils included in the study.

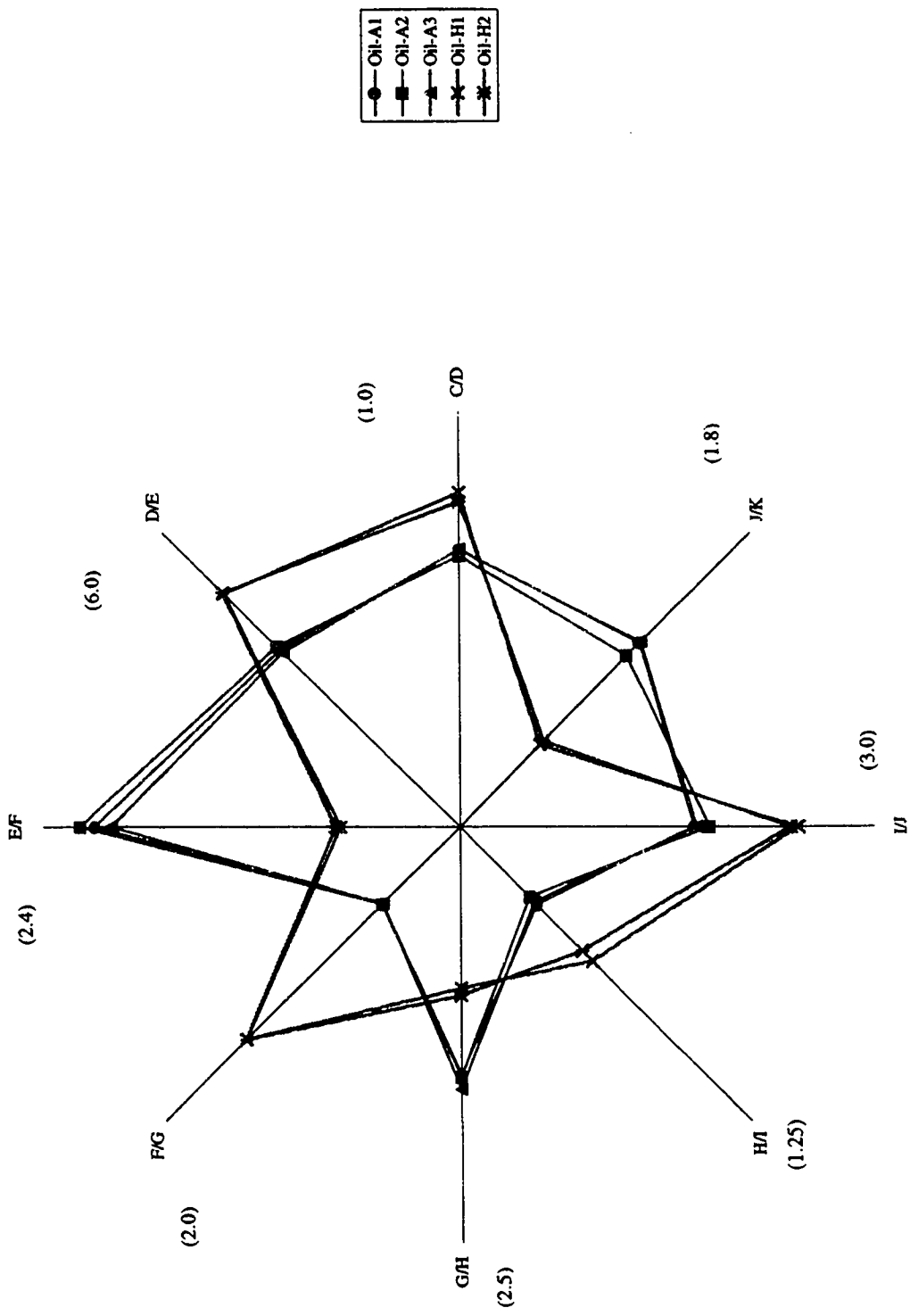

Figure 4.51 a. MRSD-1 of field A oils contrasted with field H oils.

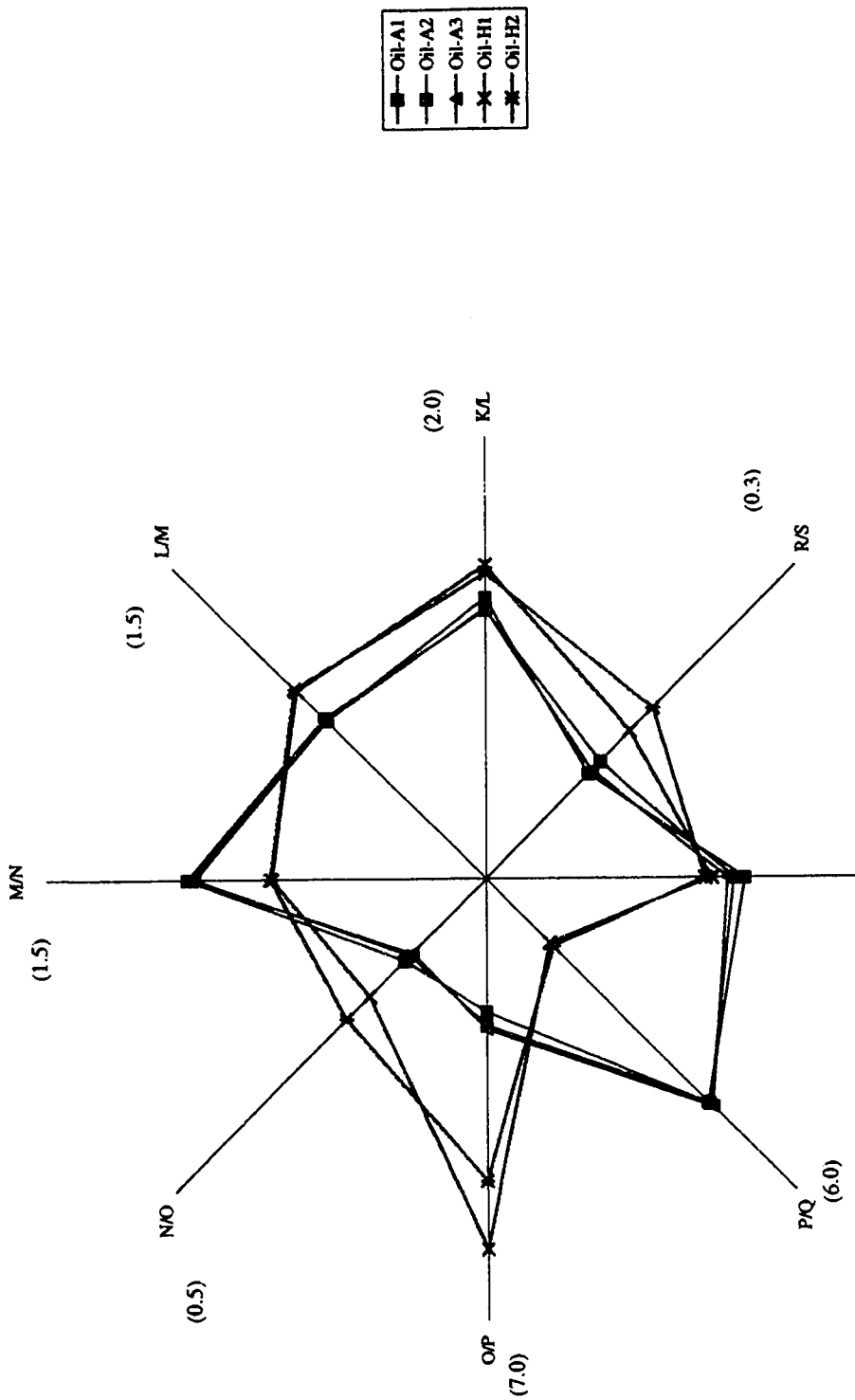

Figure 4.51 b. MRSD-2 of field A oils contrasted with field H oils.

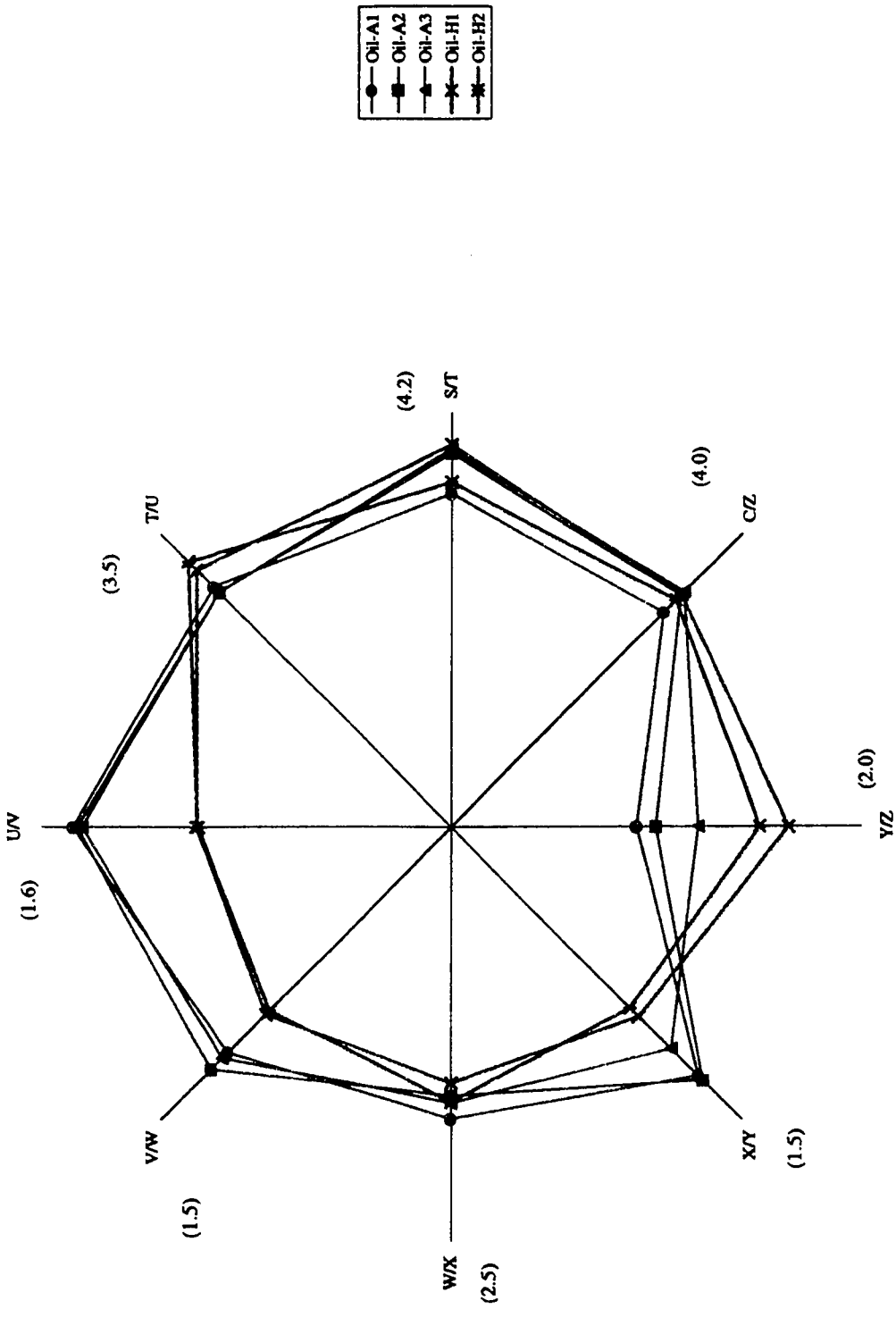

Figure 4.51 c. MRSD-3 of field A oils contrasted with field H oils.

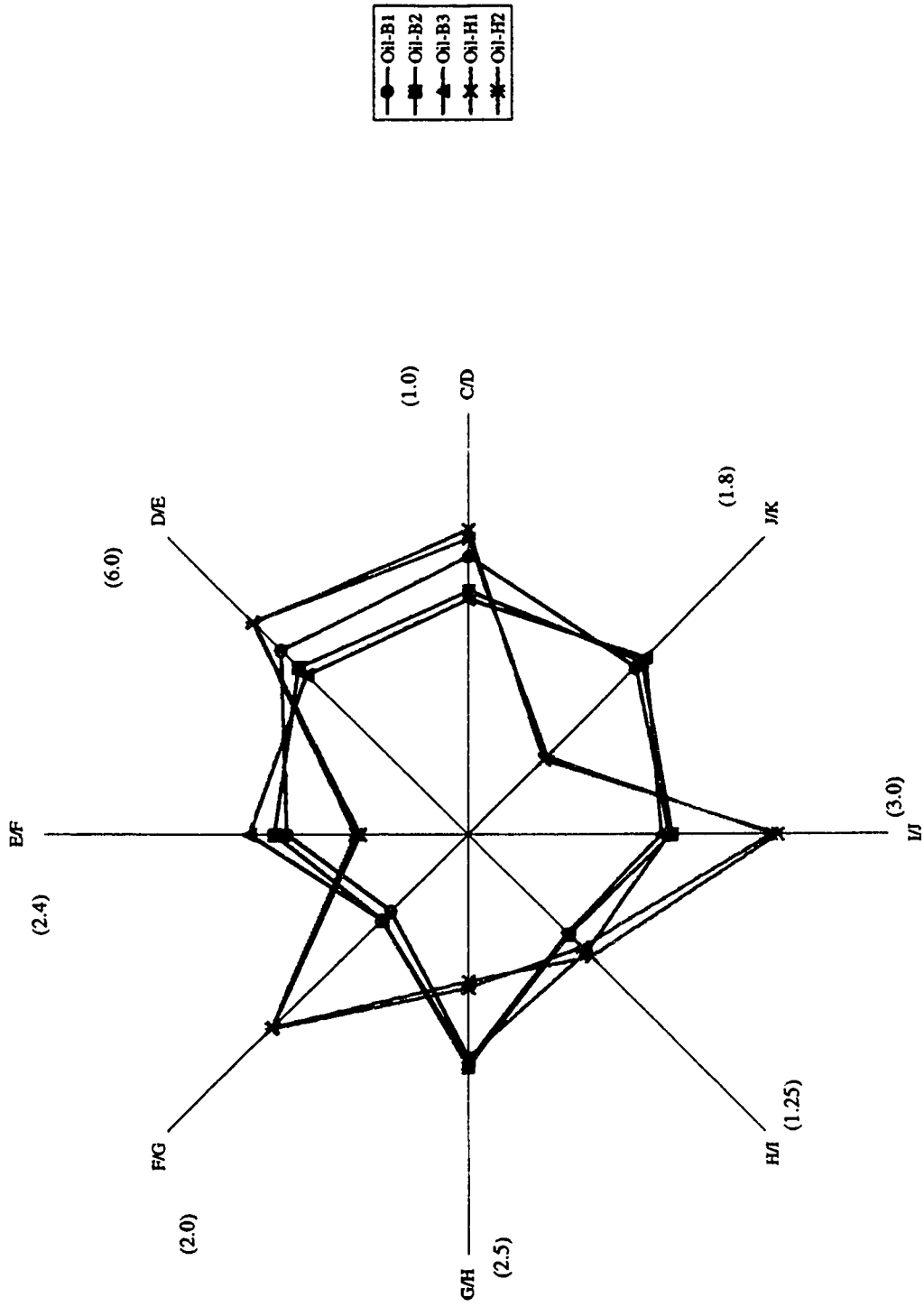

Figure 4.52 a. MRSD-1 of field B oils contrasted with field H oils.

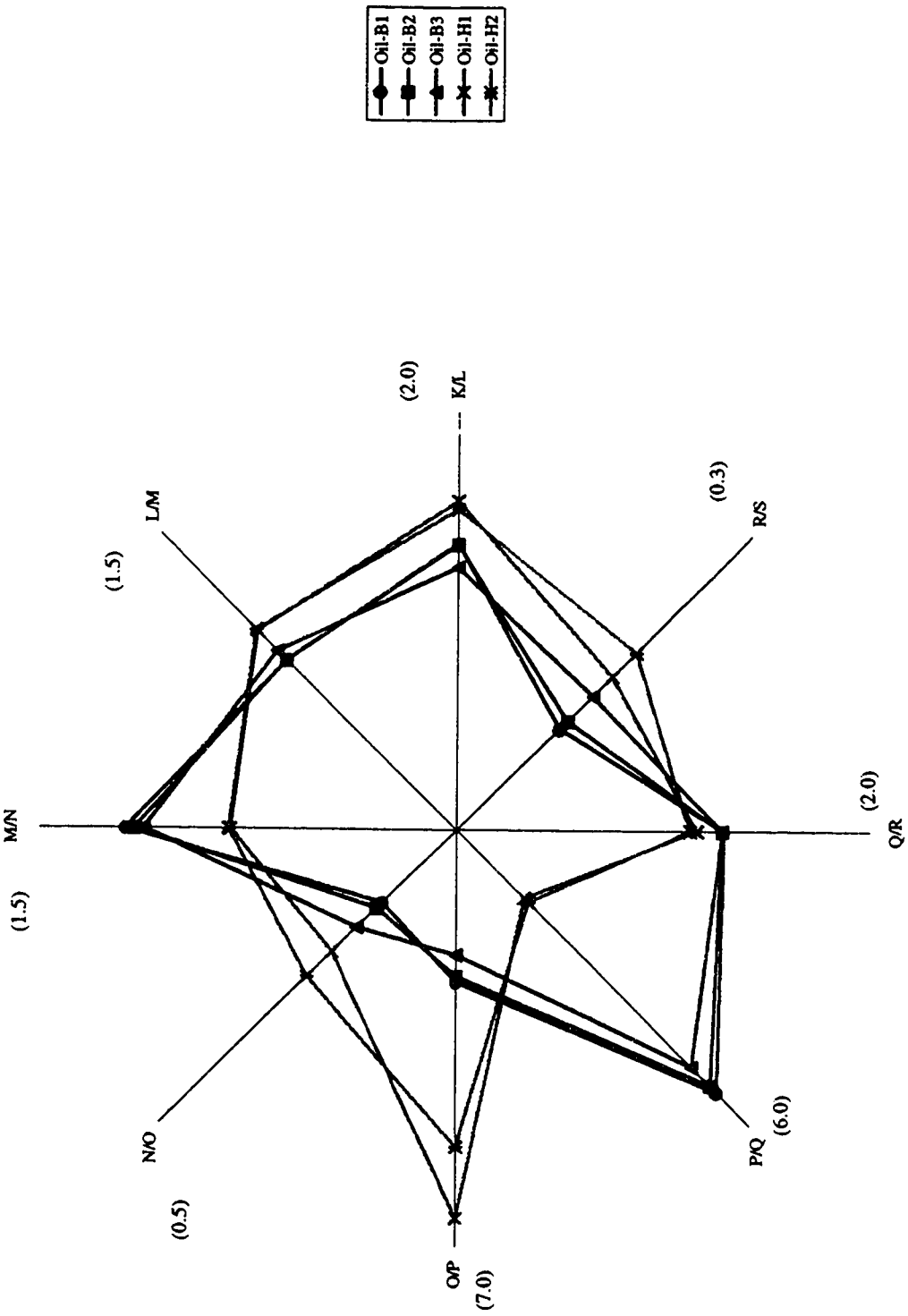

Figure 4.52 h. MRSD-2 of field B oils contrasted with field H oils.

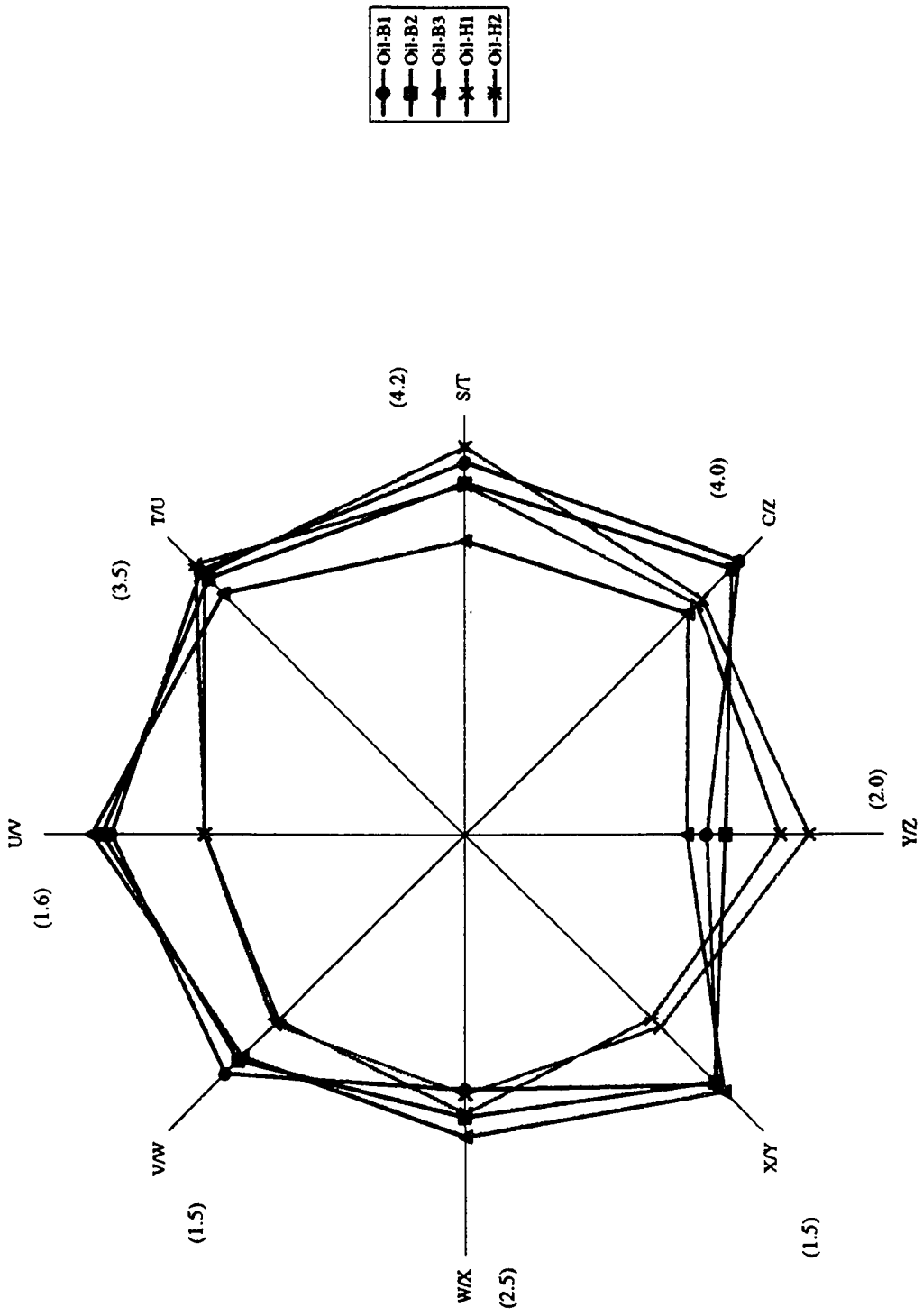

Figure 4.52 c. MRSD-3 of field B oils contrasted with field H oils.

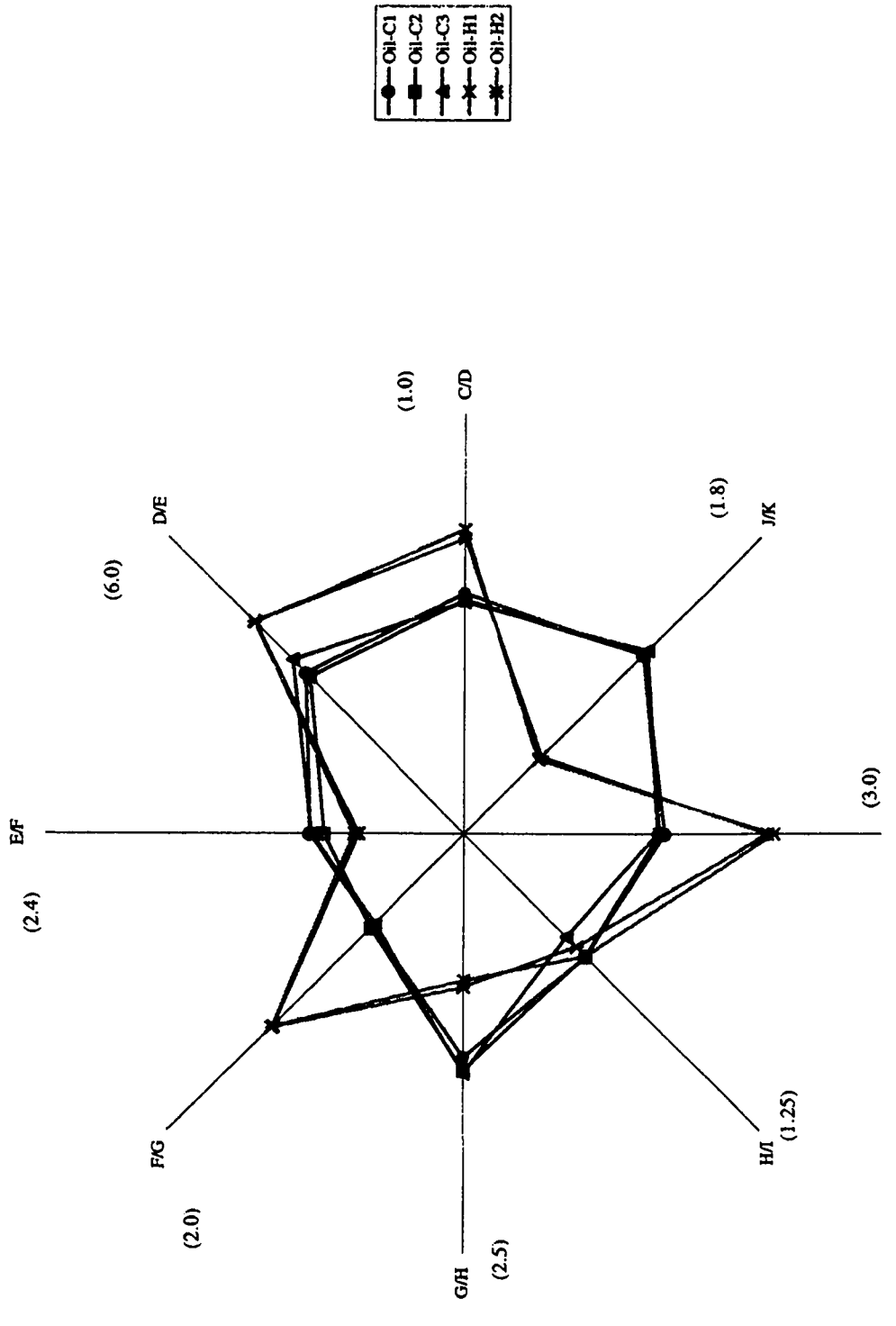

Figure 4.53 a. MRSD-1 of field C oils contrasted with field H oils.

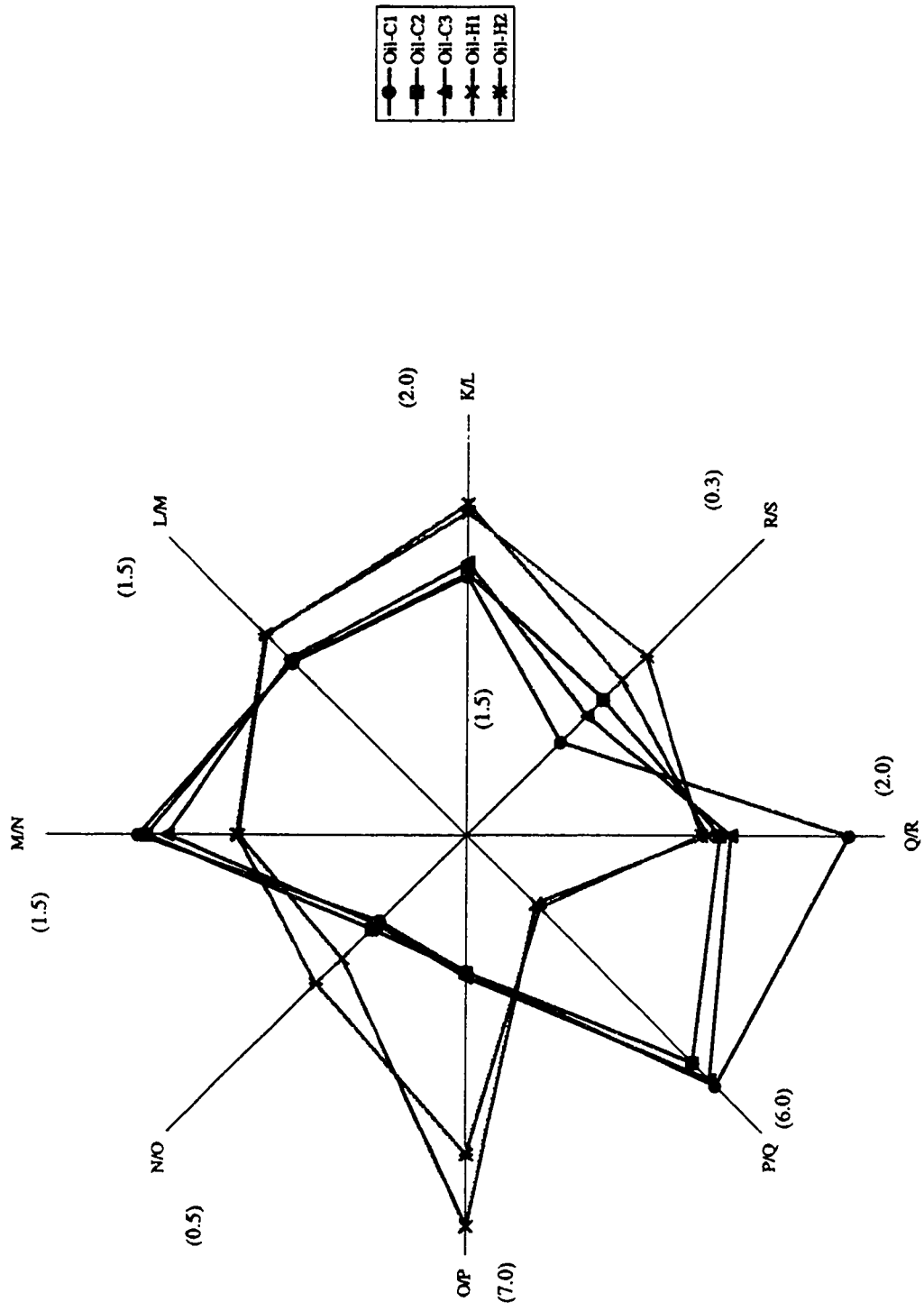

Figure 4.53 b. MRSD-2 of field C oils contrasted with field H oils.

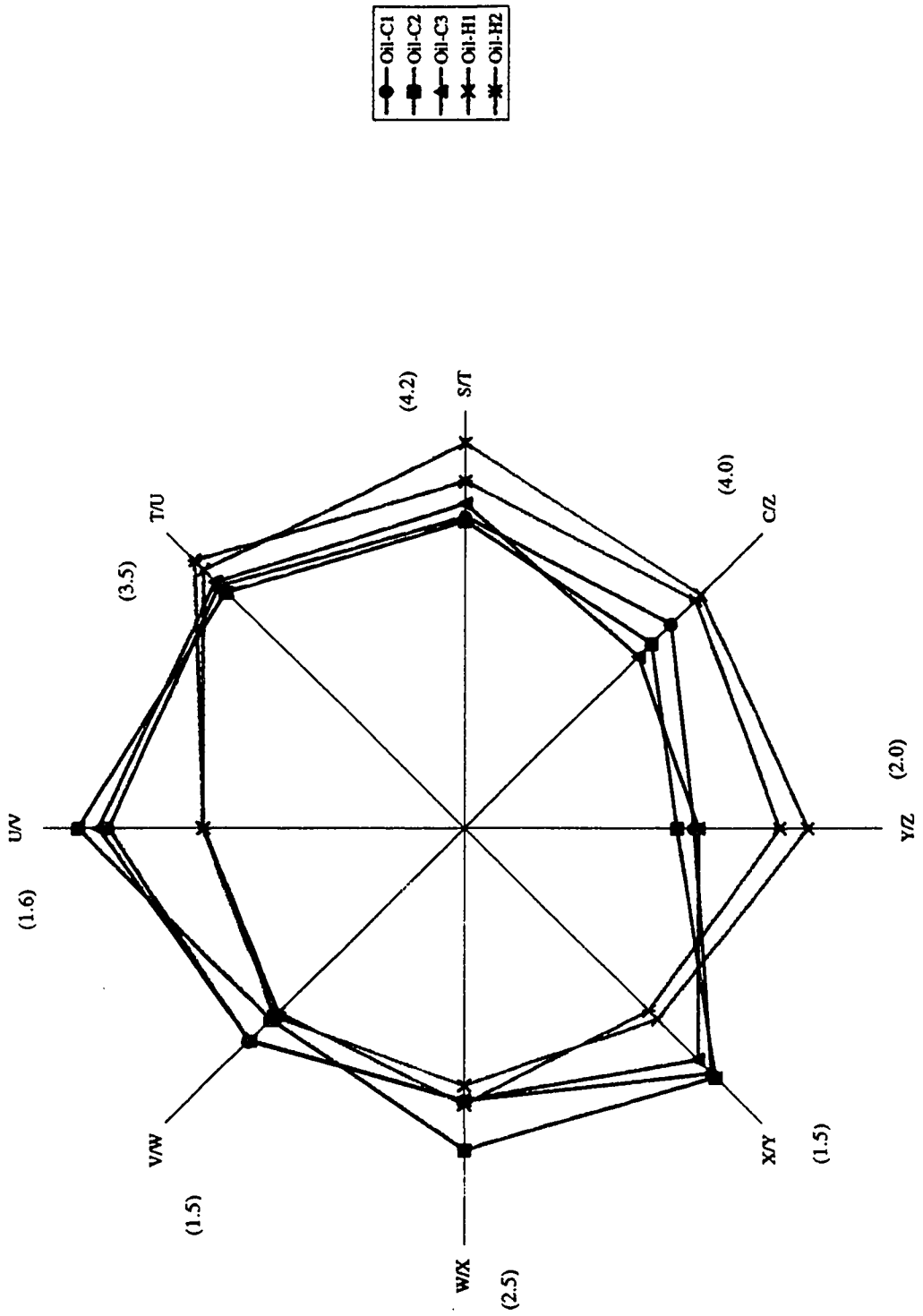

Figure 4.53 c. MRSD-3 of field C oils contrasted with field H oils.

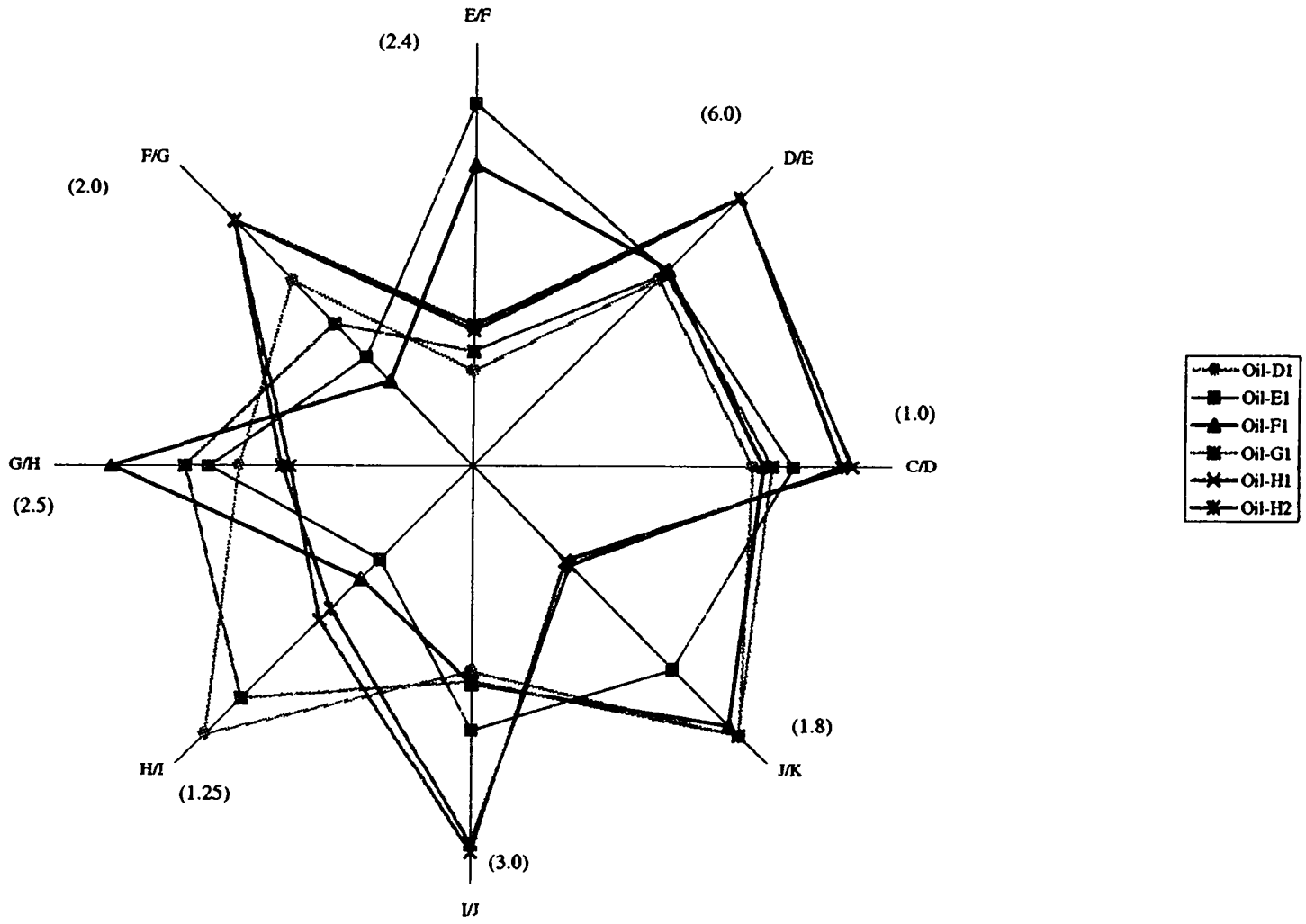

Figure 4.54 a. MRSD-1 of oils from fields D, E, F, and G contrasted with field H oils.

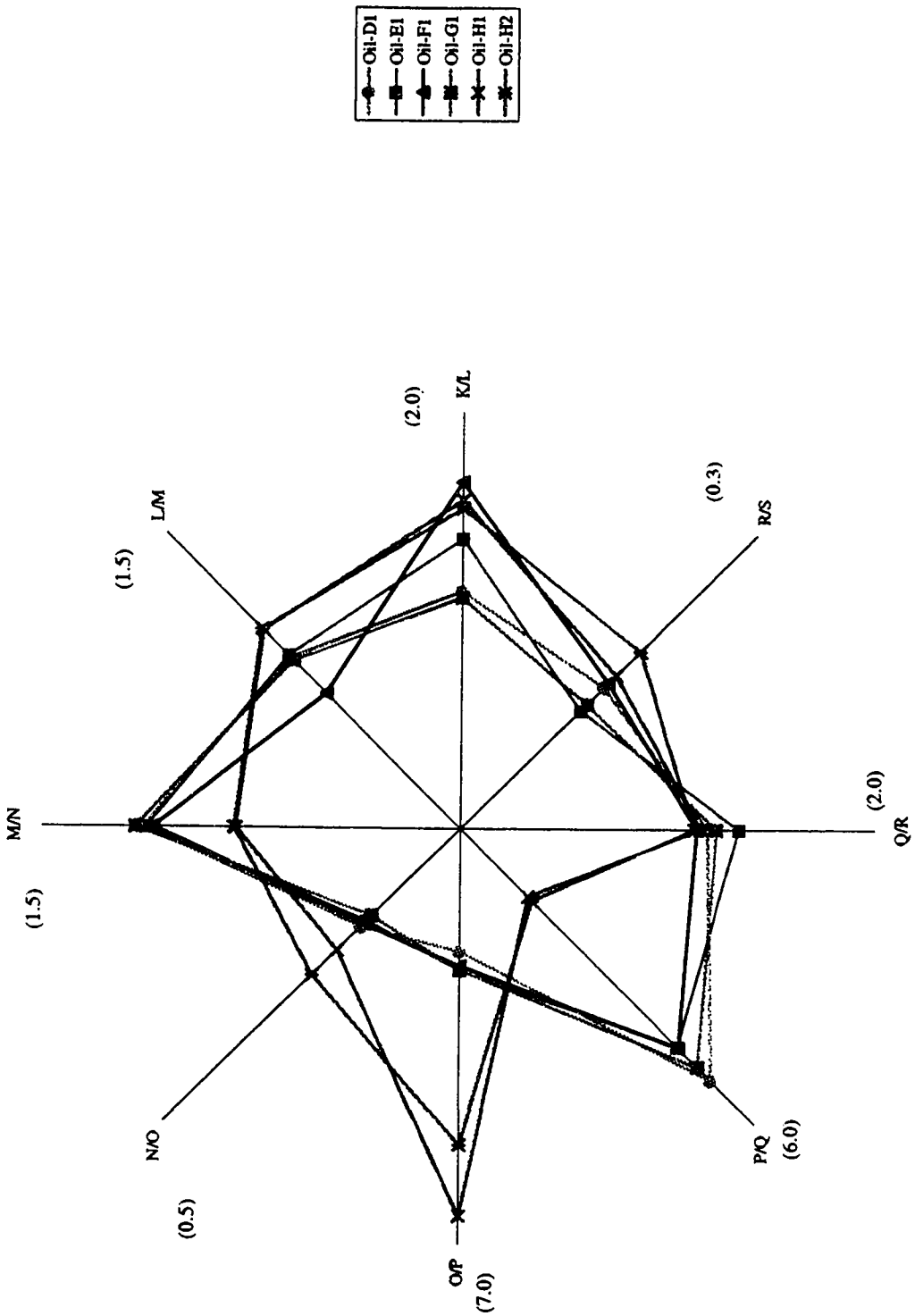

Figure 4.54 b. MRSD-2 of oils from fields D, E, F, and G contrasted with field H oils.

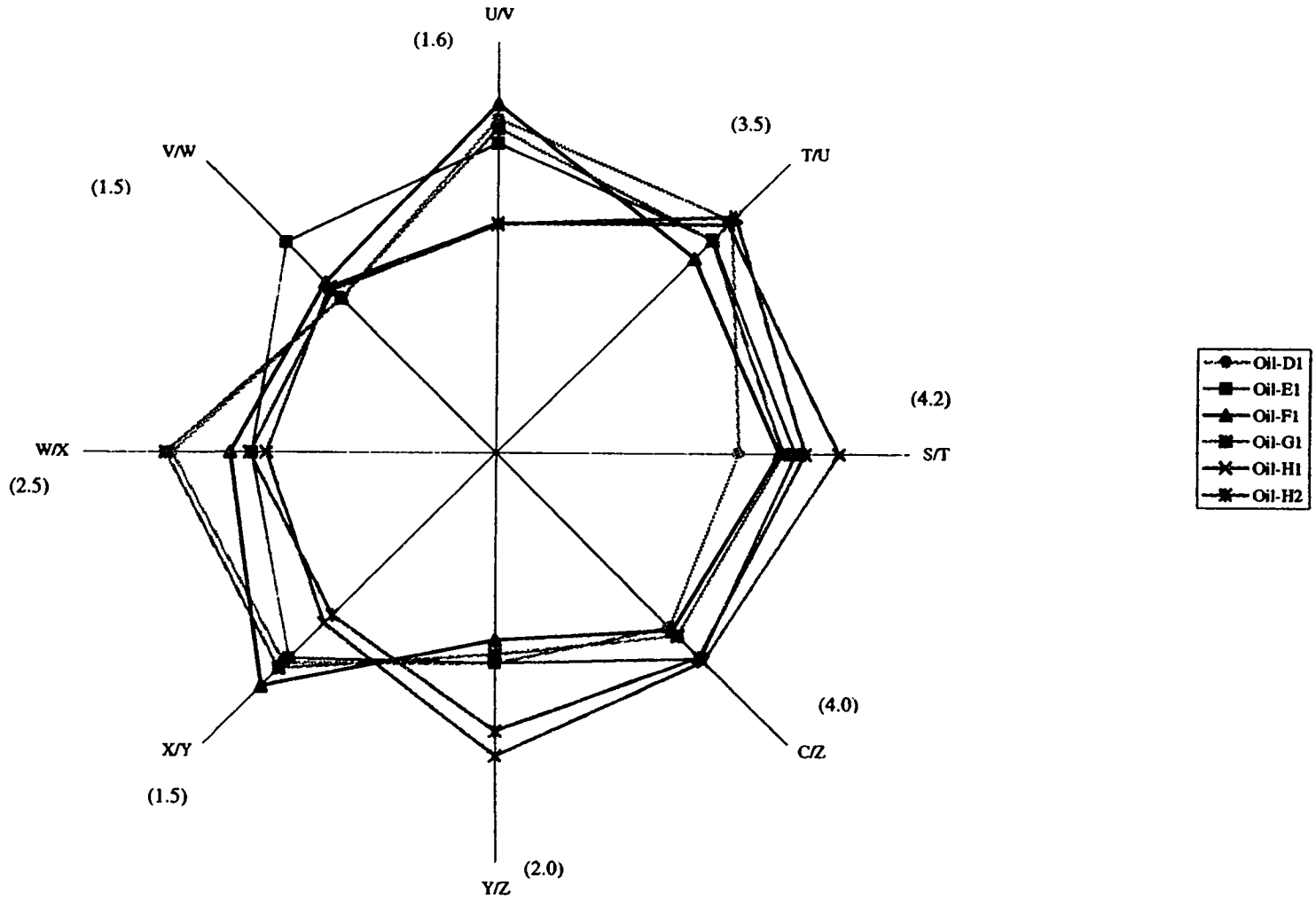

Figure 4.54 c. MRSD-3 of oils from fields D, E, F, and G contrasted with field H oils.

If one looks at the overall picture in its three parts depicted in Figures 4.50a, b, and c, one can see that oil E1 follows the same general patterns followed by oils from field A, and oil F1 is somewhat close, in its pattern, to oils from field B.

Figures 4.35b through 4.49b, which show the n-C_{15} to n-C_{22} compounds, contain the commonly studied peaks of n-C_{17} (peak "O"), pristane (peak "P"), n-C_{18} (peak "S"), and phytane (peak "T"). A plot can be constructed using ratios of (pristane/n-C_{17}) and (phytane /n-C_{18}). Figure 4.55 is such a plot. This type of plot offers a maturity scale in which maturity increases towards the origin of the plot for oils which have previously been determined to consist of a single family. This maturity trend is due to the fact that the abundance of both pristane and phytane, relative to n-C_{17} and n-C_{18}, respectively, decrease with increasing maturity. From Figure 4.55, one can see that oil D1 is the least mature amongst the Paleozoic fluids.

The pristane/phytane ratio for each of the Paleozoic fluids is noticeably greater than one, while the same ratio for the Eastern Province oils is less than one. This indicates that the environment of deposition for source rocks of Central Arabian fluids is dysoxic (Pr/Ph > 1) while that for source rocks of the Eastern Arabian oils is a reducing environment (Pr/Ph < 1).

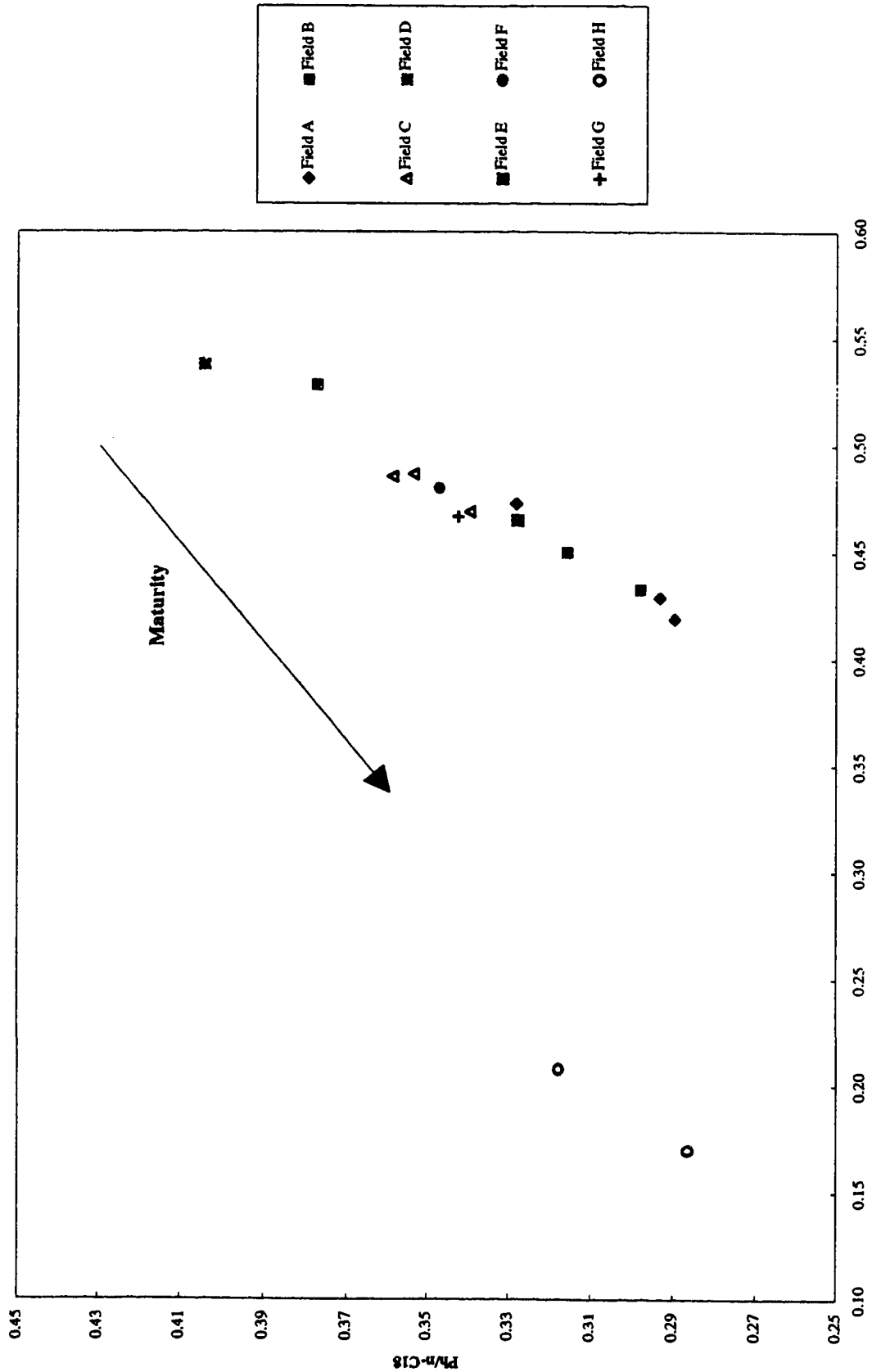

Figure 4.55. (Pristane/n-C17) *vs* . (Phytane /n-C18) for all oils included in the

4.4 GAS CHROMATOGRAPHY - MASS SPECTROMETRY (GC/MS)

4.4.1 THE SATURATE FRACTION

Hopanes and steranes are the two biomarker classes most commonly studied in the saturate fraction of crude oils. However, because of the advanced maturity of the Central Arabian oils and condensate considered in this study, they do not contain hopanes or steranes useful for correlation in concentrations large enough to enable us to detect them on the GCMS. Figures 4.56 through 4.59 (Appendix D) depict the GCMS fragmentograms of the saturate fractions of selected Central Arabian oils. Part (a) of each figure depicts the m/z 191 (hopanes) fragmentogram and part (b) depicts the m/z 217 (steranes) fragmentogram. The hopanes appear to be either completely absent or, if present, are in trace amounts in all Central Arabian oils and condensate included in this study. Steranes, however, are present to some extent in some oils and are absent from others as seen in the figures. This situation did not permit using these biomarkers for any correlation studies. High signal-to-noise ratios in some of the fragmentograms may be contributing to the obstruction of these biomarkers.

Figure 4.60a depicts the m/z 191 (hopanes) GCMS fragmentogram of oil H1 (Jurassic from Eastern Province) and Figure 4.60b depicts the m/z 217 (steranes) GCMS fragmentogram of the same oil. Figures 4.60a and 4.60b

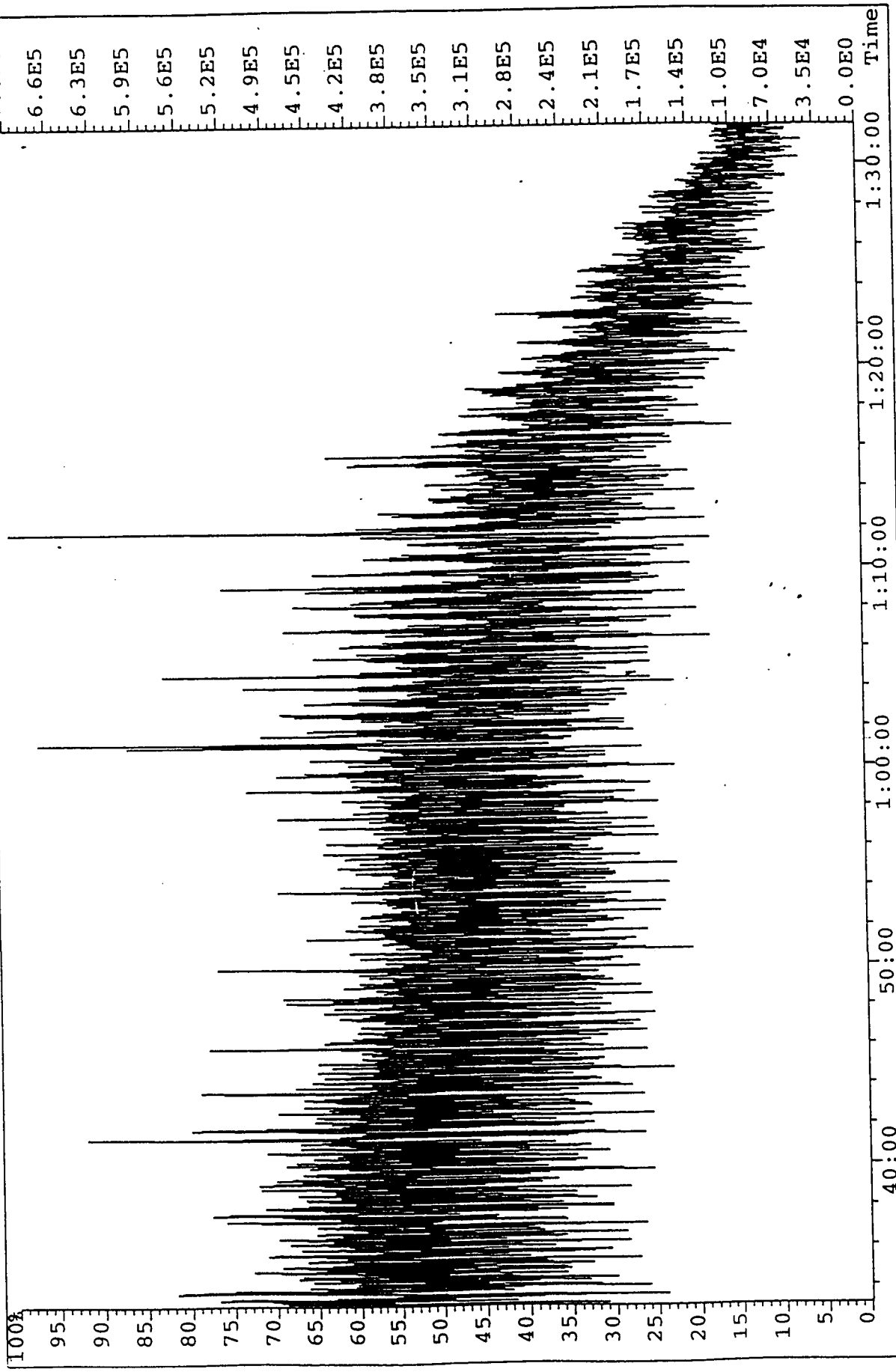

Figure 4.56 a. GCMS chromatogram (m/z 191) of the saturate fraction of oil A1.

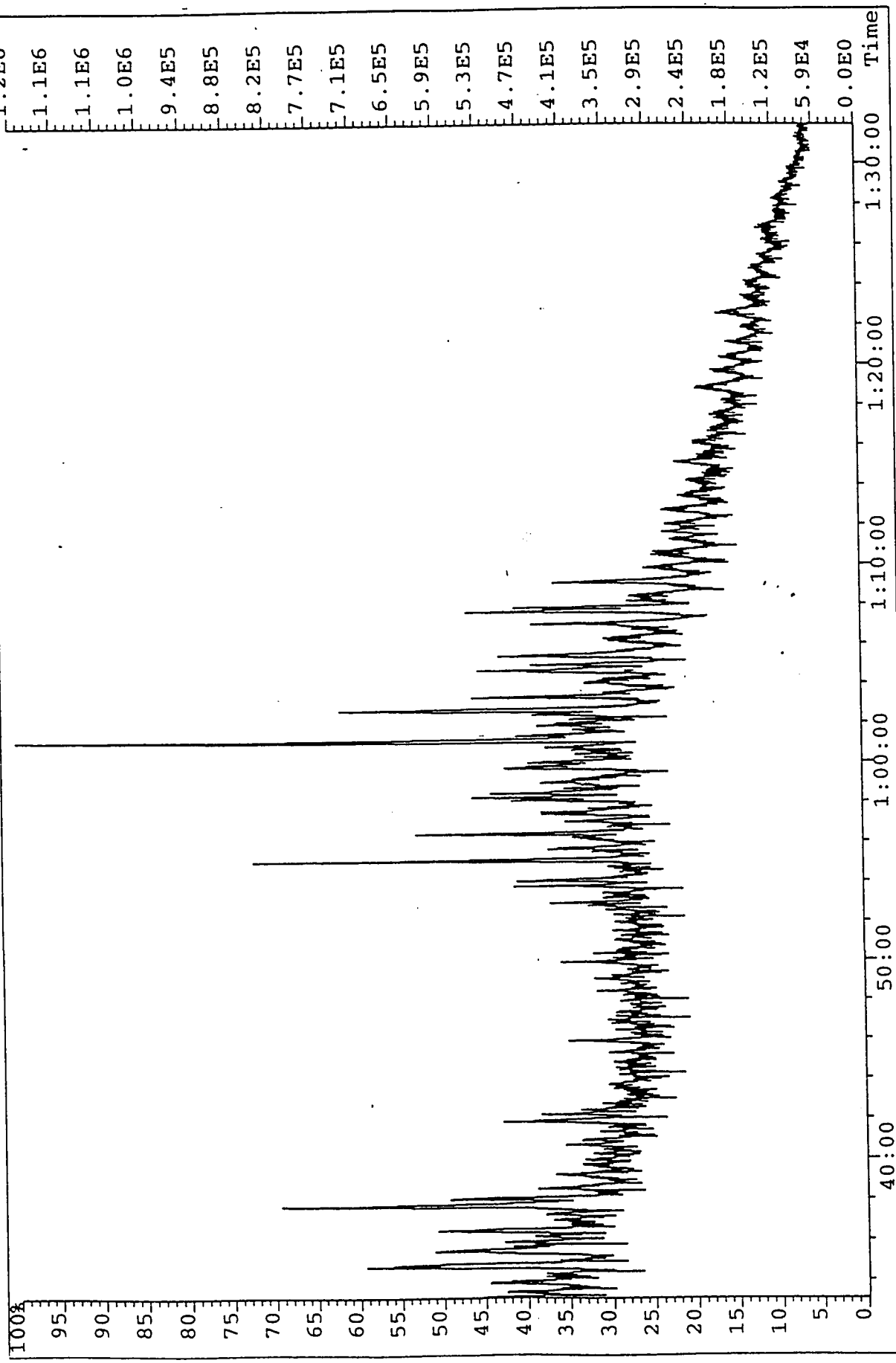

Figure 4.56 b. GCMS chromatogram (m/z 217) of the saturate fraction of oil A1.

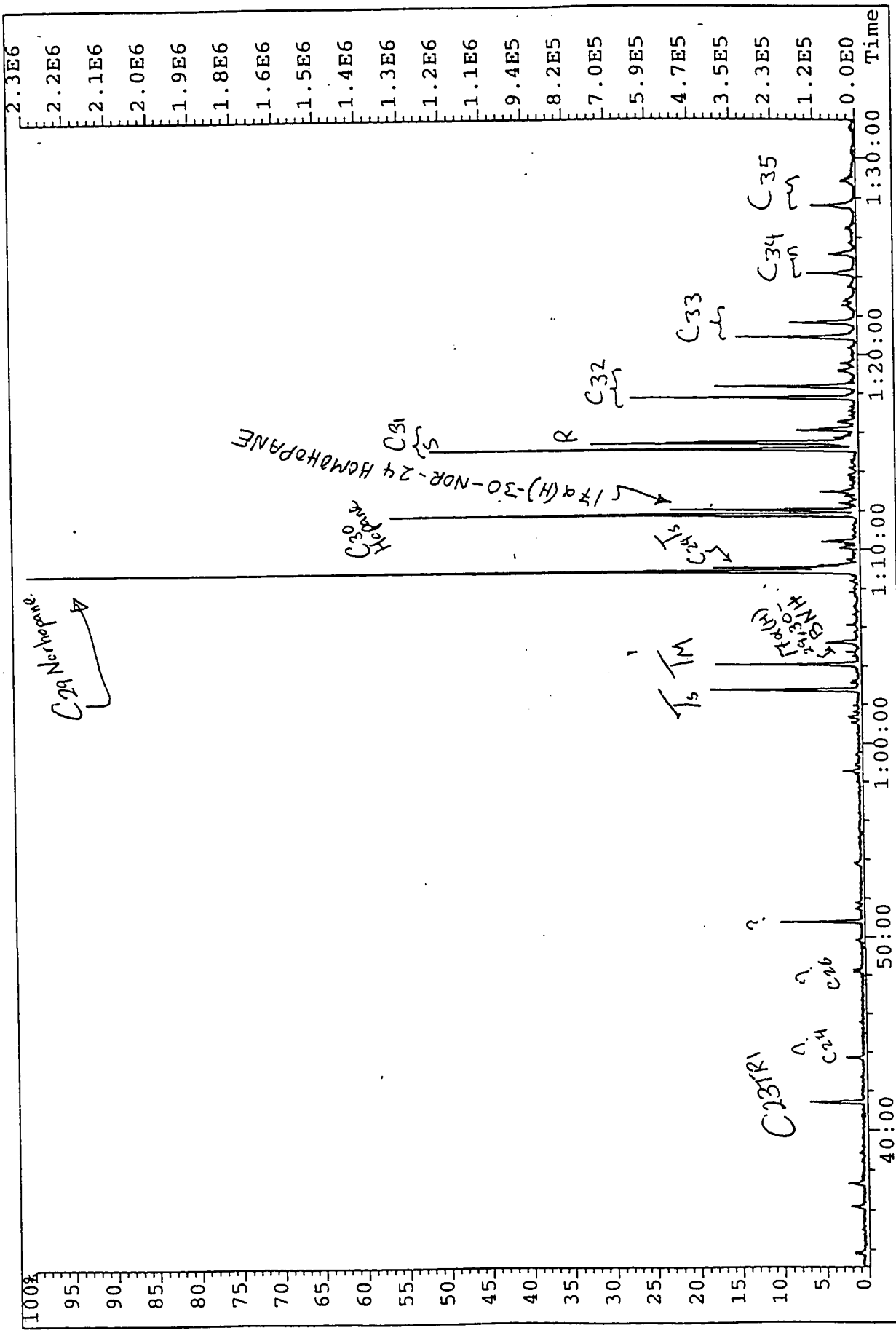

Figure 4.60 a. GCMS chromatogram (m/z 191) of the saturate fraction of oil H1.

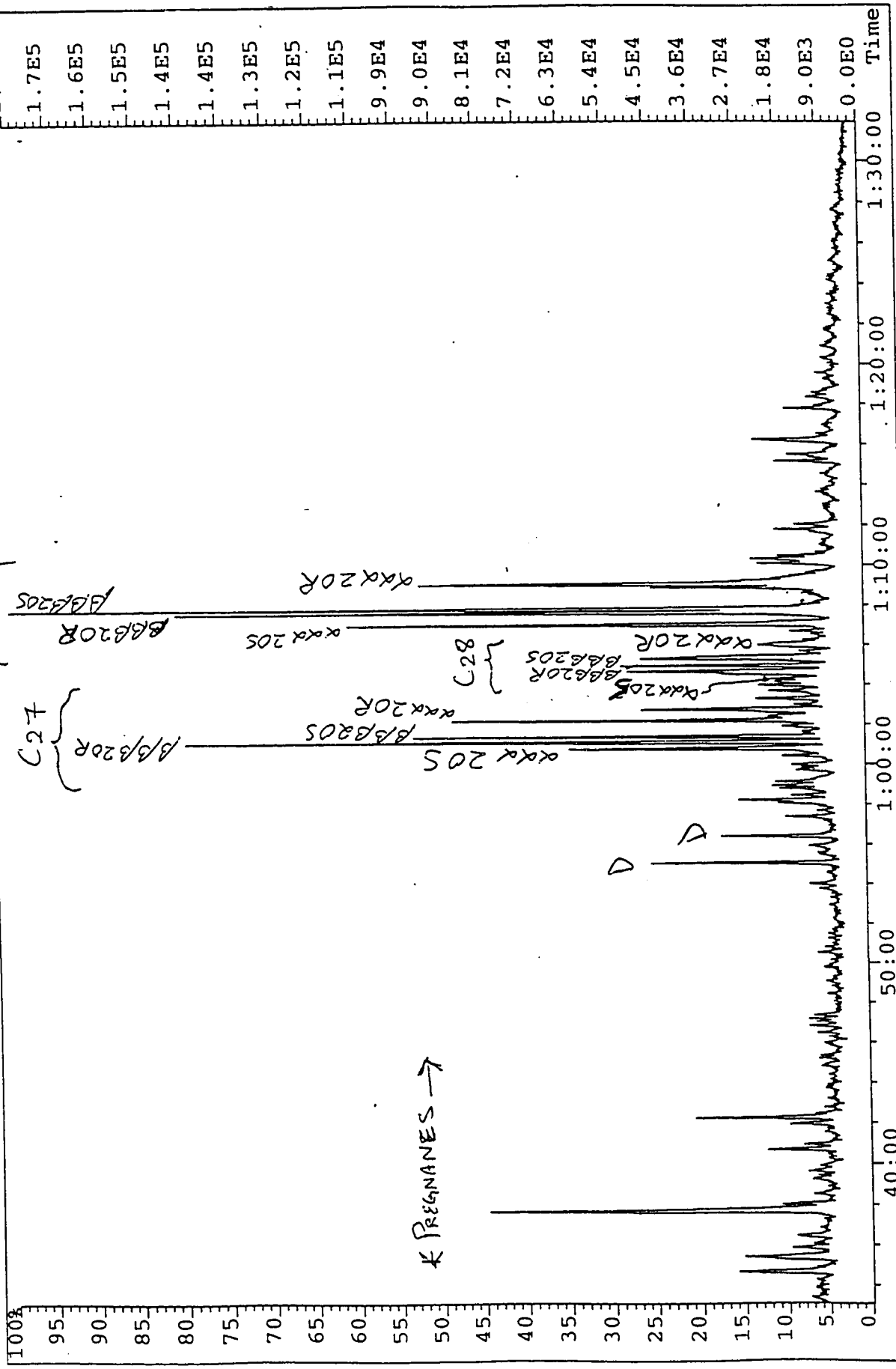

Figure 4.60 b. GCMS chromatogram (m/z 217) of the saturate fraction of oil H1.

provide the keys to m/z 191 and m/z 217 fragmentograms. It is clear from Figures 4.60a and 4.60b that oil H1 contains high enough concentrations of both hopanes and steranes to allow identification of individual biomarkers, which is not the case for the Paleozoic oils and condensate.

4.4.2 THE AROMATIC FRACTION

Due to the lack of the conventionally applied biomarkers (hopanes and steranes) in the Central Arabian oils and condensate, it was decided to look for unconventional biomarkers in the aromatic fraction. Phenanthrene and its methylated isomers are amongst the promising compounds that one may find in the aromatic fraction of crude oils. The diagnostic ion for phenanthrene is m/z 178 and that for the methylated isomers is m/z 192.

Figures 4.61 through 4.75 (Appendix E) depict the GCMS fragmentograms of the aromatic fraction of all oils included in the present study. Part (a) of each figure shows m/z 178 and part (b) shows m/z 192. Part (a) of each figure shows a single major peak, which is that of phenanthrene. Part (b) of each figure shows four major peaks which are, in order of increasing elution time, those of 3-MP, 2-MP, 9-MP, and 1-MP. Figures 4.61a and 4.61b provide the keys to m/z 178 and m/z 192 fragmentograms. Table 4.6 lists the abundances of phenanthrene and these compounds in all oils included in this

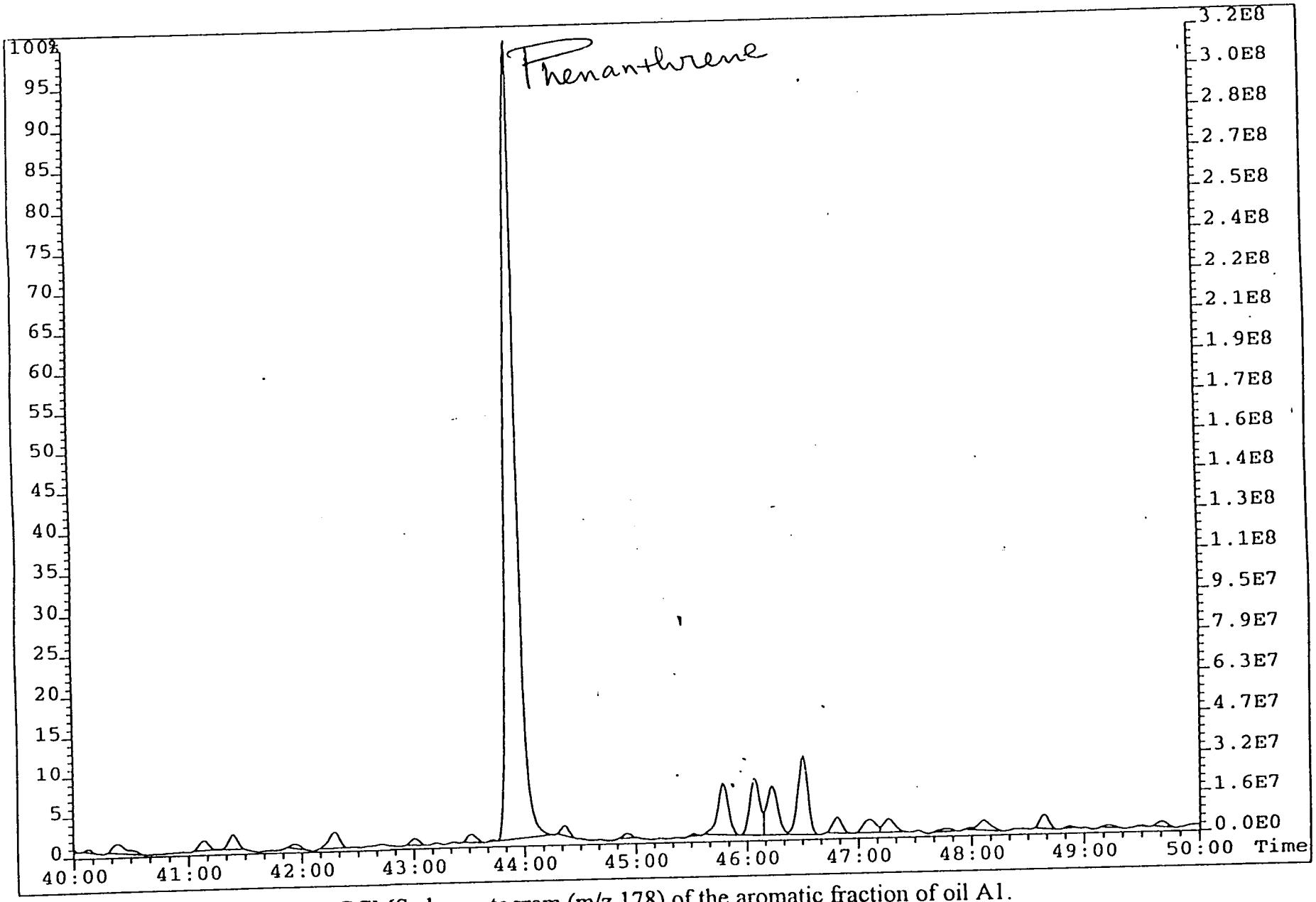

Figure 4.61 a. GCMS chromatogram (m/z 178) of the aromatic fraction of oil A1.

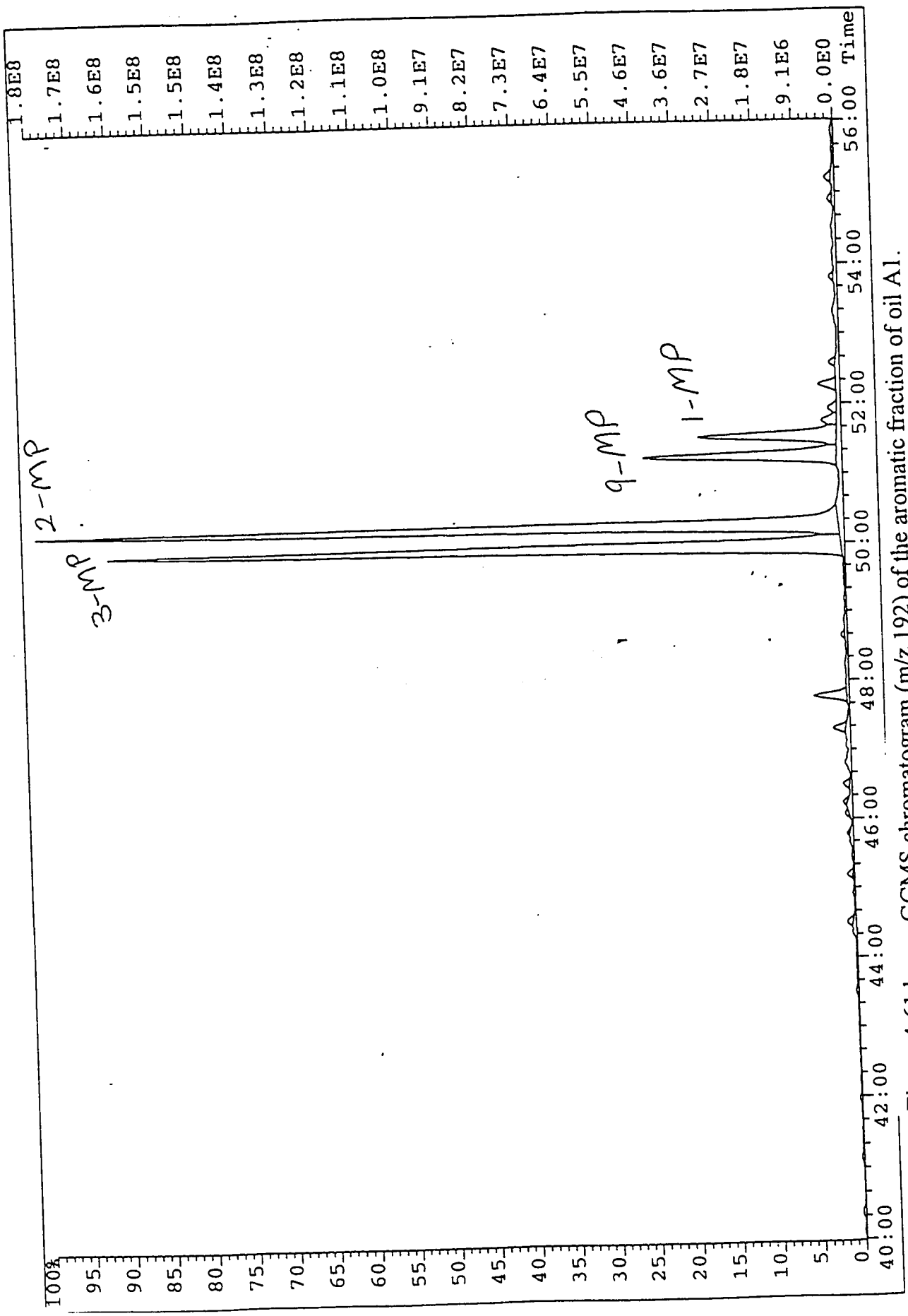

Figure 4.61 b. GCMS chromatogram (m/z 192) of the aromatic fraction of oil A1.

Table 4.6: Abundances of phenanthrene and its methylated isomers in all oils included in the study

Sample Code	Phen*	3-MePhen*	2-MePhen*	9-MePhen*	1-MePhen	MPI 1	MPR	R_c (for 0.65% ≤ R_m ≤ 1.35%)	R_c (for 1.35% < R_m ≤ 2.00%)
Oil-A1	2.17E+09	1.65E+09	1.18E+09	3.10E+08	2.24E+08	1.57	5.25	N. A.@	1.36
Oil-A2	2.29E+08	1.34E+08	1.58E+08	3.70E+07	2.73E+07	1.49	5.79	N. A.@	1.41
Oil-A3	3.77E+08	2.38E+08	3.26E+08	5.77E+07	6.11E+07	1.71	5.33	N. A.@	1.28
Oil-B1	2.32E+07	1.69E+07	2.32E+07	1.09E+07	1.17E+07	1.31	1.99	1.19	N. A.@
Oil-B2	3.82E+08	2.61E+08	3.75E+08	1.59E+08	1.85E+08	1.32	2.03	1.19	N. A.@
Oil-B3	3.62E+07	3.32E+07	4.43E+07	2.11E+07	2.28E+07	1.45	1.94	1.27	N. A.@
Oil-C1	2.03E+08	8.30E+07	9.51E+07	9.29E+07	5.24E+07	0.77	1.82	0.86	N. A.@
Oil-C2	7.74E+07	4.44E+07	6.01E+07	3.24E+07	3.35E+07	1.09	1.79	1.06	N. A.@
Oil-C3	4.39E+07	2.48E+07	3.27E+07	1.66E+07	1.73E+07	1.11	1.89	1.07	N. A.@
Oil-D1	1.11E+07	5.57E+06	8.54E+06	1.10E+07	1.05E+07	0.65	0.81	0.79	N. A.@
Oil-E1	4.57E+07	2.98E+07	4.06E+07	1.43E+07	1.43E+07	1.42	2.84	N. A.@	1.45
Oil-F1	4.31E+08	2.58E+08	3.79E+08	7.27E+07	9.80E+07	1.59	3.87	N. A.@	1.35
Oil-G1	2.72E+07	1.71E+07	2.40E+07	2.37E+07	2.33E+07	0.83	1.03	0.90	N. A.@
Oil-H1	5.57E+06	1.73E+06	2.99E+06	5.88E+06	3.94E+06	0.46	0.76	0.68	N. A.@
Oil-H2	1.91E+06	7.27E+05	1.11E+06	2.74E+06	1.54E+06	0.45	0.72	0.67	N. A.@

* Data is based on absolute areas from the GCMS results.
@ N. A. = Not Applicable
MPI 1 = {1.5*[2-MP]+[3-MP]}/{[P]+ [1-MP] + [9-MP]}
MPI 2 = {3*[2-MP]}/{[P]+ [1-MP] + [9-MP]}
Rc (for 0.65% ≤ Rm ≤ 1.35%) = 0.60 MPI 1 + 0.40
Rc (for 1.35% < Rm ≤ 2.00%) = -0.60 MPI 1 + 2.30
MPR = [2-MP]/[1-MP]

study. The values in the table are based on area integration of each peak. These abundances are then used to calculate various parameters that are reported in the literature, such as the maturity-sensitive Methylphenanthrene Index (MPI 1), which is used in the calculation of the "calculated reflectance", $\%R_C$. The Methylphenanthrene Ratio (MPR) is calculated from the ratio of the abundances of 2-MP to 1-MP and provides the criterion as to whether equation 2.1 or 2.2 should be used in calculating $\%R_C$. The criterion is that equation 2.1 should be used for samples with MPR values of less than 2.24 and equation 2.2 should be used for samples with MPR values of higher than 2.24 [44, 48, 54, 56].

These two equations are reprinted here:

$$R_c \text{ (for } 0.65 \leq R_m \leq 1.35) = 0.60 \text{ MPI 1} + 0.40 \qquad (2.1)$$

$$R_c \text{ (for } 1.35 < R_m \leq 2.00) = -0.60 \text{ MPI 1} + 2.30 \qquad (2.2).$$

Oils from field A (Central Arabia) have low gas/oil ratios (GOR) and MPR values that are greater than 2.24 (average = 5.46), thus equation 2.2 was used to determine their calculated vitrinite reflectance values ($\%R_C$). The $\%R_C$ values (average = 1.35%) of the three oils from field A indicate the $\%R_m$ value of the source rock at the time of generation, *i.e.*, the source rock was at the "late-post mature" stage of oil generation. Low GOR for such high gravity oils may be taken as an indication of water-washing since water-washing results in depleting

the gas in the oil phase and, in turn, depleting the gas cap present over the oil *via* a dissolution phenomenon [57].

The $\%R_C$ of these oils are on the high end of oil generation; this may be an artificial elevation resulting from water-washing, not true maturity. Water-washing may deplete phenanthrene concentration to a greater extent than it depletes the concentration of methylphenanthrenes, thus altering the outcome of the equation, *c.f.* Figure 4.76.

Since aqueous solubility data for phenanthrene and methylphenanthrenes are not available, I reached the above conclusion (about increased solubility of phenanthrene relative to methylphenanthrenes) from solubility trends of benzene, toluene, and dimethylbenzene, which decrease by about an order of magnitude with each addition of a methyl group [14].

Oils from field B (Central Arabia) have low GOR and MPR values that are less than 2.24 (average = 1.99) meaning that equation 2.1 should be used for the calculations of $\%R_c$. The calculated $\%R_C$ values have an average of 1.22%. Taking these values to correspond to the $\%R_m$ value of the source rock at the time of generation, means that the source rock was in the "late mature" stage of oil generation. Since this is also a low GOR field, the $\%R_C$ values obtained may again be an artifact of water-washing rather than real maturity.

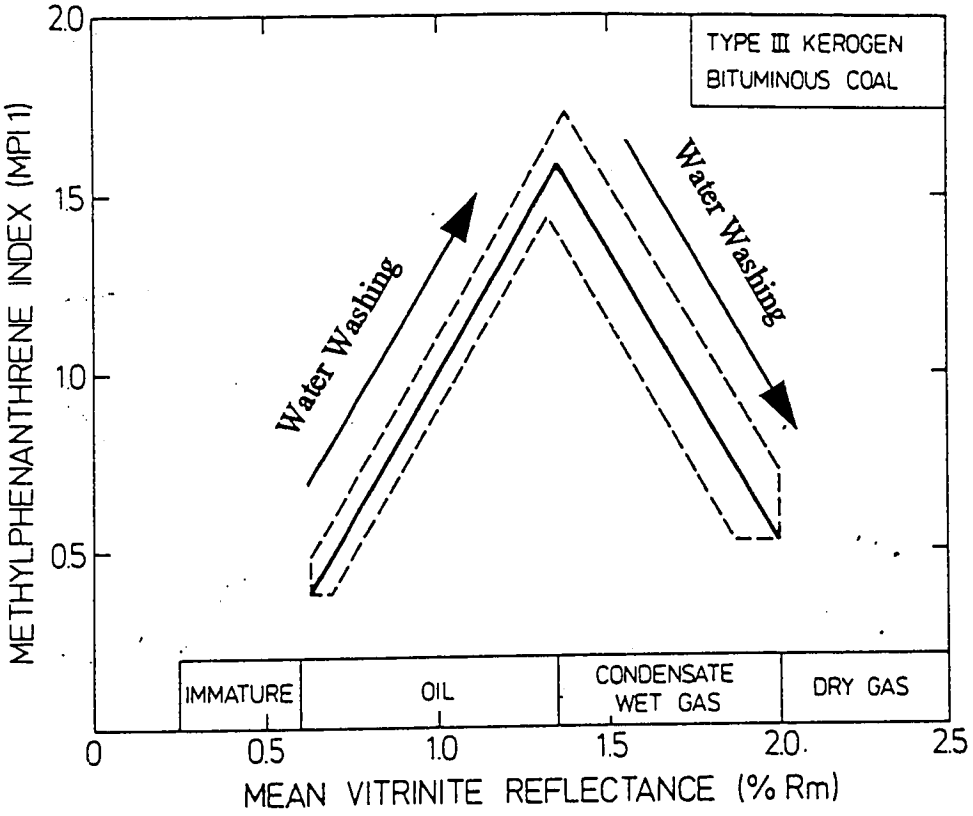

Figure 4.76. Relationship between Methylphenanthrene Index (MPI 1) and mean vitrinite reflectance (%R_m) as based on data from Type-III kerosene-bearing rock and bituminous coal samples (modified after Radke and Welte, 1981).

Field C (Central Arabia) oils have MPR values that are less than 2.24 (average = 1.83), thus equation 2.1 was used in calculating the $\%R_C$ values of these oils. The calculated $\%R_C$ show an average of 0.99%. These $\%R_C$ values suggest that the source rock was at the "late mature" stage of oil generation. Field C has a slightly higher GOR than fields A and B. Thus, it may not be as heavily water-washed as those two fields. However, the $\%R_C$ is more reasonable than that for fields A and B.

Oils D1 and G1 (Central Arabia) have GOR values that are considerably higher than all the above fields, and MPR values that are less than 2.24. The $\%R_C$ values (using equation 2.1) are 0.79% and 0.90%, respectively, suggesting that they were generated from source rocks that were at the "peak mature" stage of oil generation, with oil G1 generated at a stage bordering on the "late mature" stage. Maturity seen here may be closer to reality than at fields A, B, or C.

The oil from field E (Central Arabia) has a low GOR and an MPR value that is greater than 2.24 and corresponding $\%R_C$ value (using equation 2.2) of 1.45%. The same reasoning given for field A oils is also applicable here.

F1 (Paleozoic condensate from the Eastern Province) has the highest GOR of all the Paleozoic fluids considered in this study. It has an MPR value that is greater than 2.24 and corresponding $\%R_C$ value (using equation 2.2) of 1.35%.

This suggests that it was generated from a source rock at the "post mature" stage of oil generation and is in agreement with its believed true maturity.

Field H oils (Jurassic, Eastern Province) have MPR values that are less than 2.24 and $\%R_c$ values (using equation 2.2) of 0.68% (Oil-H1) and 0.67% (Oil-H2). These $\%R_c$ values indicate that these oils were generated from a source rock that was at the early "peak mature" stage of oil generation.

Calculated reflectance values ($\%R_C$) for Paleozoic oils and condensate show that oils from fields A, B, and E (low GOR, high API) were generated when the source rock was at the "late-post" mature stage. These $\%R_C$ values, however, are unlikely in view of the fact that at such values of $\%R_C$, only gas should be produced by the source rock. However, we find black oils. Because of the low GOR of the field, water-washing may be causing preferential depletion of phenanthrene relative to methylphenanthrenes, thus affecting (raising) the MPI 1 values and resulting in an artificially high $\%R_C$.

The $\%R_C$ values for oils from field C (higher GOR than A and B, high API) show that they were generated when the source rock was at the "late mature" stage or that they have been affected by water-washing though not as heavily as fields A and B. $\%R_C$ values for this field are more reliable than those of field A and B.

The $\%R_C$ values for oils from fields D and G indicate that these oils were generated when the source rock was at the "peak mature" and bordering on the "late mature" stage. These two fields have considerably higher GORs. Thus, maturity at these fields assessed on the basis of $\%R_C$ is closer to reality than at fields A and B.

These $\%R_C$ values show that the condensate from field F was generated when the source rock was at the "post" mature stage.

Calculated $\%R_c$ values for the Eastern Province Jurassic oils suggest that they were generated from source rock which was at the "peak" mature stage.

CHAPTER 5

CONCLUSIONS

The following conclusions are drawn from the previously described results and discussions.

Bulk properties: API gravity values of Paleozoic Central Arabian oils are much higher than Jurassic oils from the Eastern Province. Percent sulfur and nitrogen contents of these Paleozoic oils are exceedingly low, and especially so when compared with Jurassic oils from the Eastern Province. Bulk properties reveal similarities between Fields B and C, D and G, as well as E and F.

Pristane/phytane ratios indicate that source rocks of the Central Arabian oils were deposited under dysoxic conditions and that source rocks of the Eastern Province oils were deposited under highly reducing conditions.

The mid-range star diagrams (MRSD) show that all Paleozoic fluids (Central Arabian oils and the condensate from Eastern Province) follow patterns that are different from those followed by oils from the Eastern Province. Fields B and C follow fairly similar patterns on the MRSDs. MRSDs also show that the two oils from field D and G have, for the most part, similar patterns, which is in agreement with their similar bulk properties.

Central Arabian oils are exceedingly lean in conventional biomarkers (*e.g*, hopanes and steranes). These biomarkers are not present in high enough concentrations and the compounds that are present are not diagnostic enough to permit using them for correlation purposes.

The methylphenanthrene ratio (MPR) values of the oils from Central Arabia are all higher than those of Jurassic oils from the Eastern Province, with the exception of the oils from fields D and G. These exceptions may result from the effects of water-washing on all Central Arabian fields except D and G. The latter two fields exhibit MPR values that are closer to the Eastern Province Jurassic oils than to Central Arabian oils.

Calculated reflectance values (%RC) for Paleozoic oils and condensate indicate the following:

(a) oils from fields A, B, and E (low gas/oil ratio (GOR), high API gravity) were generated when the source rock was at the "late-post" mature stage. Their $\%R_C$ values, however, are unlikely in view of the fact that at such values of $\%R_C$, only gas should be produced by the source rock. However, we find black oils.

(b) Because of the low GOR of the field, water-washing may be causing preferential depletion of phenanthrene relative to methylphenanthrenes,

thus affecting (raising) the MPI 1 values and resulting in an artificially high $\%R_C$.

(c) oils from field C (higher GOR than A and B, high API gravity) were generated when the source rock was at the "late mature" stage or that they have been affected by water-washing though not as greatly as fields A and B. Calculated reflectance ($\%R_C$) values for this field are more reliable than those of field A and B.

(d) oils from field D and G were generated when the source rock was at the "peak mature" and bordering on the "late mature" stage. These two fields have considerably higher GORs. Thus, maturity at these fields assessed on the basis of $\%R_C$ is closer to reality than at fields A and B.

(e) condensate from field F was generated when the source rock was at the "post" mature stage.

Calculated %Rc values for the Eastern Province Jurassic oils suggest that they were generated from source rock which was at the "peak" mature stage.

CHAPTER 6

REFERENCES

[1] Abu-Ali, M. A., U. A. Franz, J. Shen, F. Monnier, M. D. Mahmoud, and T. M. Chambers, 1991, Hydrocarbon Generation and Migration in the Paleozoic Sequence of Saudi Arabia, SPE 21376, p. 345-356.

[2] Beydoun, Z. R., 1988, The Middle East: Regional Geology and Petroleum Resources, Scientific Press, P. O. Box 21, Beaconsfield, Bucks, HP9 1NS, U. K.

[3] Cole, G. A., M. A. Abu-Ali, S. M. Aoudeh, W. J. Carrigan, H. H. Chen, E. L. Colling, W. J. Gwathney, A. A. Al-Hajji, H. I. Halpern, P. J. Jones, S. H. Al-Sharidi, and M. H. Tobey, 1994, Organic Geochemistry of the Paleozoic Petroleum System of Saudi Arabia: , Energy & Fuels, v. 8, p. 1425-1442.

[4] Husseini, M. I., 1991, Tectonic and Depositional Model of the Arabian Plates During the Silurian-Devonian, AAPG Bulletin, v. 75, No. 1, p. 108-120.

[5] Halpern H. I., 1995, Confidential Aramco Publication.

[6] Halpern H. I., 1995, Development and Applications of Light Hydrocarbon Based Star Diagrams, AAPG Bulletin, v. 76, No. 6, p. 801-815.

[7] Zhilin, C., Z. Guangjia, and R. Alexander, 1994, A Biomarker study of immature crude oils from the Shengli oil field, People's Republic of China, Chemical Geology, v. 113, p. 117-132.

[8] Peters K. E., and J. M. Moldowan, 1993, The Biomarker Guide, The Biomarker Guide. Prentice-Hall, Inc., Englewood Cliffs, New Jersey.

[9] Moldowan, J. M., K. E. Peters, R. M. K. Carlson, M. Schoel, and M. A. Abu-Ali, 1994, Diverse Applications of Petroleum Biomarker Maturity Parameters, AJSE, v. 19, No. 2B, p. 272-298.

[10] Peters, K. E., A. Eh. Kontorovich, B. J. Huizinga, J. M. Moldowan, and C. Y. Lee, 1994, Multiple Oil Families in the West Siberian Basin, AAPG Bulletin, v.78, No. 6, p. 893-909.

[11] Warburton G. A., and J. E. Zumberge, 1983, Determination of Petroleum Sterane Distribution by Mass Spectrometry with Selective Metastable Ion Monitoring, Analytical Chemistry. V. 55. p. 123-126.

[12] Lanças, F. M., E. Carrilho, G. H. N. Deane, and M. C. F. Camilo, June, 1989, Group-Type Fractionation of Petroleum and Alternative Fuels by Column Liquid Chromatography, Journal of High Resolution Chromatography, v. 12, p. 368-371.

[13] Miles J. A., 1991, Illustrated Glossary of Petroleum Geochemistry, Illustrated Glossary of Petroleum Geochemistry, Oxford Scientific Publications, Calredon Press, Oxford.

[14] Tissot B. P., and D. H. Welte, 1984, Petroleum Formation and Occurrence, 2nd edition Springer-Verlag, Berlin Heidelberg, Germany. 699 p.

[15] Alexander R., A. V. Larcher, R. I. Kagi, and P. L. Price, 1992, An oil-Source Correlation Study Using Age-Specific Plant-Derived Aromatic Biomarkers, Biological Markers in Sediments and Petroleum. Ed. by Moldowan J. M., P. Albrecht, and R. P. Philp.

[16] Connan J., 1993, Molecular Geochemistry in Oil Exploration, Applied Petroleum Geochemistry, edited by M. L. Bordenave, Chapter I.7, p. 175-204.

[17] Barker C., 1979, Organic Geochemistry in Petroleum Exploration, AAPG Education Course Note Series # 10.

[18] Philp R. P., 1986, Geochemistry in the search for oil, Feb. 10, Chemical & Engineering News, V. 64, p. 28-43.

[19] Vandenbroucke M., 1993, Migration of Hydrocarbons, Applied Petroleum Geochemistry. Ed. by Bordenave, Editions Technip, Paris, p. 123-148.

[20] Tran K. Le, and B. Philippe, 1993, Oil and Rock Extract Analysis, Applied Petroleum Geochemistry, edited by M. L. Bordenave, Chapter II.4, p. 373-394.

[21] Clayton J. L., & J. D. King, 1987, Effects of weathering on biological marker and aromatic hydrocarbon composition of organic matter in Phosphoria shale outcrop, Geochim. et Comochim. Acta, V. 51, p. 2153-2157.

[22] Bordenave M. L., J. Espitalie, P. Leplat, J. L. Oudin, and M. Vandenbroucke, 1993, Screening Techniques for Source Rock Evaluation, Applied Petroleum Geochemistry. Ed. by Bordenave, Editions Technip, Paris, p. 217-278.

[23] Daly A. R., May 7, 1990, Oil and bitumen fingerprinting on exploration, Oil & Gas Journal, p. 156-159.

[24] Blanc Ph., and J. Connan, 1993, Crude Oil in Reservoirs: Factors Affecting Their Composition, Applied Petroleum Geochemistry. Ed. by Bordenave, Editions Technip, Paris, p. 149-174.

[25] Tissot B. P., May, 1984, Recent Advances in Petroleum Geochemistry Applied to Hydrocarbon Exploration, AAPG Bulletin, V. 68, No. 5, p. 545-563.

[26] Eglinton G., 1969, Hydrocarbons and fatty acids in living organisms and recent and ancient sediments, Advances in Organic Geochemistry, 1968, p. 1-24.

[27] Henderson W., V. Wollrab, and G. Eglinton, 1969, Identification of steranes and triterpanes from a geological source by capillary GC & MS, Advances in Organic Geochemistry, 1968, p. 181-207.

[28] Mackenzie A. S., G. A. Wolff, & J. R. Maxwell, 1983, Fatty acids in some biodegraded petroleums, possible origins and significance, Proceedings, Advances in Organic Geochemistry, 1981, Continent. Shelf Inst., Norway, p. 637-649.

[29] Rodrigues K., 1988, Oil source bed recognition and crude oil correlation, Trinidad, West Indies, Advances in Organic Geochemistry 1987; Organic Geochemistry, V. 13, Nos. 1-3, p. 365-371.

[30] Philp R. P., & J. N. Oung, August 1st, 1988, Biomarkers; occurrence, utility, and detection, Analytical Chemistry, V. 6, No. 15, p. 887A-94A+.

[31] Horsfield B., and J. Rullkotter, 1994, Diagenesis, Catagenesis, and Metagenesis of Organic Matter, The Petroleum System-from source to trap: AAPG Memoir 60. Ed. by Magoon L. B., and Dow W. G. p. 189-199.

[32] Seifert W. K., and J. M. Moldowan, 1978, Applications of steranes, terpanes, and monoaromatics to the maturation, migration, and source of crude oils , Geochimica et Cosmochimica Acta, V. 42 (1), p. 77-95.

[33] Grantham P. J., 1986, The Occurrence of unusual C_{27} and C_{29} sterane predominance in two types of Oman crude oil, Organic Geochemistry, V. 9, p. 1-10.

[34] Grantham P. J., G. W. M. Lijmbach, and J. Posthuma, 1990, Geochemistry of crude oils in Oman, Classic Petroleum Provinces. Geological Society Special Publication No. 50. Ed. by Brooks J. p. 317-328.

[35] Seifert W. K., 1978, Steranes and terpanes in kerogen pyrolysis for correlation of oils and source rocks, Geochimica et Cosmochimica Acta, V. 42 (5), p. 473-484.

[36] Seifert W. K., J. M. Moldowan, and R. W. Jones, 1979, Application of Biological Marker chemistry to Petroleum Exploration, Proceedings of the Tenth World Petroleum Congress, Bucharest, Romania. September 1979. Paper SP8, Heyden, p. 425-440.

[37] Alajbeg A. J., Muhl, S. Marin-Mudrovcic, and A. Putnikovic, 1988, Multiple parameters approach in oil-oil correlation for the Zutica field oils, Organic Geochemistry, V. 13, Nos. 1-3, p. 81-88.

[38] Zhendi W., M. Fingas, and K. Li, Sep., 1994, Fractionation of a Light Crude Oil and Identification and Quantitation of Aliphatic, Aromatic, and Biomarker Compounds by GC-FID and GC-MS, Part I, Journal of Chromatographic Science, V. 32, p. 361-366.

[39] Dunham K. W., P. A. Meyers, and J. Rullkotter, 1988, Biomarker Comparison of Michigan Basin Oils, Geochemical Biomarkers. Ed. by Yen T. F., and J. M. Moldowan, Hardwood Academic Publishers. p. 181-202.

[40] Curiale J. A., 1994, Correlation of Oils and Source Rocks-A Conceptual and Historical Perspective, The Petroleum System-from source to trap: AAPG Memoir 60. Ed. by Magoon L. B., and Dow W. G., p. 251-260.

[41] Behar F., and R. Pelet, 1988, A new Technique for Oil/Source-Rock and Oil/Oil Correlation, Geochemical Biomarkers. Ed. by Yen T. F., and J. M. Moldowan. Hardwood Academic Publishers. p. 51-70.

[42] Waples D. W., and T. Machihara, 1991, Biomarkers for Geologists, Biomarkers for Geologists. AAPG Methods in Exploration Series, No. 9.

[43] Riva A., P. G. Caccialanza, and F. Quagliaroli, 1988, Recognition of 18β(H)-oleanane in several crudes and Tertiary-Upper Cretaceous Sediments. Definition of a New Maturity Parameter, Organic Geochemistry, V. 13 (4-6), p. 671-675.

[44] Radke M., & D. H. Welte , 1981, The Methylphenanthrene Index (MPI): A Maturity Parameter based on Aromatic Hydrocarbons, Advances in Organic Geochemistry 1981, p. 504-512; John Wiley & Sons Limited.

[45] Mair B. J., and Martinez-Pico J. L., 1962, Composition of trinuclear aromatic portion of the heavy gas oil and light lubricating distillate, Proceedings of American Petroleum Institute, Section III 42, p. 173-185.

[46] Wakeham S. G., C. Schaffner, W. Giger, 1980, Diagenetic polycyclic aromatic hydrocarbons in recent sediments; structural information obtained by high performance liquid chromatography, Advances in Organic Geochemistry 1979, Physics and Chemistry of the Earth, 12, p. 353-363.

[47] Ishiwatari, R., and K. Fukushima, 1979, Generation of unsaturated and aromatic hydrocarbons by thermal alteration of young kerogen, Geochimica et Cosmochimica Acta, V. 43 ( ), p. 1343-1349.

[48] Radke M., D. H. Welte , H. Willsch, 1982, Geochemical study on a well in the Western Canada Basin: relation of the aromatic distribution pattern to maturity of organic matter, Geochim. et Comochim. Acta, V. 46, No. 3, p. 1-10.

[49] Volkman J. K., 1984, Biodegradation of aromatic hydrocarbons crude oils from the Barrow Sub-basin of Western Australia, Organic Geochemistry, V. 6, p. 619-632.

[50] Radke M., Garrigues P., and Willscht H., 1990, Methylated dicyclic and tricyclic aromatic hydrocarbons in crude oils from the Hanadil field, Indonesia, Organic Geochemistry, V. 15, No. 1, p. 17-34.

[51] Smith J. W., S. C. George, & B. D. Batts, 1995, The geosynthesis of alkylaromatics, Organic Geochemistry, V. 23, No. 1, p. 81-85.

[52] Alexander R., T. P. Bastow, S. J. Fisher, & R. I. Kagi, 1995, Geosynthesis of organic compounds: II. Methylation of phenanthrene and alkylphenanthrenes, Geochimica et Cosmochimica Acta, V. 59 (20), p. 4259-4266.

[53] Radke M., D. H. Welte , H. Willsch, 1986, Maturity parameters based on aromatic hydrocarbons: Influence of the organic matter type, Organic Geochemistry, V. 10, p. 51-63.

[54] Radke M., 1987, Organic Geochemistry of Aromatic Hydrocarbons, Advances in Geochemistry, V. 2, Academic Press, New York, p. 140-207.

[55] Cole, G. A., W. J. Carrigan, E. L. Colling, H. I. Halpern, M. R. Al-Khadhrawi, and P. J. Jones, 1994, The Organic Geochemistry of the

Jurassic Petroleum System in Eastern Saudi Arabia, Pangea: Global Environments and Resources, Canadian Society of Petroleum Geologists, Memoir 17, p.413-438.

[56] Radke M., August, 1988, Application of aromatic compounds as maturity indicators in source rocks and crude oils, Marine Petroleum Geology, V. 5, p. 224-236; also in "Advances in Organic Geochemistry", 1987, Geol. Soc. of London, UK.

[57] Halpern H. I., Personal Communication, 1995.

Appendix (A)

GC Chromatograms of the Saturate Fractions

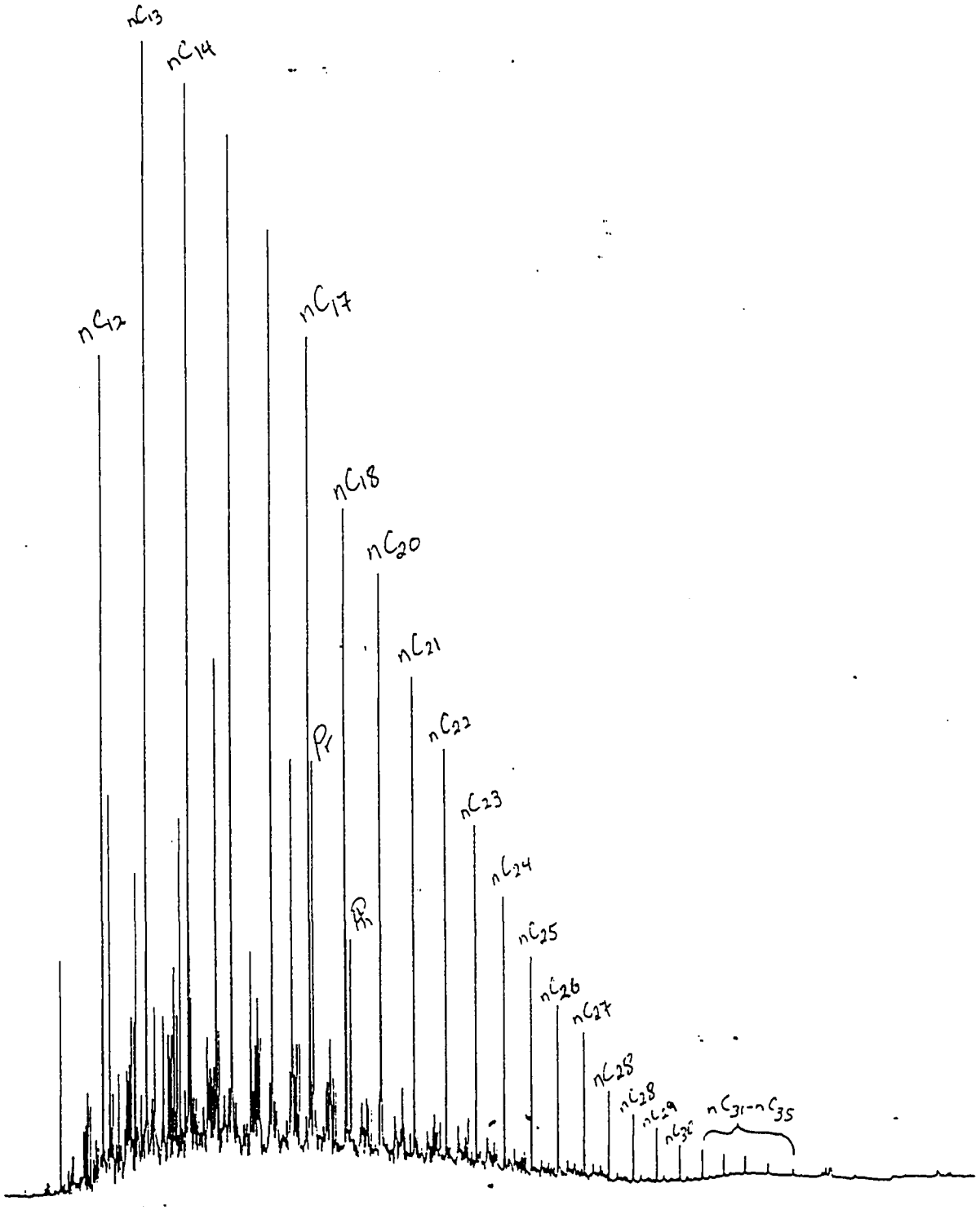

Figure 4.5. Gas chromatogram of the saturate fraction of oil A1.

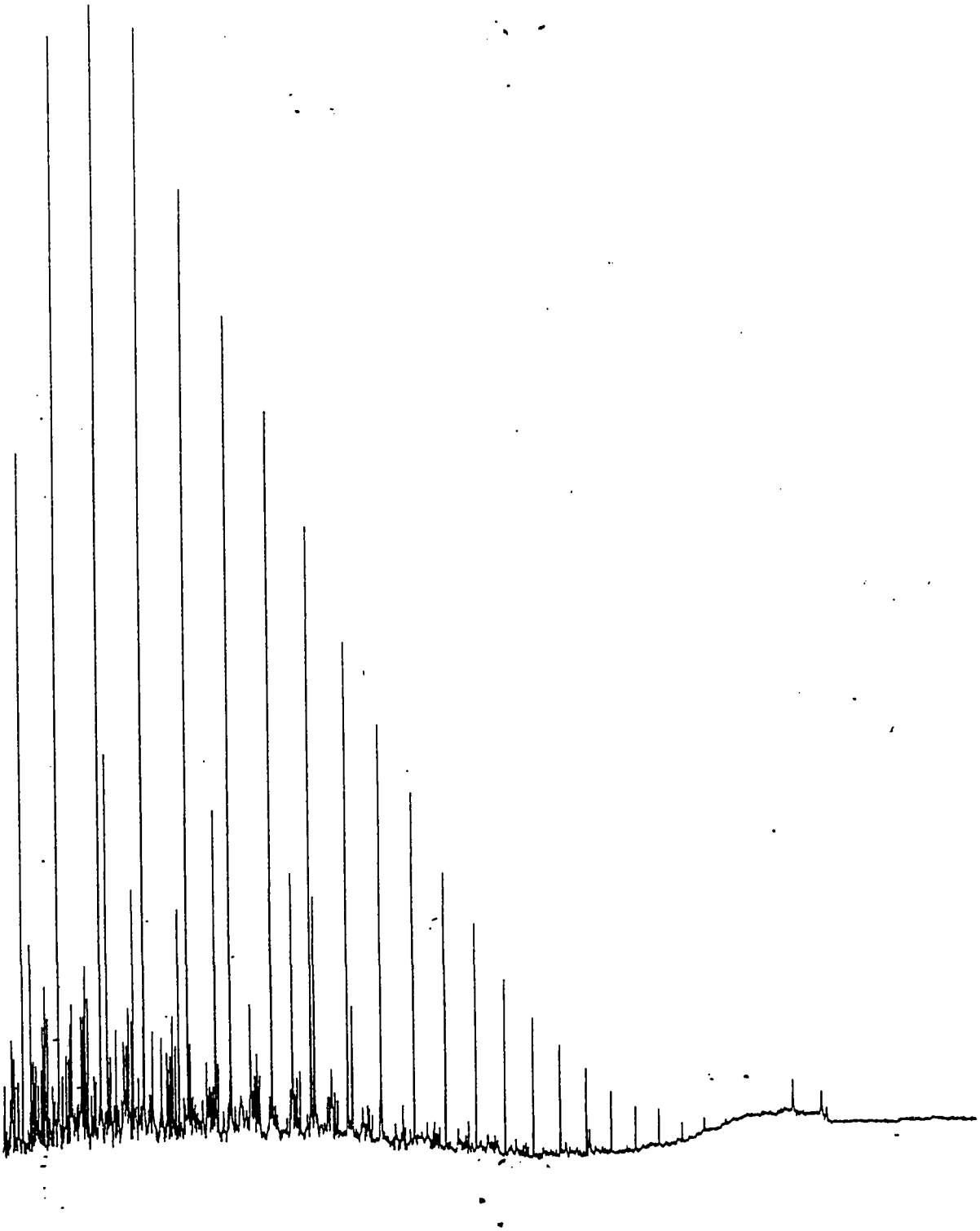

Figure 4.6. Gas chromatogram of the saturate fraction of oil A2.

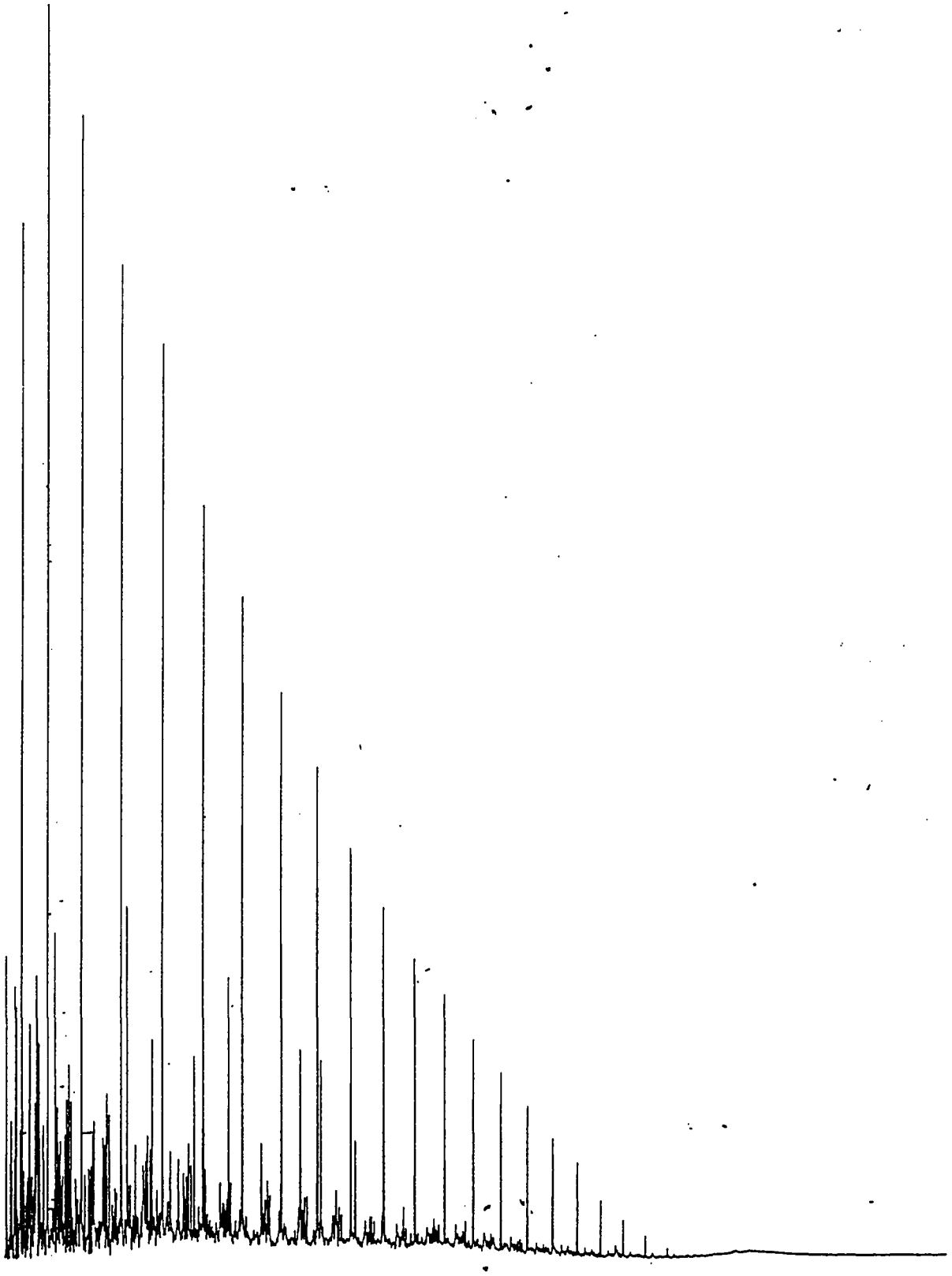

Figure 4.7. Gas chromatogram of the saturate fraction of oil A3.

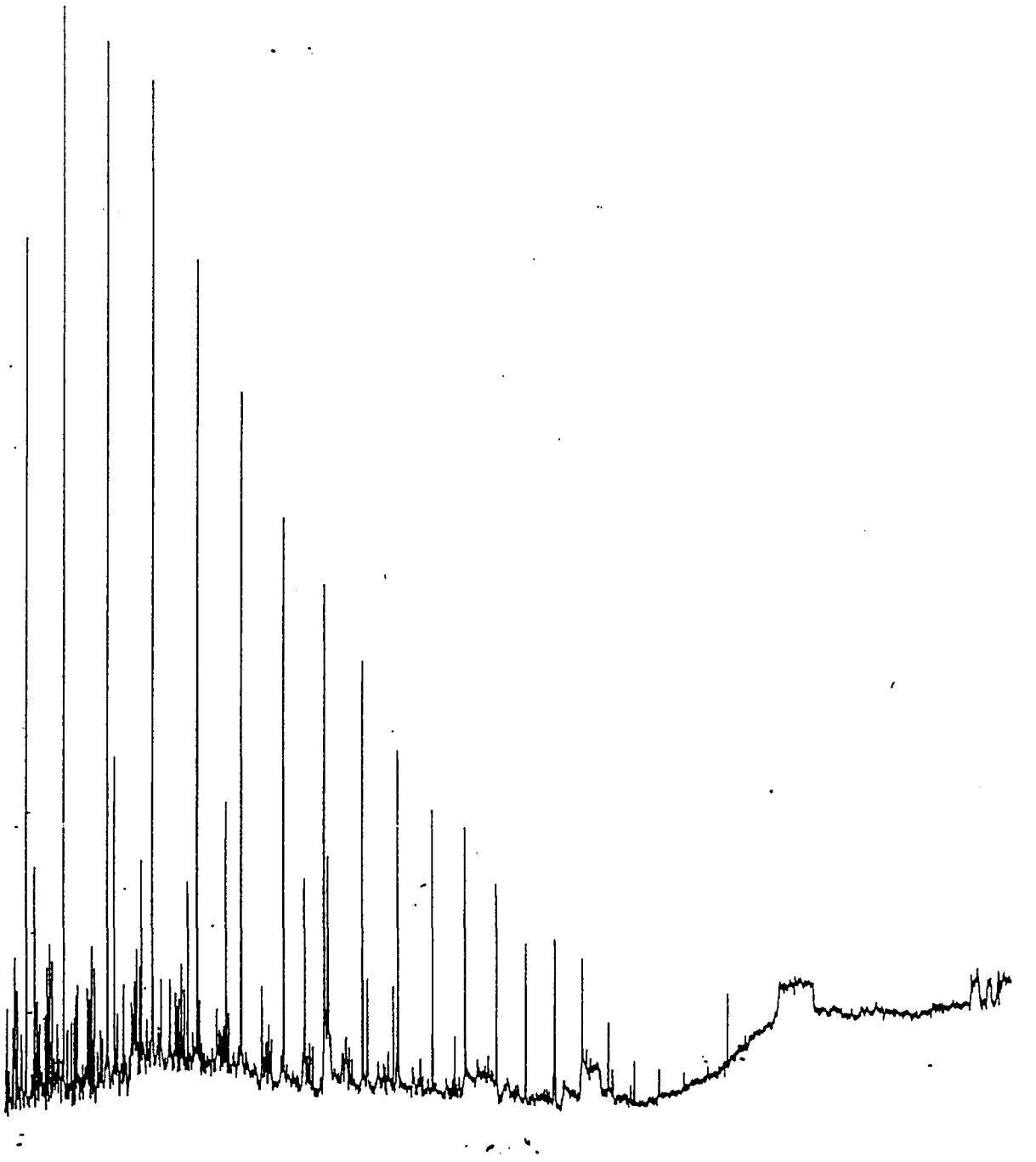

Figure 4.8. Gas chromatogram of the saturate fraction of oil B1.

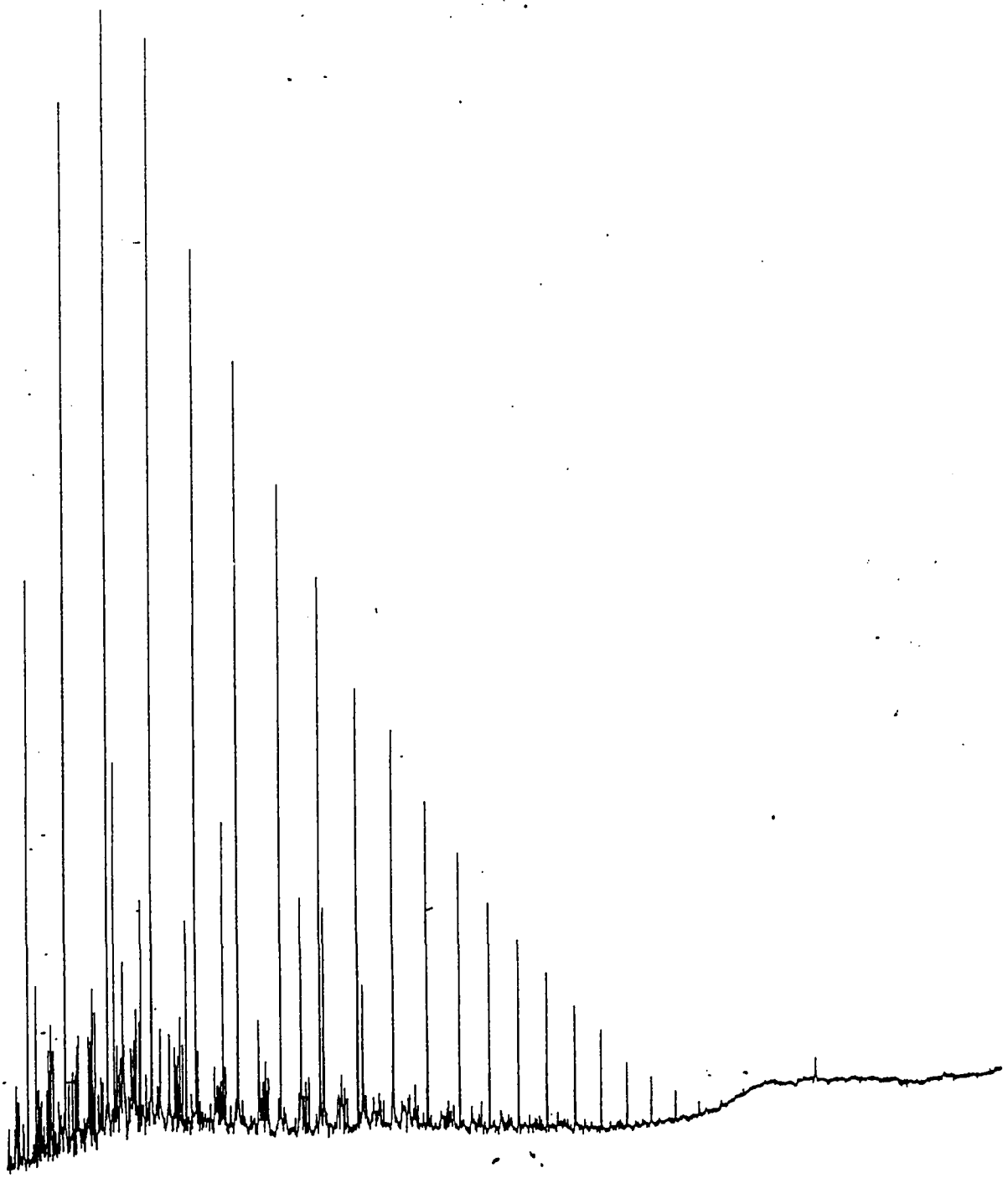

Figure 4.9. Gas chromatogram of the saturate fraction of oil B2.

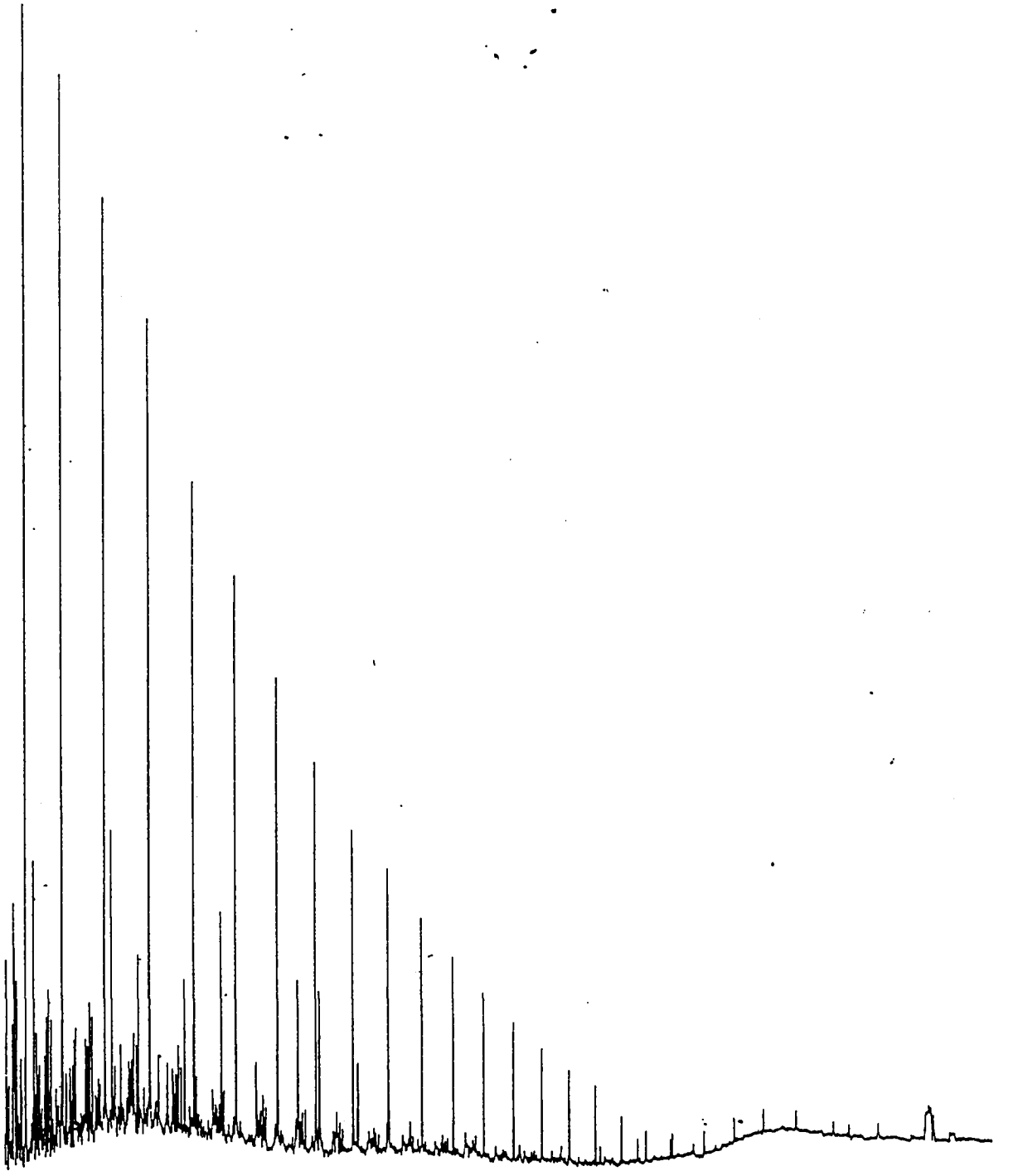

Figure 4.10. Gas chromatogram of the saturate fraction of oil B3.

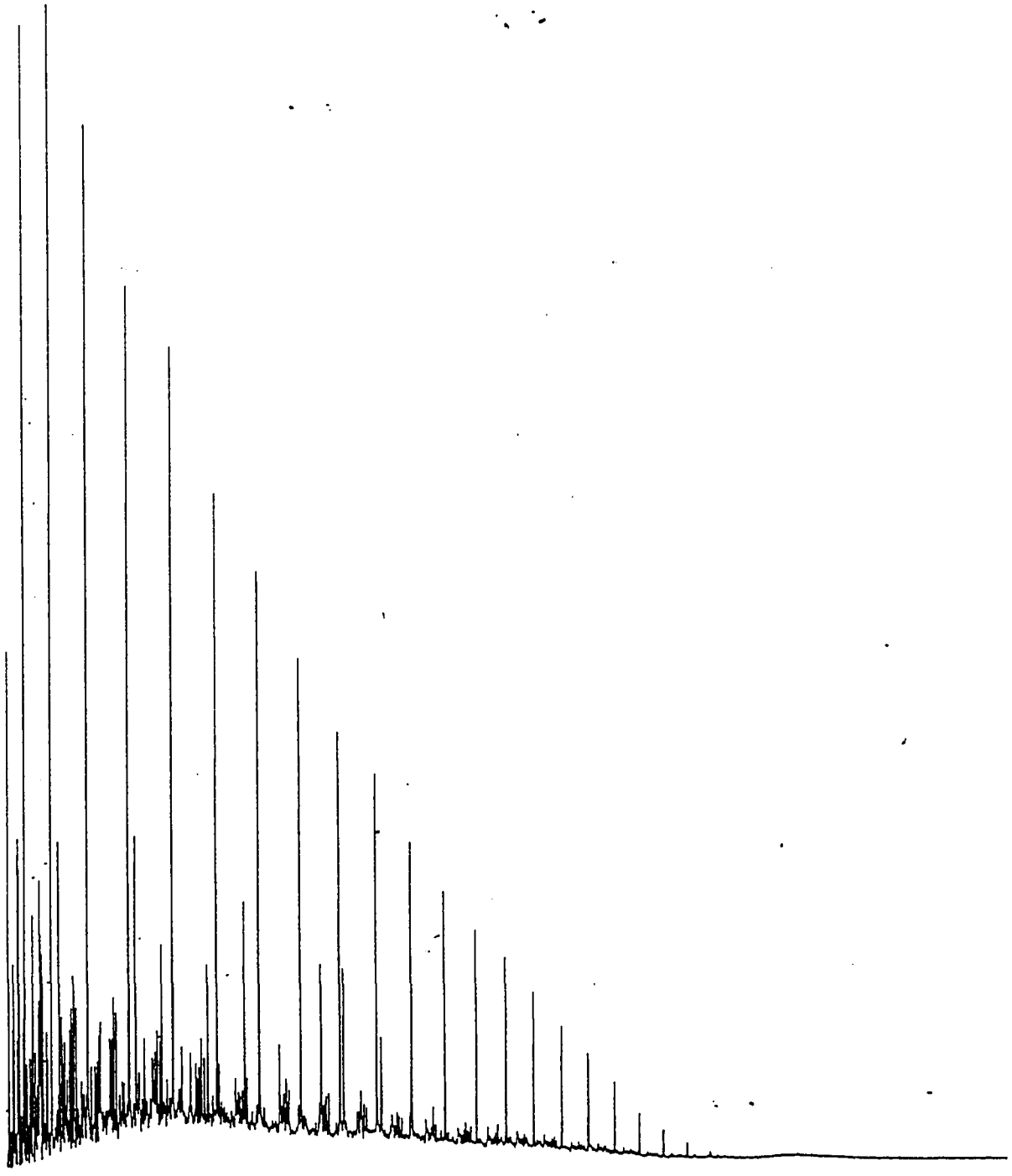

Figure 4.11. Gas chromatogram of the saturate fraction of oil C1.

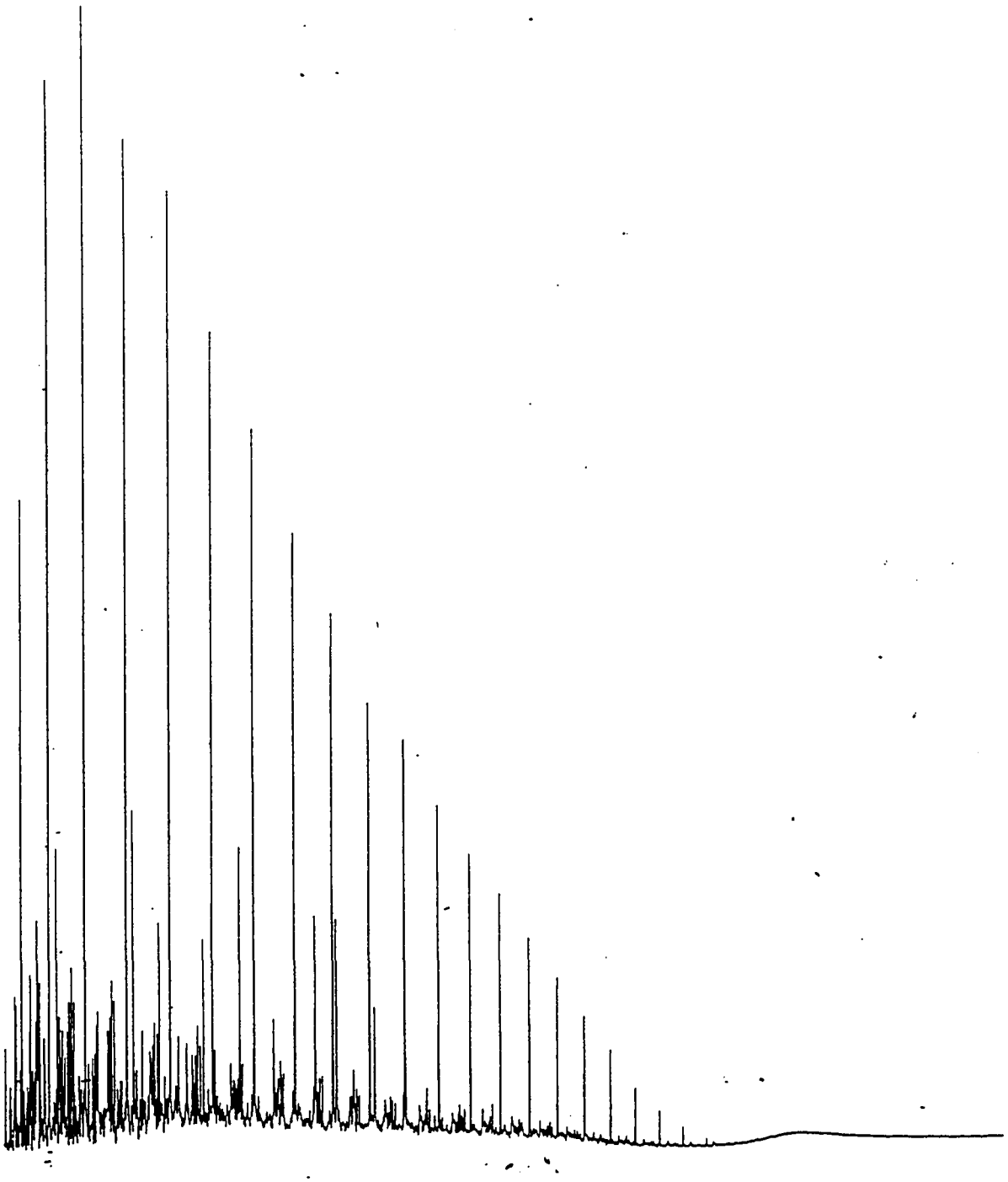

Figure 4.12. Gas chromatogram of the saturate fraction of oil C2.

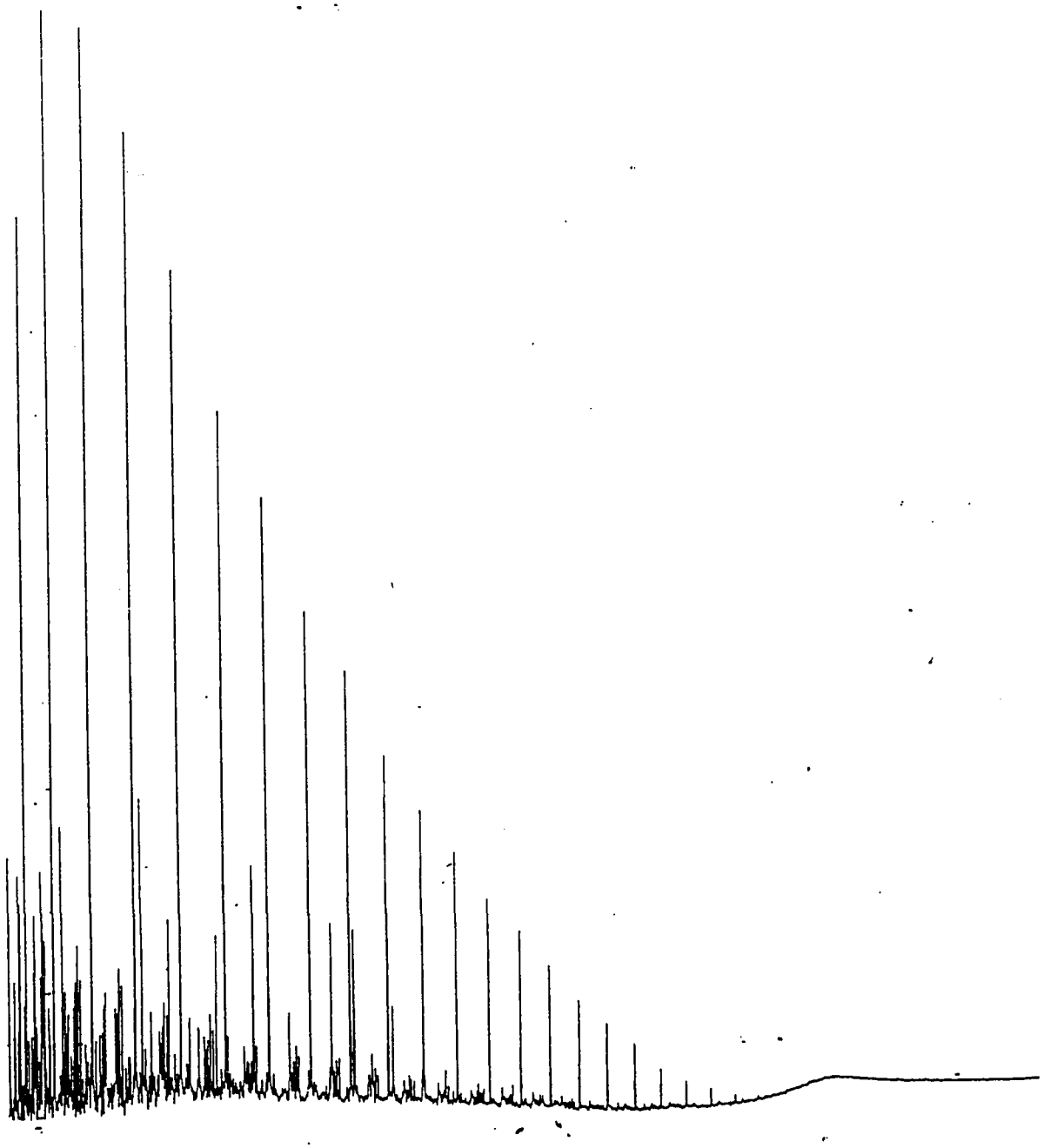

Figure 4.13. Gas chromatogram of the saturate fraction of oil C3.

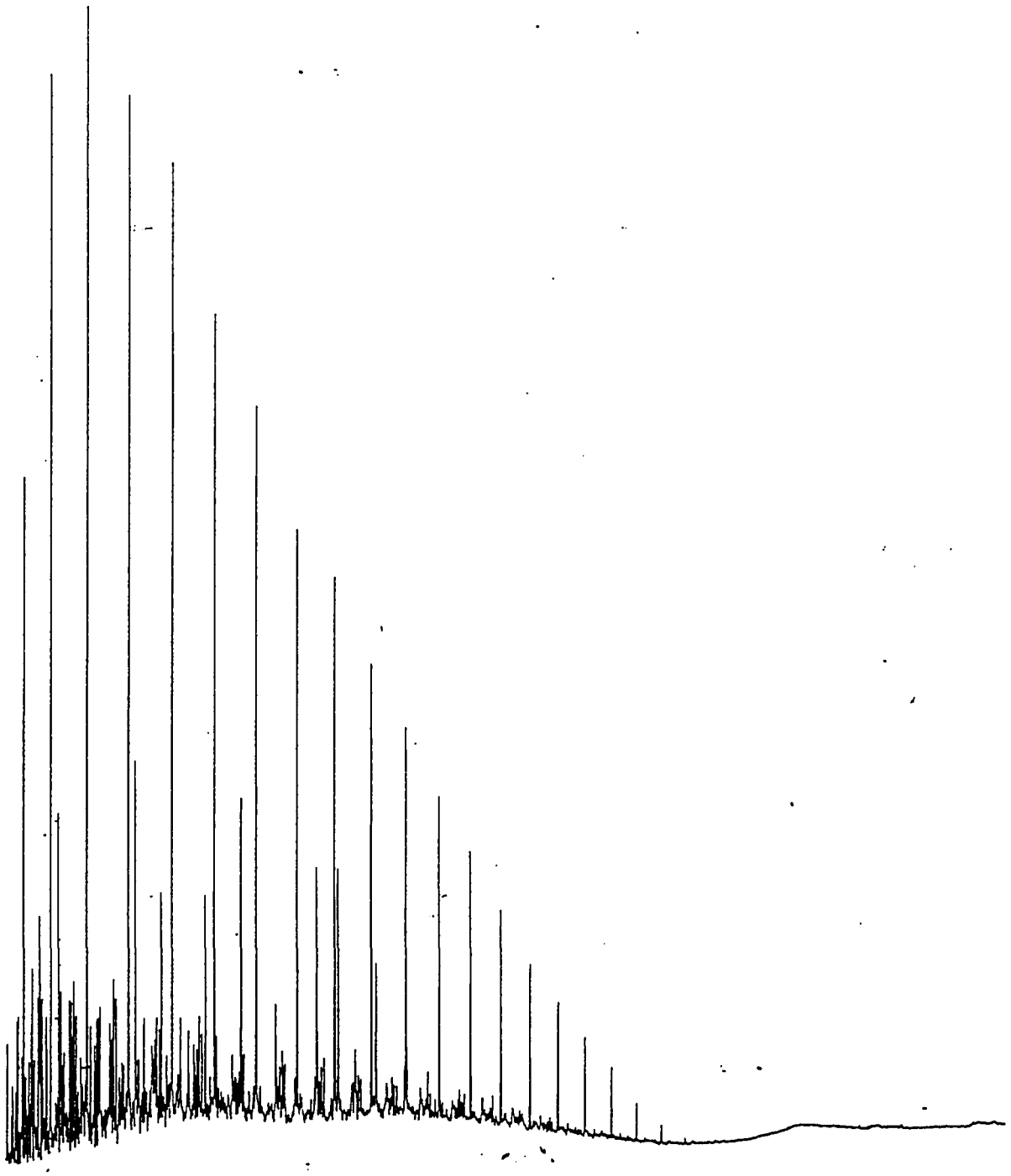

Figure 4.14. Gas chromatogram of the saturate fraction of oil D1.

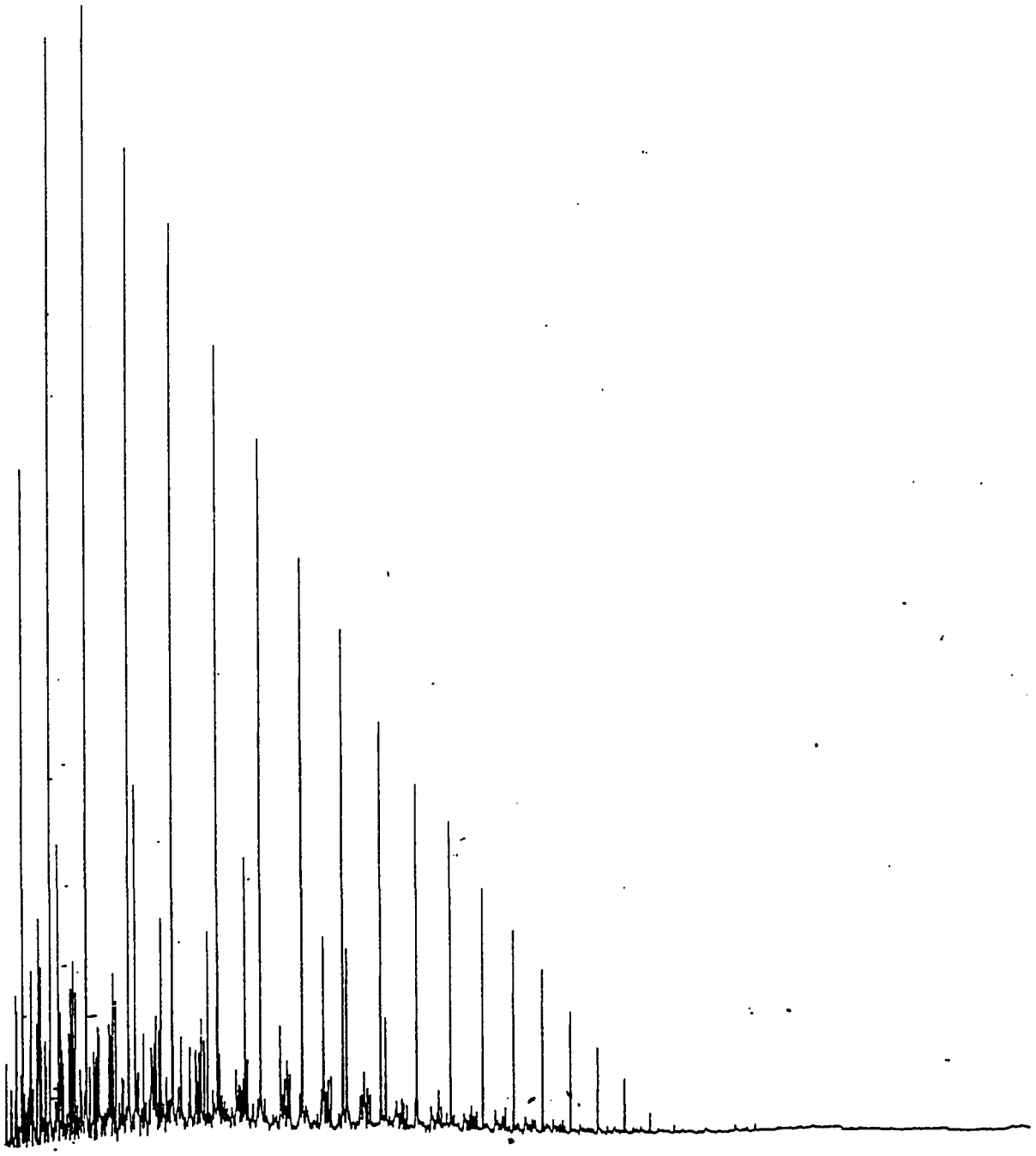

Figure 4.15. Gas chromatogram of the saturate fraction of oil E1.

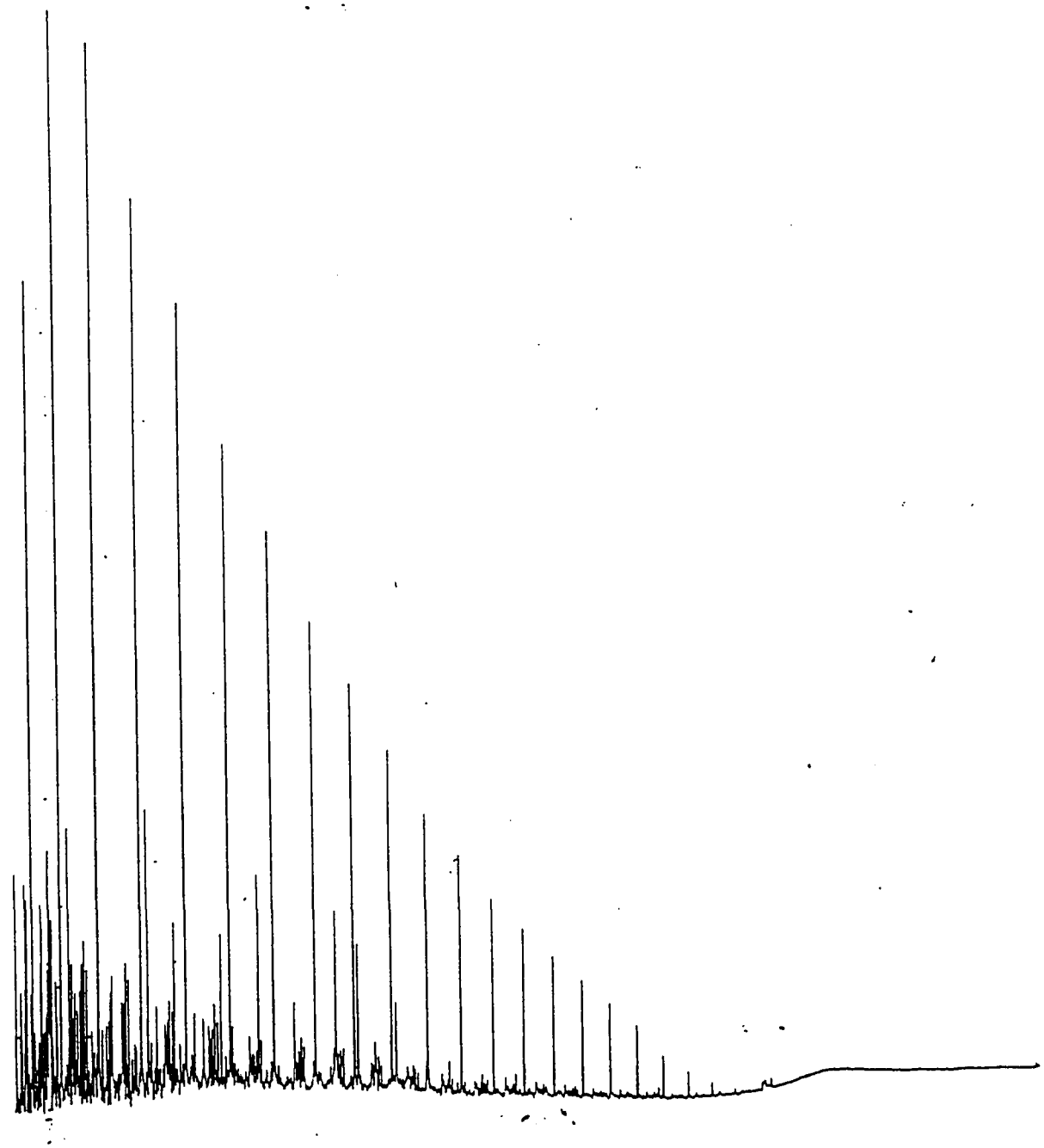

Figure 4.16. Gas chromatogram of the saturate fraction of oil F1.

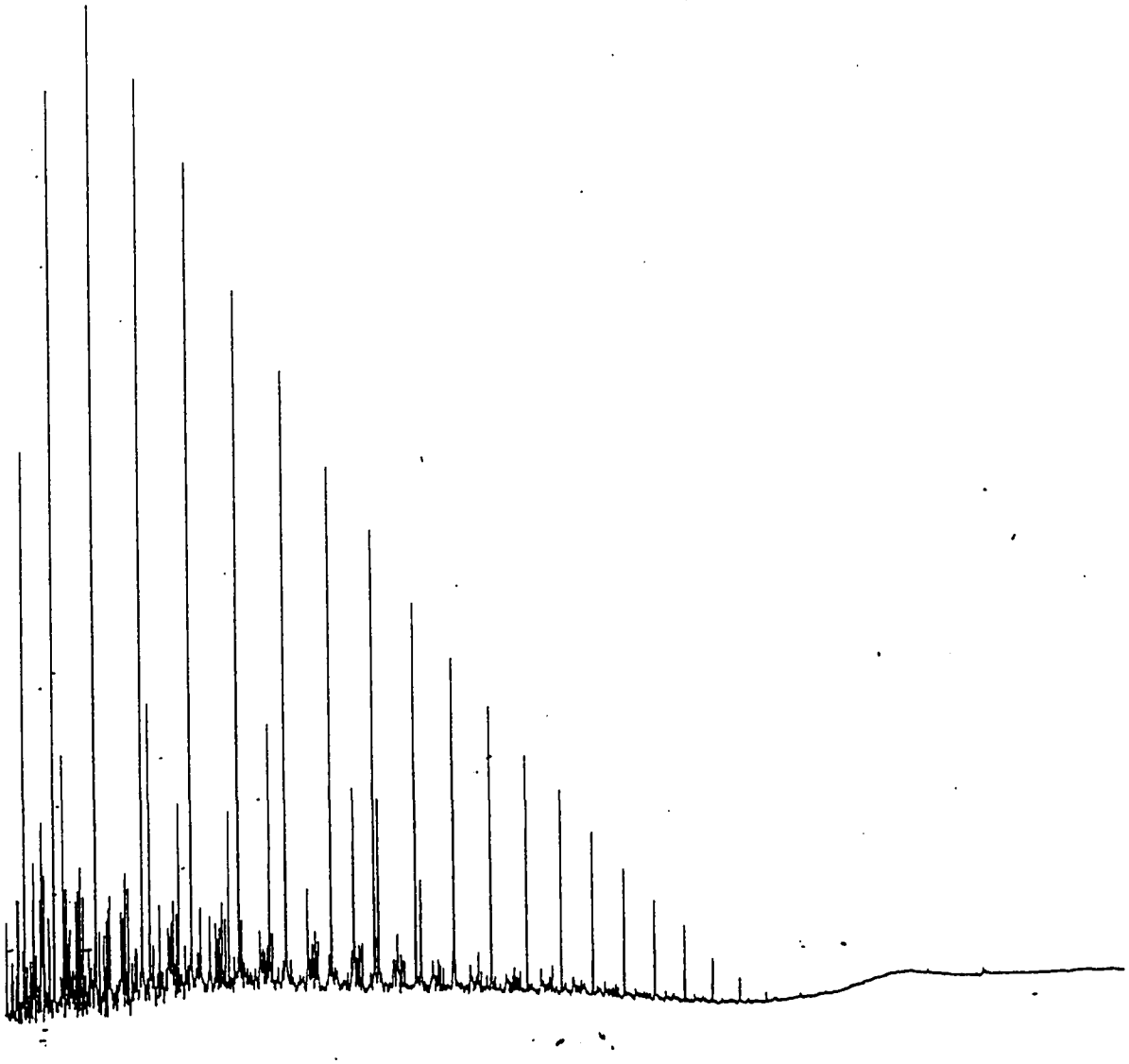

Figure 4.17. Gas chromatogram of the saturate fraction of oil G1.

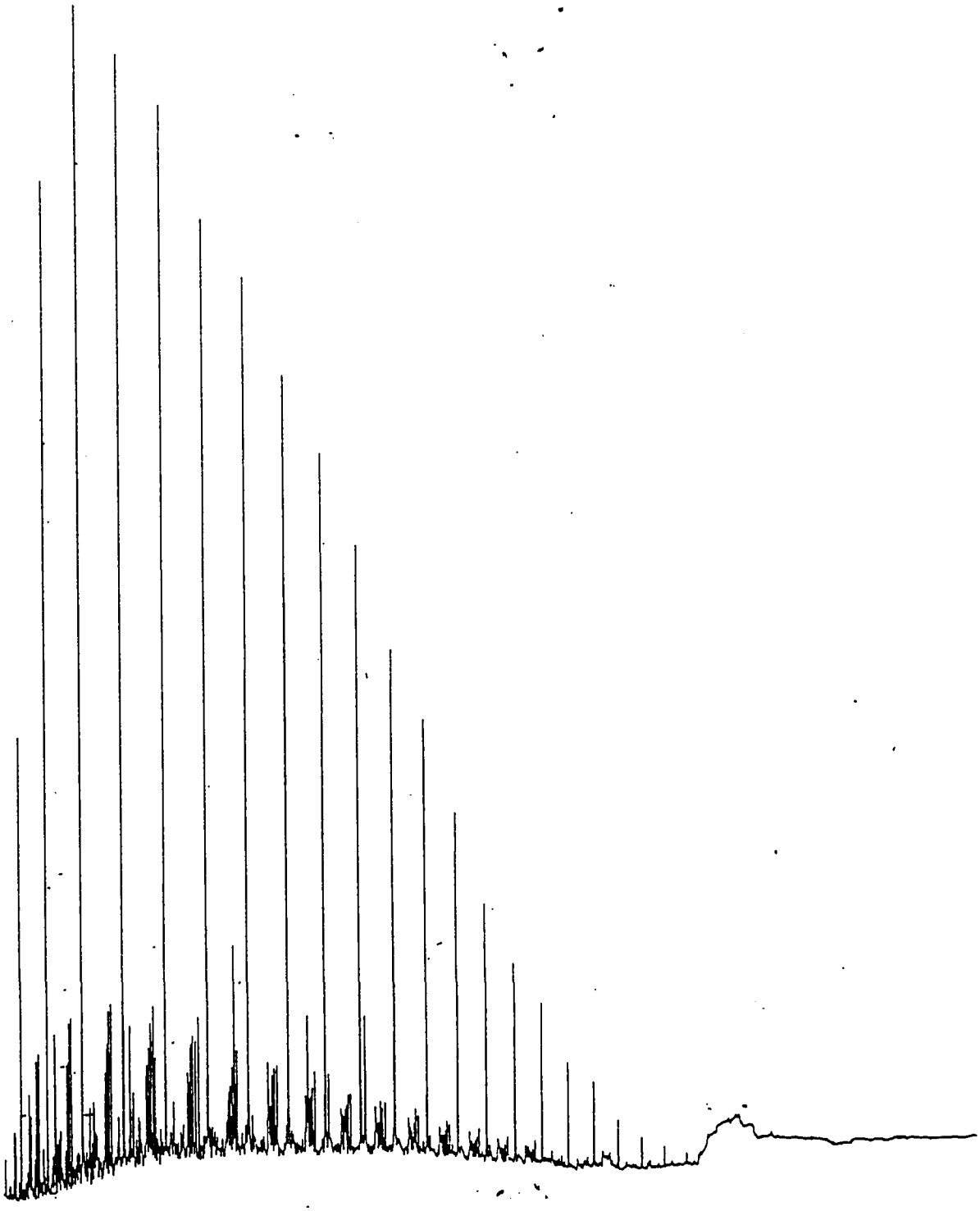

Figure 4.18. Gas chromatogram of the saturate fraction of oil H1.

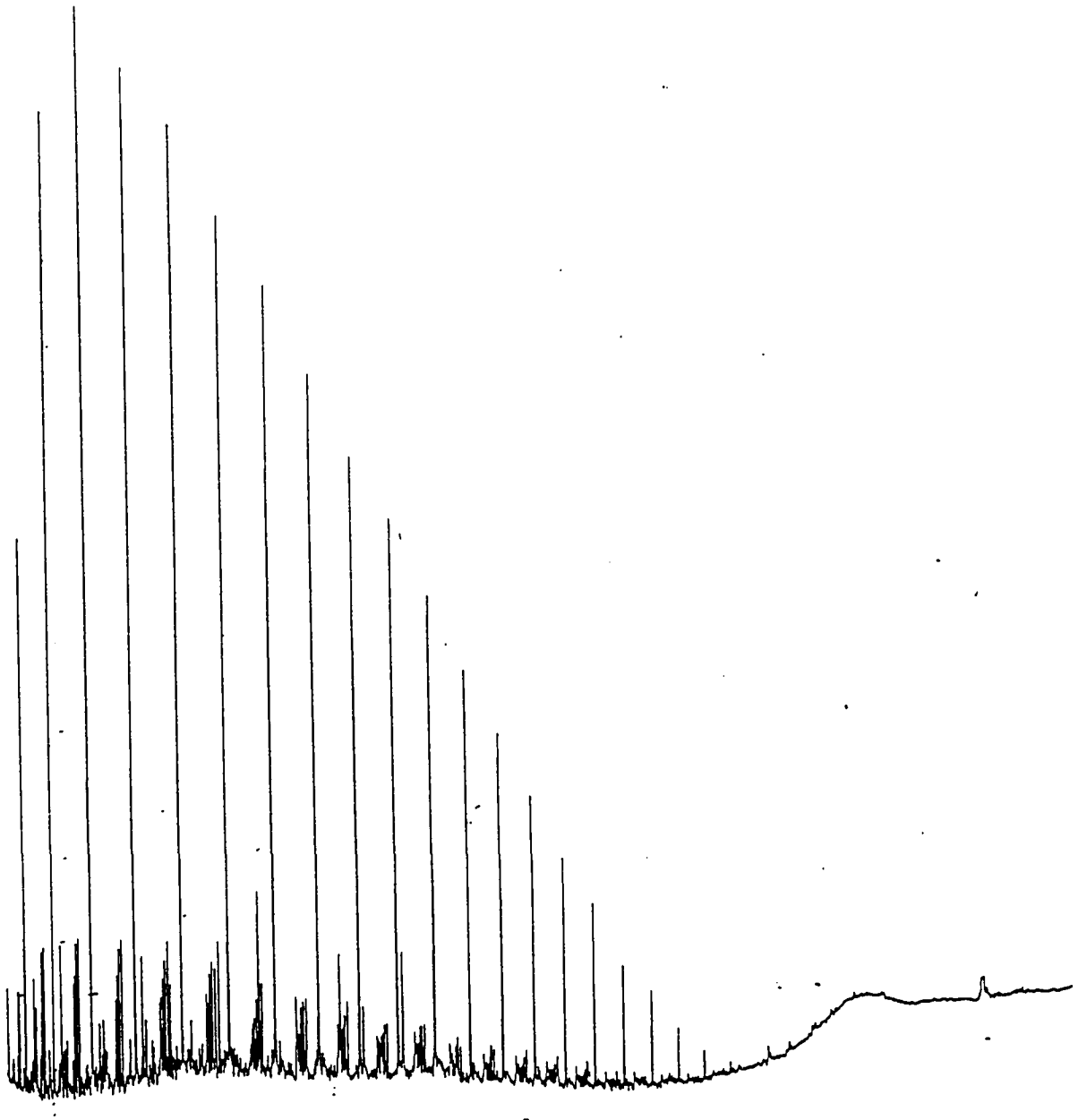

Figure 4:19. Gas chromatogram of the saturate fraction of oil H2.

Appendix (B)

GC Chromatograms of the Aromatic Fractions

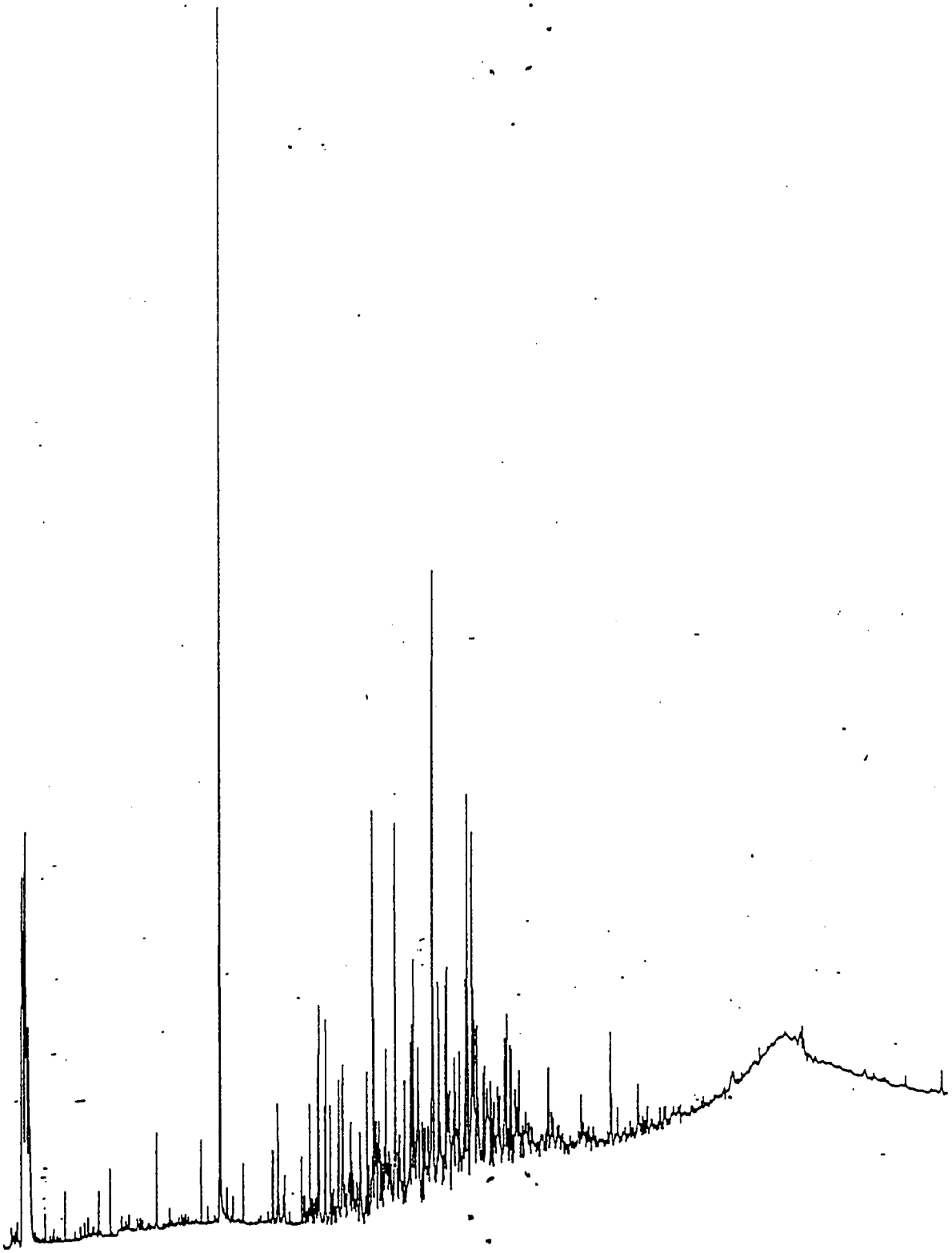

Figure 4.20 a. Gas chromatogram of the aromatic fraction of oil A1.

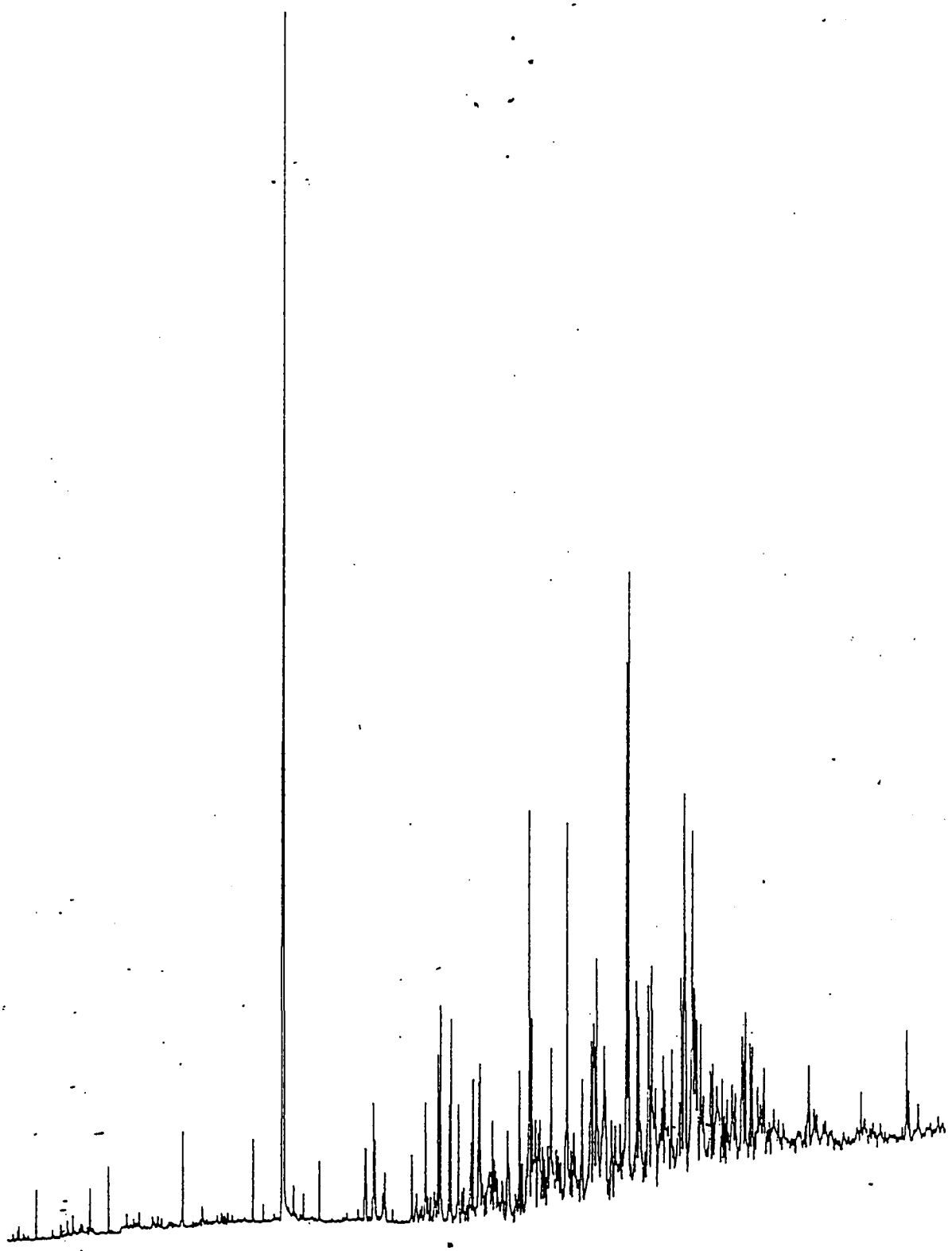

Figure 4.20 b. Gas chromatogram of the middle range (10-78 min.) of the aromatic fraction of oil A1.

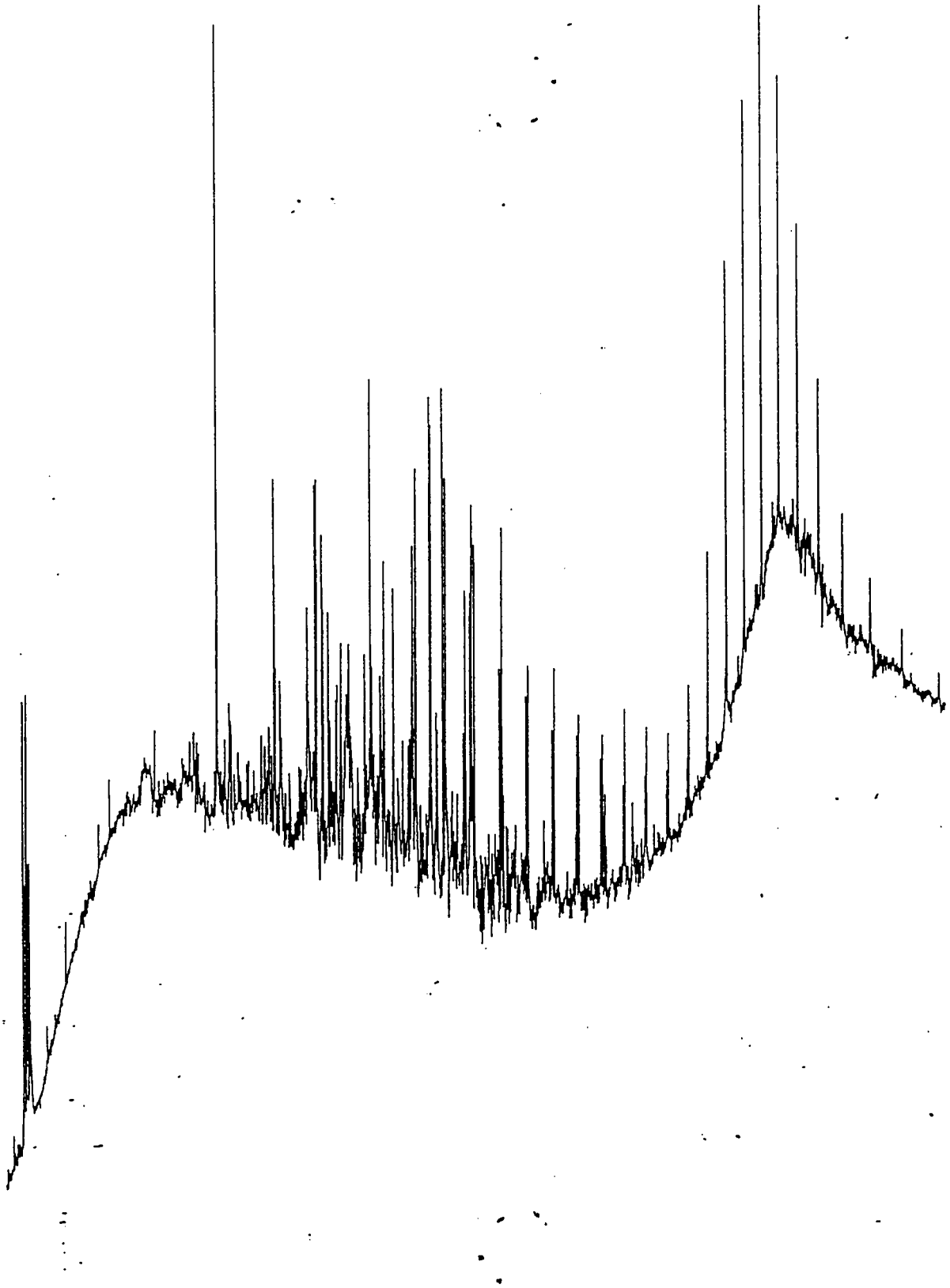

Figure 4.21 a. Gas chromatogram of the aromatic fraction of oil A2.

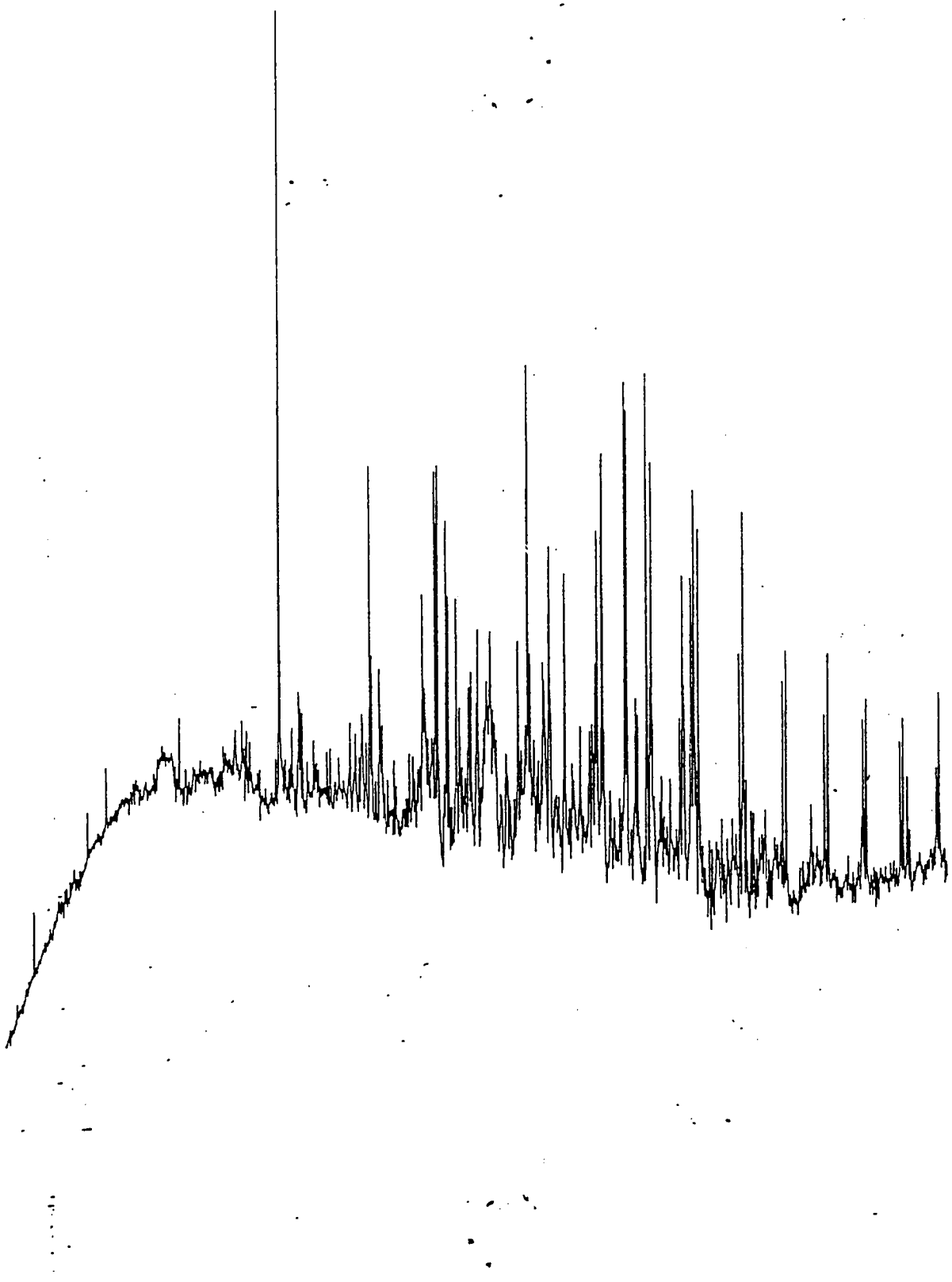

Figure 4.21 b. Gas chromatogram of the middle range (10-78 min.) of the aromatic fraction of oil A2.

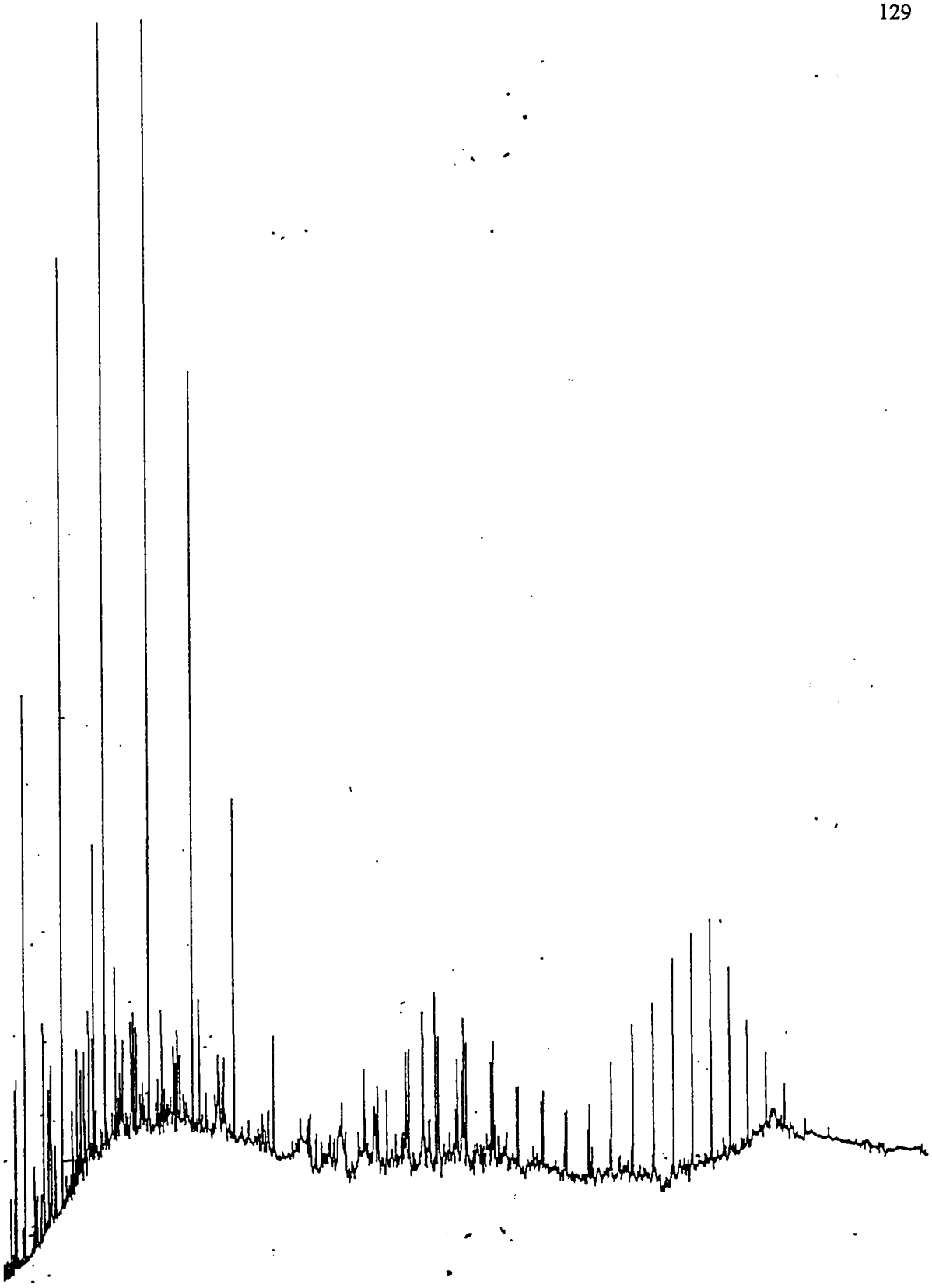

Figure 4.22 a. Gas chromatogram of the aromatic fraction of oil A3.

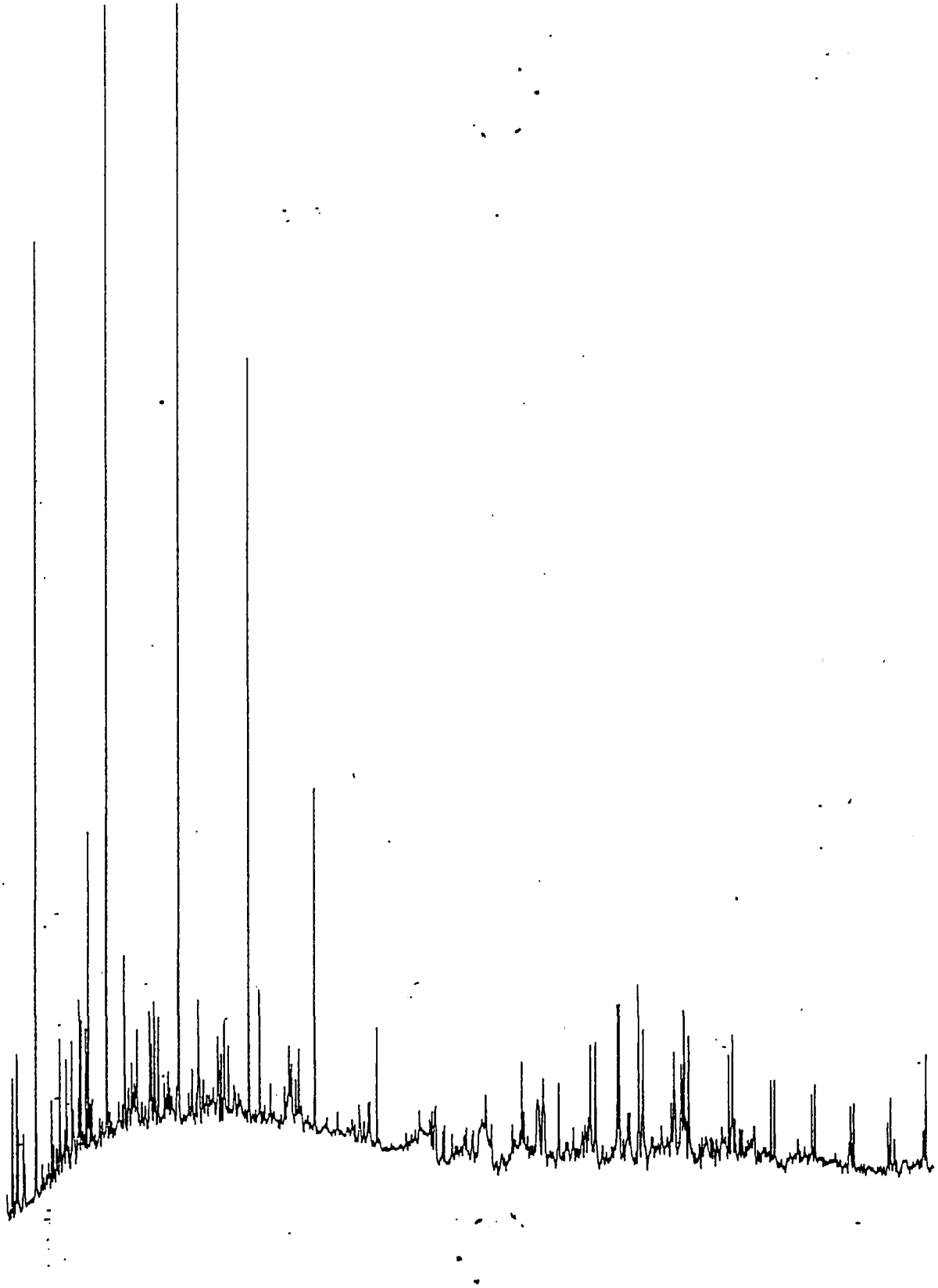

Figure 4.22 b. Gas chromatogram of the middle range (10-78 min.) of the aromatic fraction of oil A3.

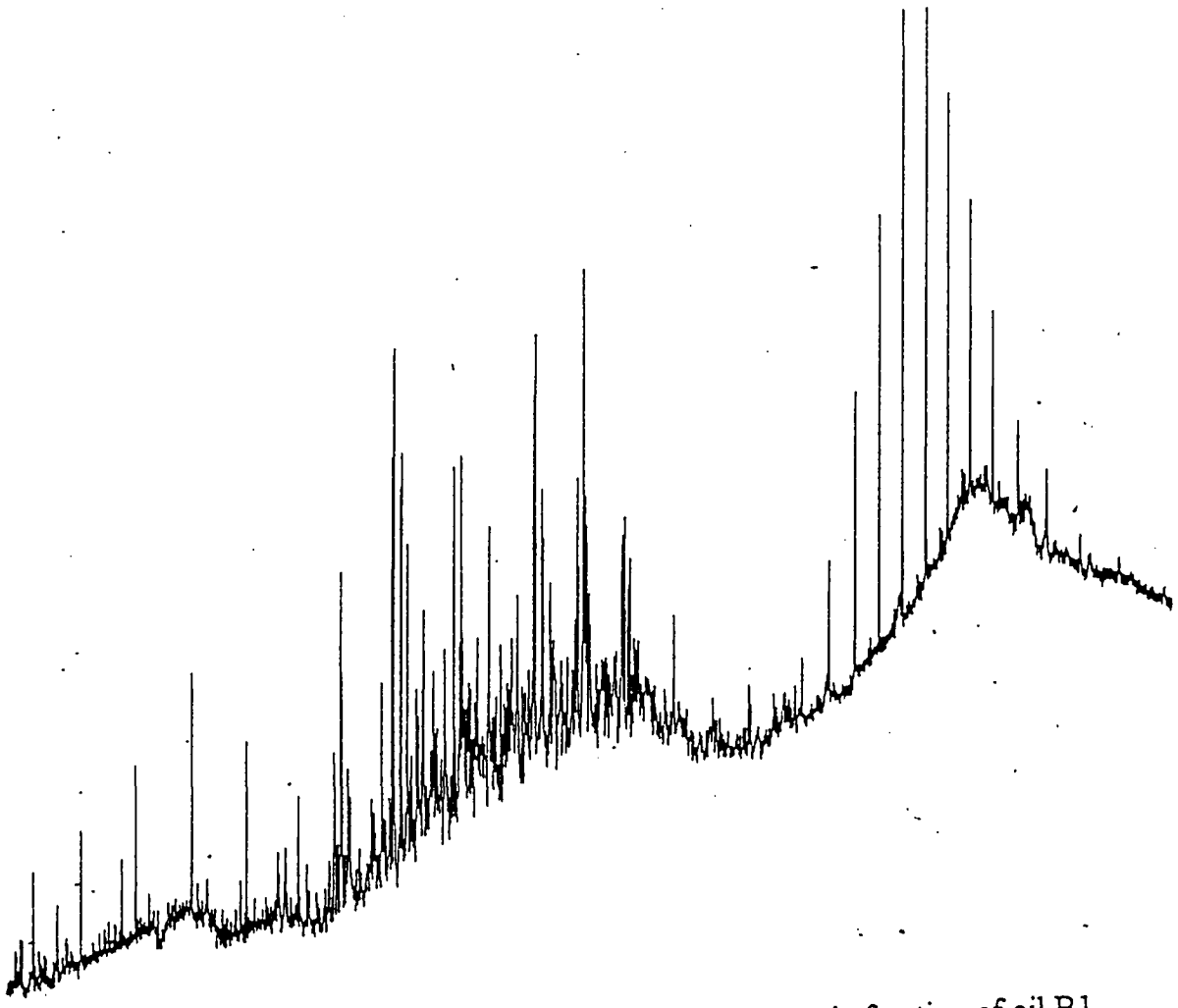

Figure 4.23 a. Gas chromatogram of the aromatic fraction of oil B1.

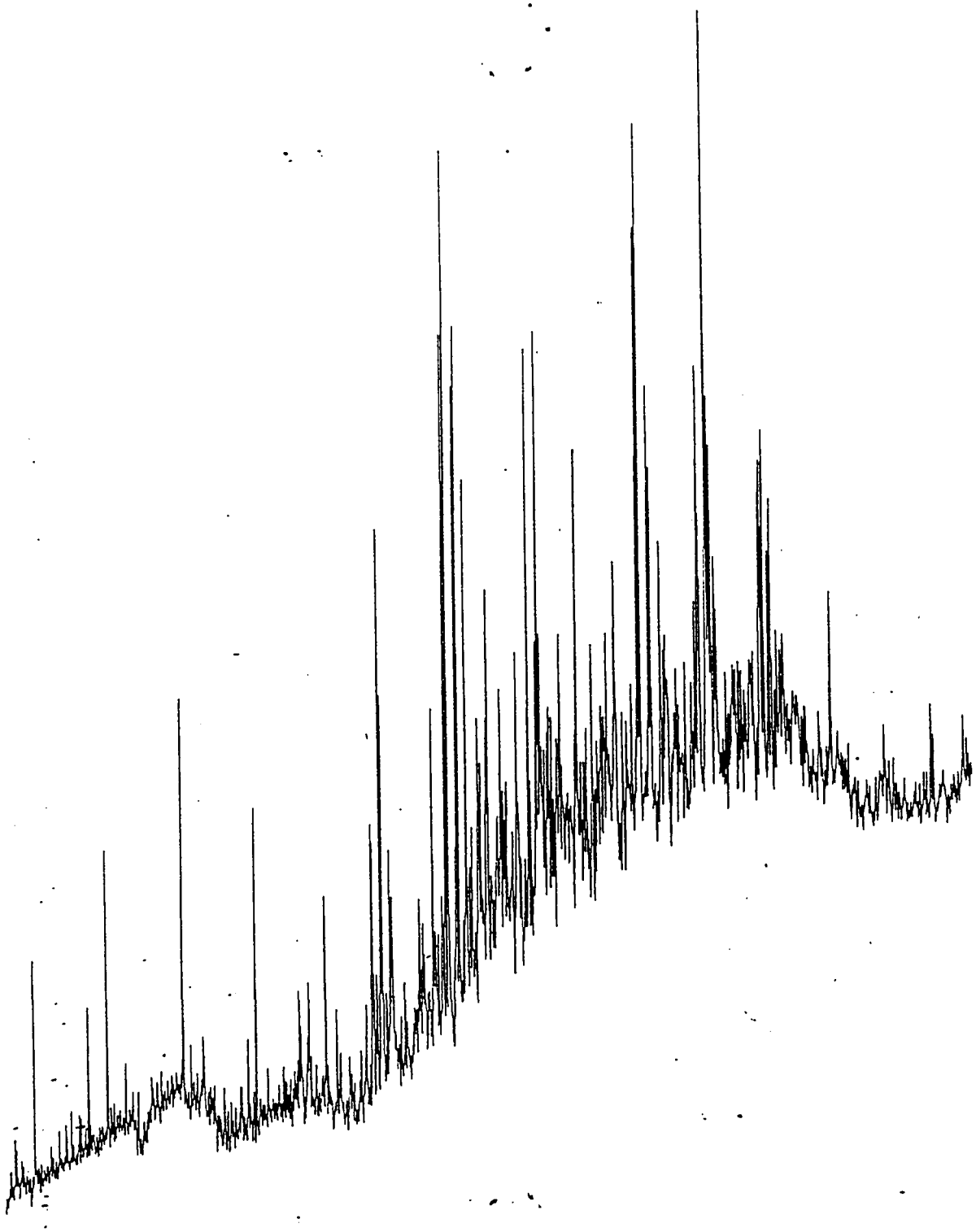

Figure 4.23 b. Gas chromatogram of the middle range (10-78 min.) of the aromatic fraction of oil B1.

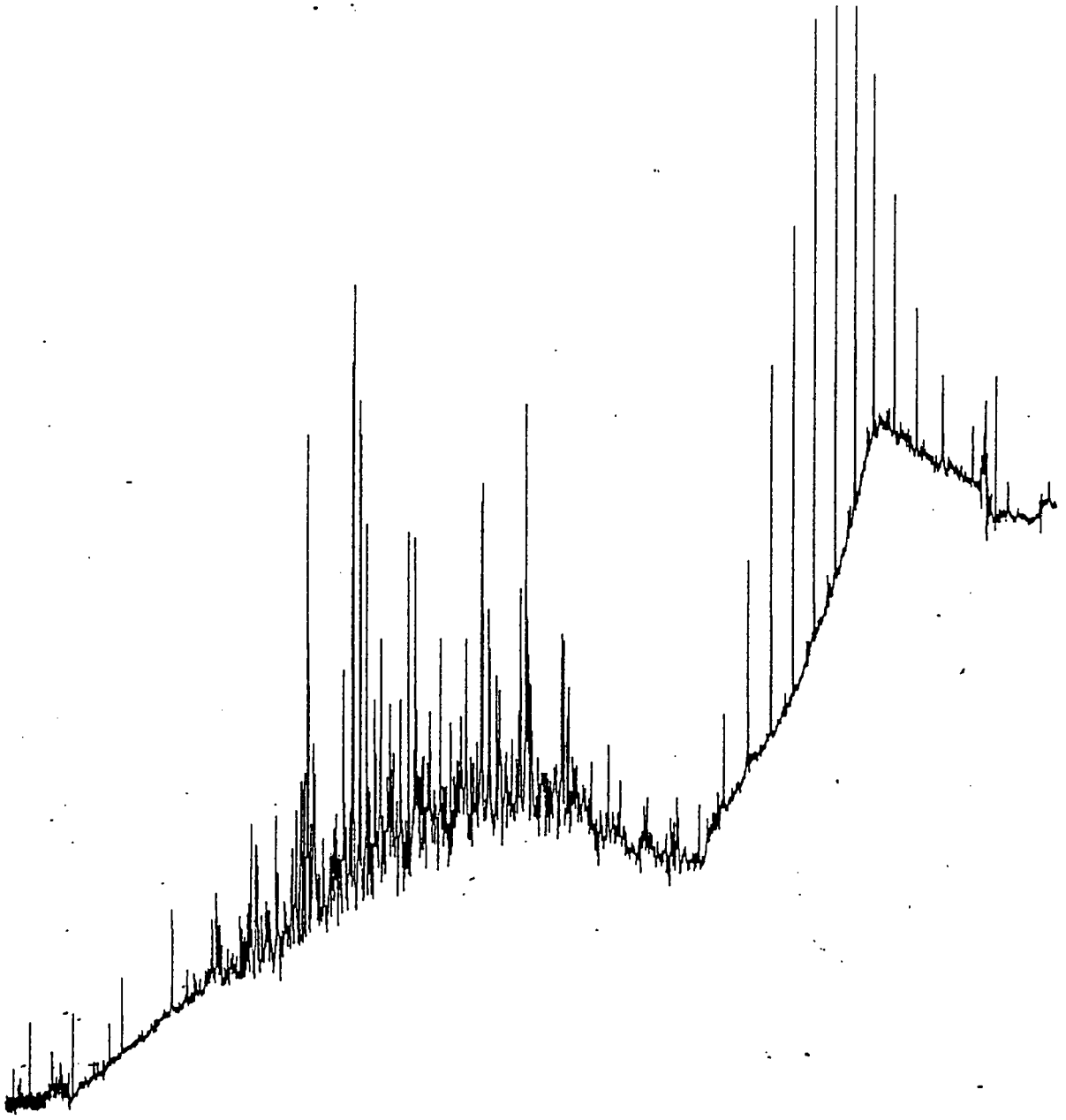

Figure 4.24 a. Gas chromatogram of the aromatic fraction of oil B2.

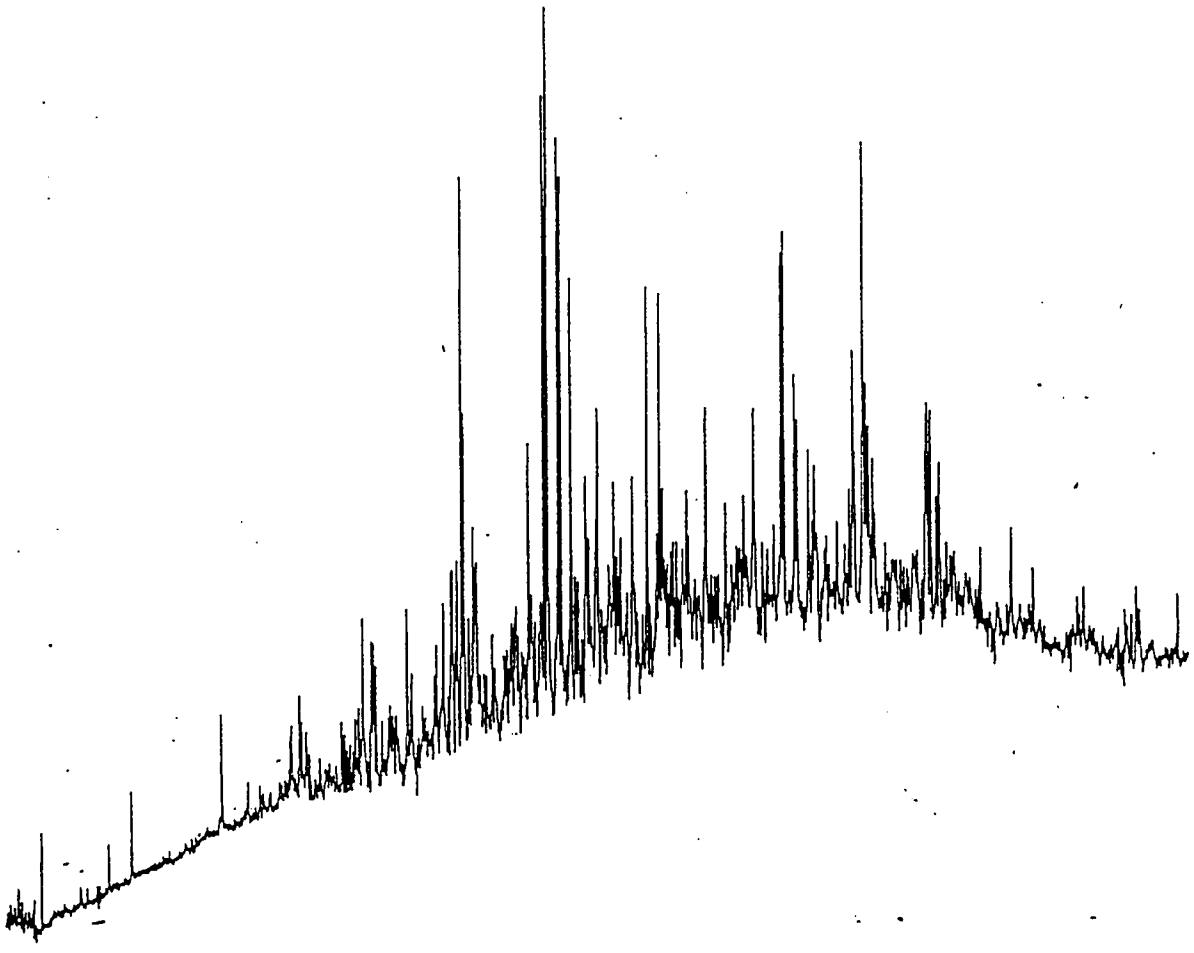

Figure 4.24 b. Gas chromatogram of the middle range (10-78 min.) of the aromatic fraction of oil B2.

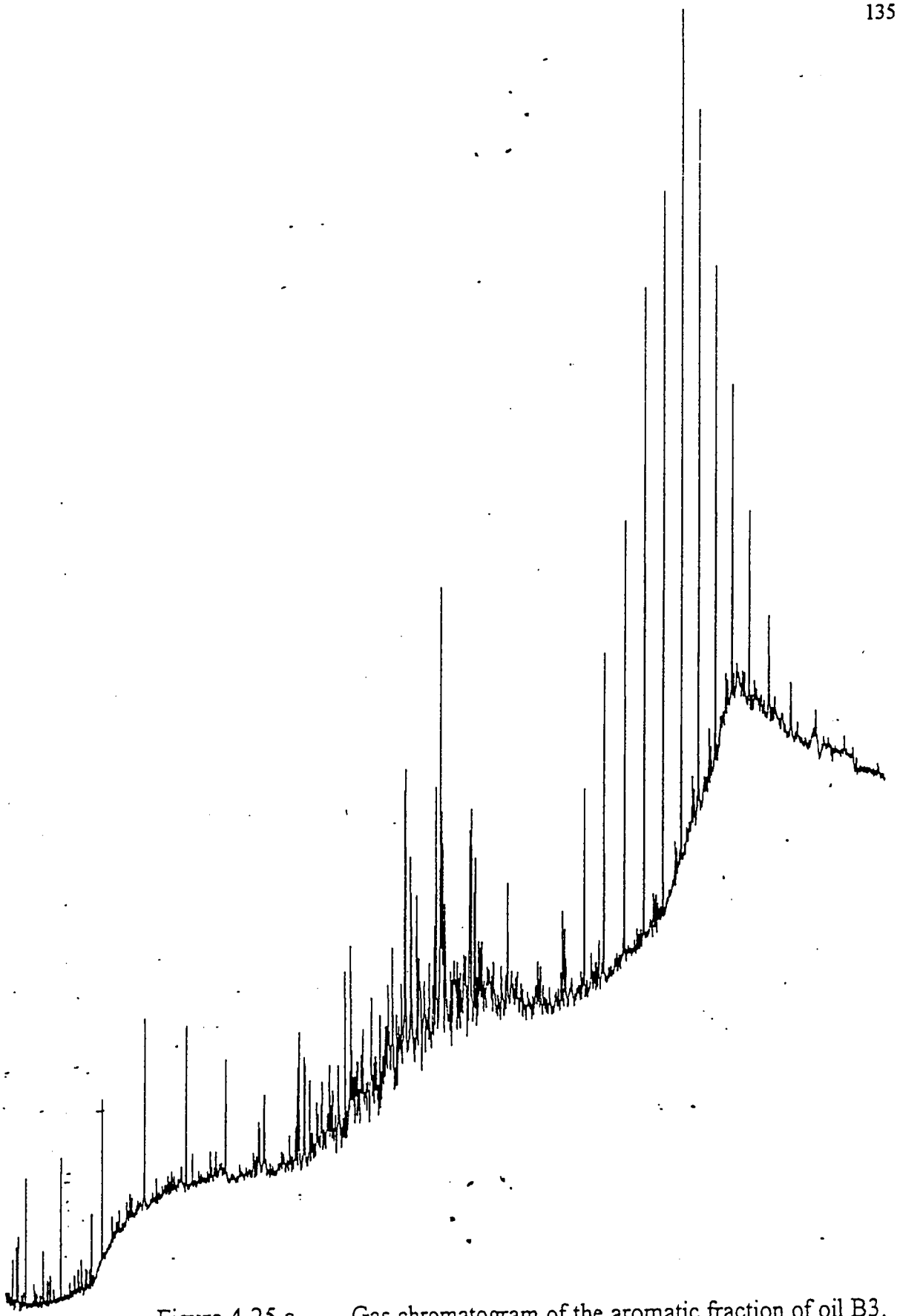

Figure 4.25 a. Gas chromatogram of the aromatic fraction of oil B3.

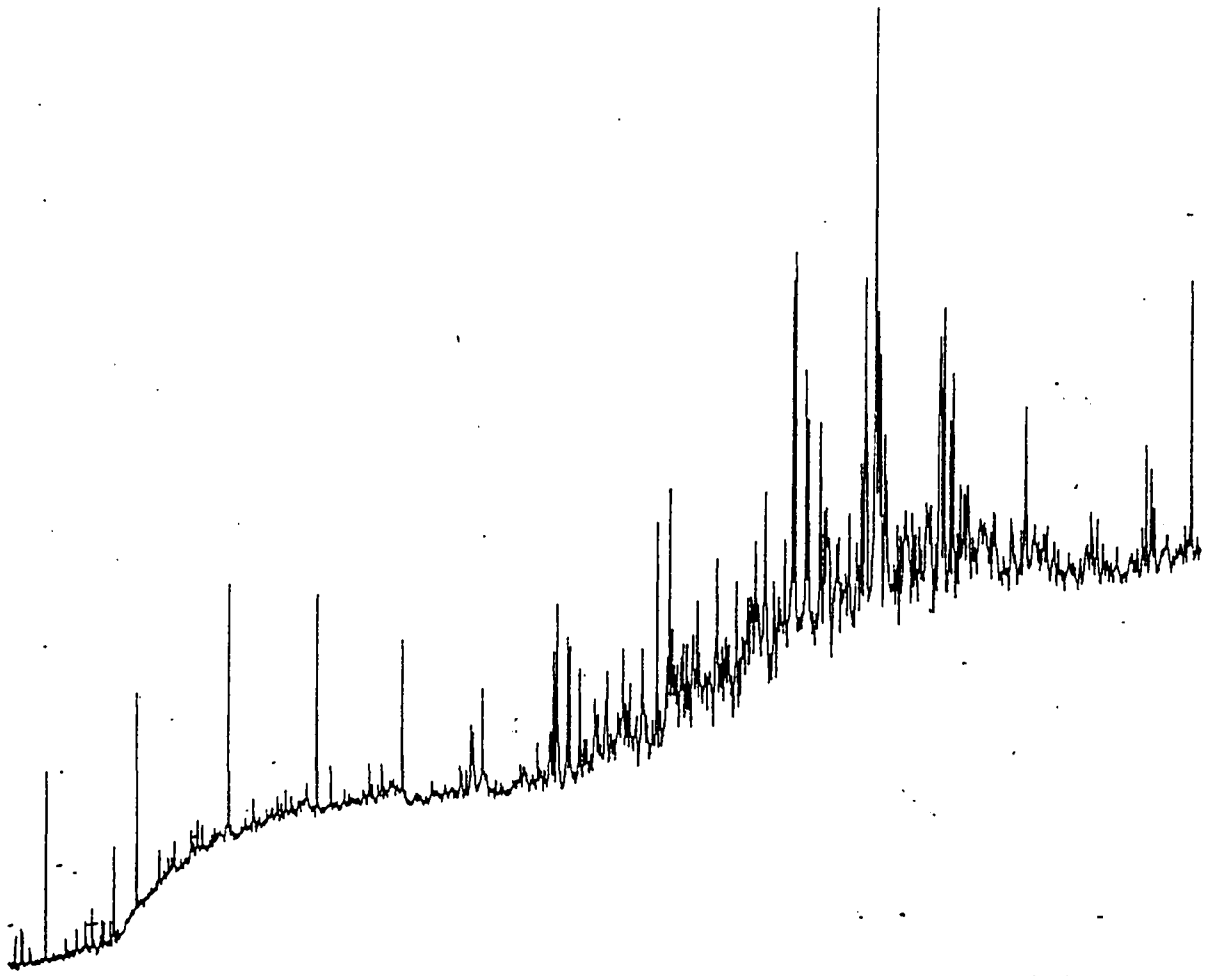

Figure 4.25 b. Gas chromatogram of the middle range (10-78 min.) of the aromatic fraction of oil B3.

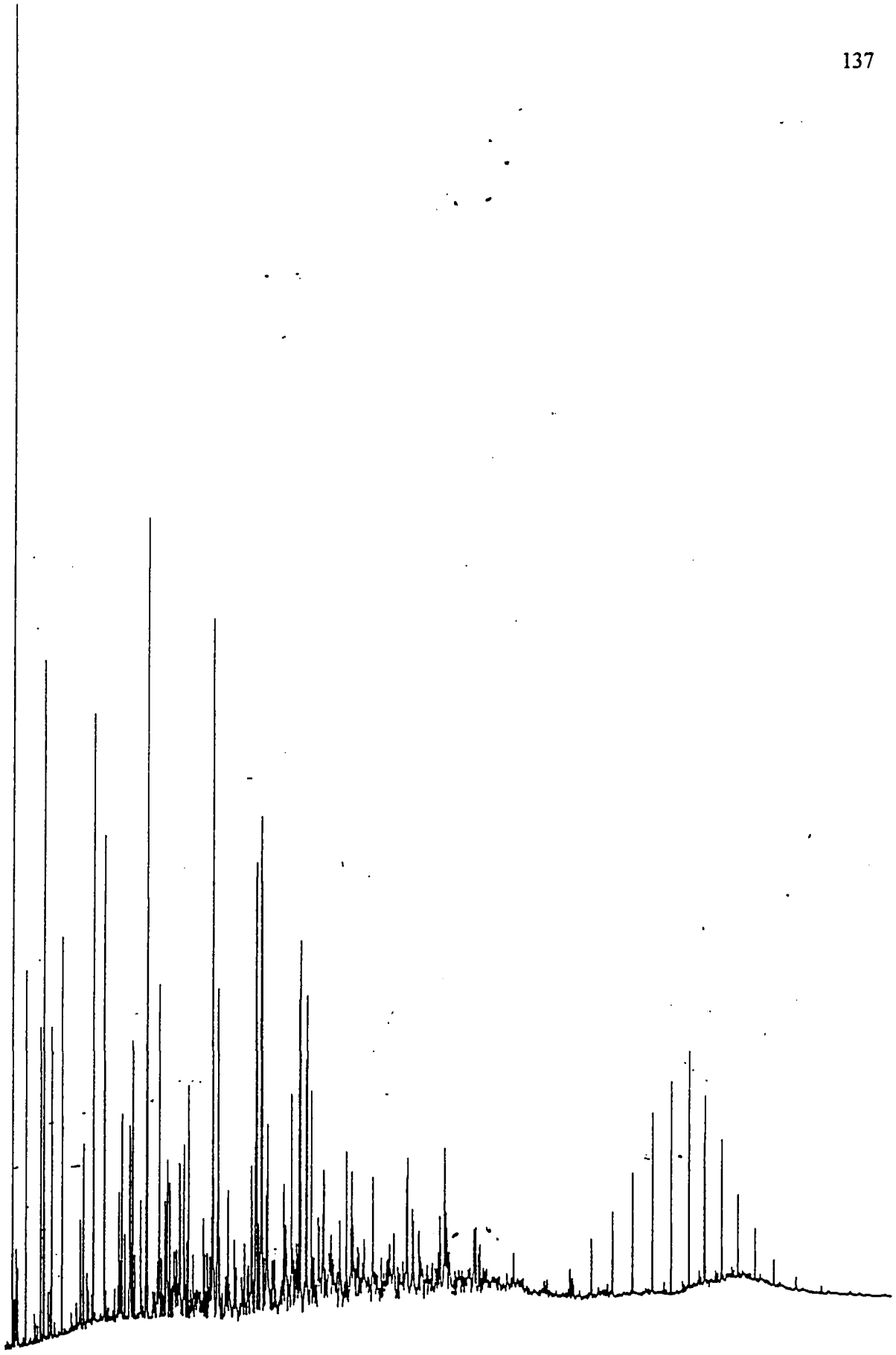

Figure 4.26 a. Gas chromatogram of the aromatic fraction of oil C1.

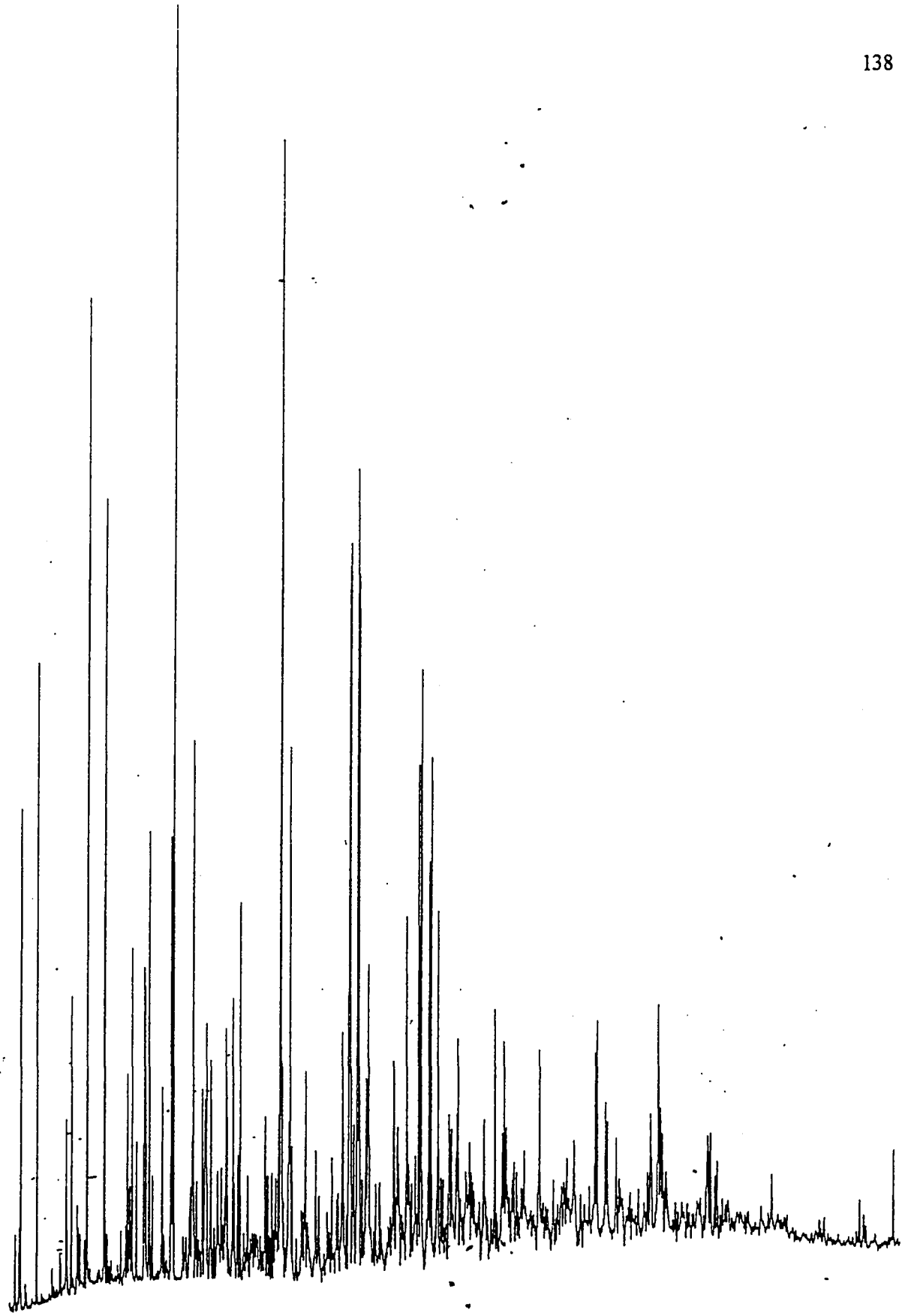

Figure 4.26 b. Gas chromatogram of the middle range (10-78 min.) of the aromatic fraction of oil C1.

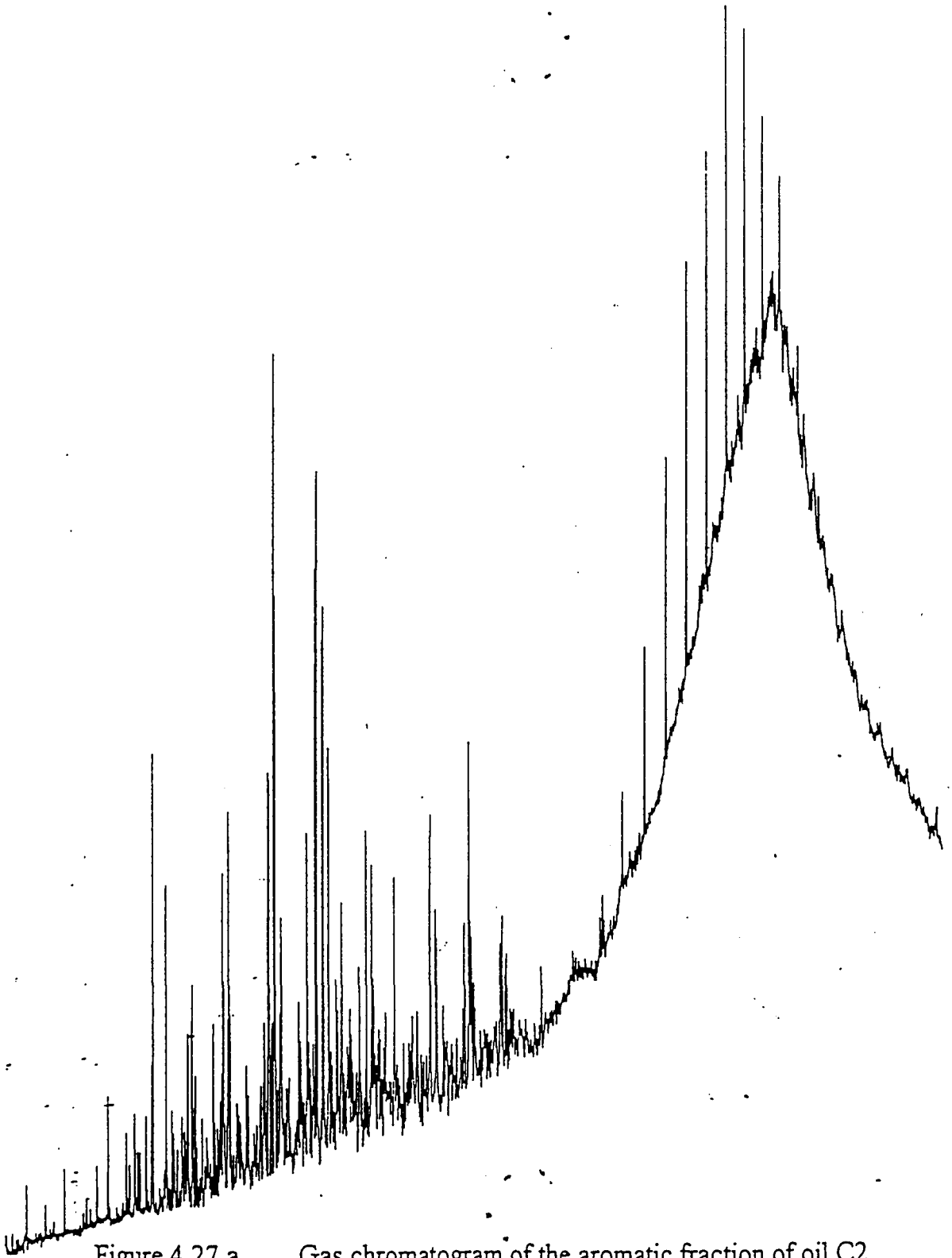

Figure 4.27 a. Gas chromatogram of the aromatic fraction of oil C2.

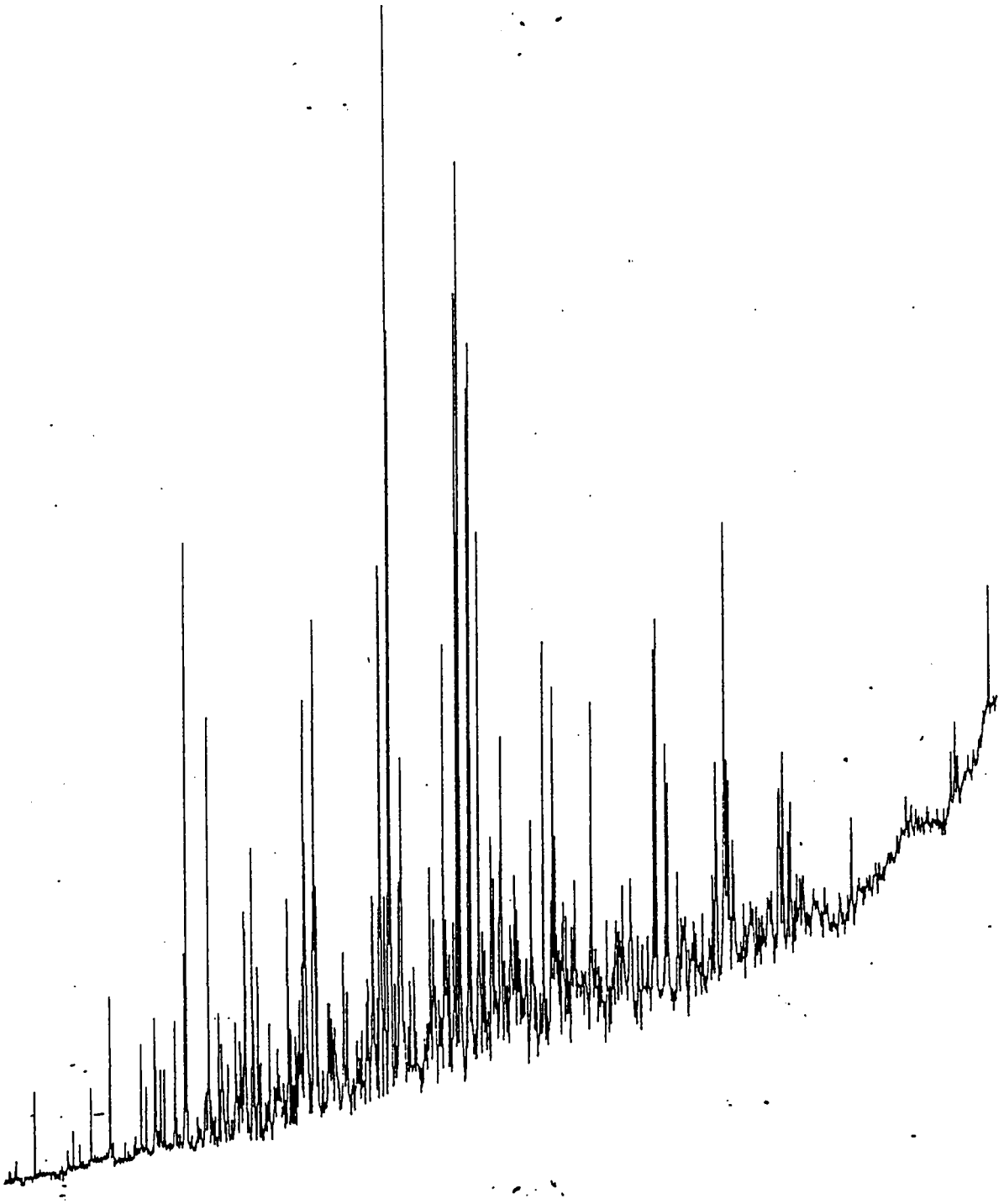

Figure 4.27 b. Gas chromatogram of the middle range (10-78 min.) of the aromatic fraction of oil C2.

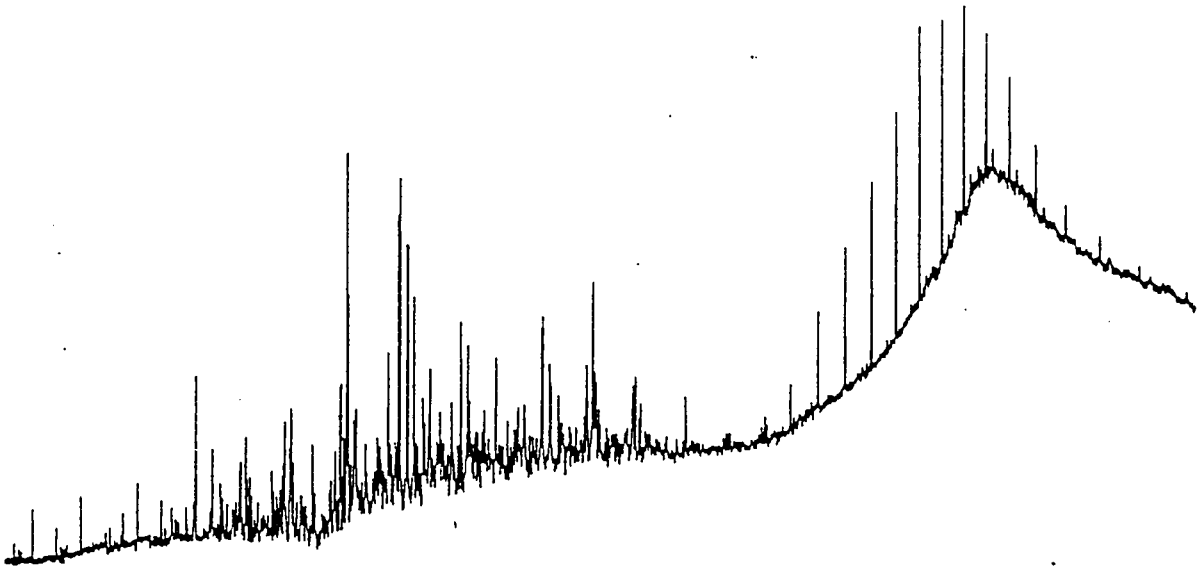

Figure 4.28 a. Gas chromatogram of the aromatic fraction of oil C3.

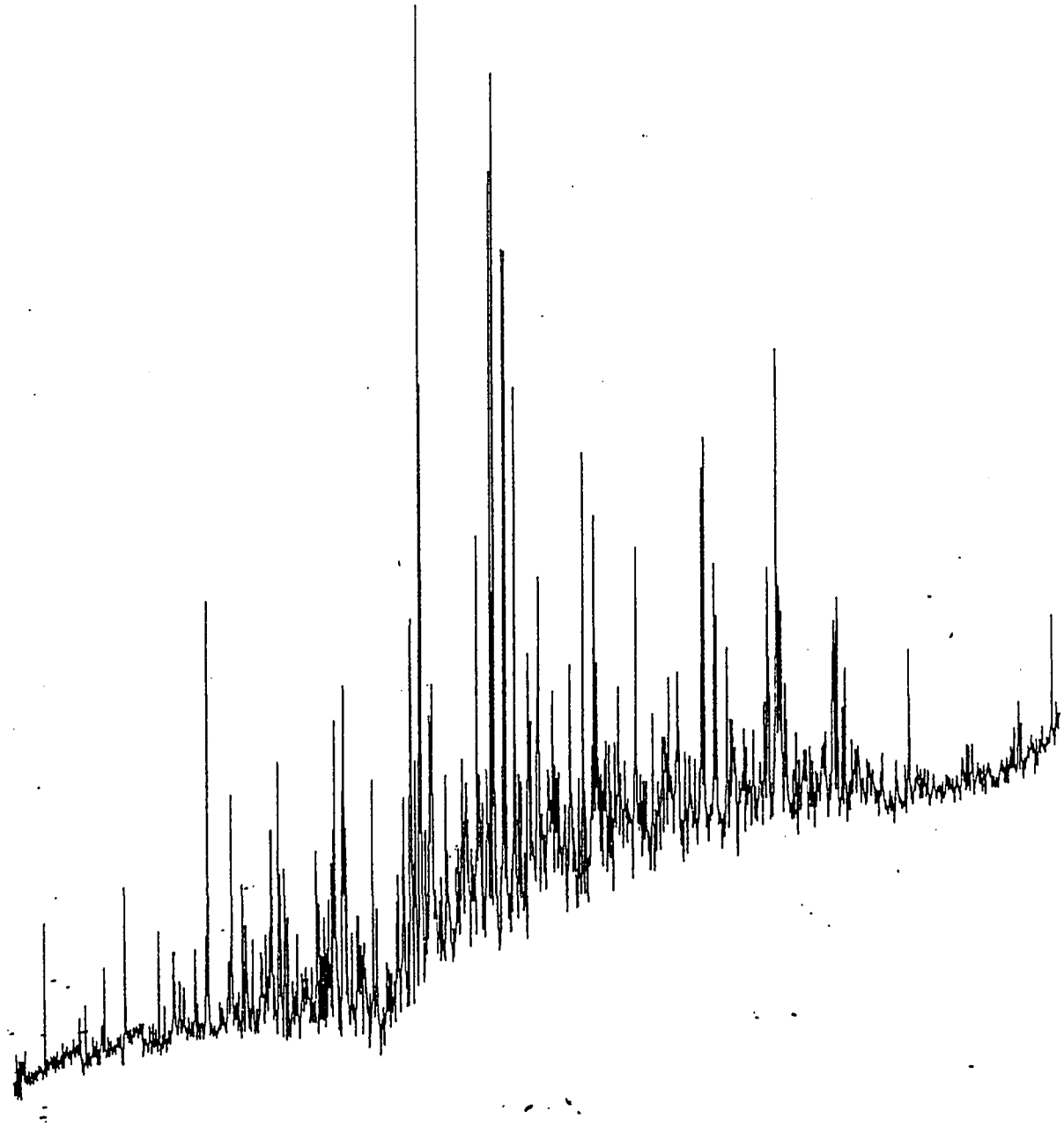

Figure 4.28 b. Gas chromatogram of the middle range (10-78 min.) of the aromatic fraction of oil C3.

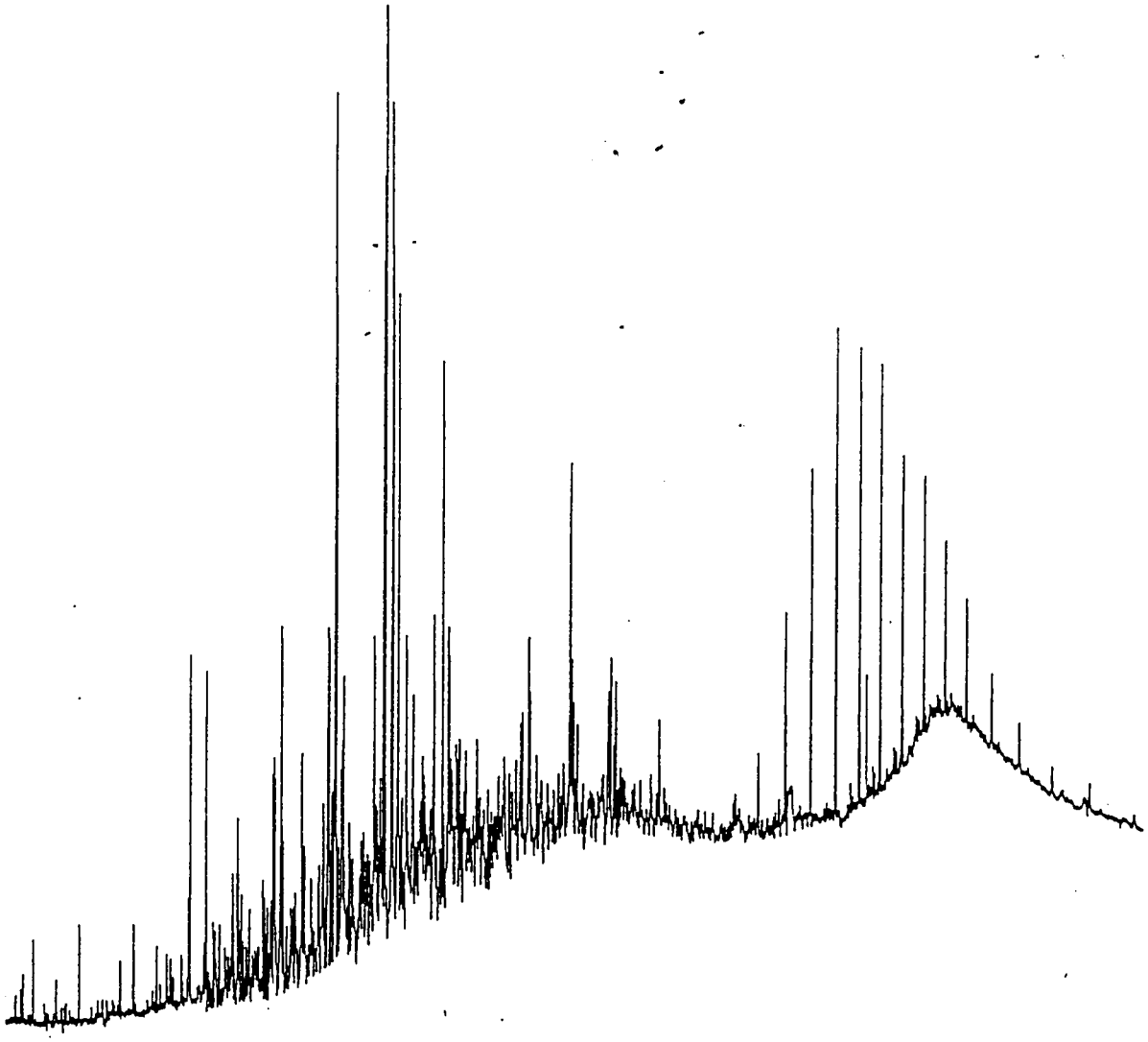

Figure 4.29 a. Gas chromatogram of the aromatic fraction of oil D1.

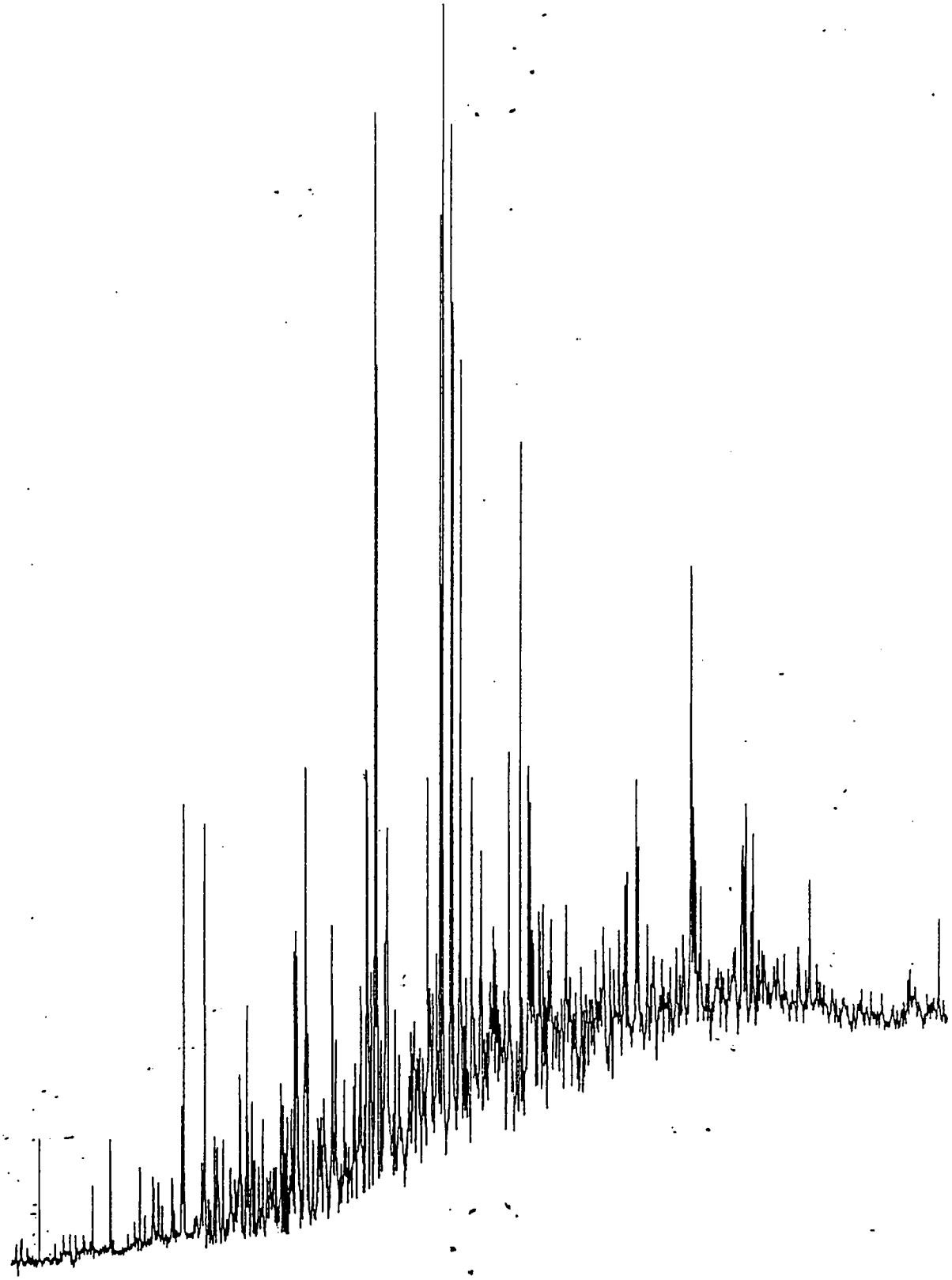

Figure 4.29 b. Gas chromatogram of the middle range (10-78 min.) of the aromatic fraction of oil D1.

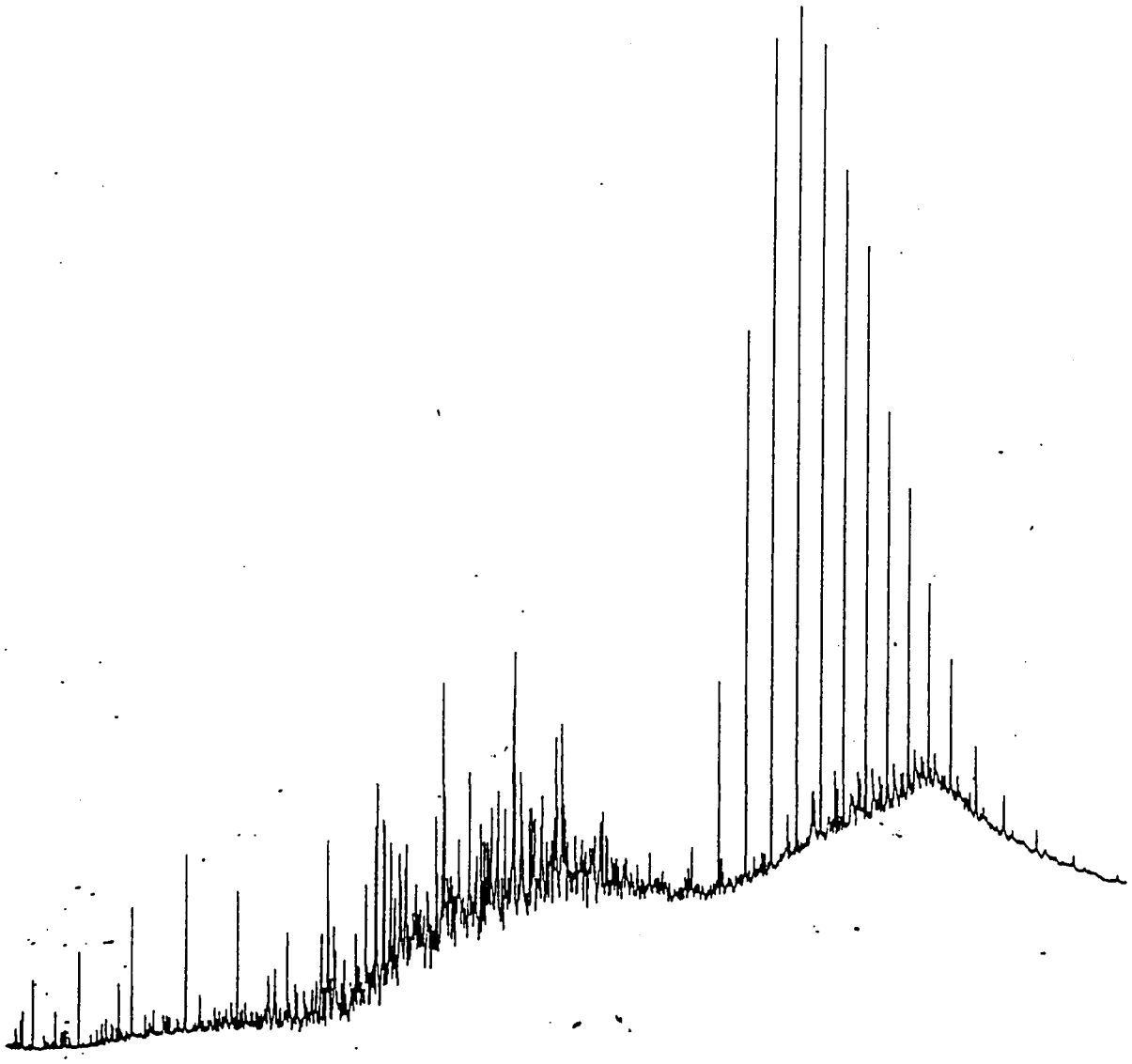

Figure 4.30 a. Gas chromatogram of the aromatic fraction of oil E1.

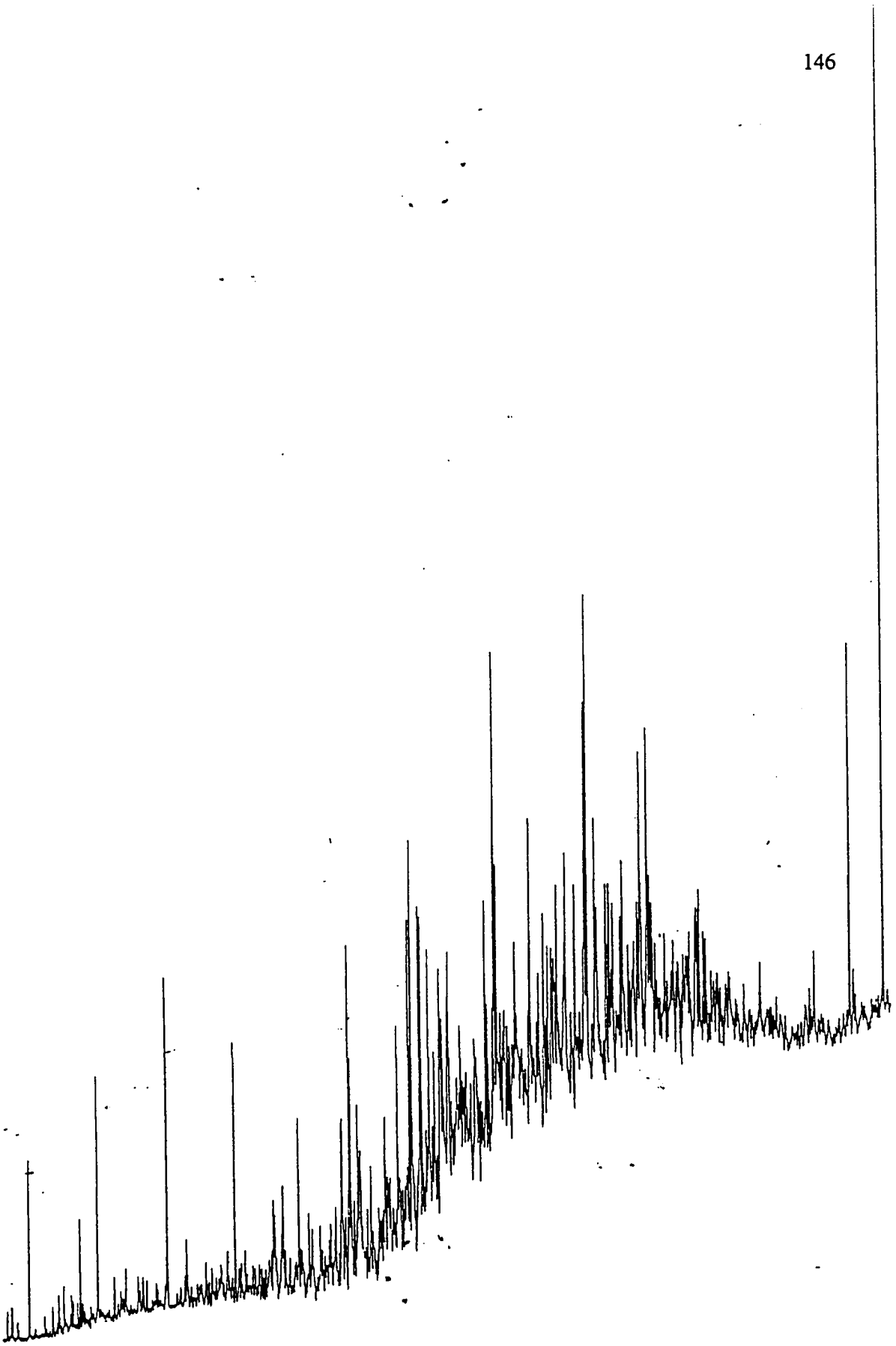

Figure 4.30 b. Gas chromatogram of the middle range (10-78 min.) of the aromatic fraction of oil E1.

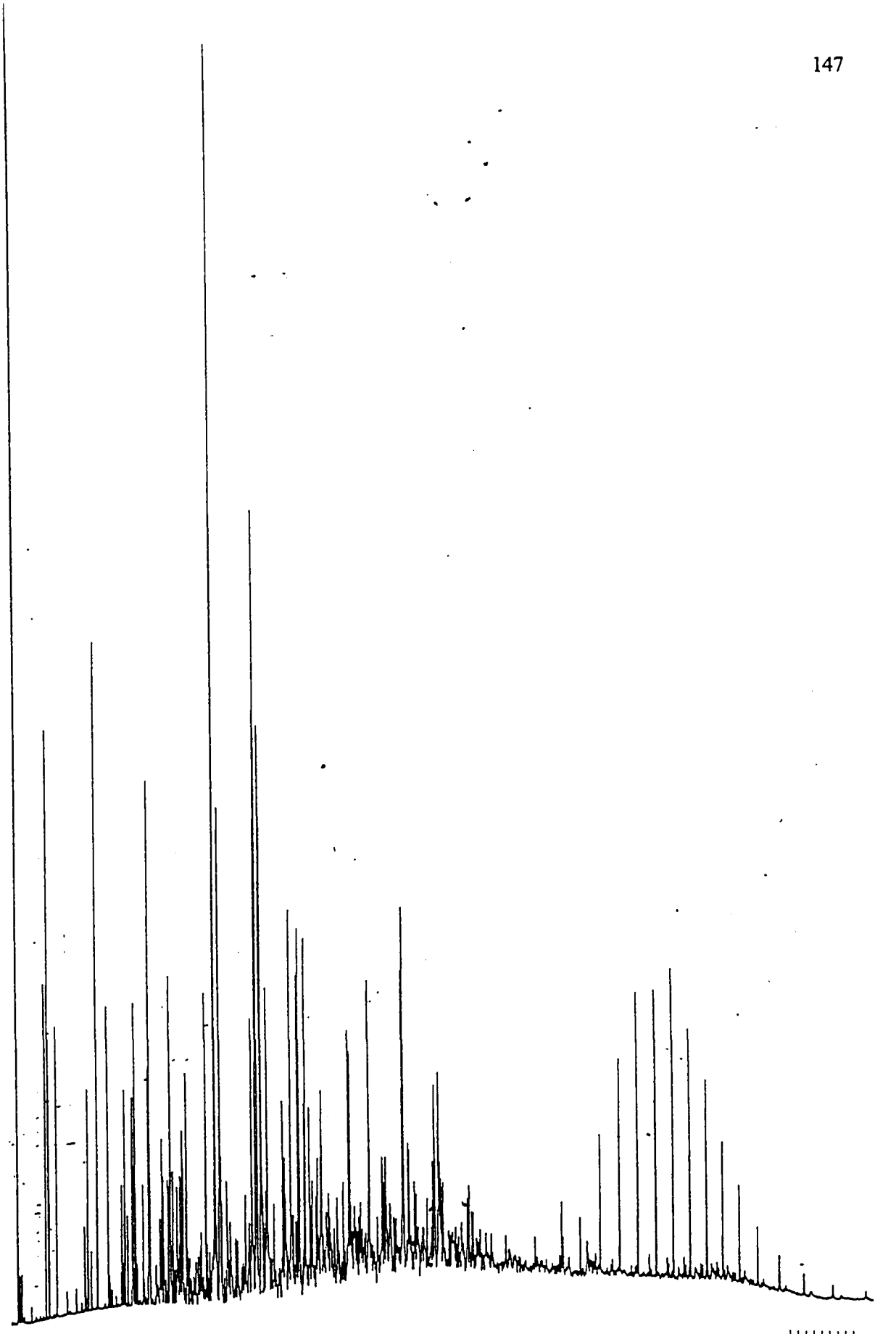

Figure 4.31 a. Gas chromatogram of the aromatic fraction of oil F1.

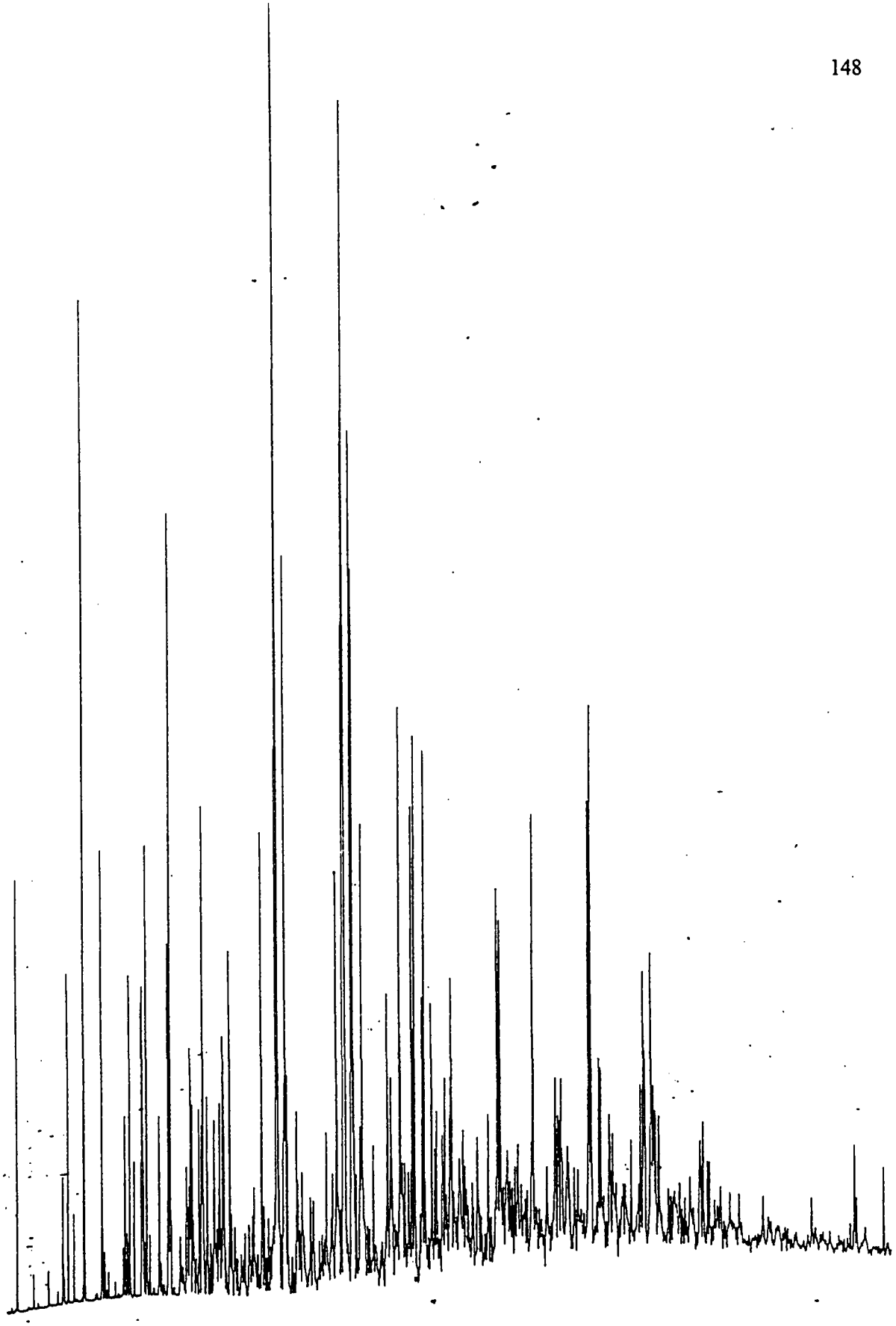

Figure 4.31 b. Gas chromatogram of the middle range (10-78 min.) of the aromatic fraction of oil F1.

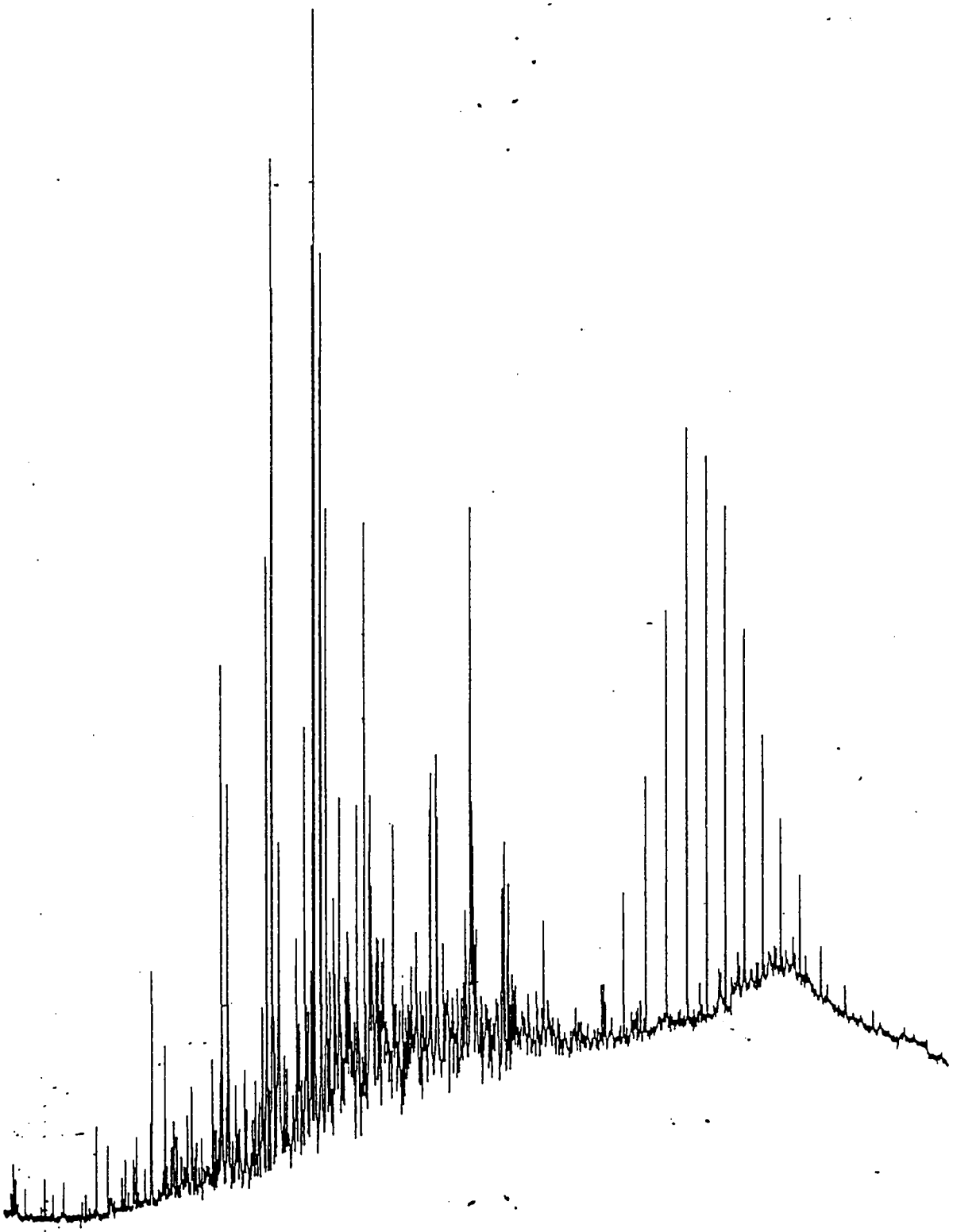

Figure 4.32 a. Gas chromatogram of the aromatic fraction of oil G1.

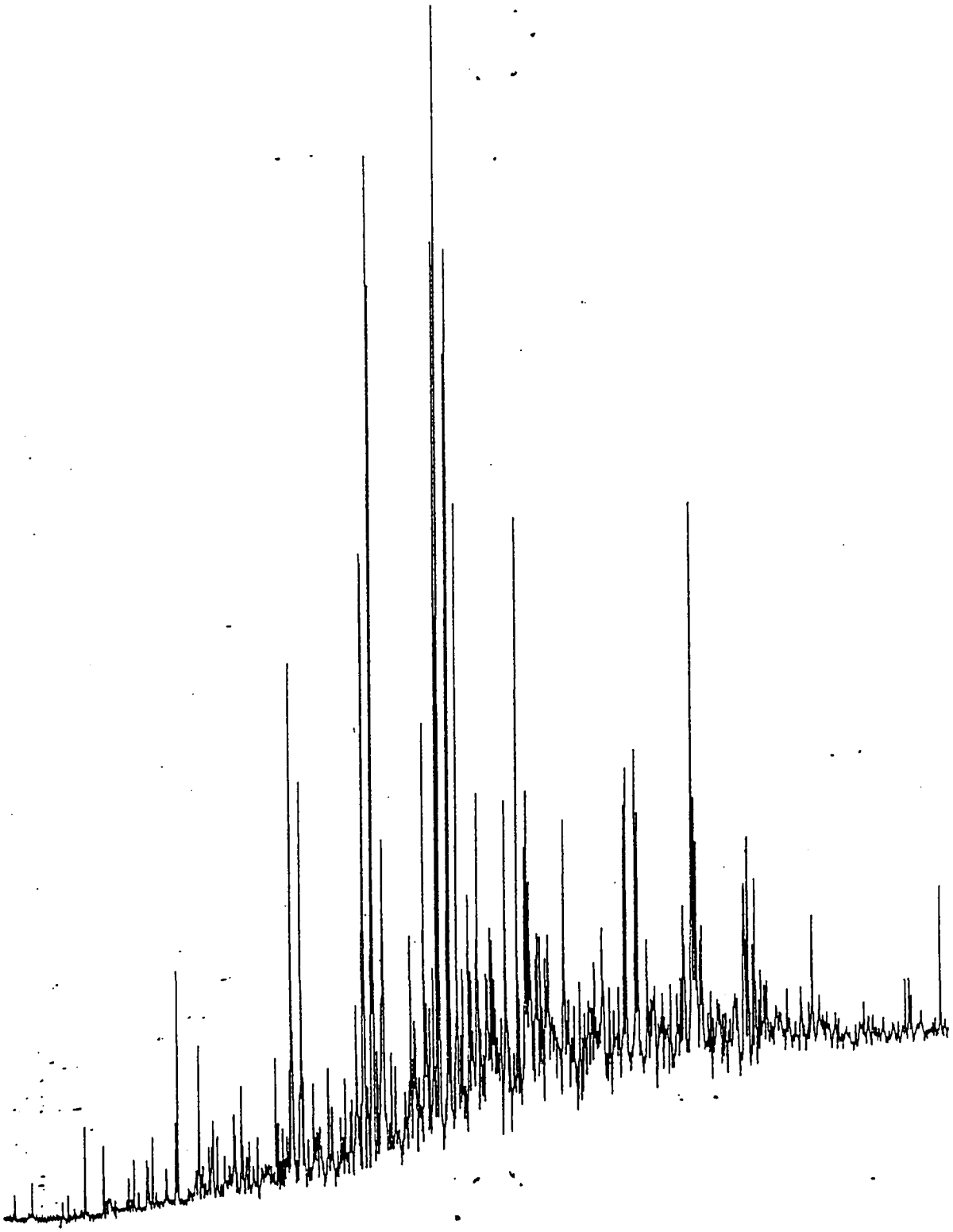

Figure 4.32 b. Gas chromatogram of the middle range (10-78 min.) of the aromatic fraction of oil G1.

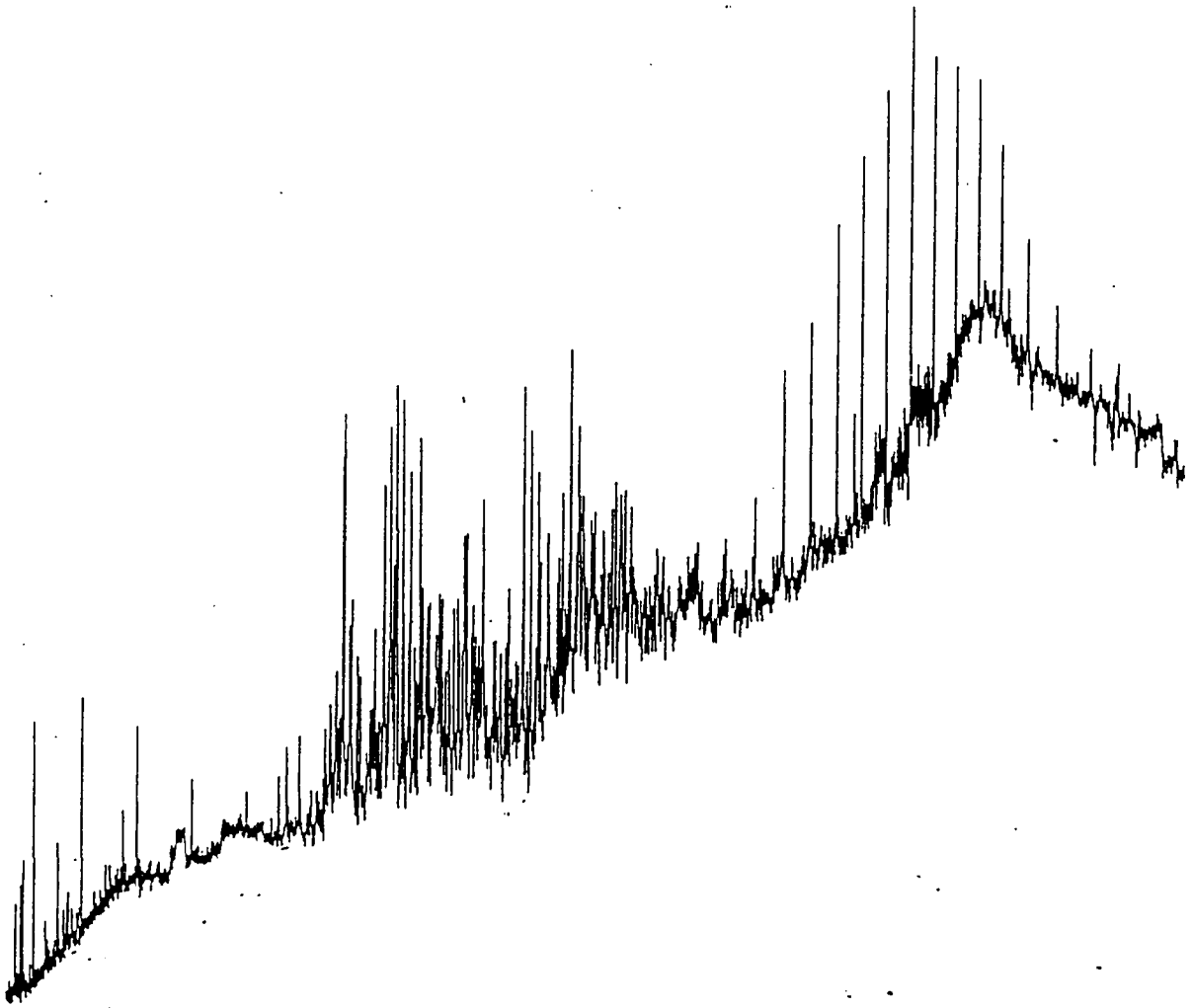

Figure 4.33 a. Gas chromatogram of the aromatic fraction of oil H1.

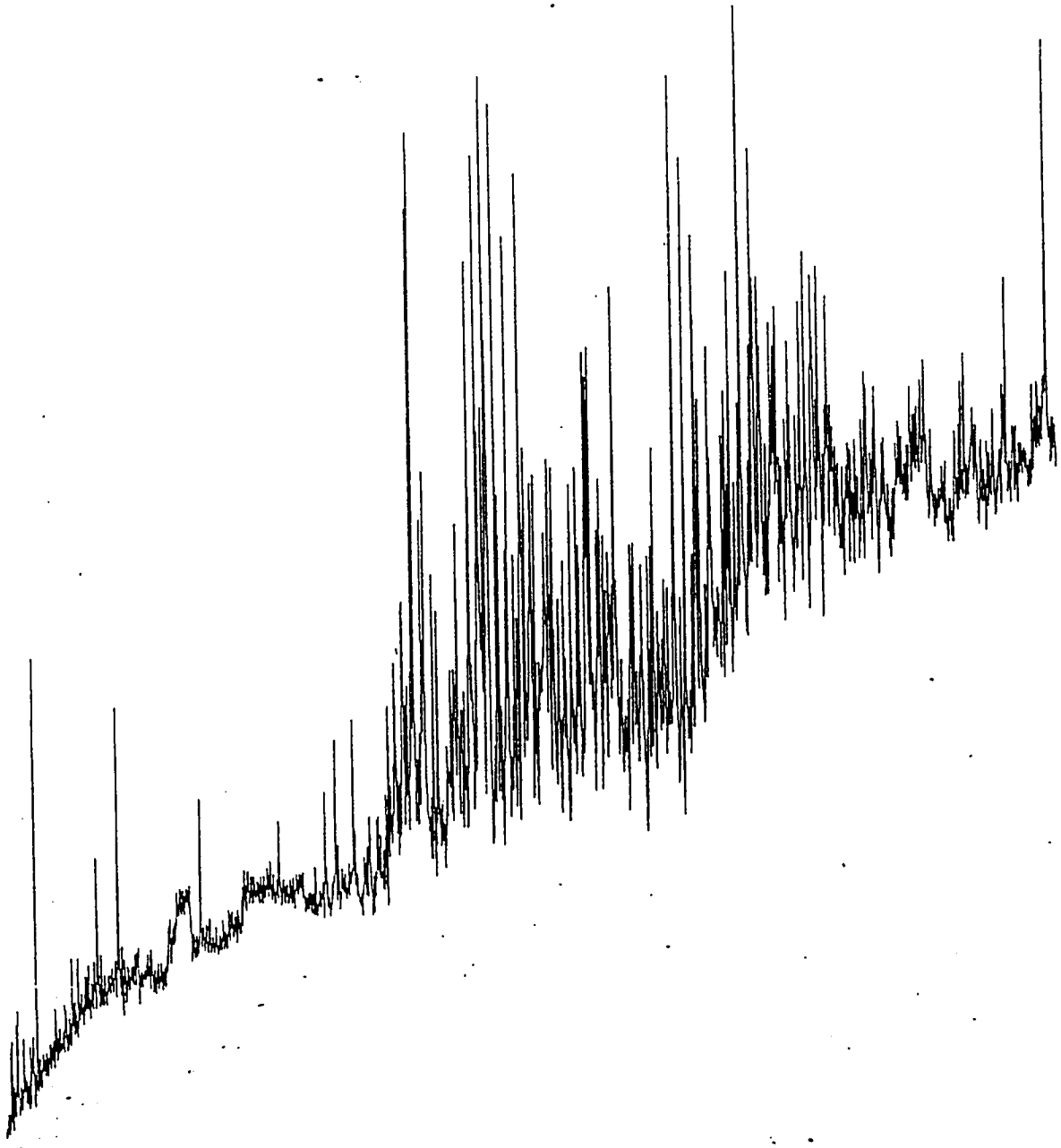

Figure 4.33 b. Gas chromatogram of the middle range (10-78 min.) of the aromatic fraction of oil H1.

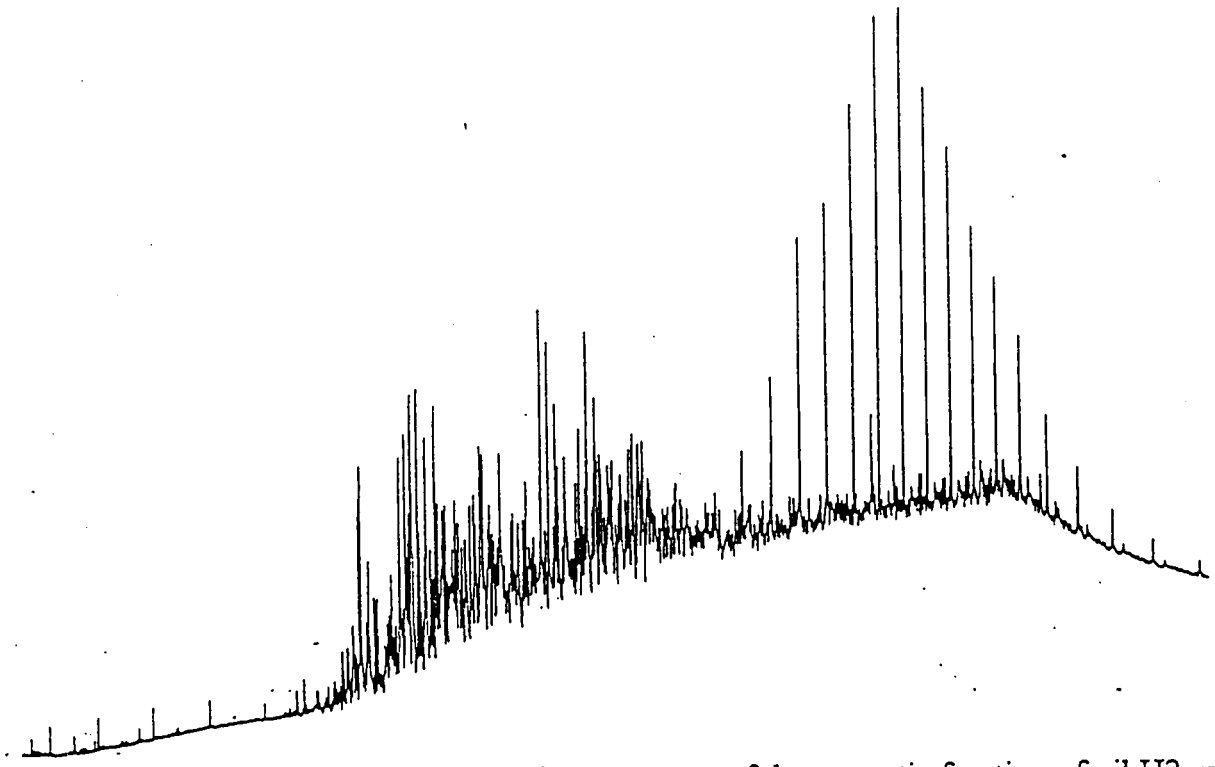

Figure 4.34 a. Gas chromatogram of the aromatiç fraction of oil H2. —

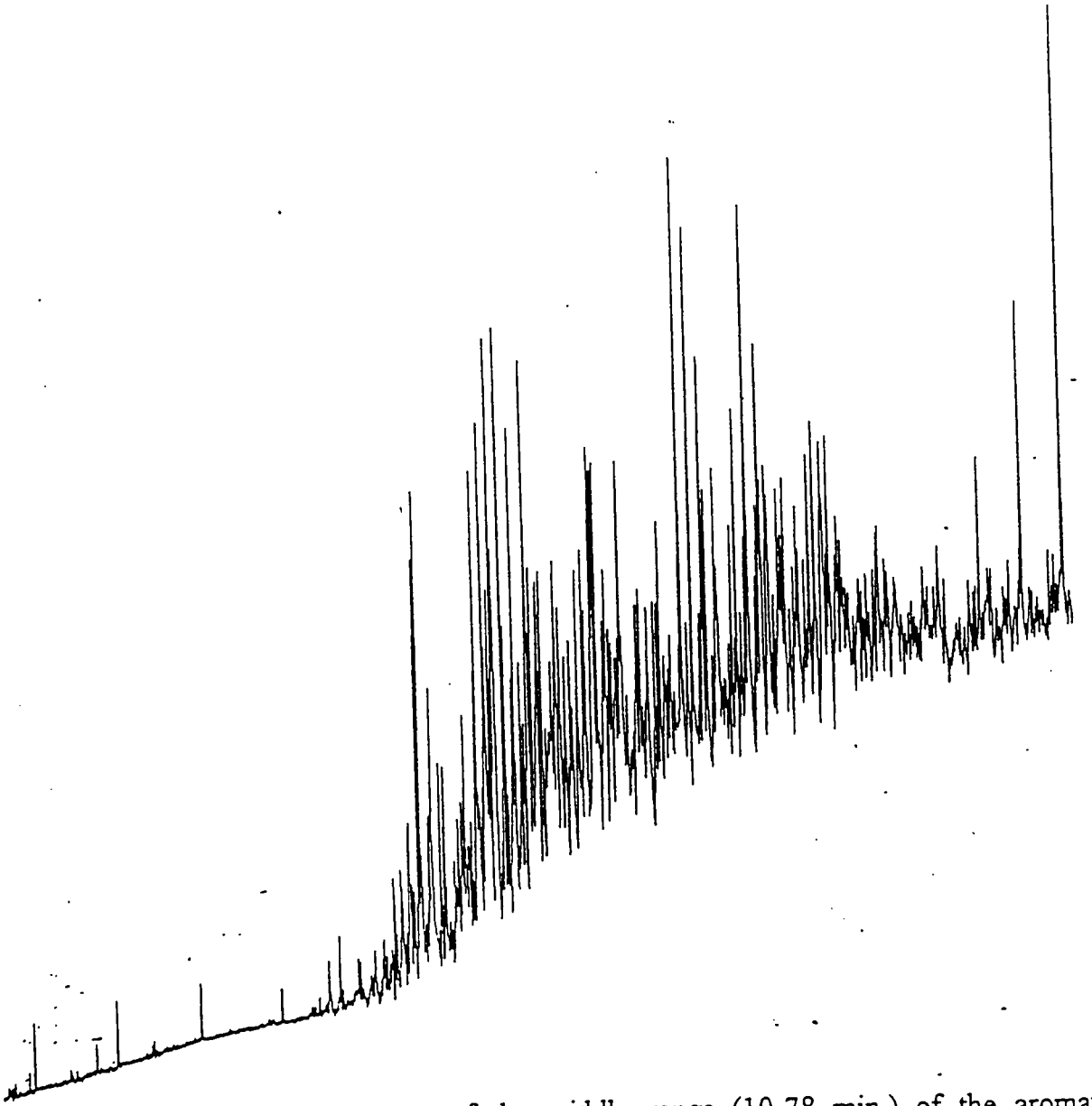

Figure 4.34 b. Gas chromatogram of the middle range (10-78 min.) of the aromatic fraction of oil H2.

Appendix (C)

Whole-Oil GC Chromatograms

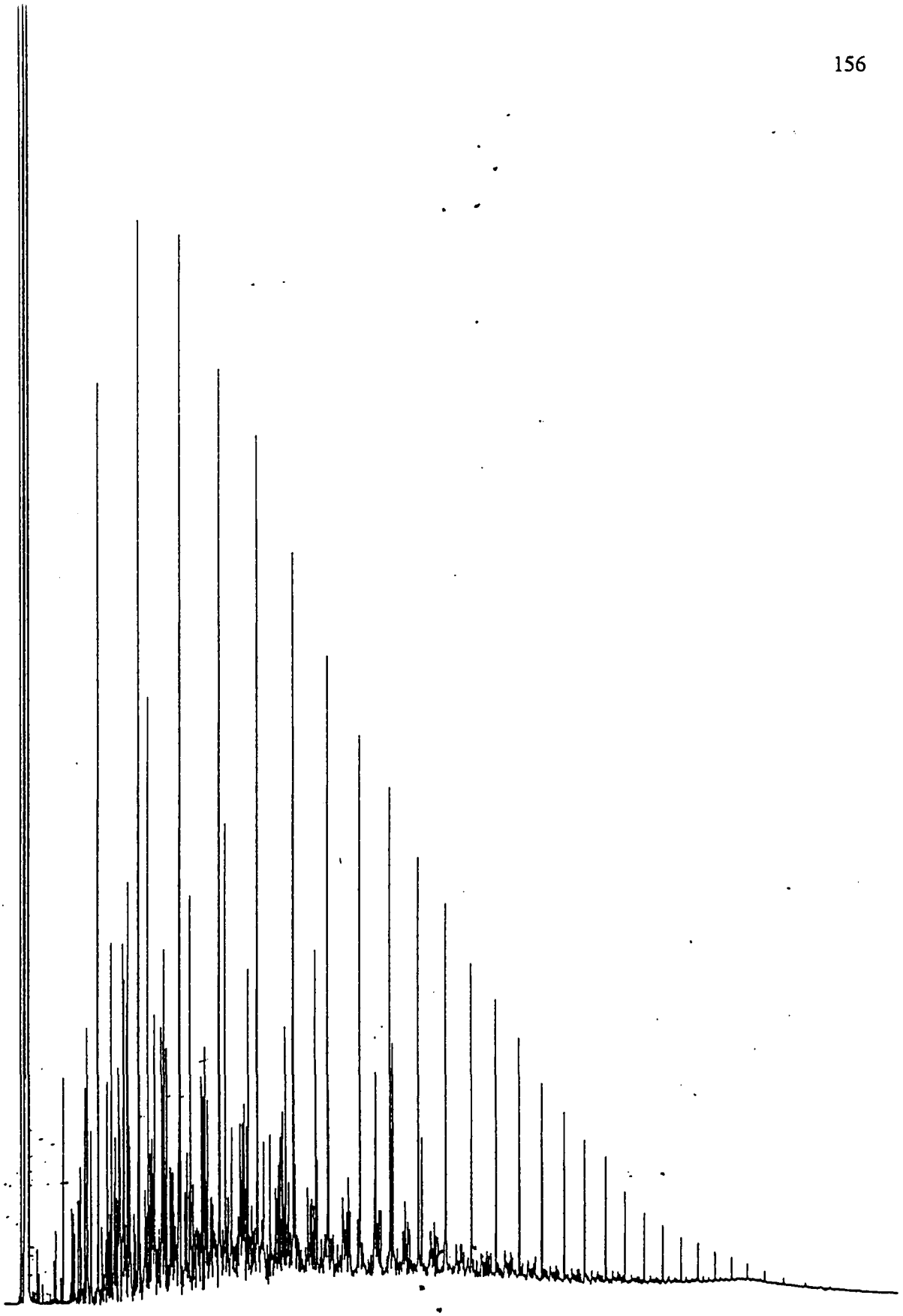

Figure 4.35 a. Whole-oil gas chromatogram of oil A1.

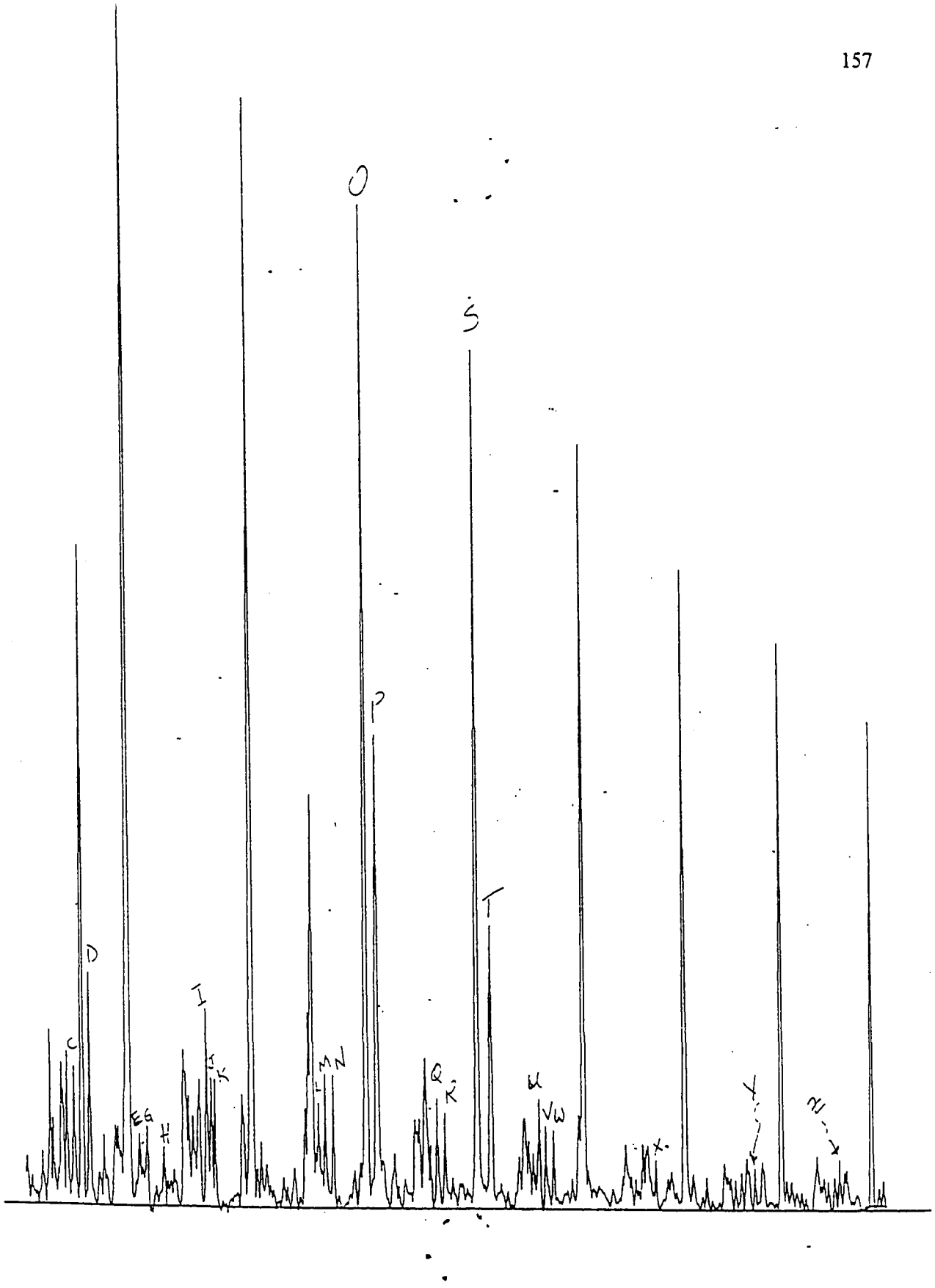

Figure 4.35 b. Whole-oil gas chromatogram of the middle range (38-67 min.) of oil A1.

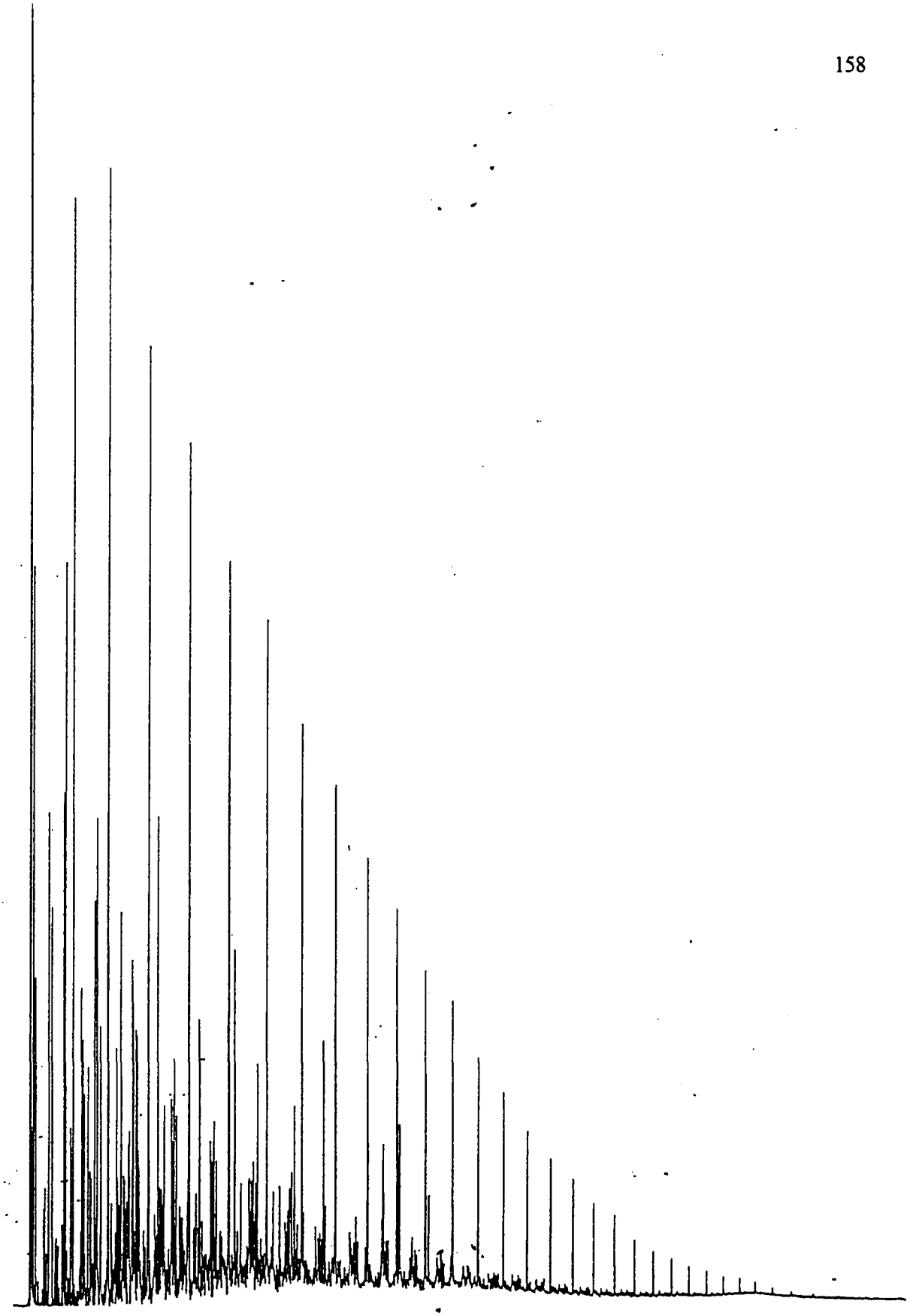

Figure 4.36 a. Whole-oil gas chromatogram of oil A2.

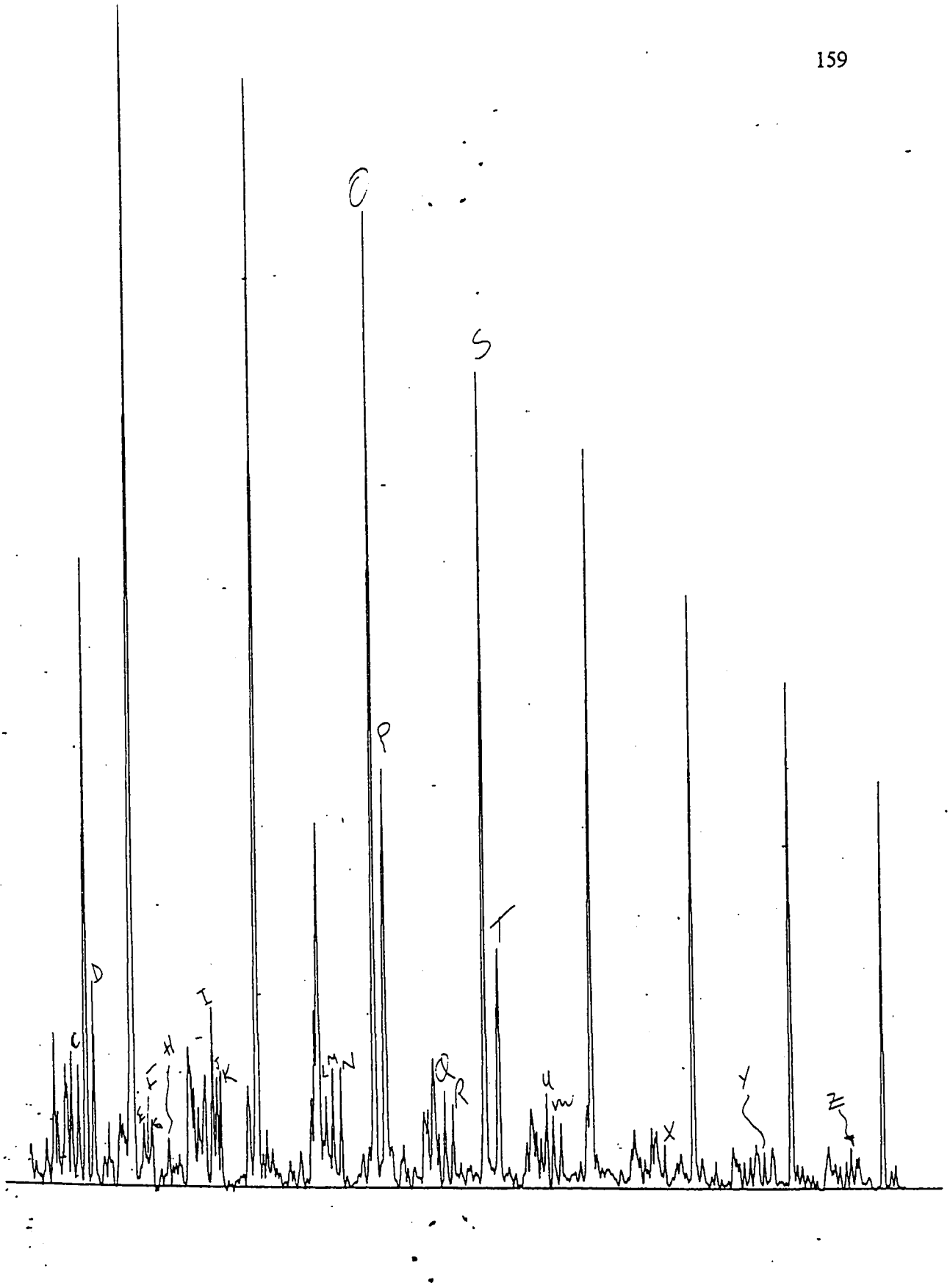

Figure 4.36 b. Whole-oil gas chromatogram of the middle range (38-67 min.) of oil A2.

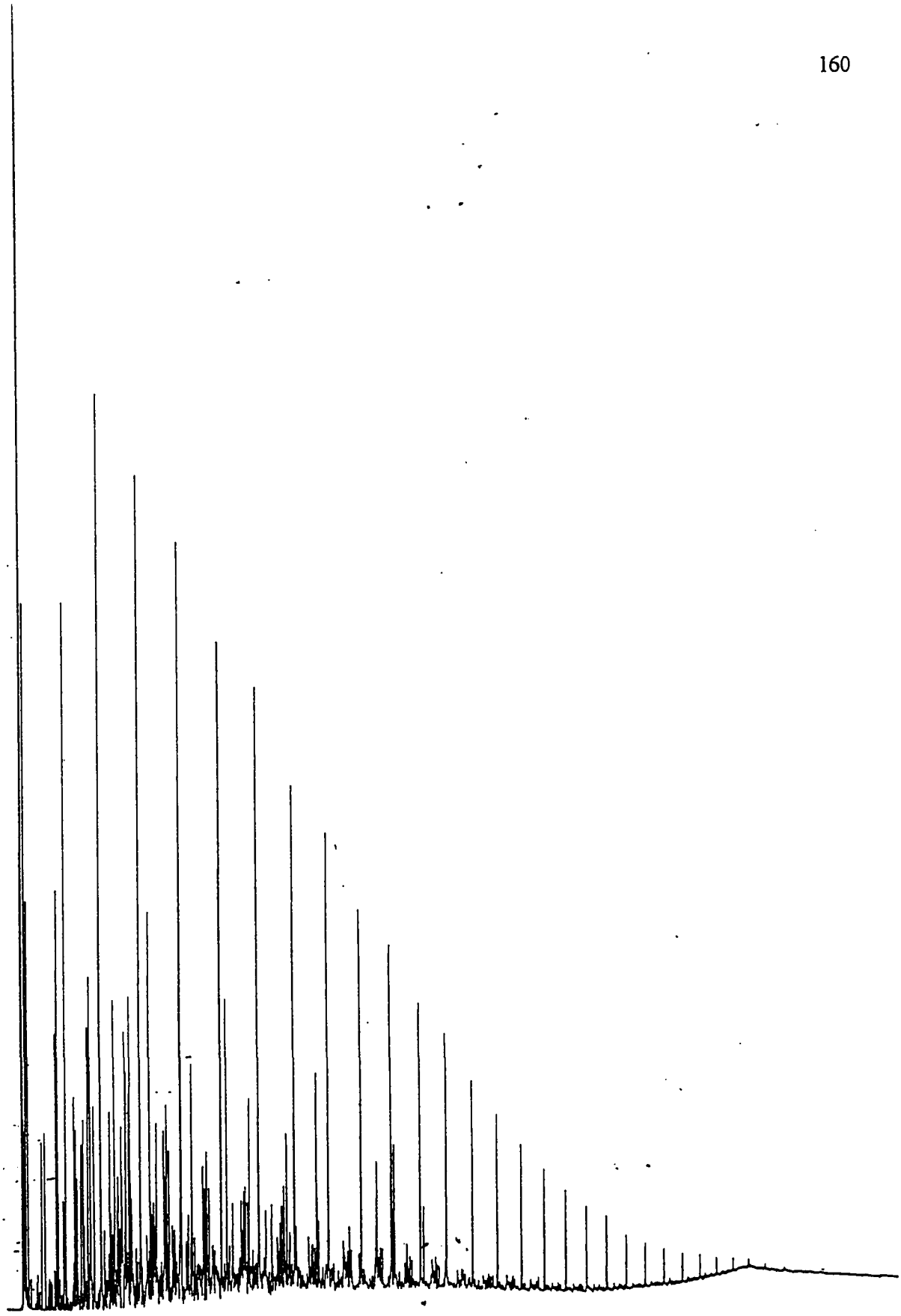

Figure 4.37 a. Whole-oil gas chromatogram of oil A3.

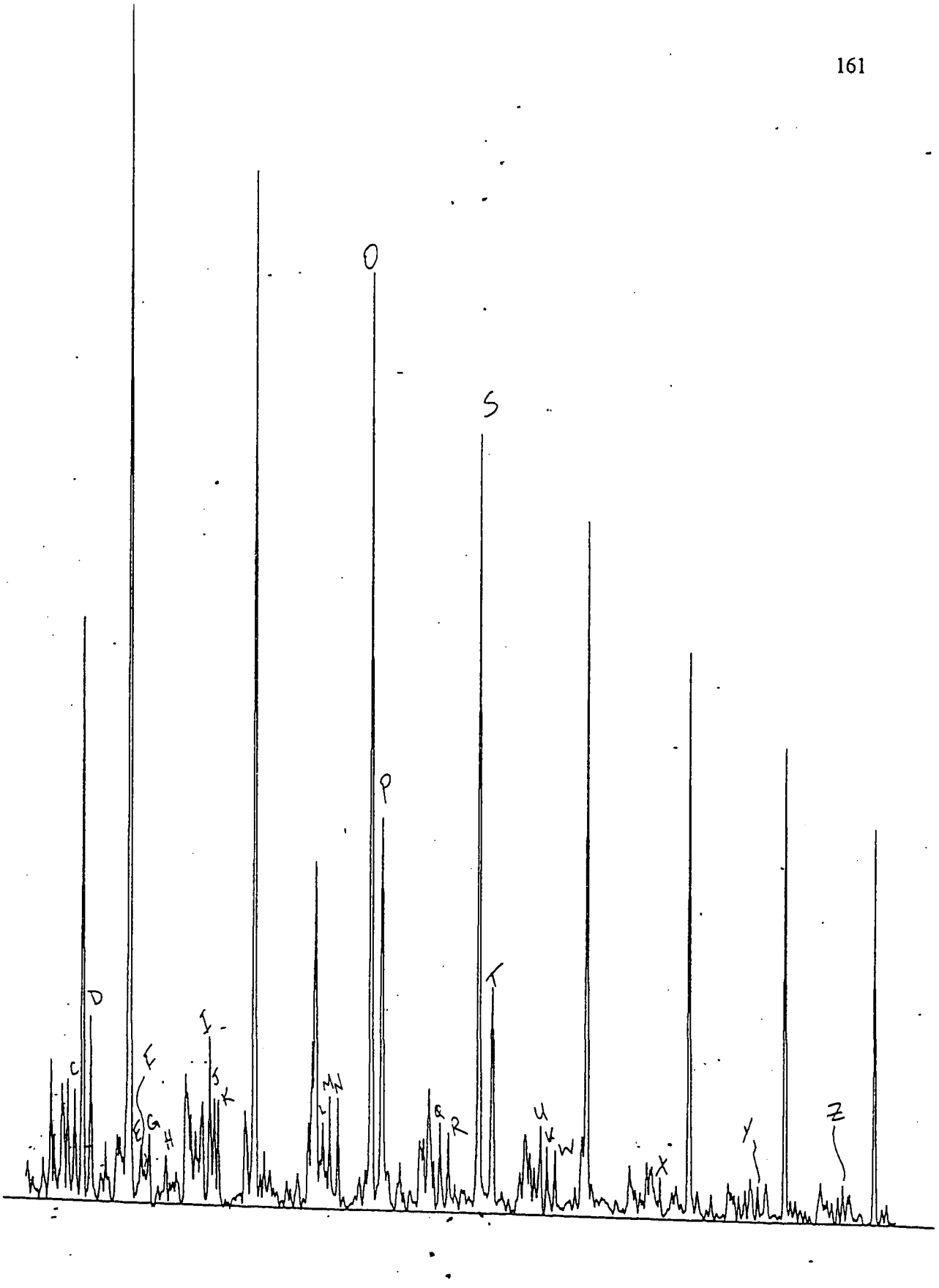

Figure 4.37 b. Whole-oil gas chromatogram of the middle range (38-67 min.) of oil A3.

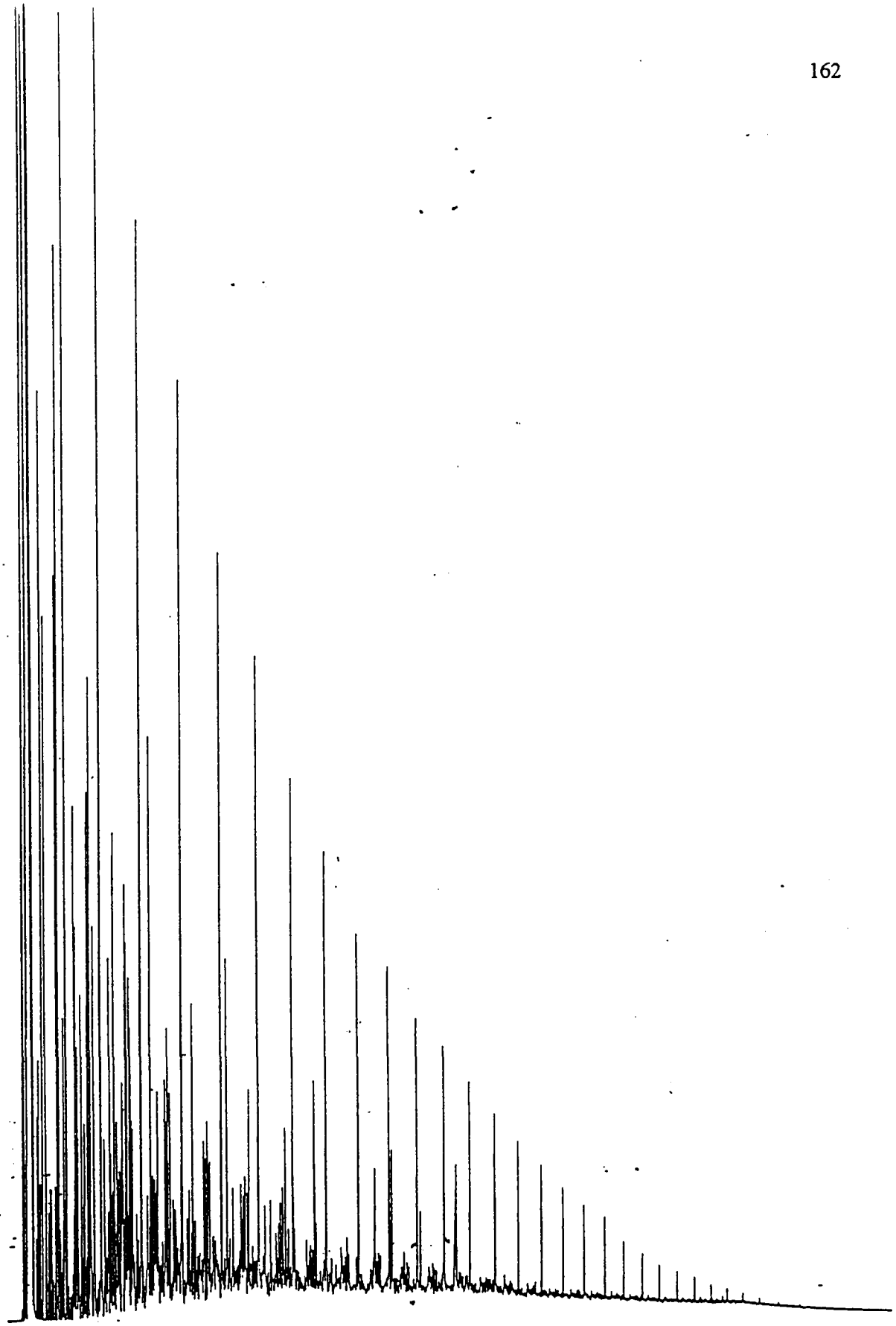

Figure 4.38 a. Whole-oil gas chromatogram of oil B1.

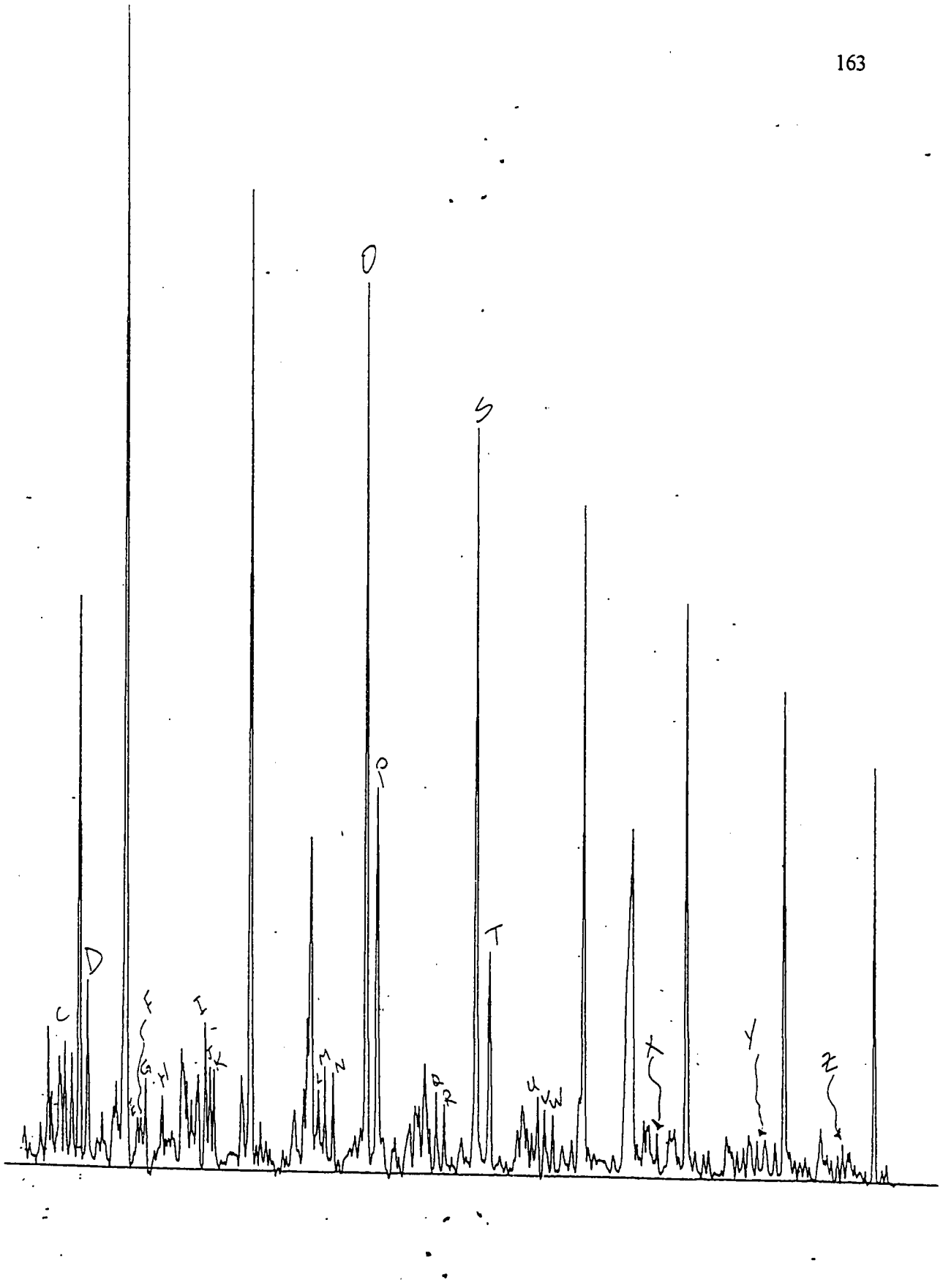

Figure 4.38 b. Whole-oil gas chromatogram of the middle range (38-67 min.) of oil B1.

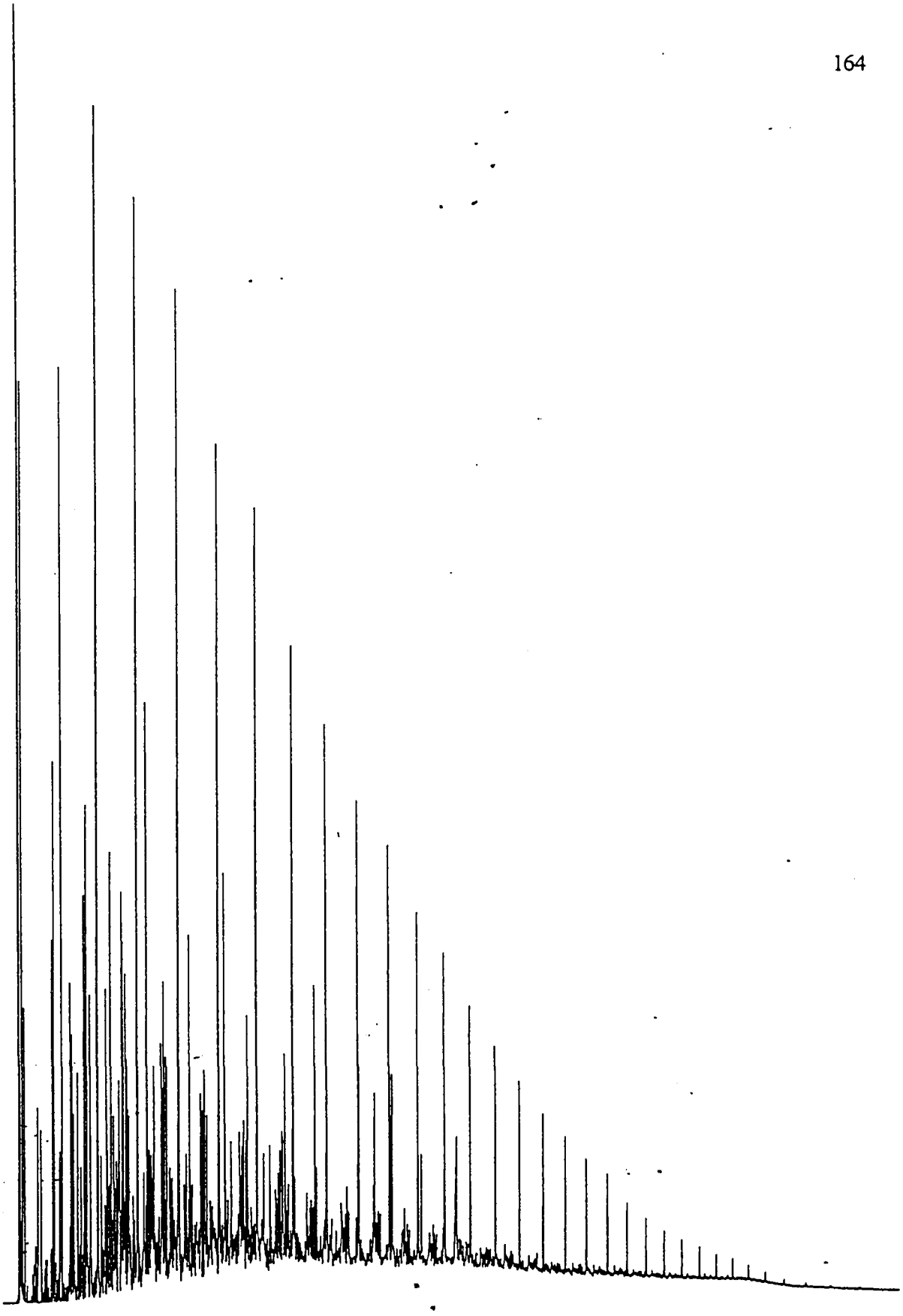

Figure 4.39 a. Whole-oil gas chromatogram of oil B2.

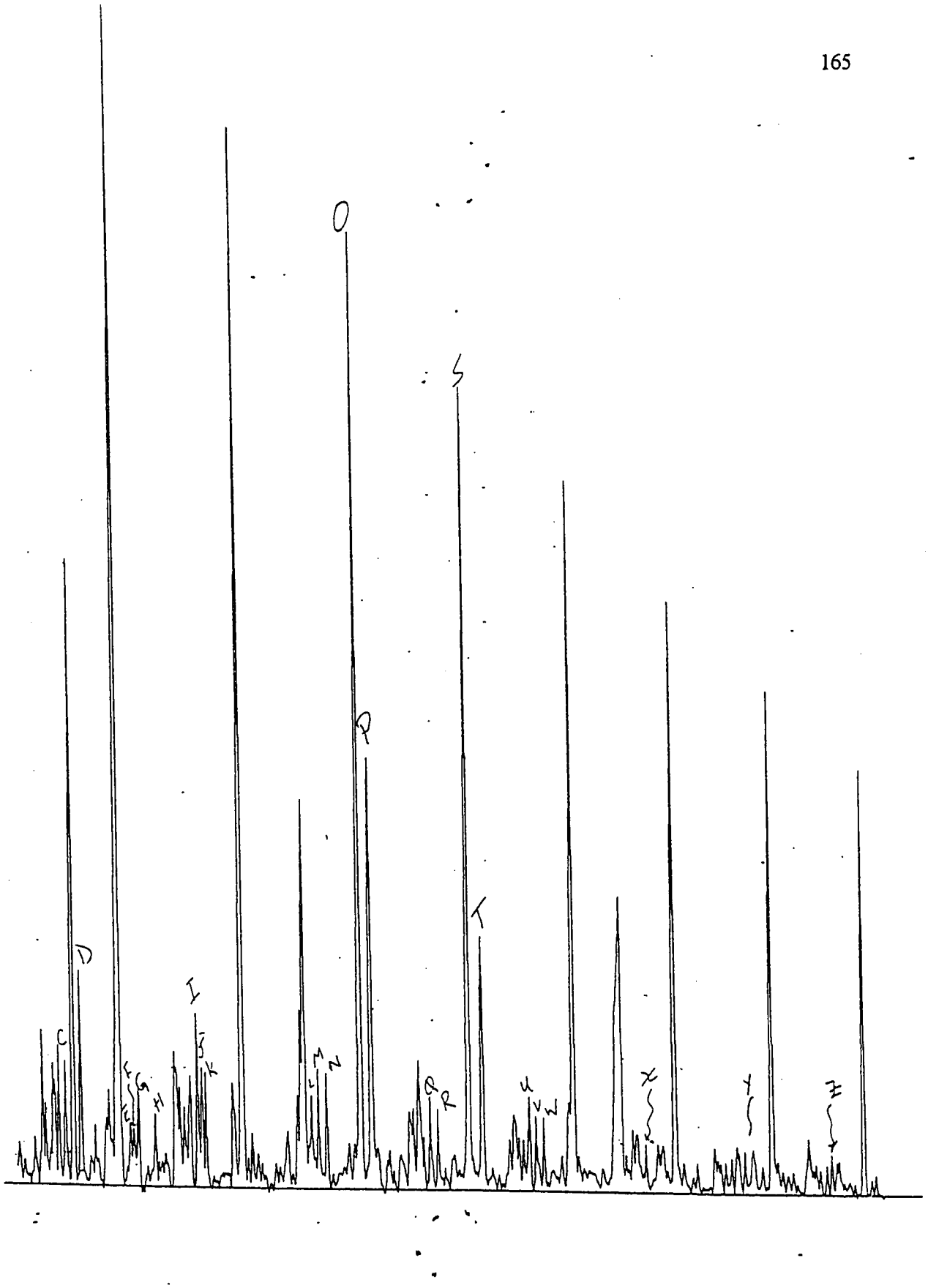

Figure 4.39 b. Whole-oil gas chromatogram of the middle range (38-67 min.) of oil B2.

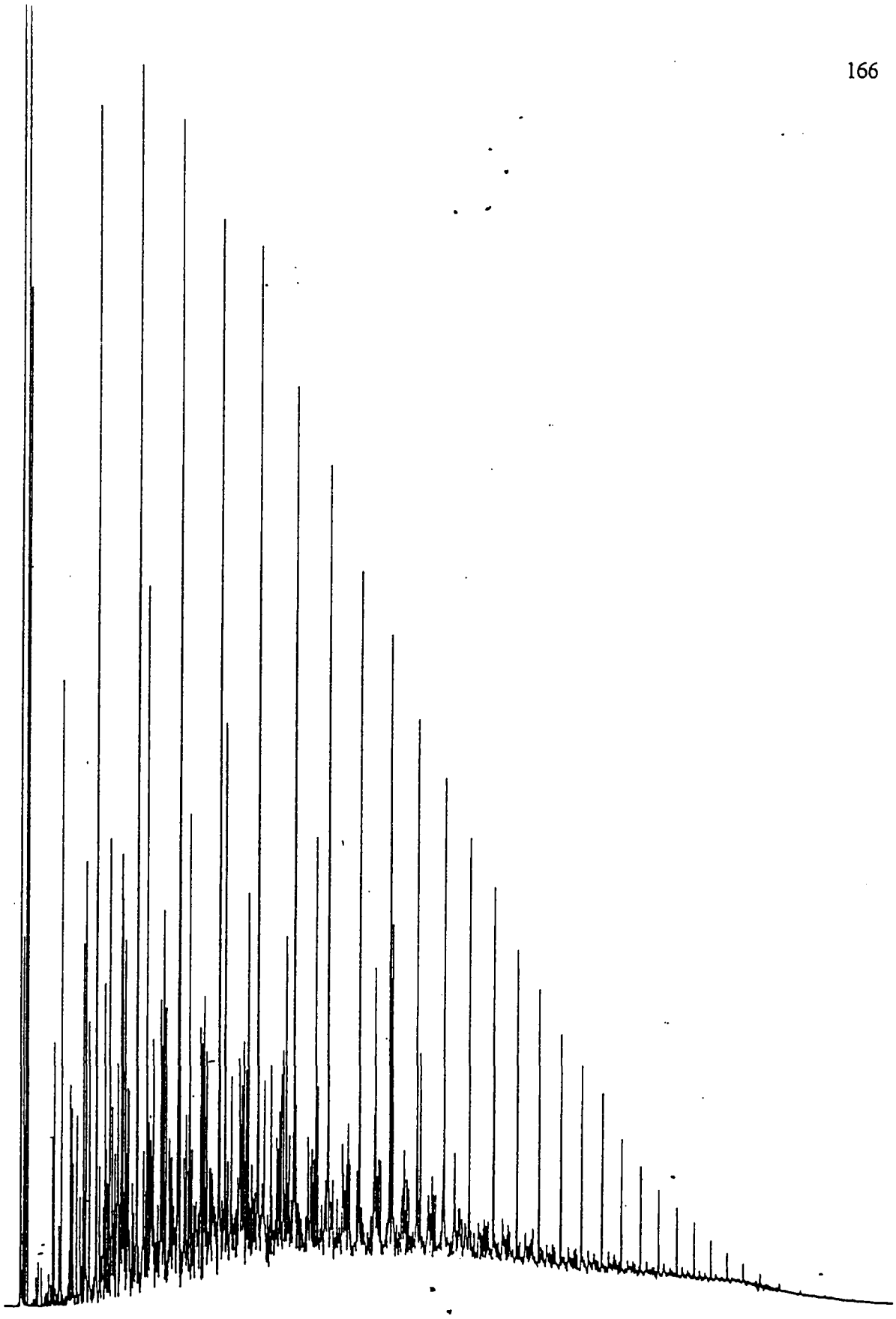

Figure 4.40 a. Whole-oil gas chromatogram of oil B3.

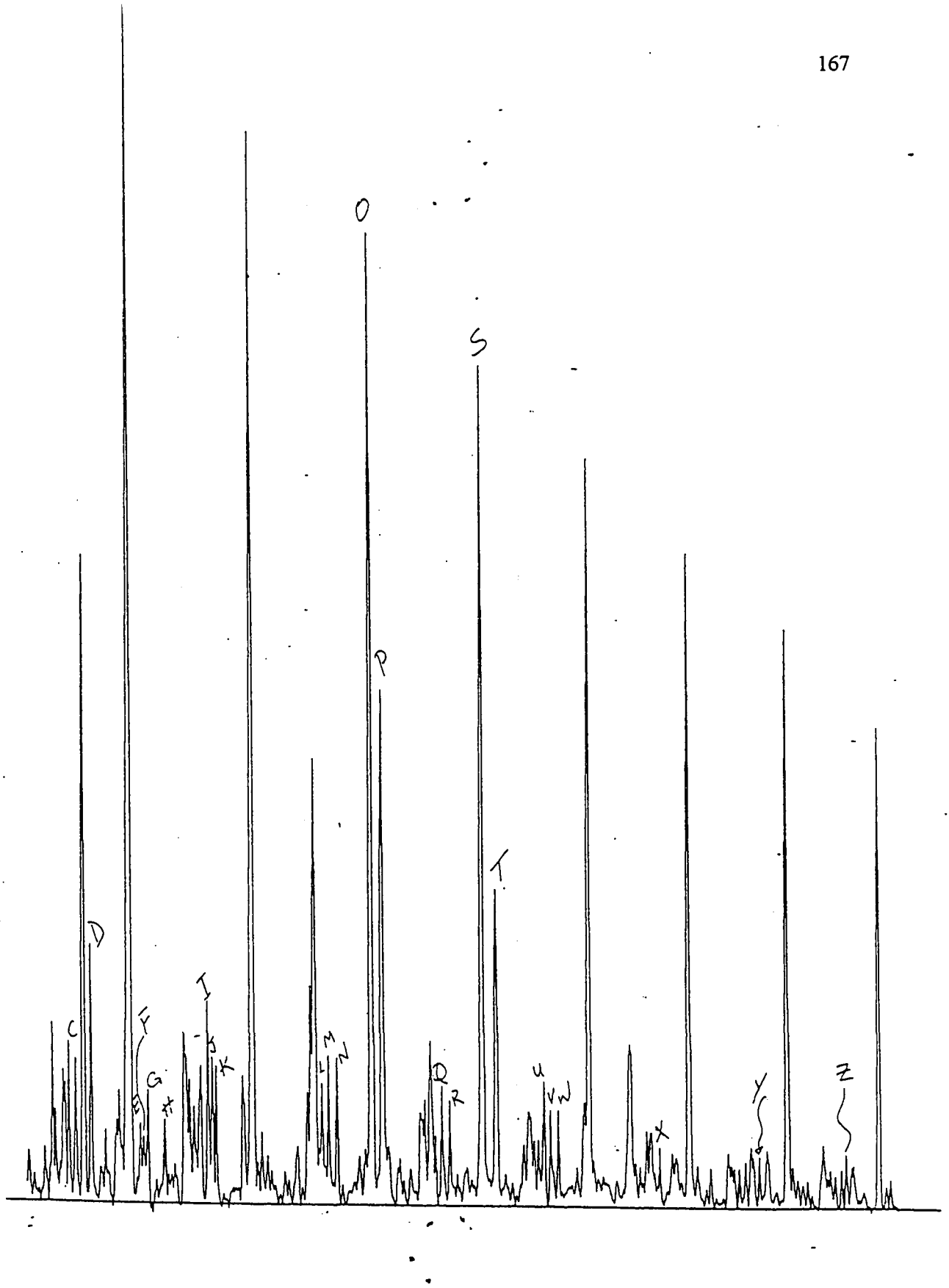

Figure 4.40 b. Whole-oil gas chromatogram of the middle range (38-67 min.) of oil B3.

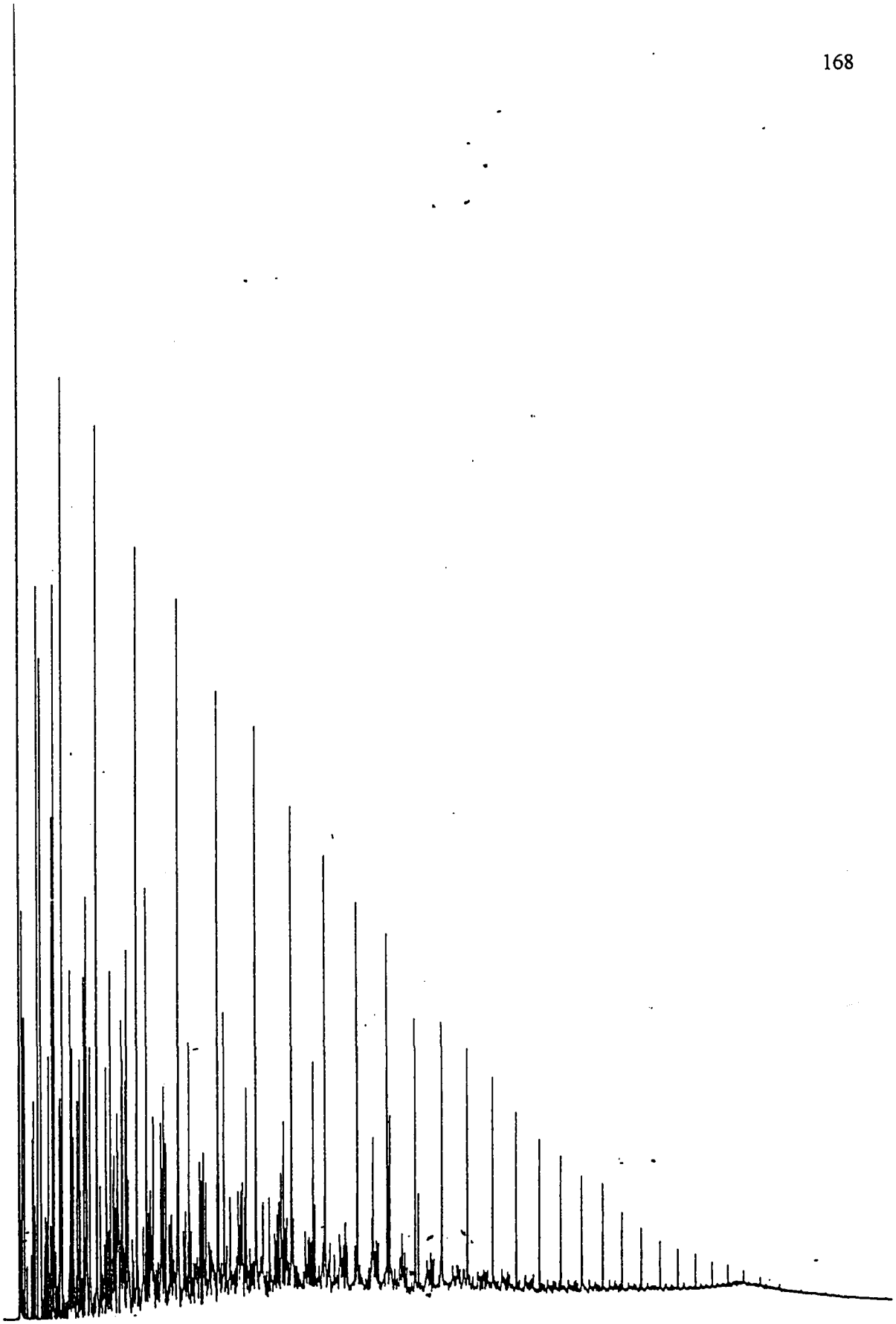

Figure 4.41 a. Whole-oil gas chromatogram of oil C1.

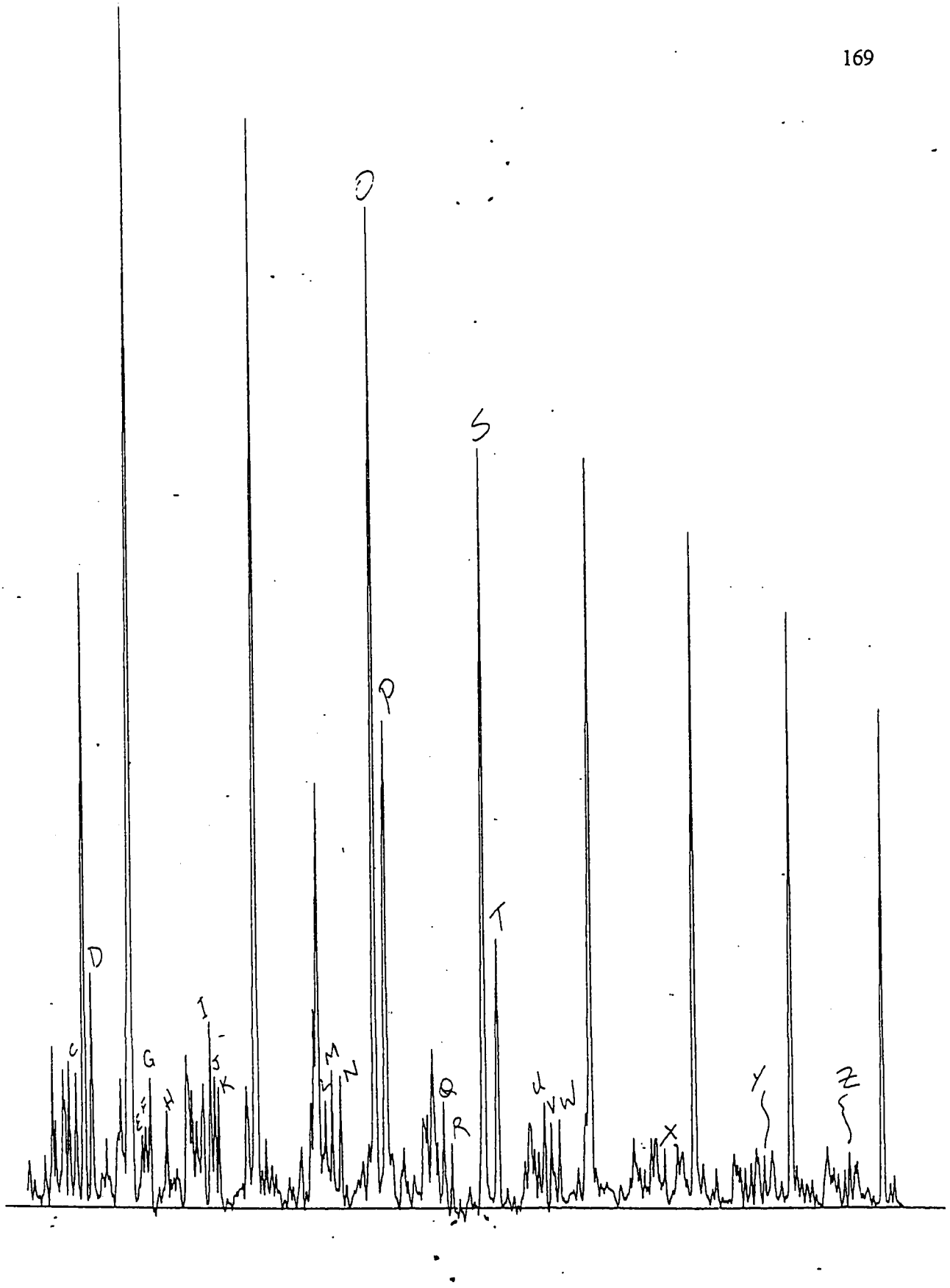

Figure 4.41 b. Whole-oil gas chromatogram of the middle range (38-67 min.) of oil C1.

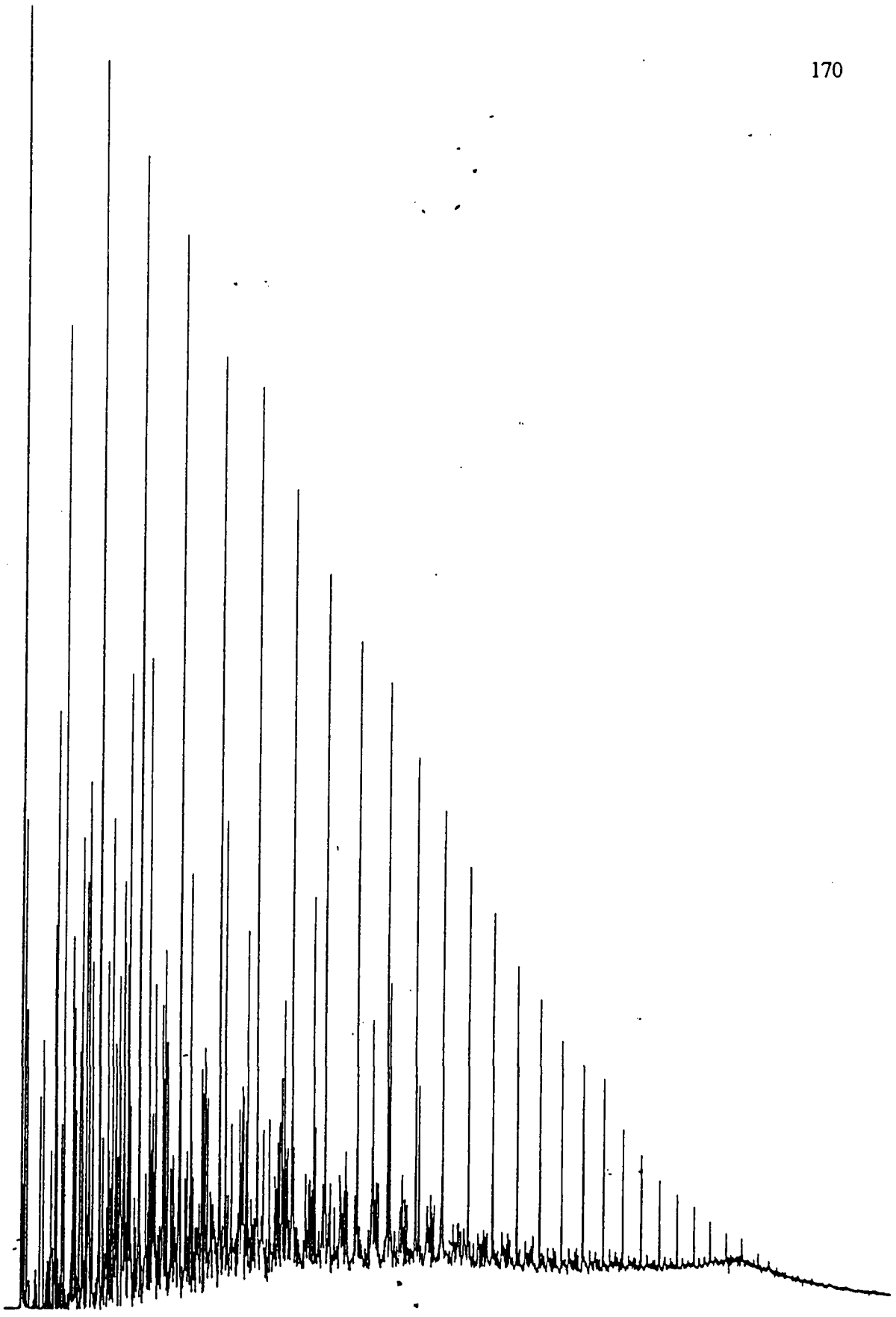

Figure 4.42 a. Whole-oil gas chromatogram of oil C2.

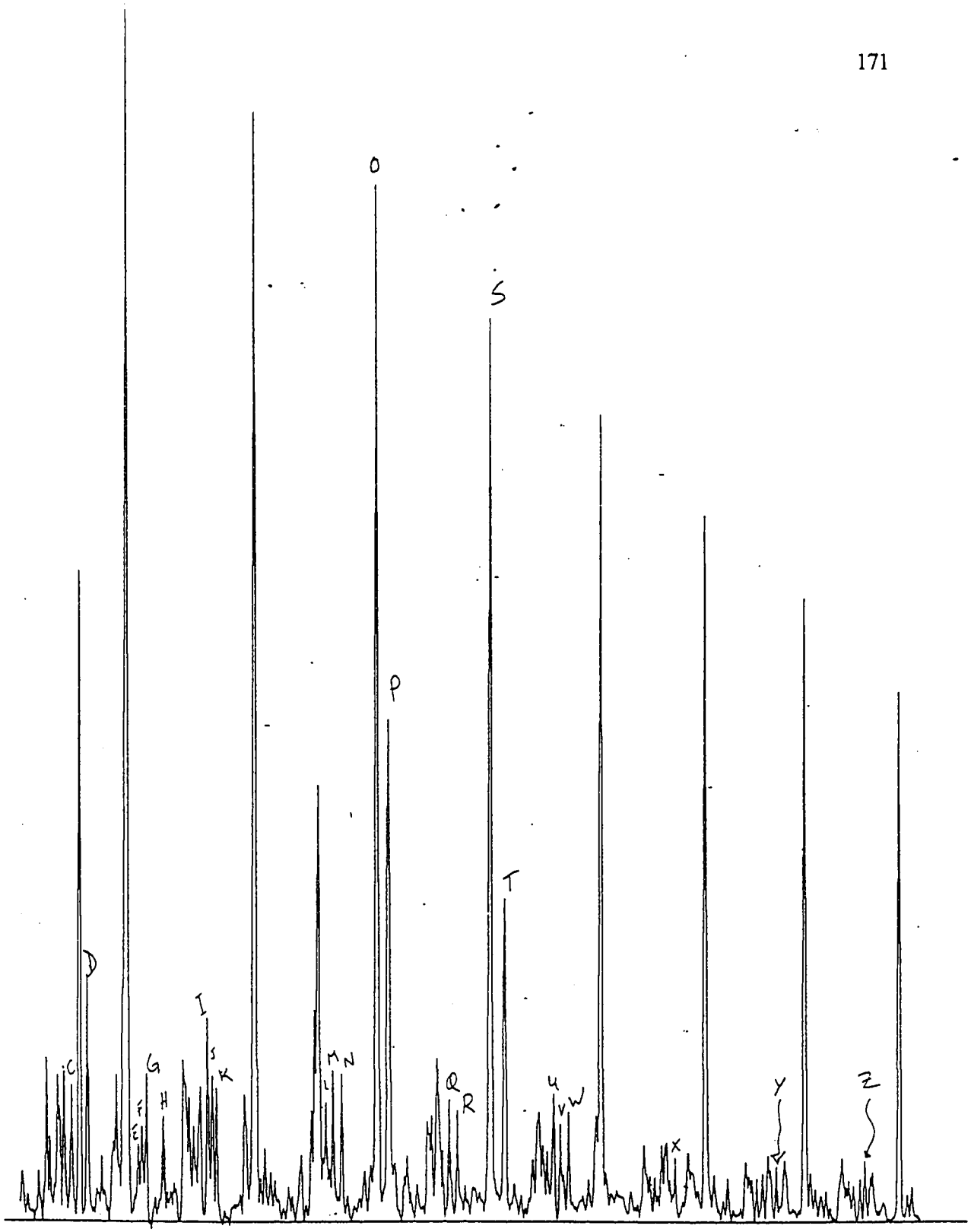

Figure 4.42 b. Whole-oil gas chromatogram of the middle range (38-67 min.) of oil C2.

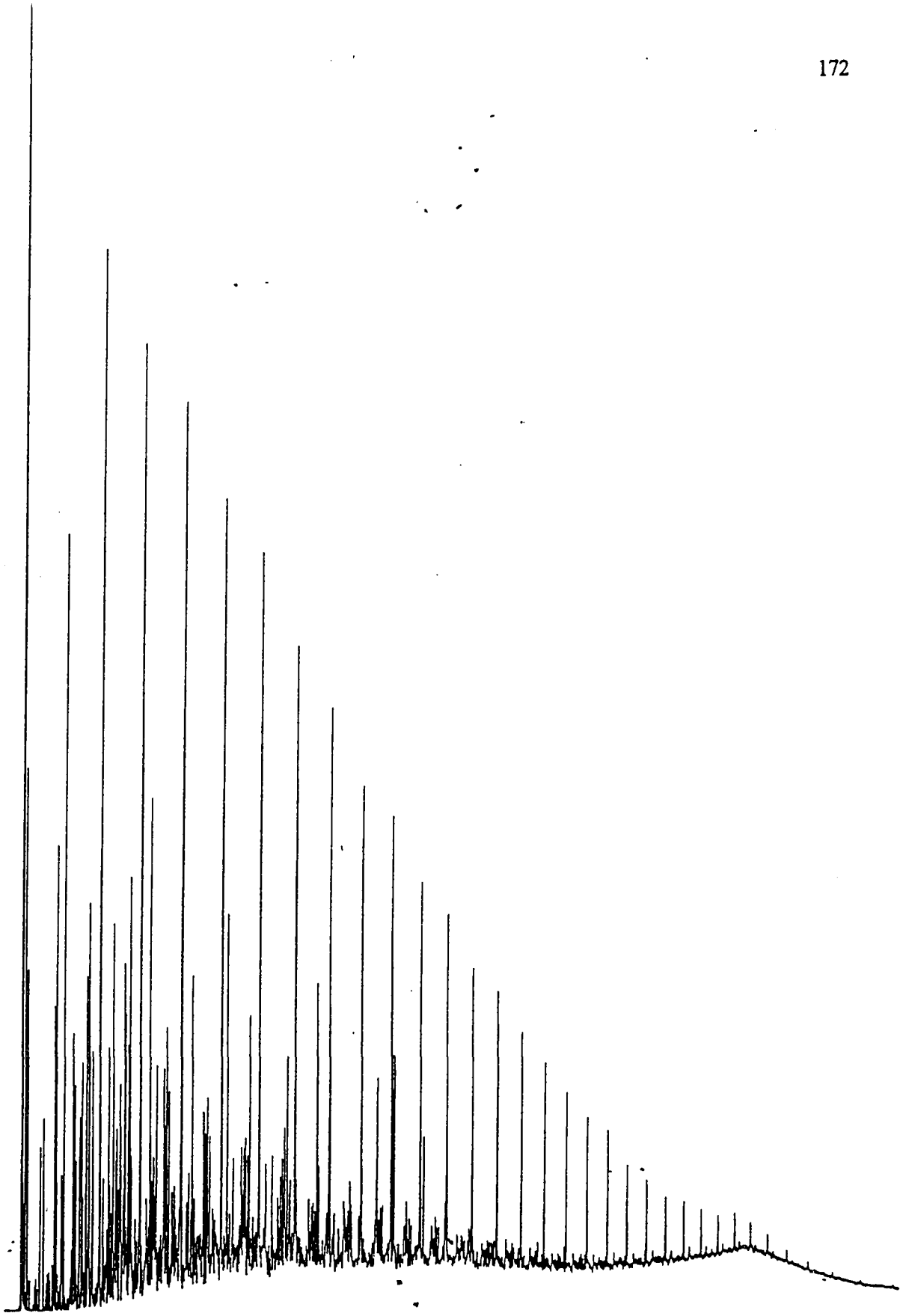

Figure 4.43 a. Whole-oil gas chromatogram of oil C3.

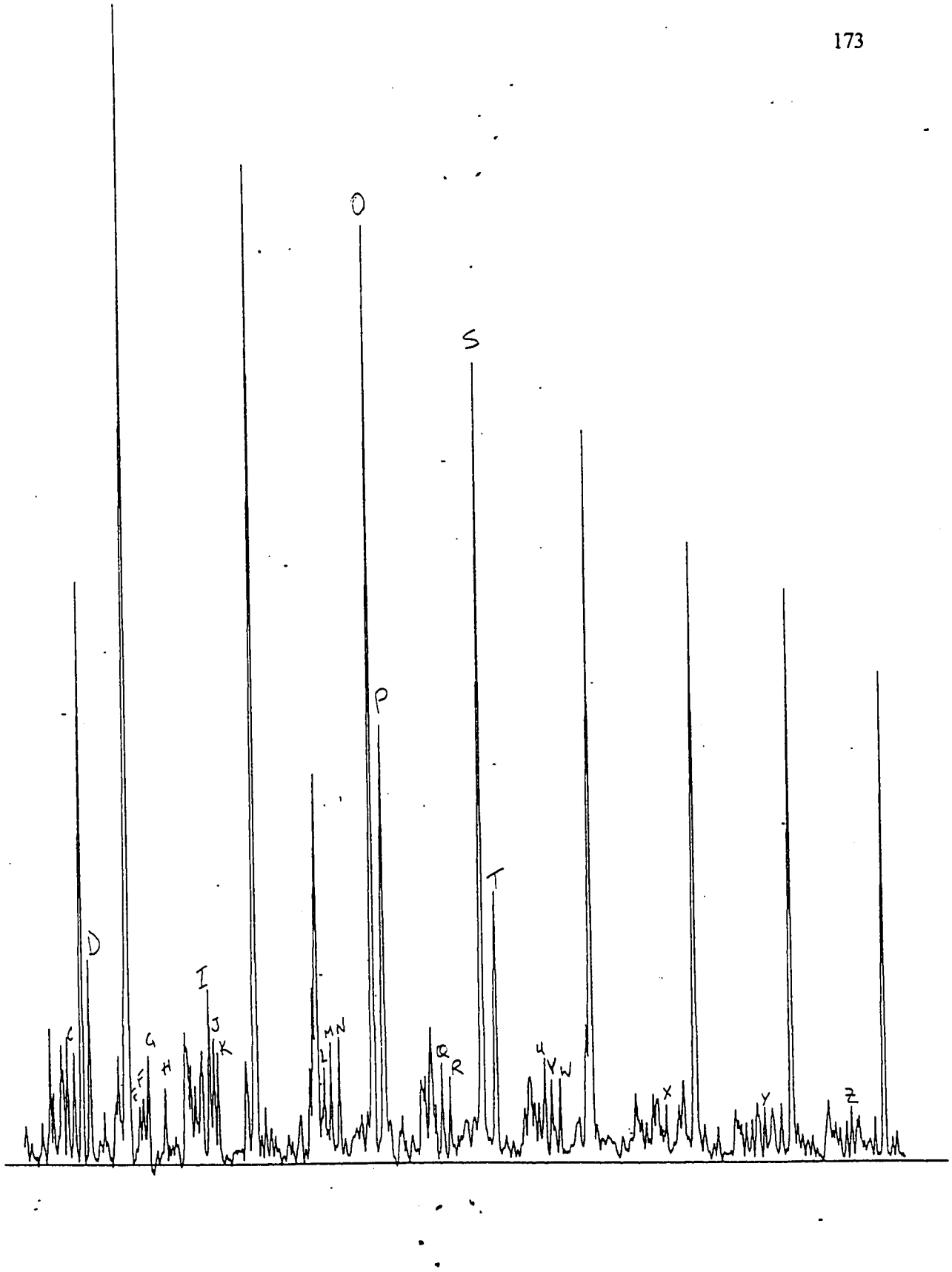

Figure 4.43 b. Whole-oil gas chromatogram of the middle range (38-67 min.) of oil C3.

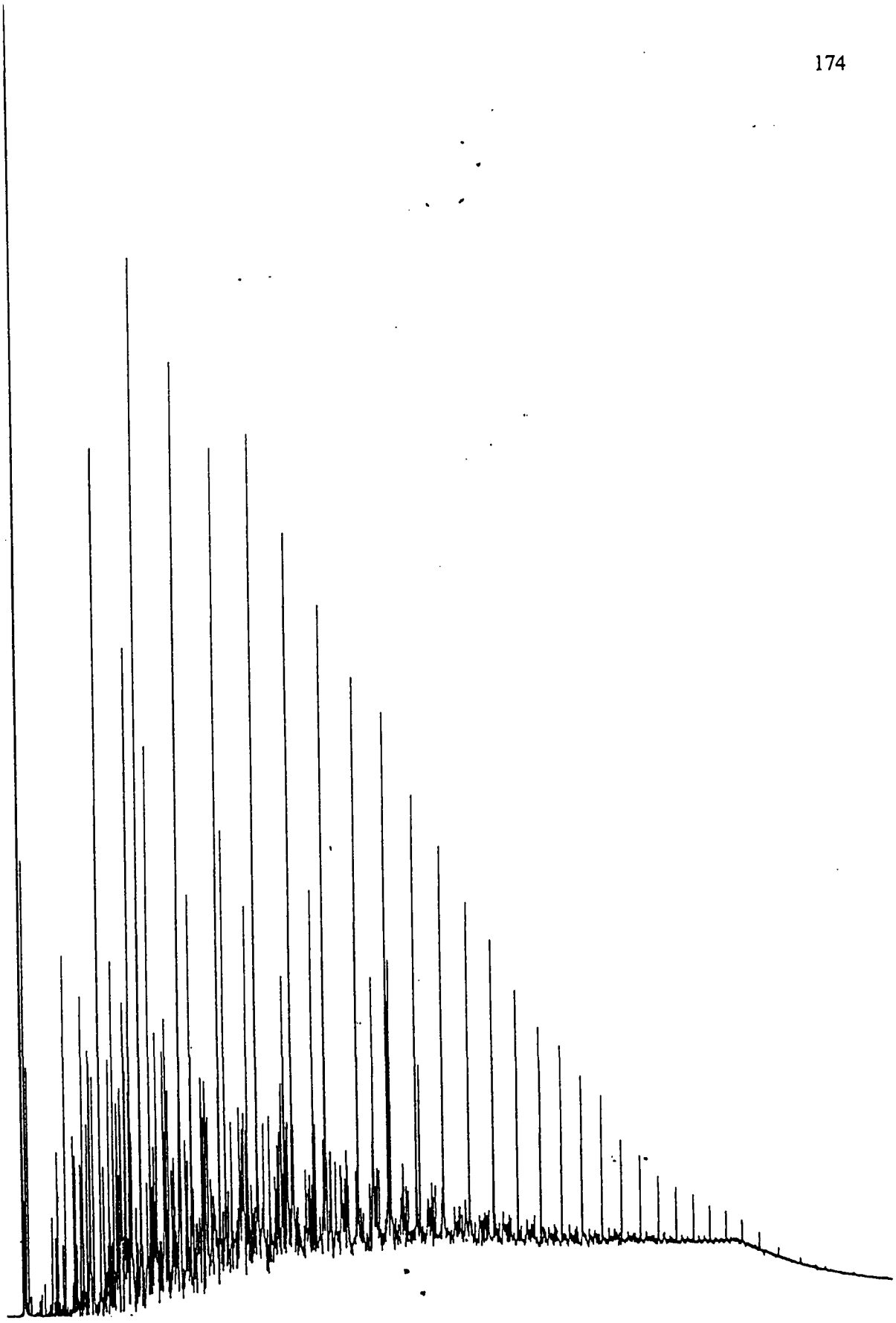

Figure 4.44 a. Whole-oil gas chromatogram of oil D1.

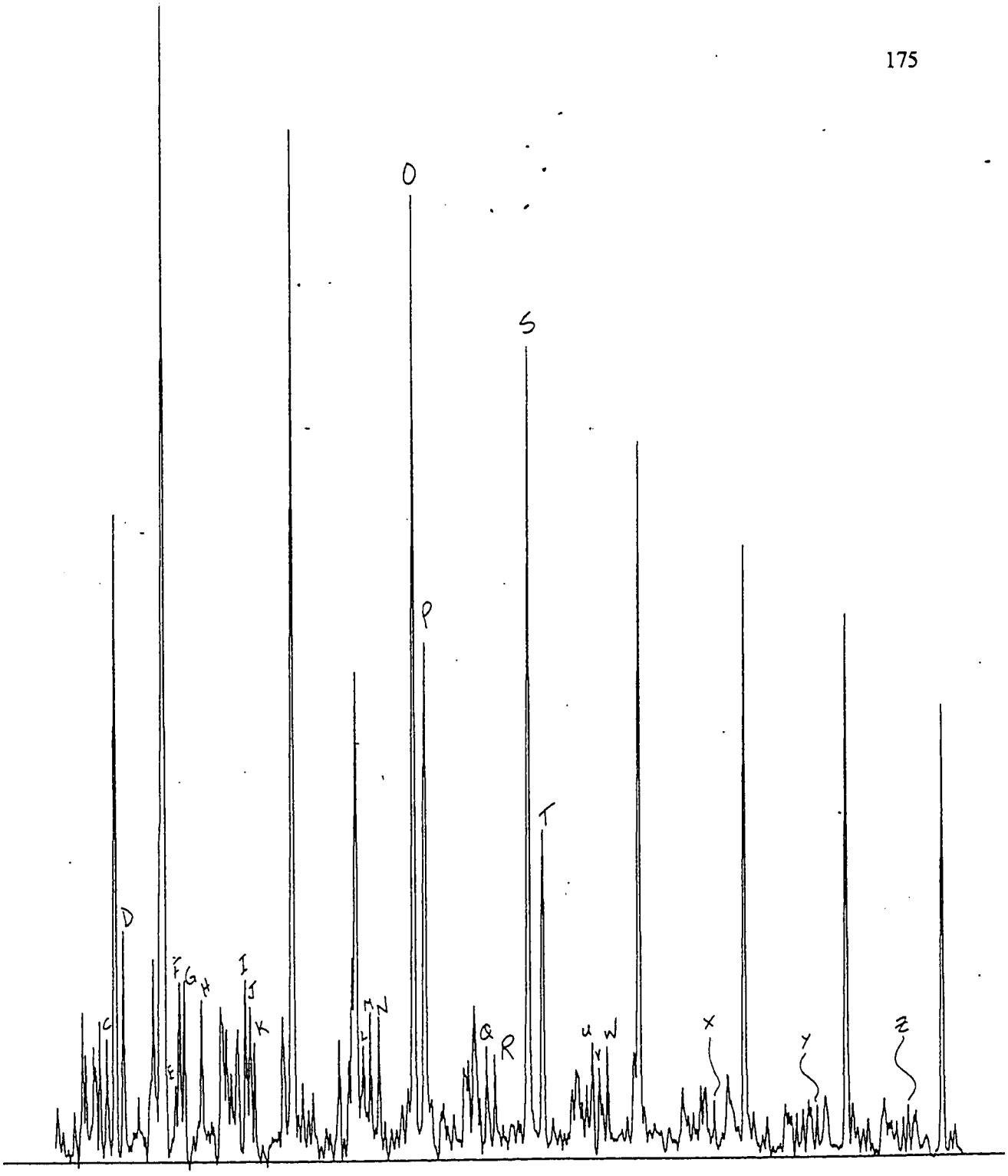

Figure 4.44 b. Whole-oil gas chromatogram of the middle range (38-67 min.) of oil D1.

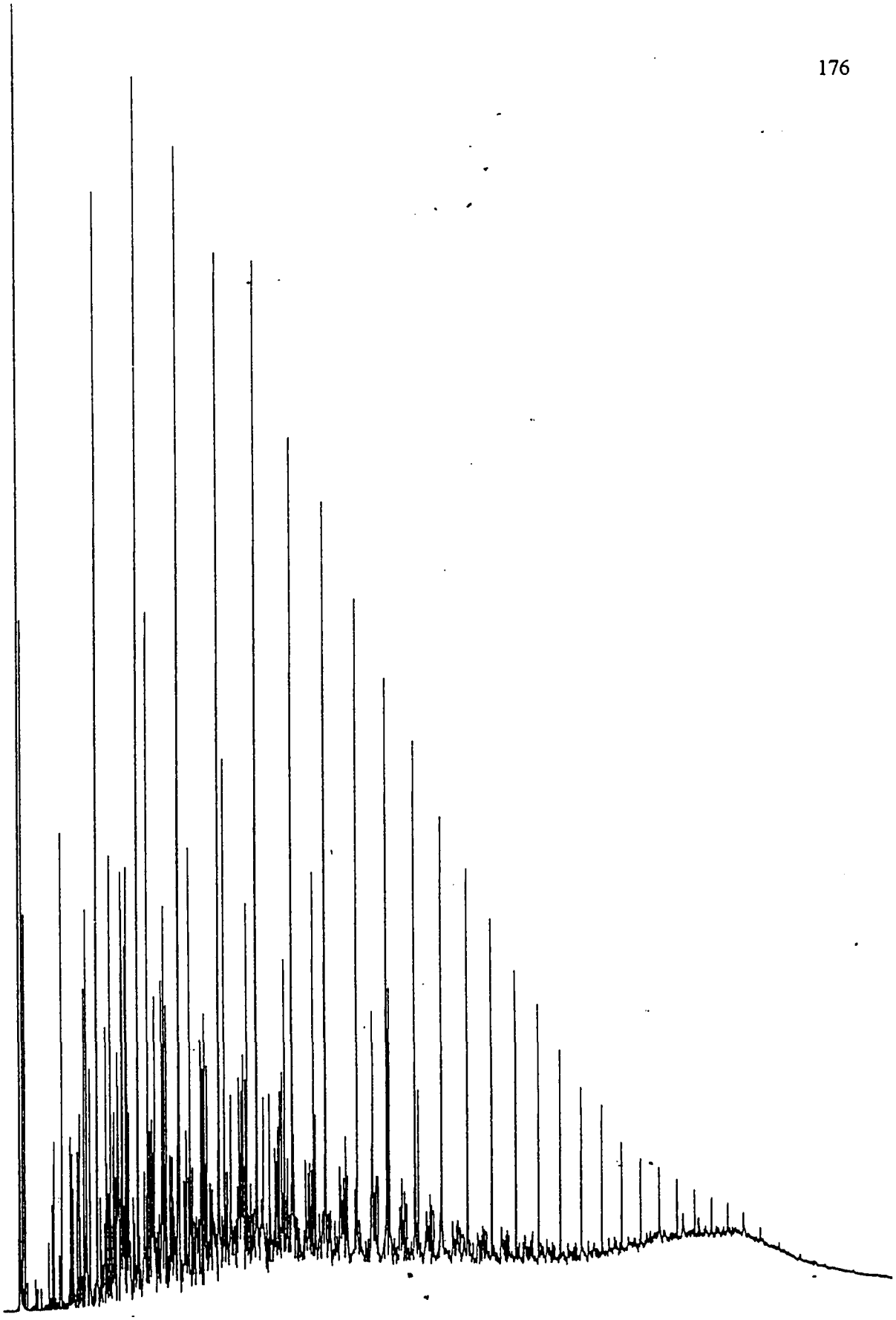

Figure 4.45 a. Whole-oil gas chromatogram of oil E1.

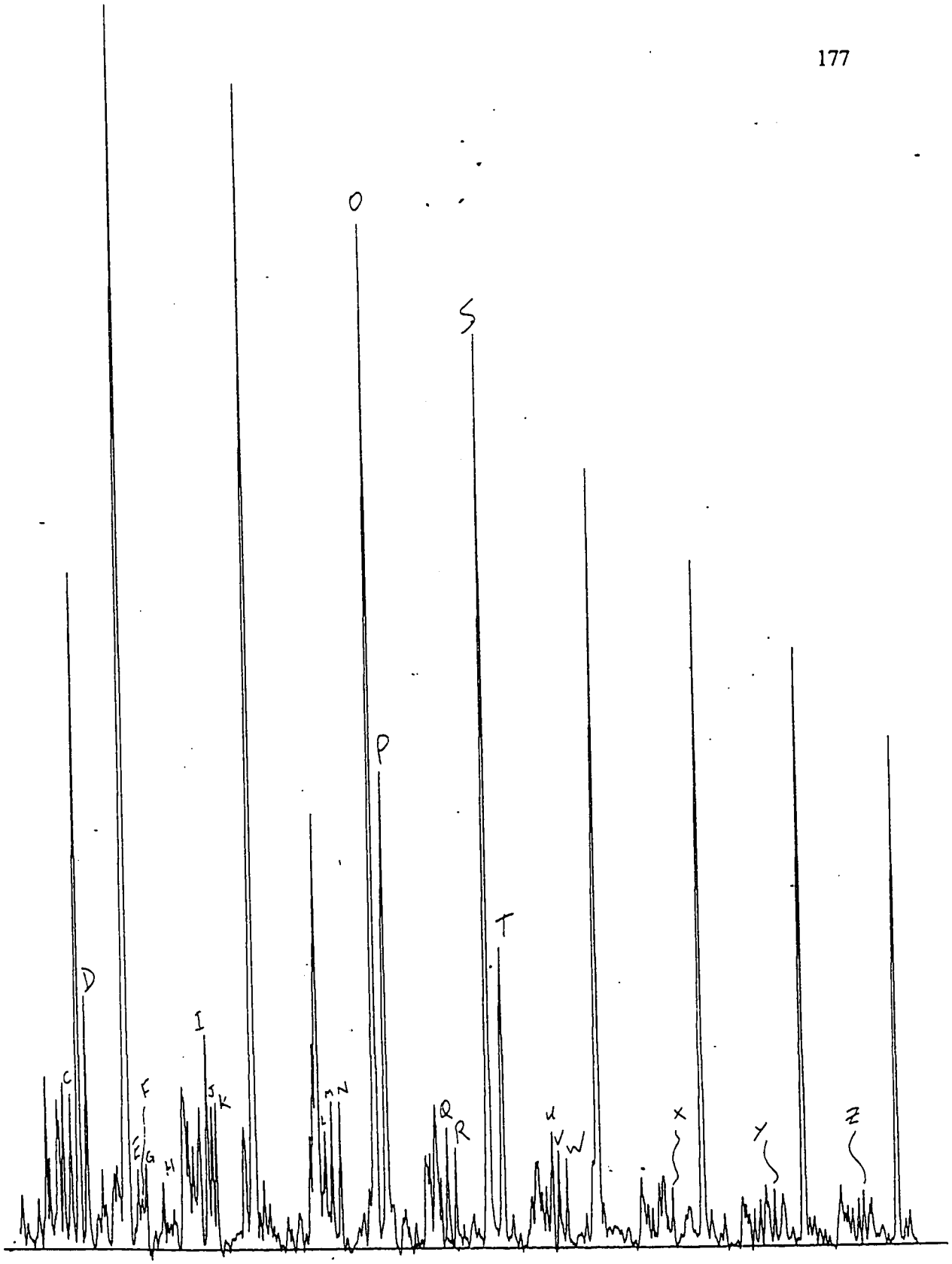

Figure 4.45 b. Whole-oil gas chromatogram of the middle range (38-67 min.) of oil E1.

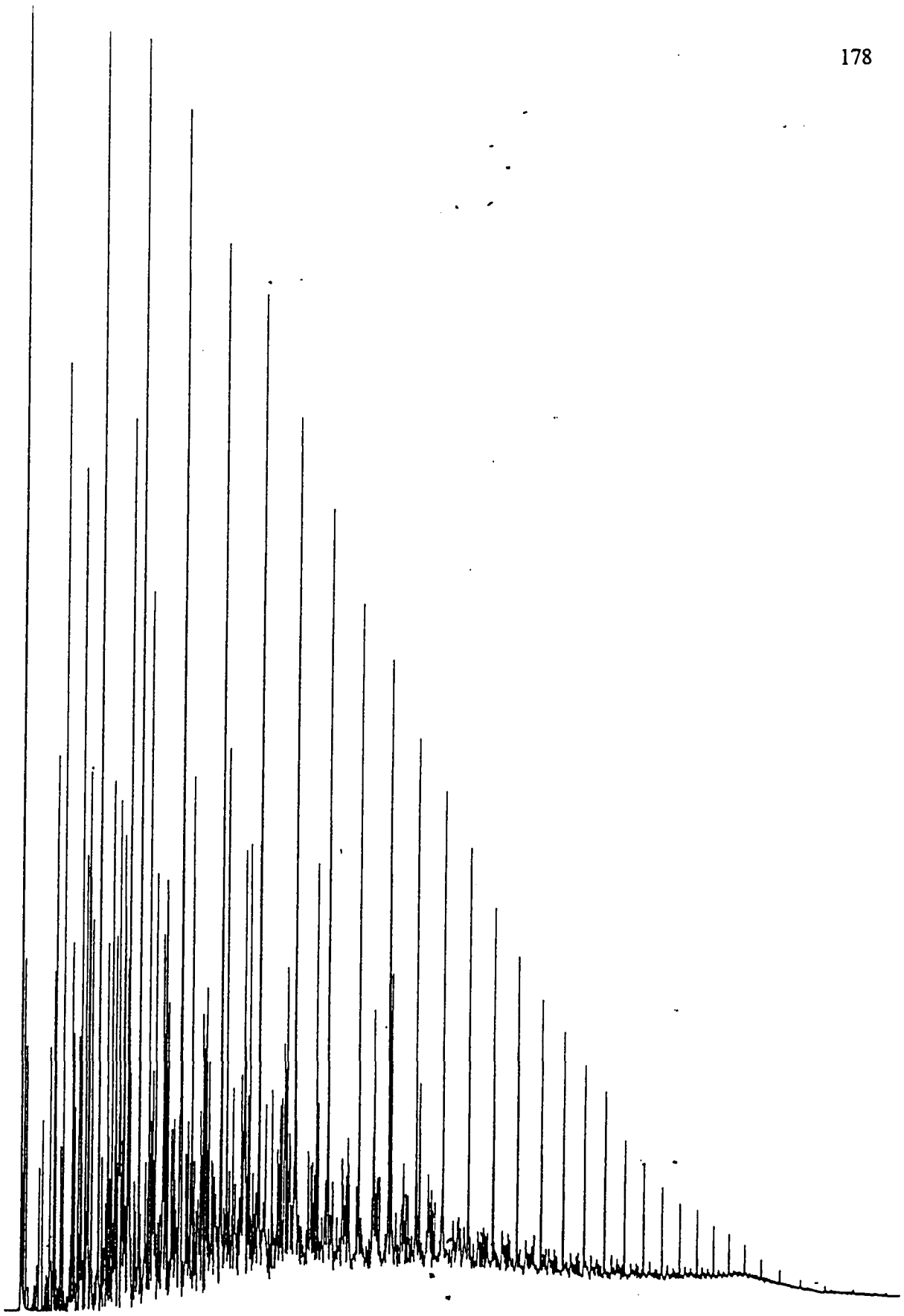

Figure 4.46 a. Whole-oil gas chromatogram of oil F1.

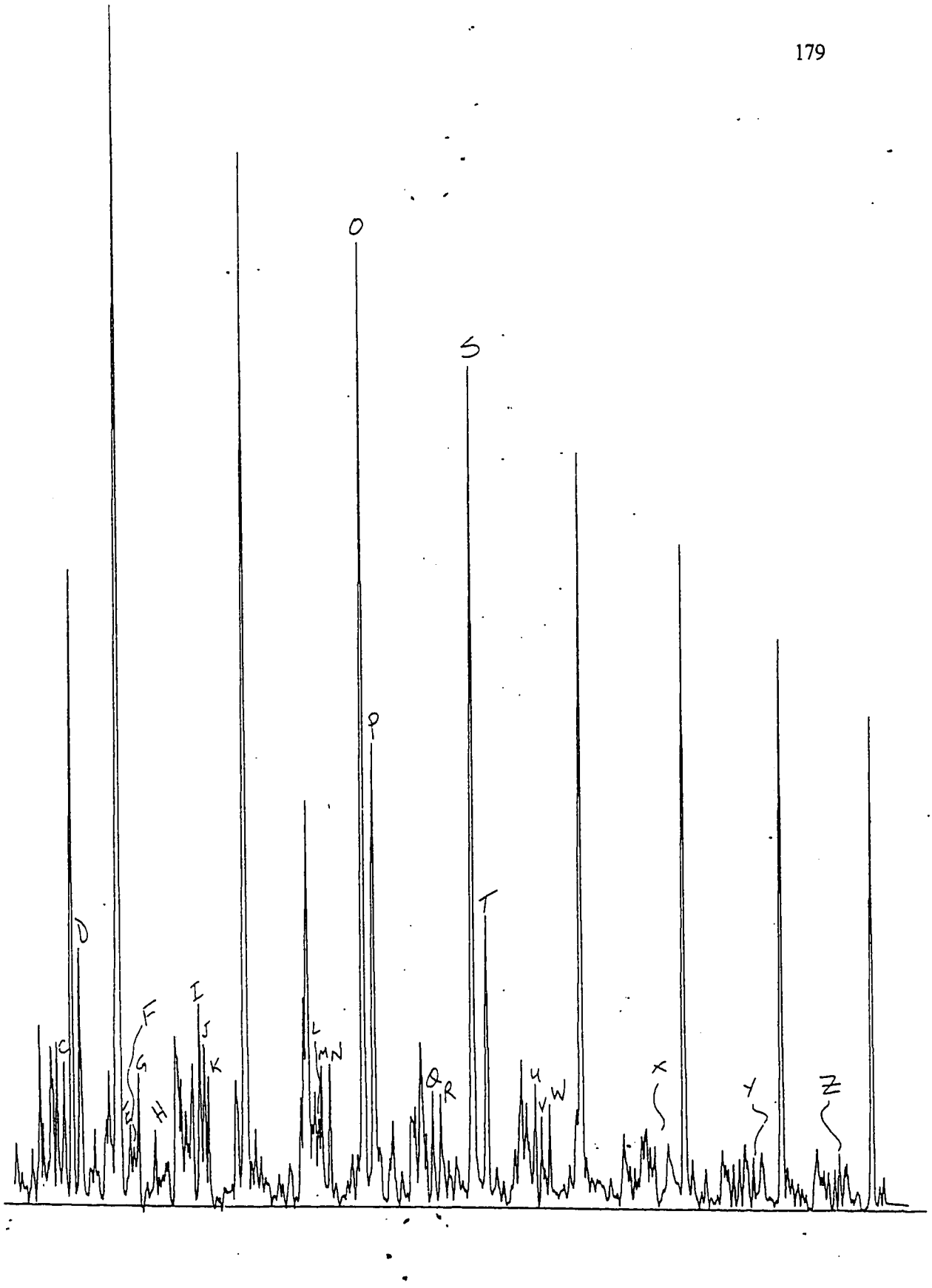

Figure 4.46 b. Whole-oil gas chromatogram of the middle range (38-67 min.) of oil F1.

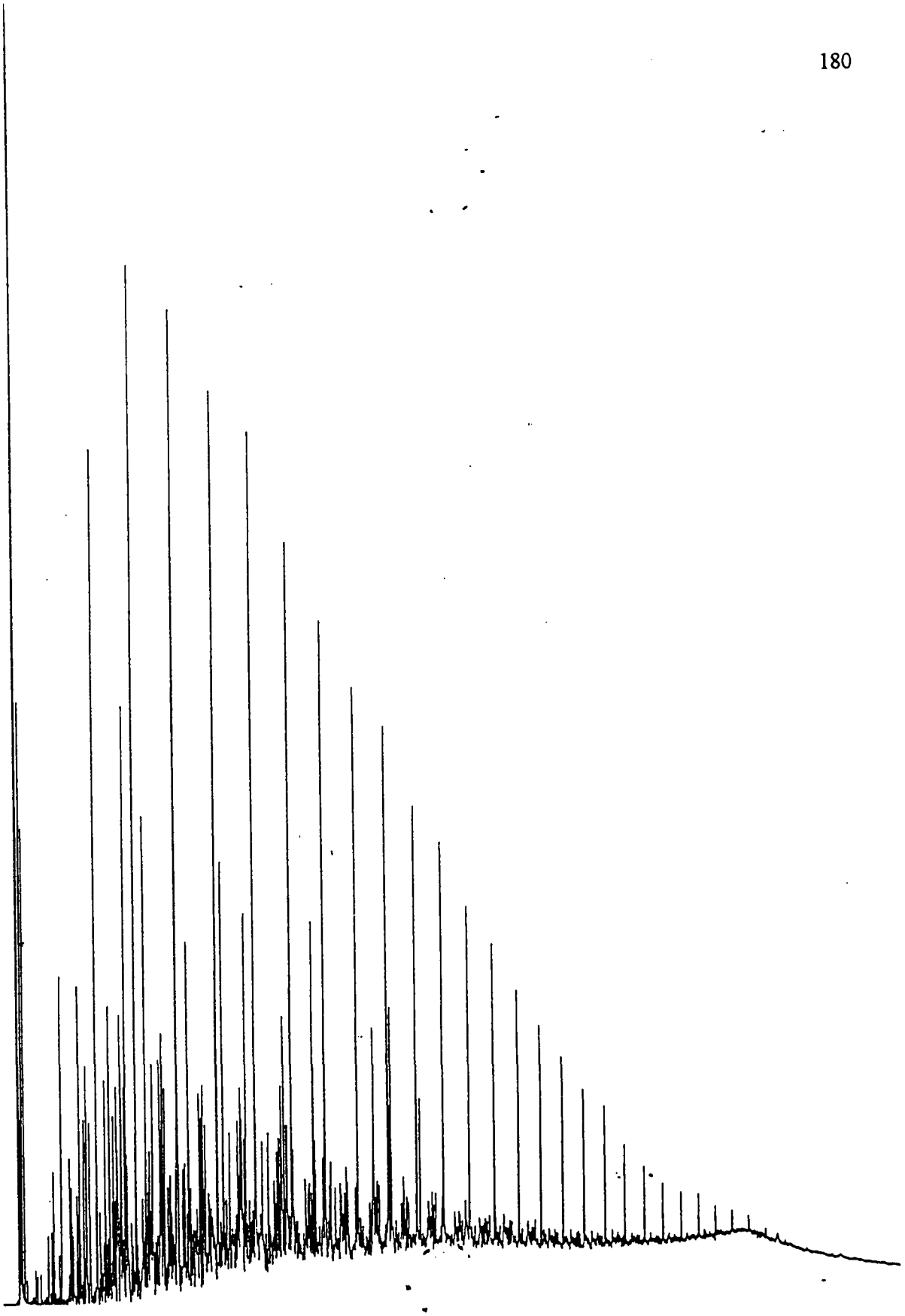

Figure 4.47 a. Whole-oil gas chromatogram of oil G1.

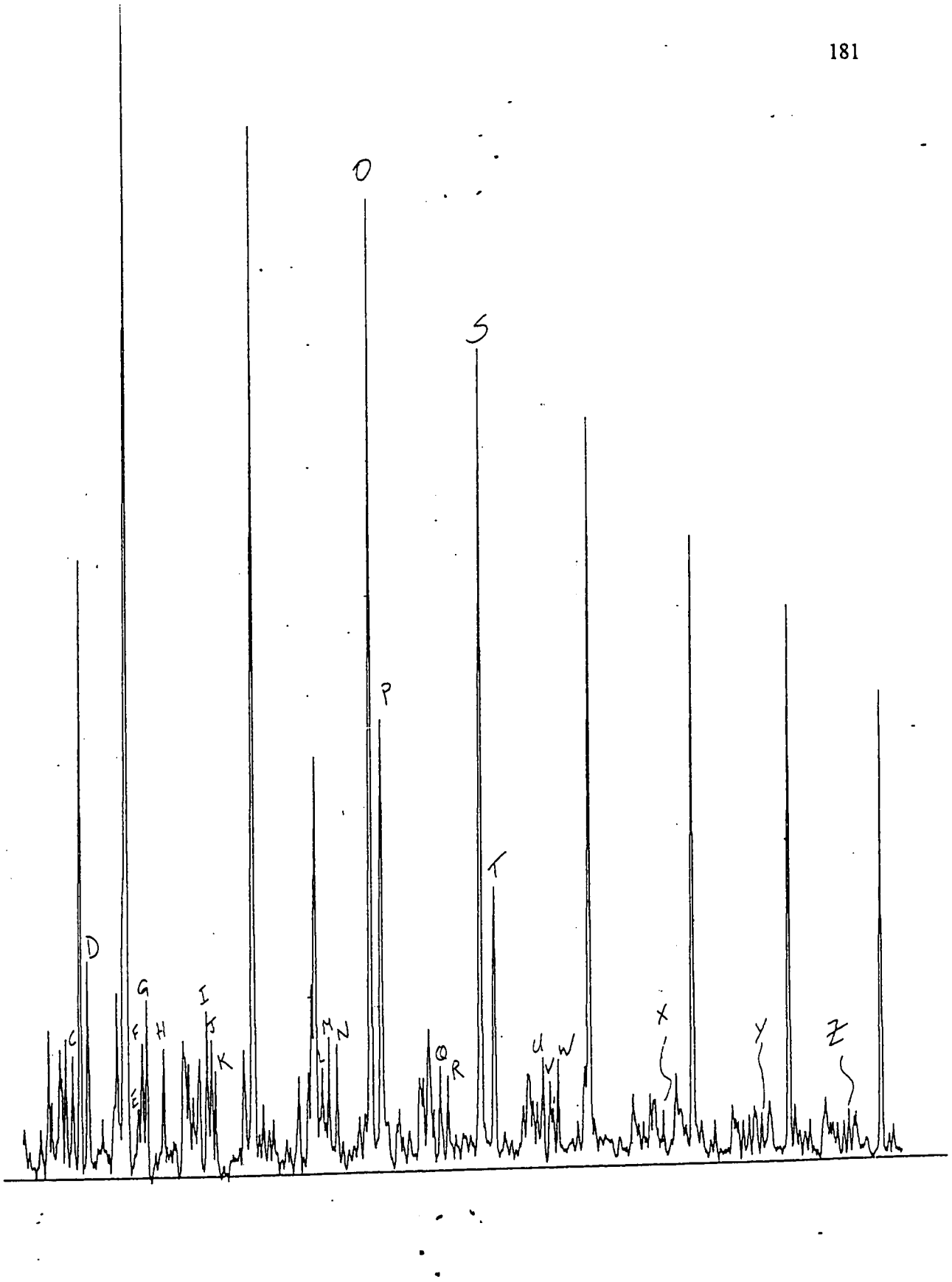

Figure 4.47 b. Whole-oil gas chromatogram of the middle range (38-67 min.) of oil G1.

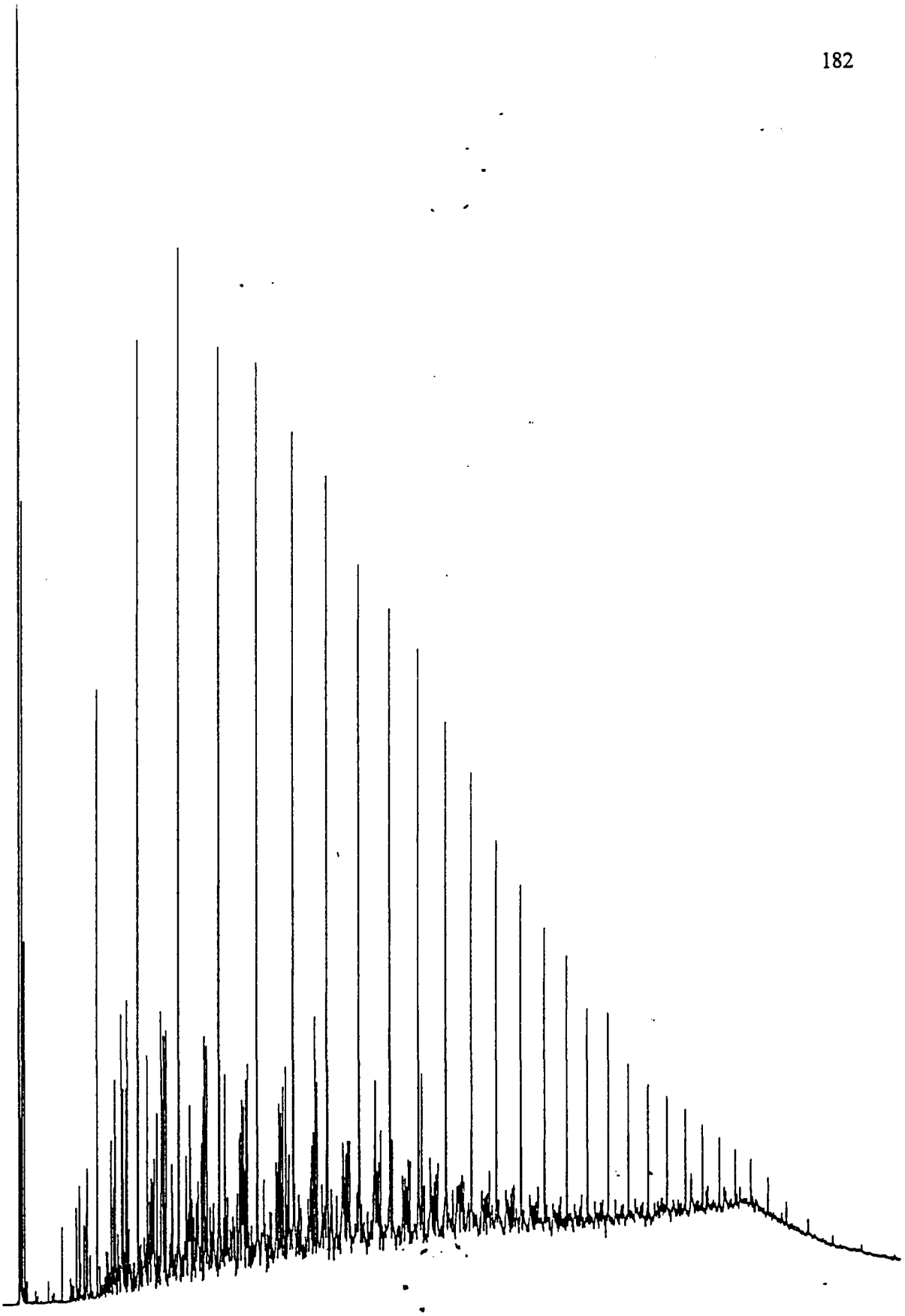

Figure 4.48 a. Whole-oil gas chromatogram of oil H1.

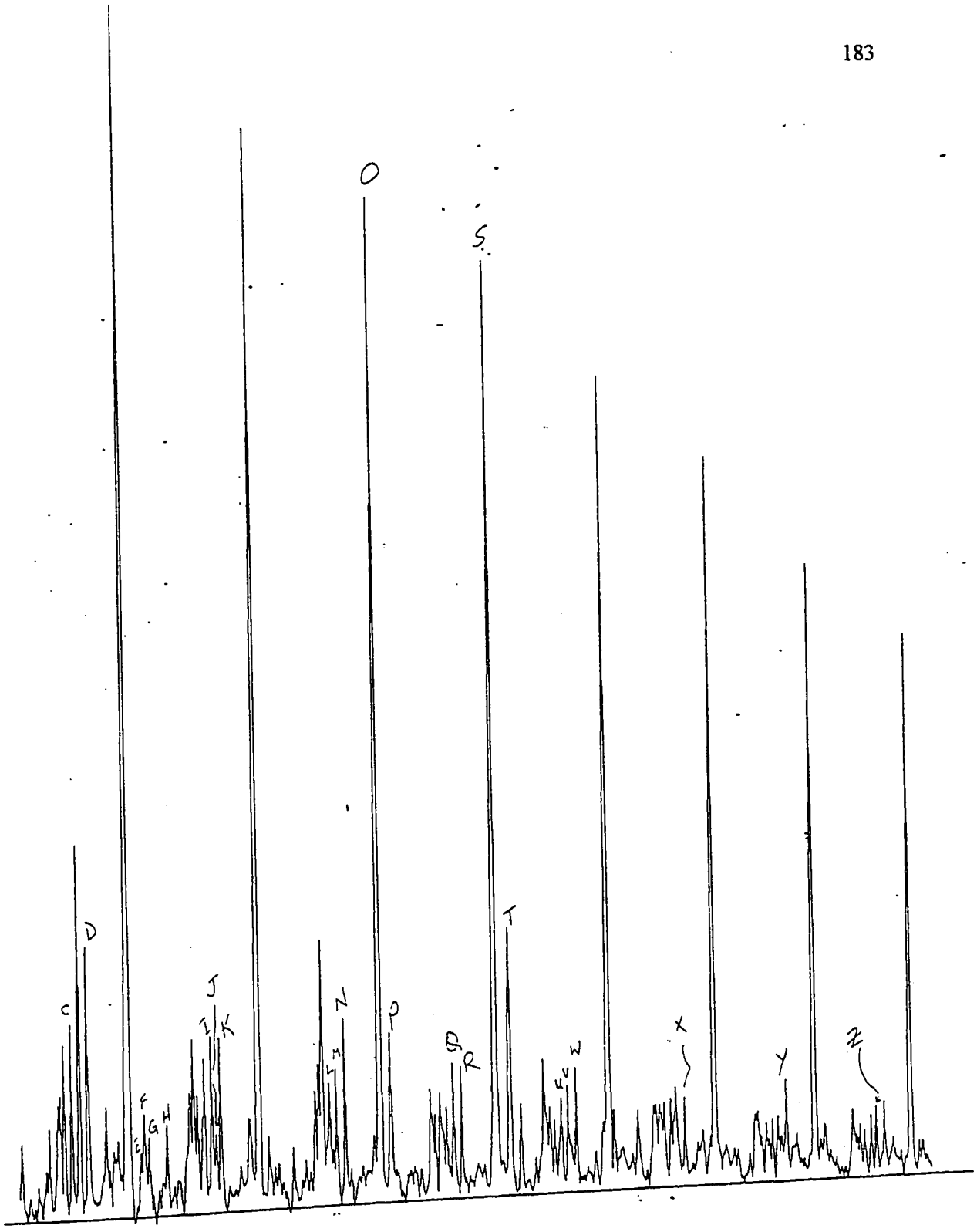

Figure 4.48 b. Whole-oil gas chromatogram of the middle range (38-67 min.) of oil H1.

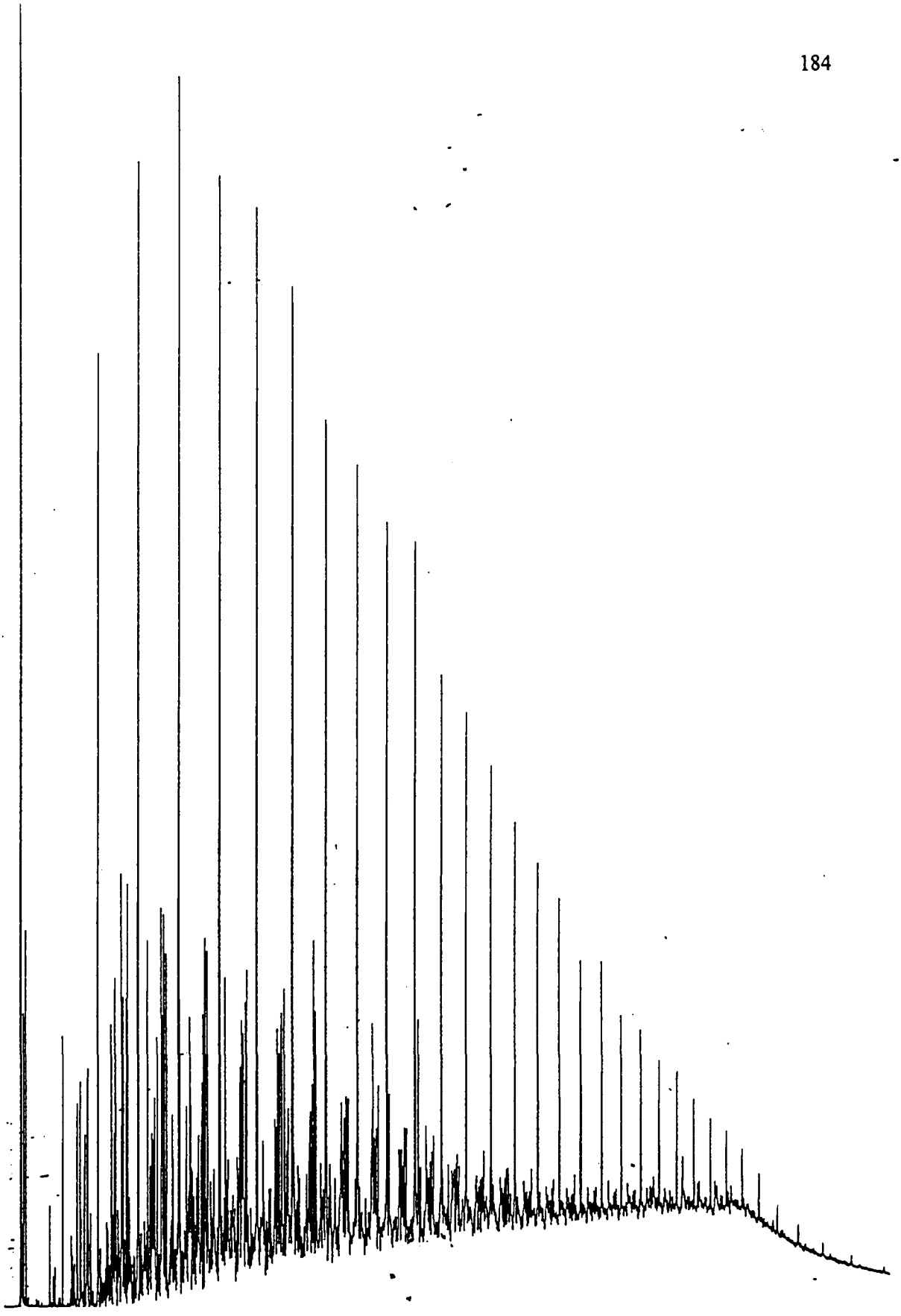

Figure 4.49 a. Whole-oil gas chromatogram of oil H2.

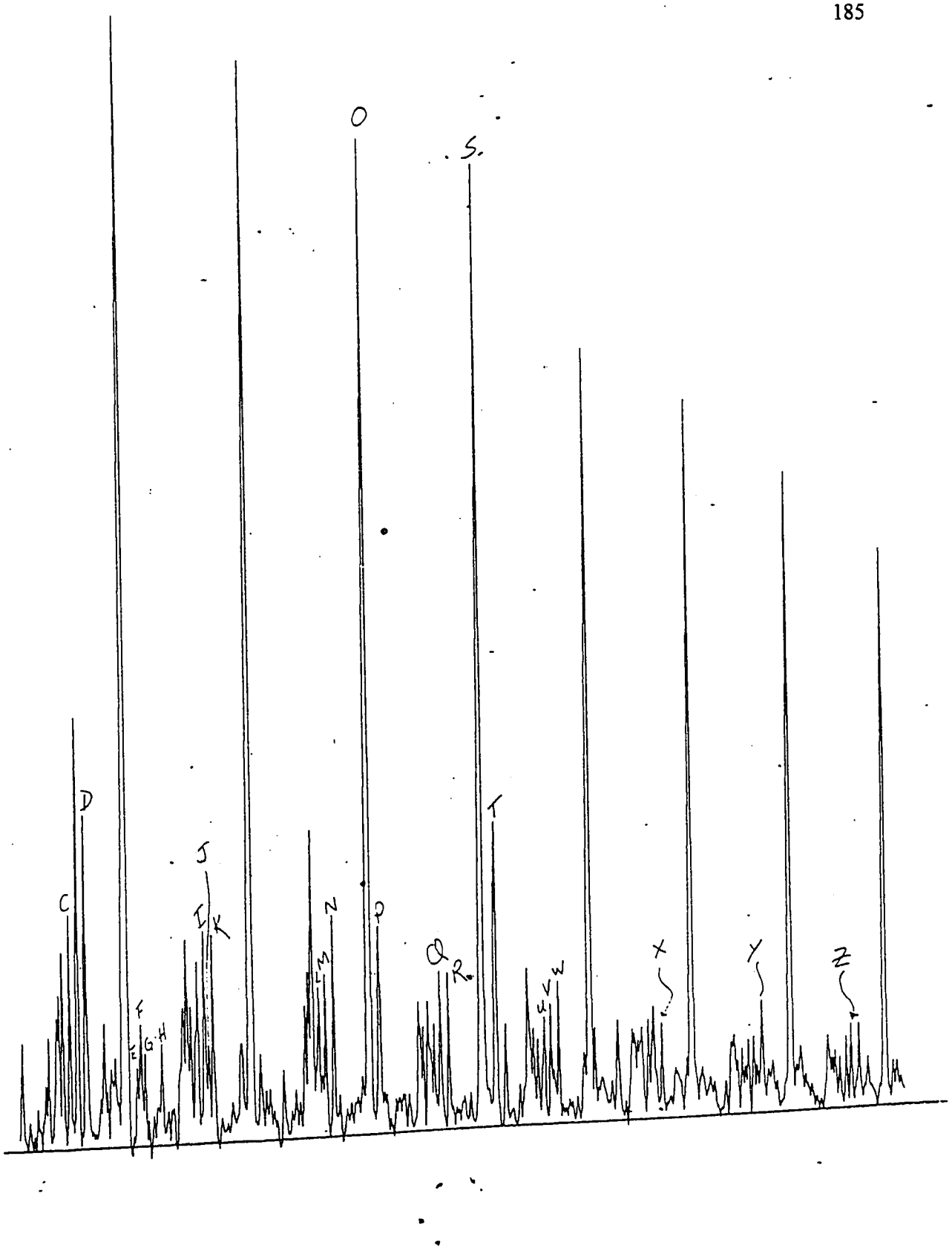

Figure 4.49 b. Whole-oil gas chromatogram of the middle range (38-67 min.) of oil H2._

Appendix (D)

GC/MS Fragmentograms of the Saturate Fractions

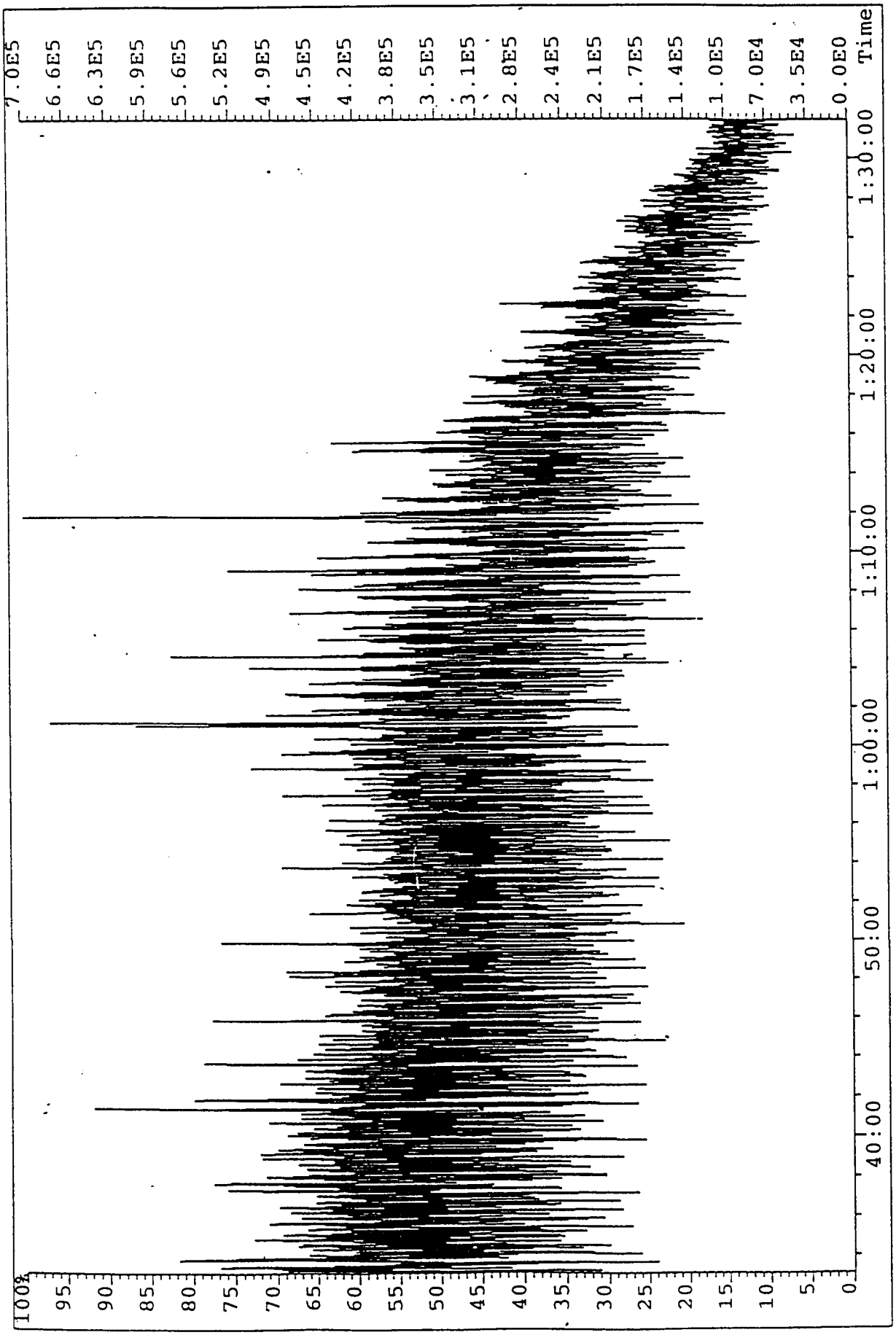

Figure 4.56 a. GCMS chromatogram (m/z 191) of the saturate fraction of oil A1.

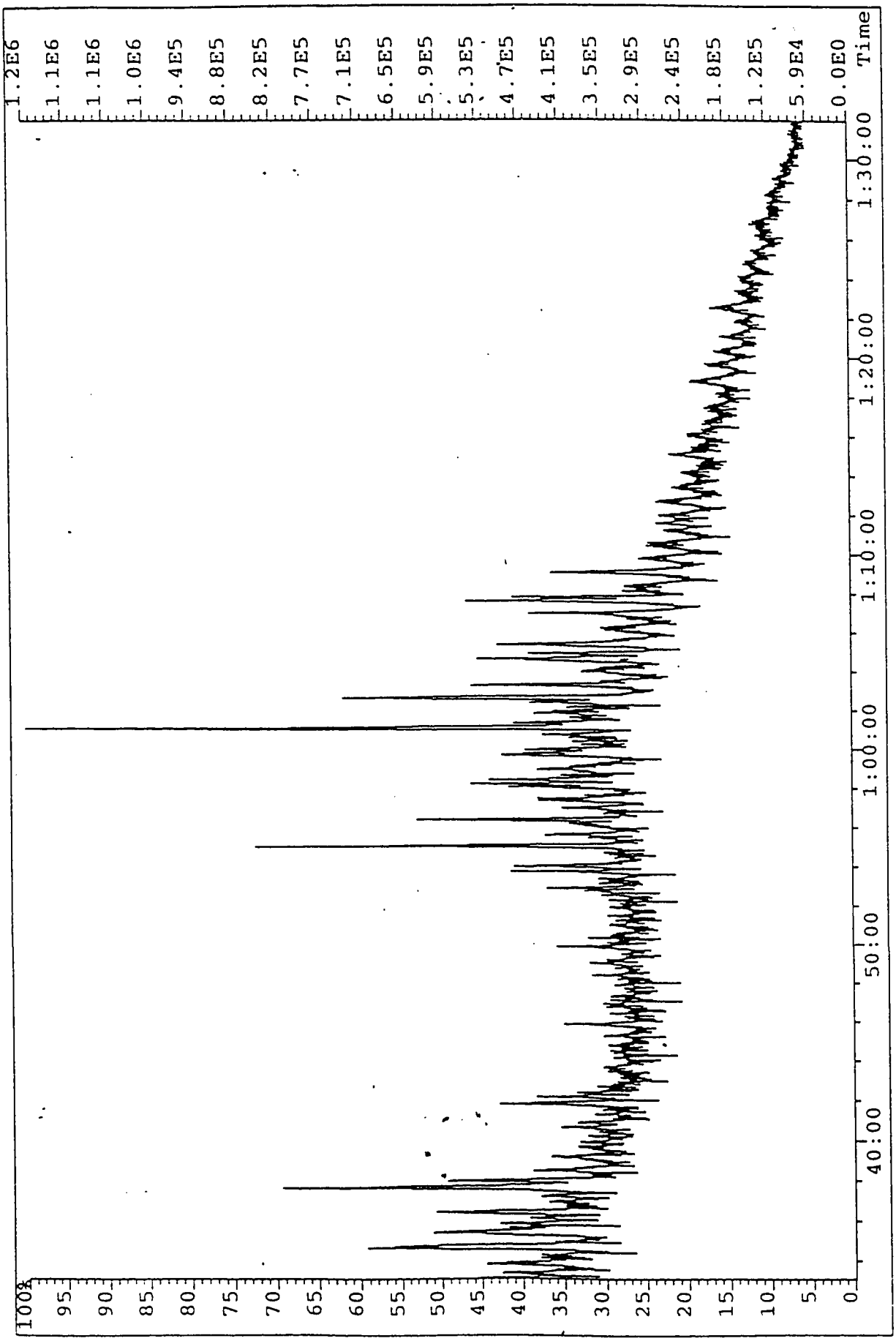

Figure 4.56 b. GCMS chromatogram (m/z 217) of the saturate fraction of oil A1.

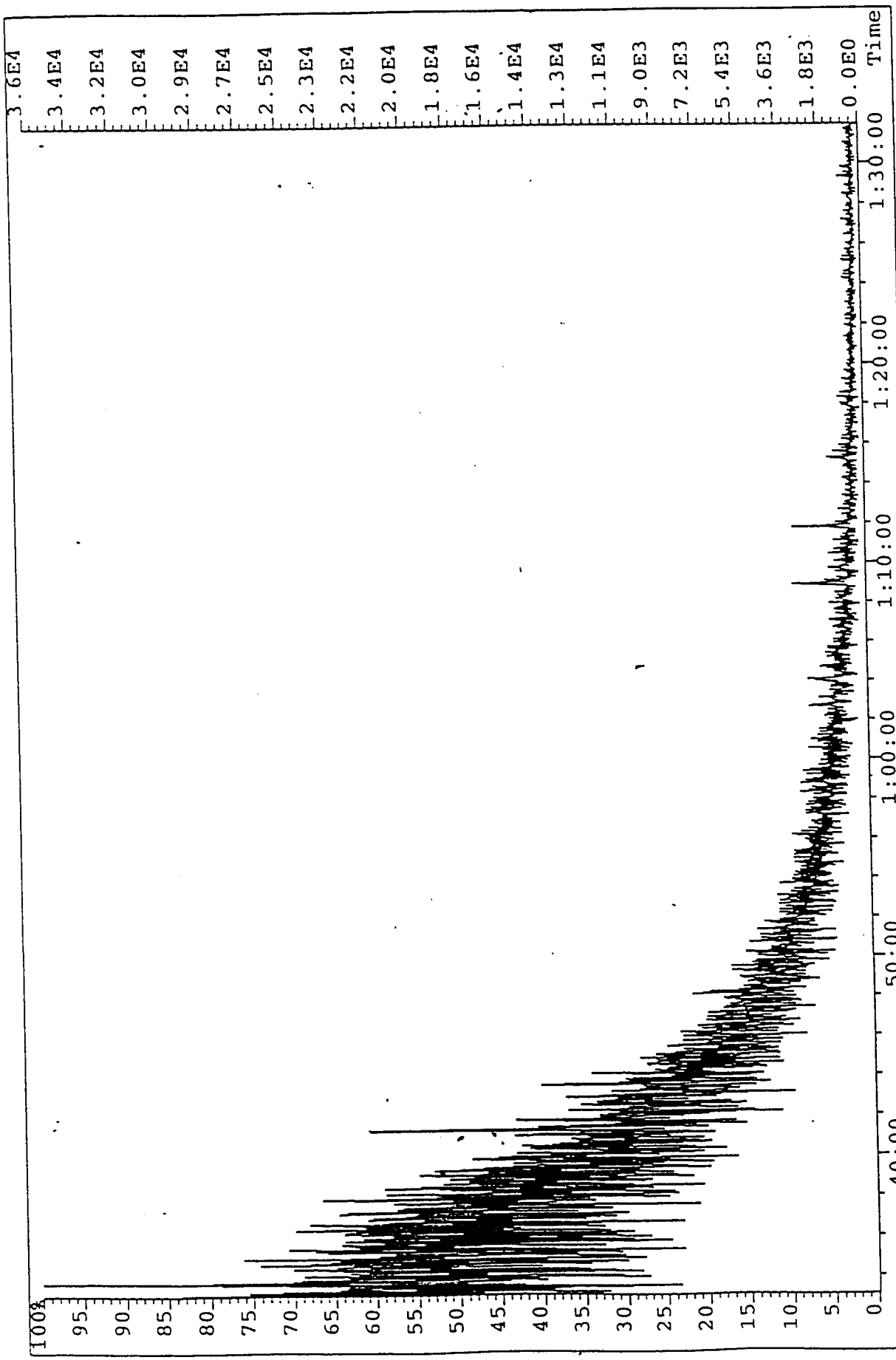

Figure 4.57 a. GCMS chromatogram (m/z 191) of the saturate fraction of oil A3.

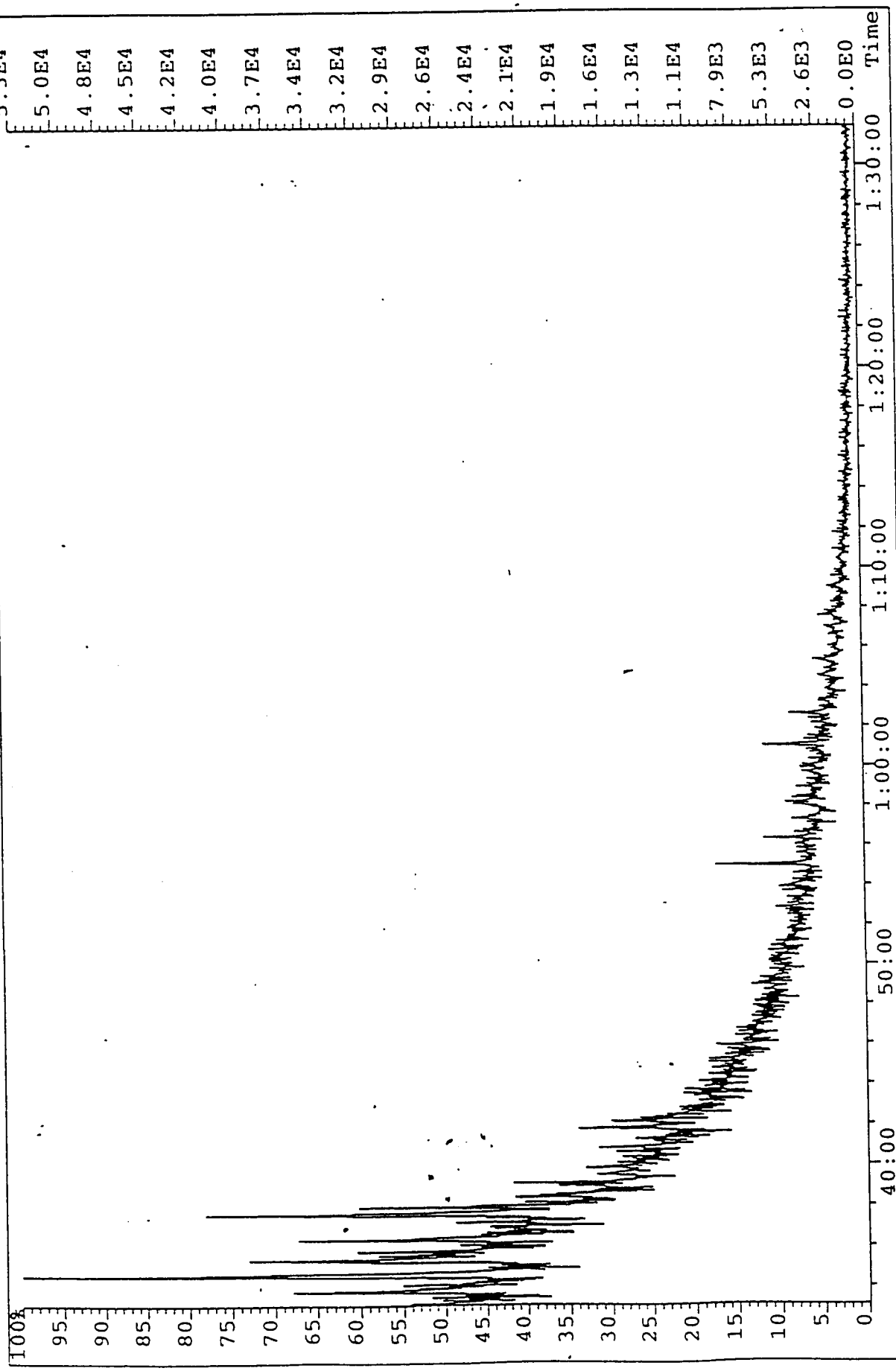

Figure 4.57 b. GCMS chromatogram (m/z 217) of the saturate fraction of oil A3.

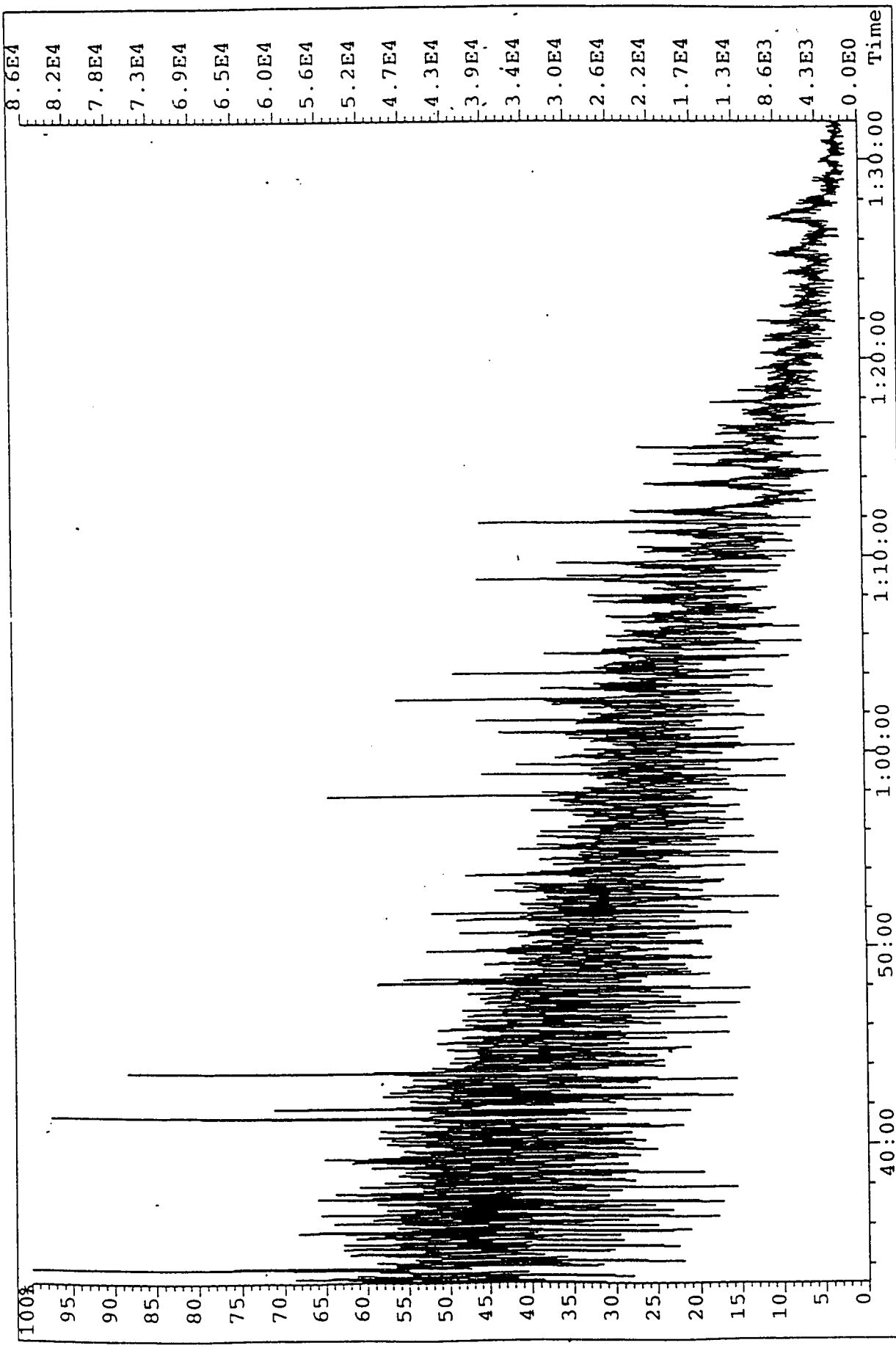

Figure 4.58 a. GCMS chromatogram (m/z 191) of the saturate fraction of oil B1.

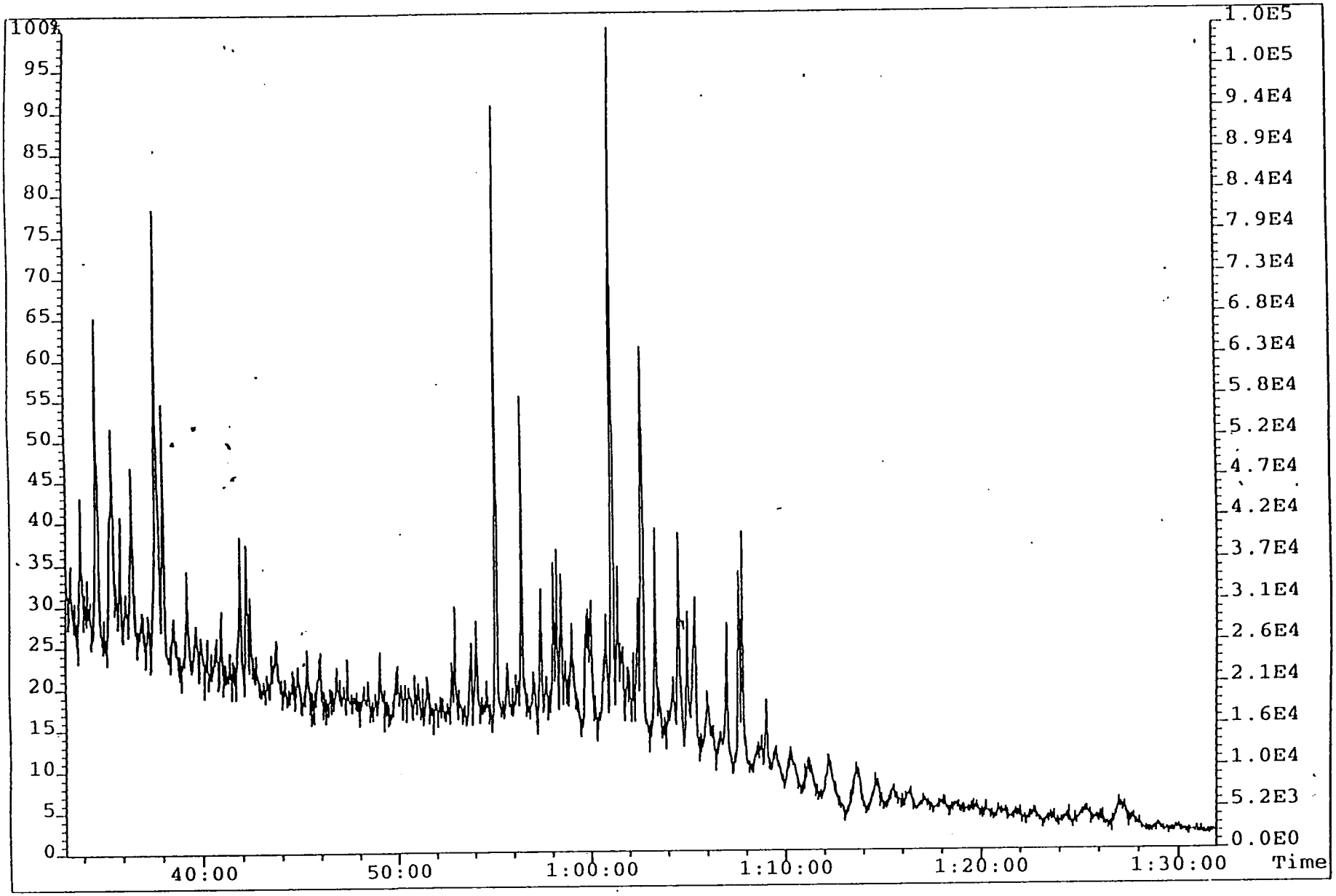

Figure 4.58 b. GCMS chromatogram (m/z 217) of the saturate fraction of oil B1.

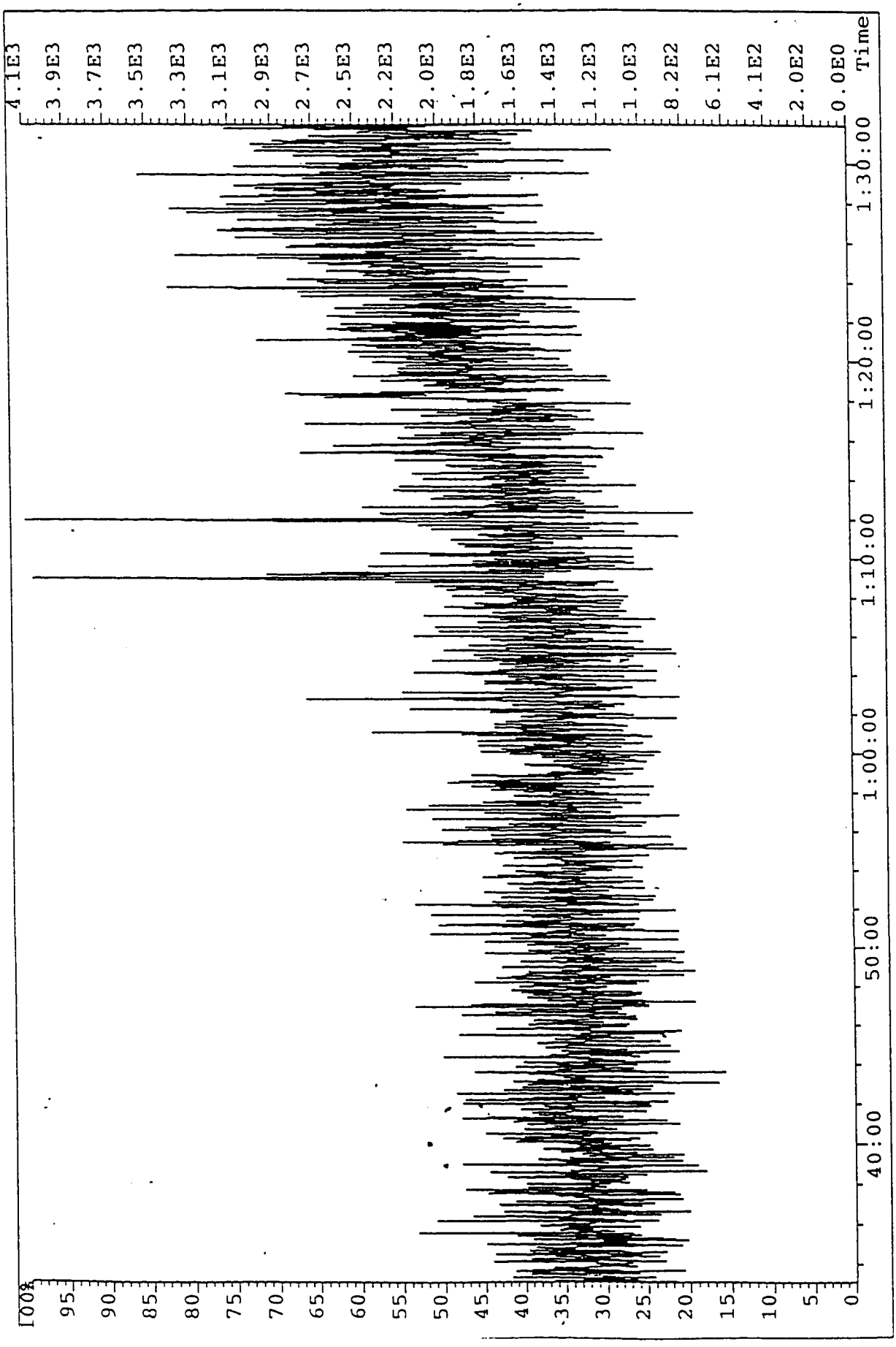

Figure 4.59 a. GCMS chromatogram (m/z 191) of the saturate fraction of oil C3.

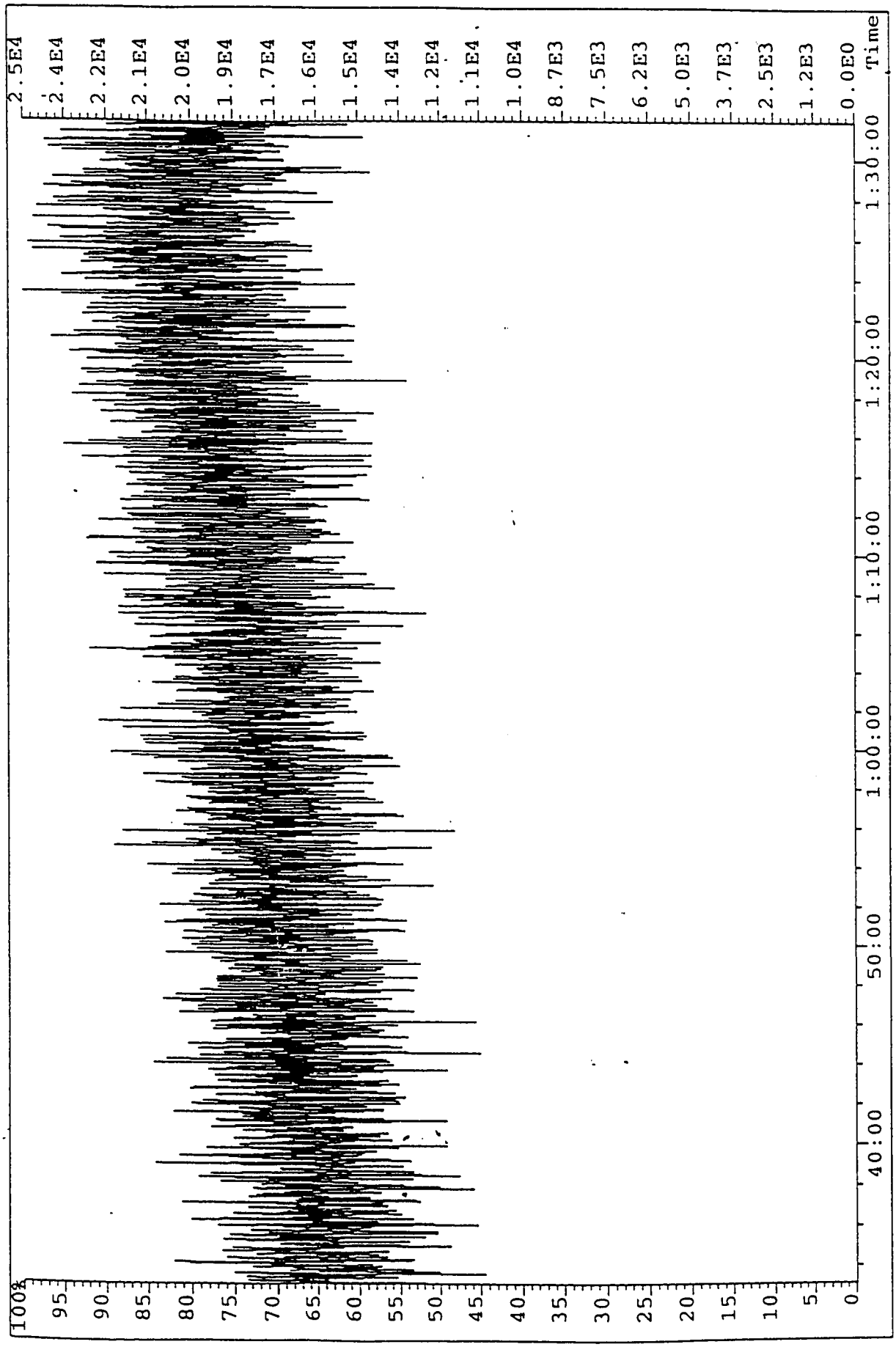

Figure 4.59 b. GCMS chromatogram (m/z 217) of the saturate fraction of oil C3.

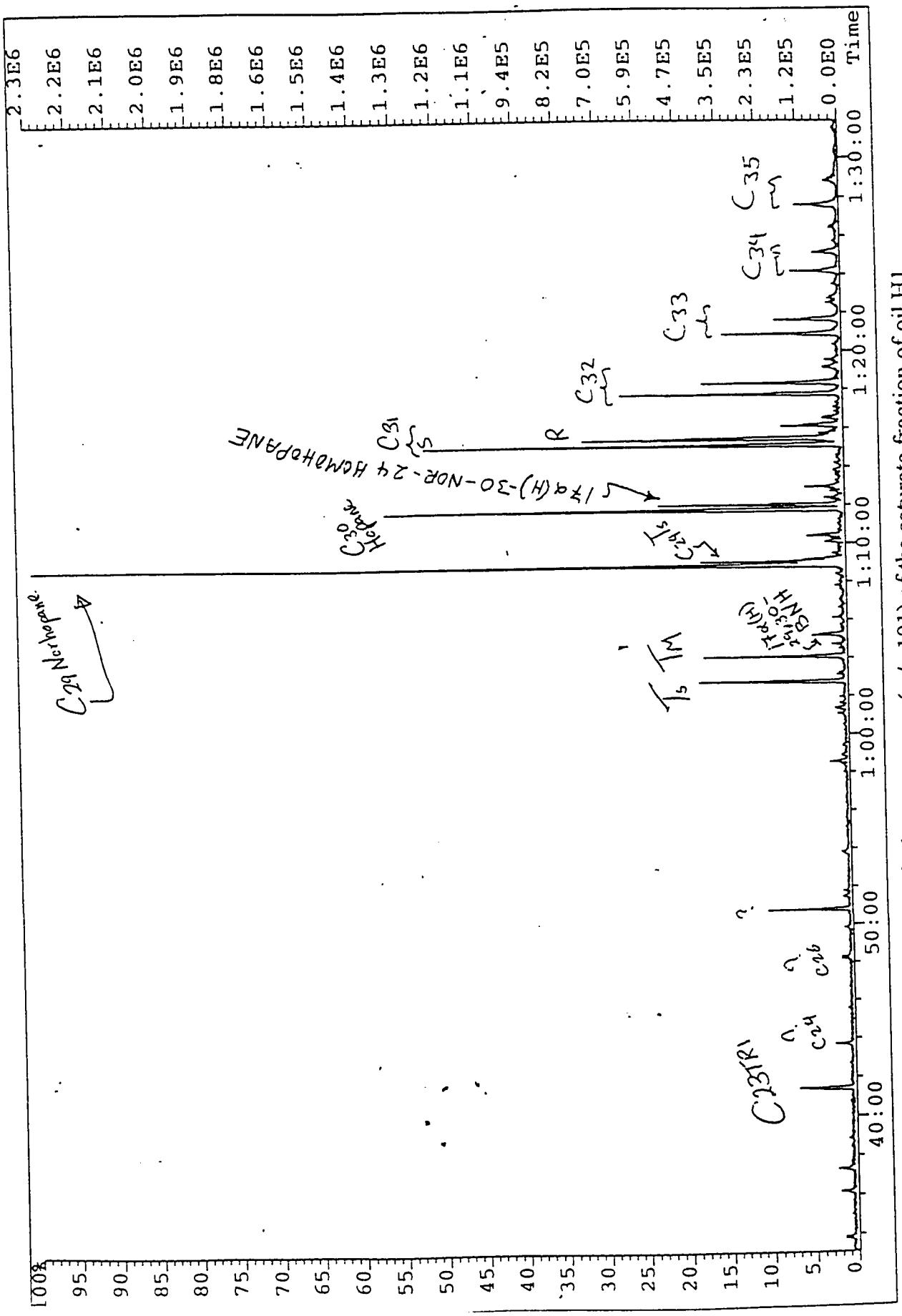

Figure 4.60 a. GCMS chromatogram (m/z 191) of the saturate fraction of oil H1.

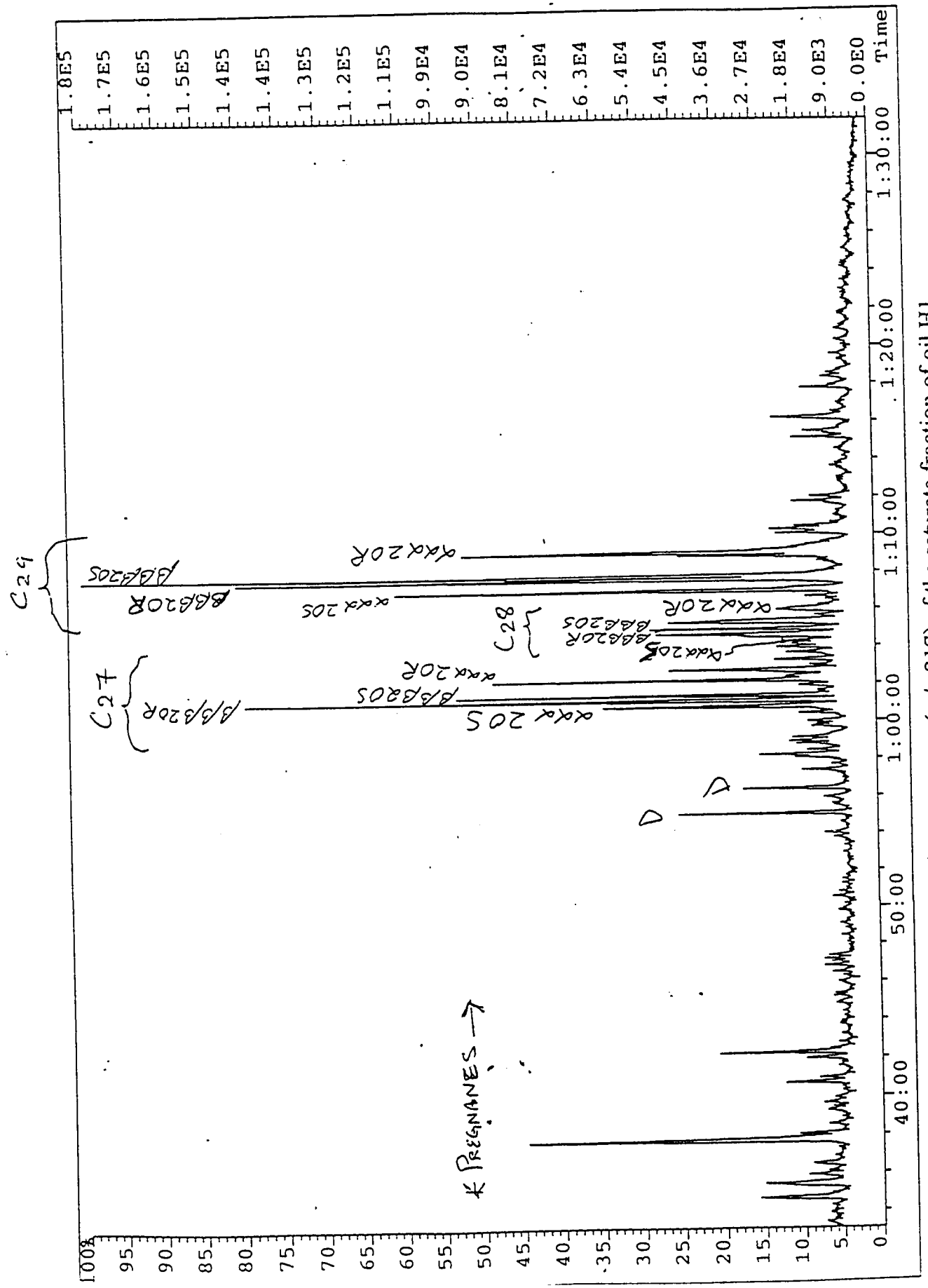

Figure 4.60 b. GCMS chromatogram (m/z 217) of the saturate fraction of oil H1.

Appendix (E)

GC/MS Fragmentograms of the Aromatic Fractions

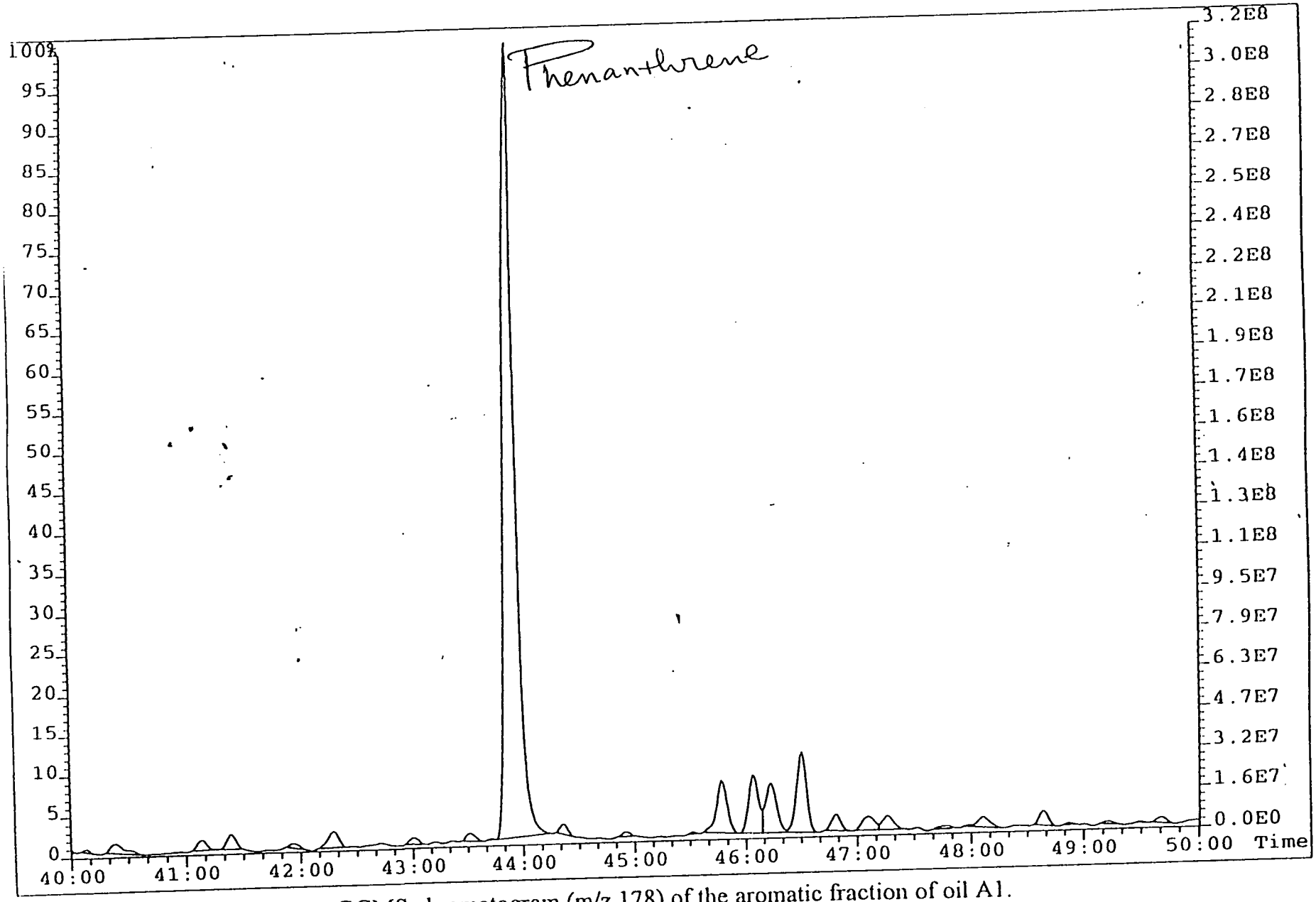

Figure 4.61 a. GCMS chromatogram (m/z 178) of the aromatic fraction of oil A1.

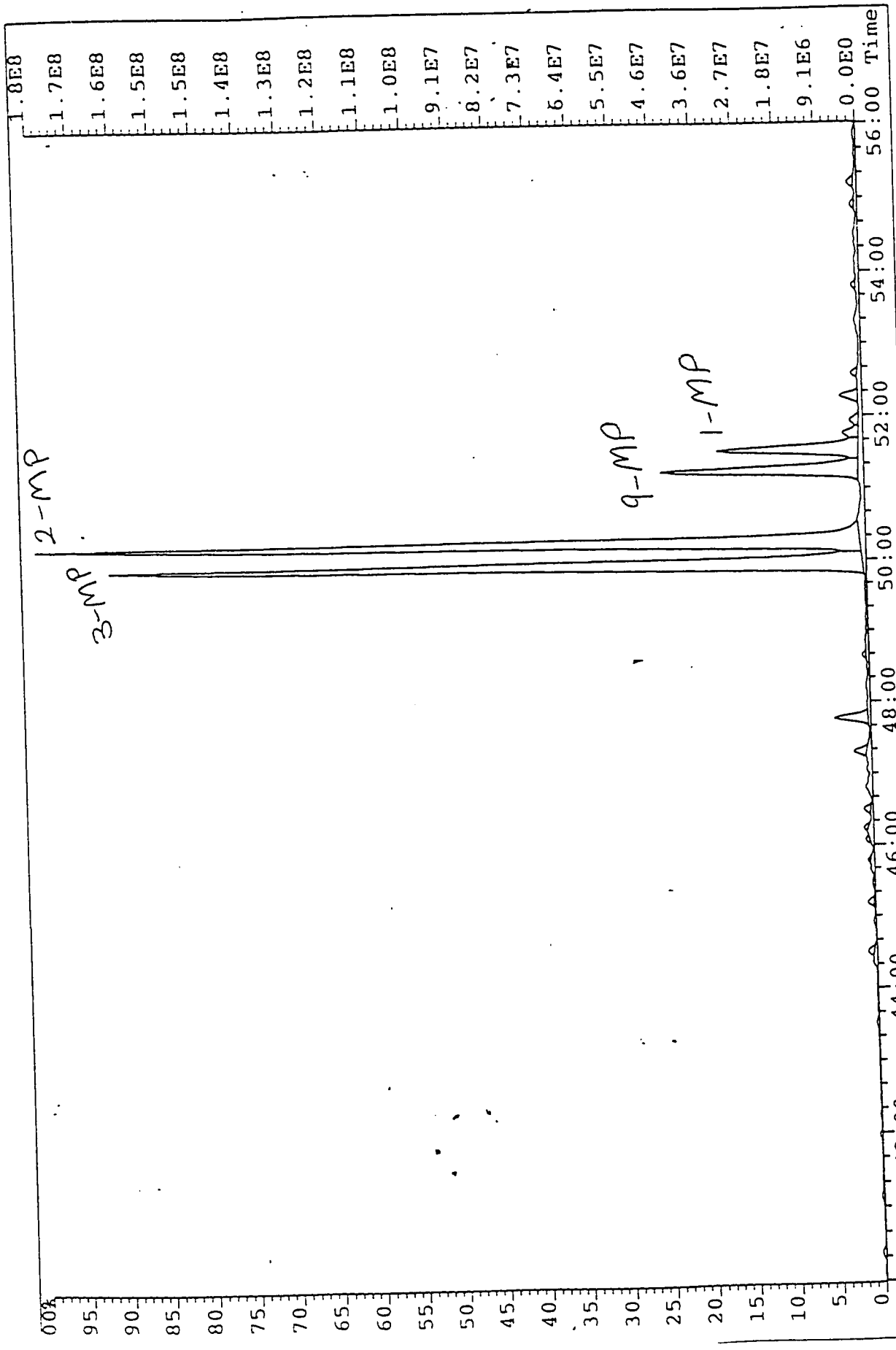

Figure 4.61 b. GCMS chromatogram (m/z 192) of the aromatic fraction of oil A1.

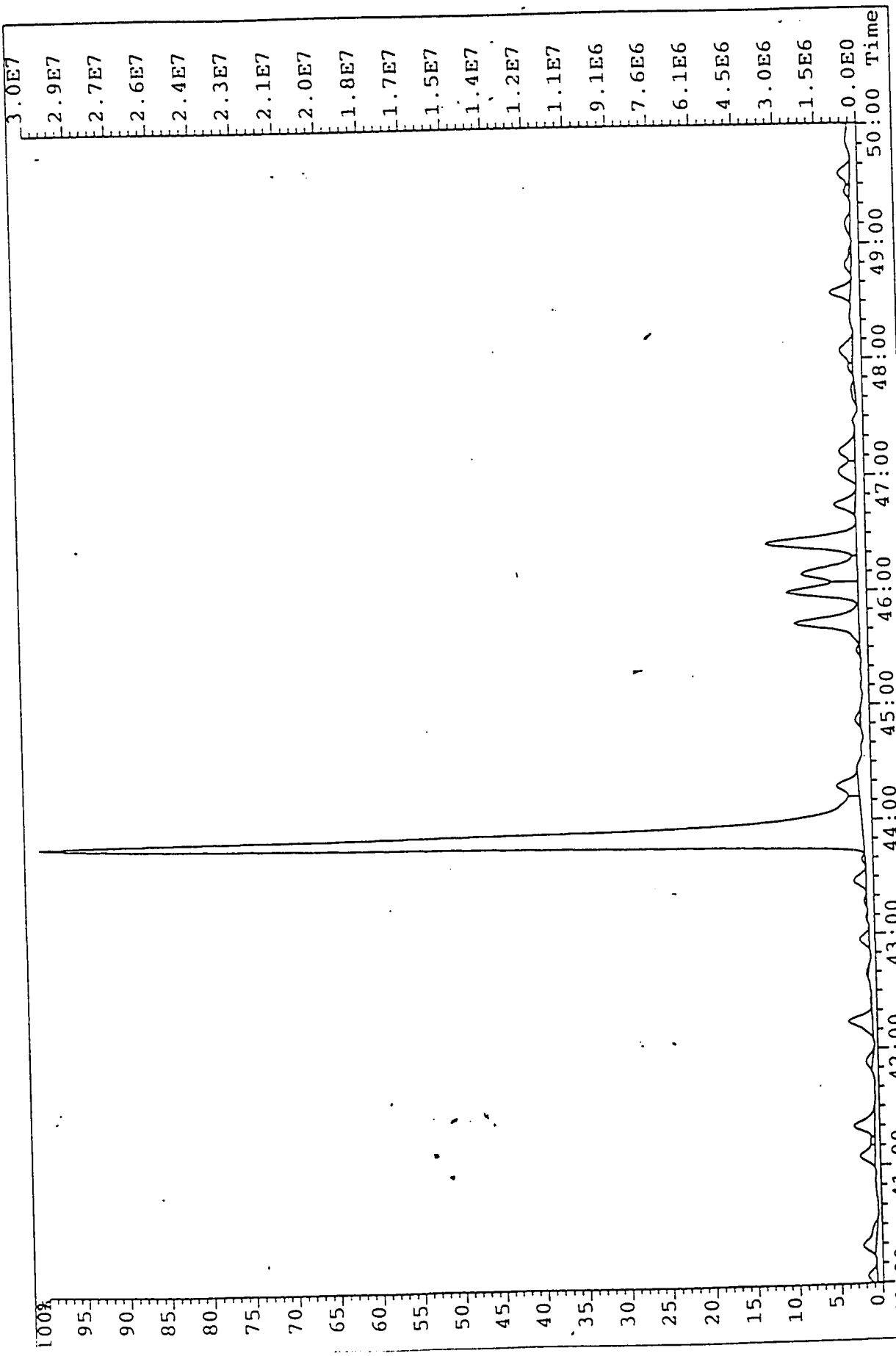

Figure 4.62 a. GCMS chromatogram (m/z 178) of the aromatic fraction of oil A2.

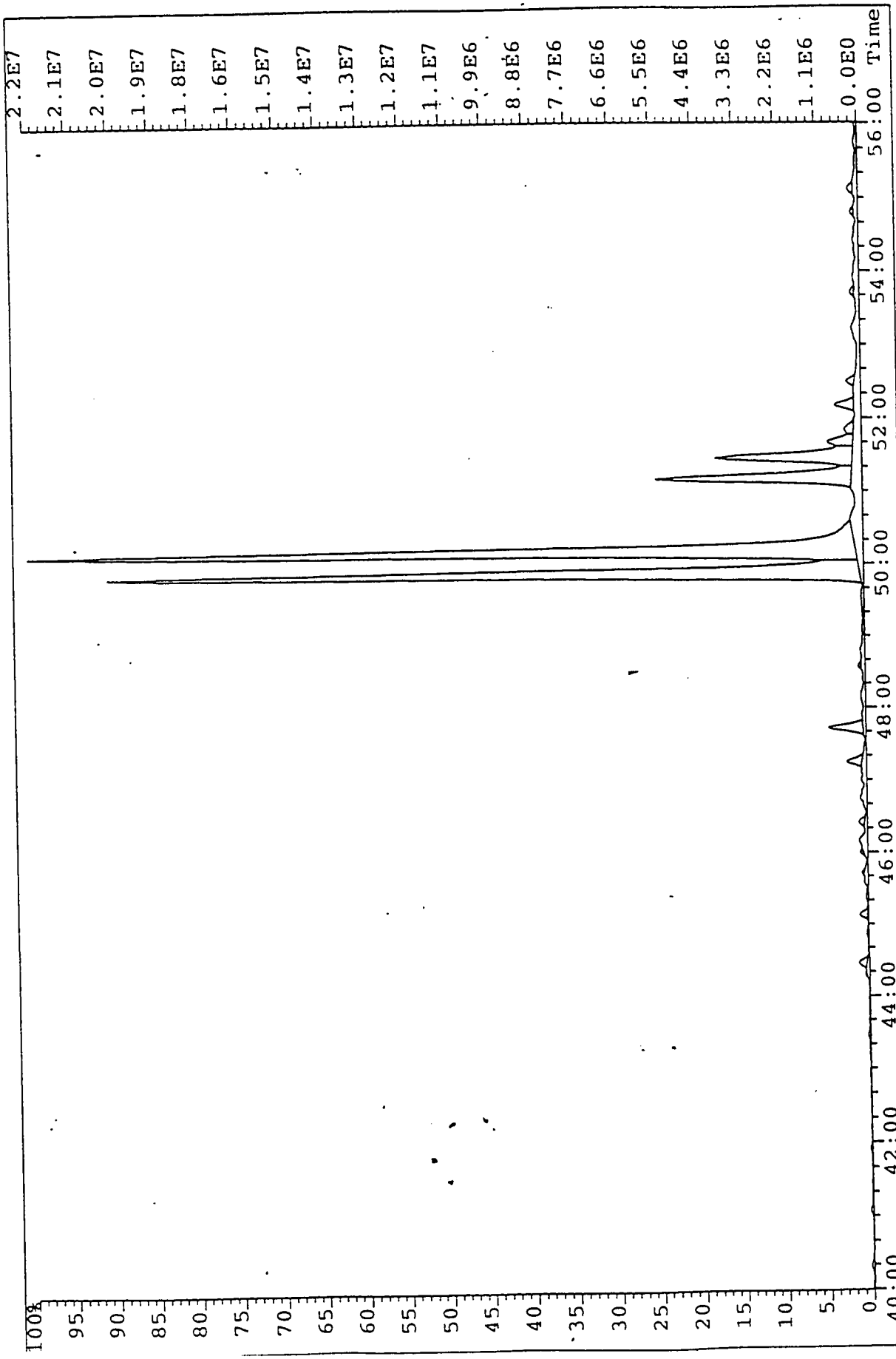

Figure 4.62 b. GCMS chromatogram (m/z 192) of the aromatic fraction of oil A2.

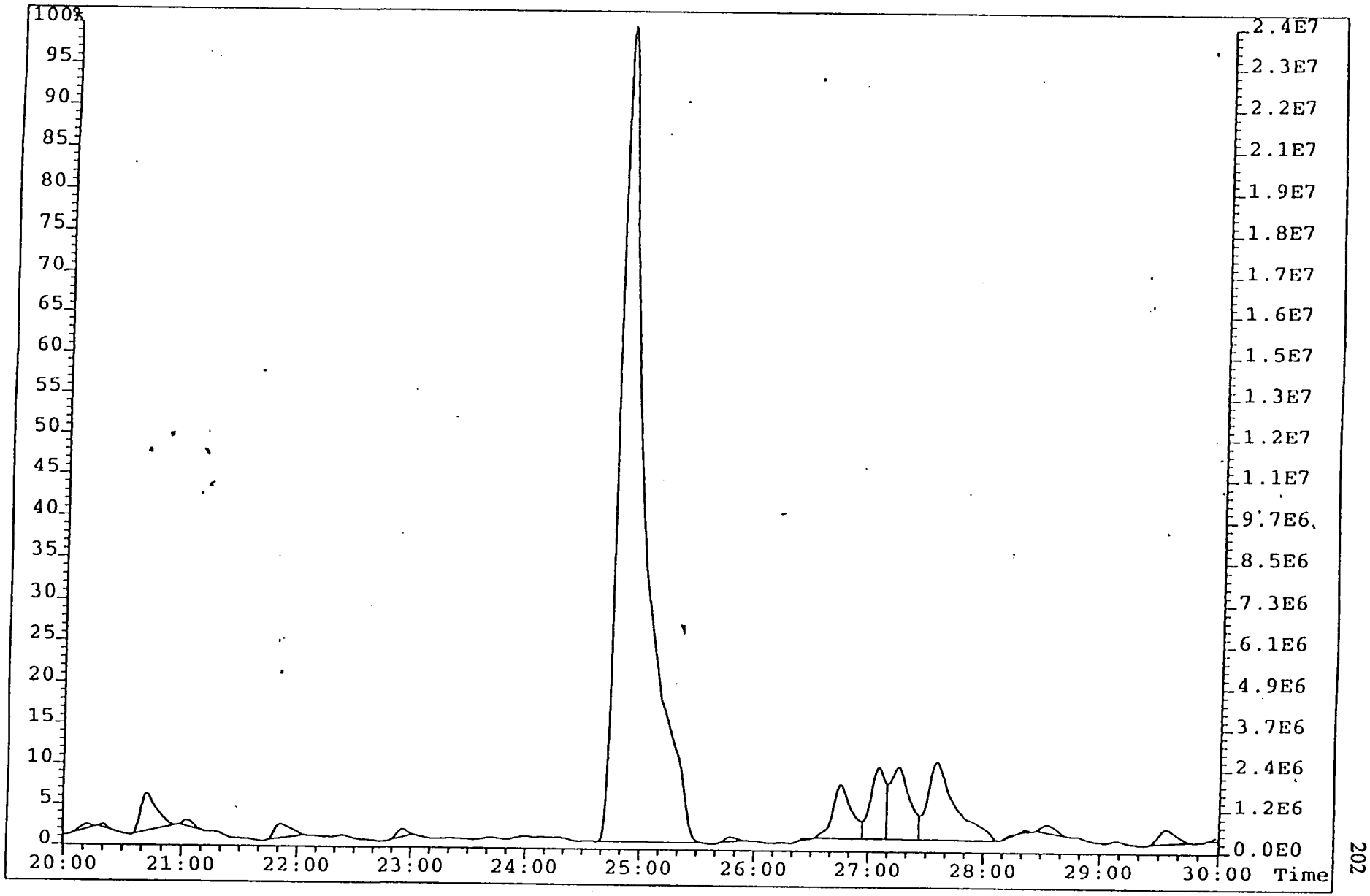

Figure 4.63 a. GCMS chromatogram (m/z 178) of the aromatic fraction of oil A3.

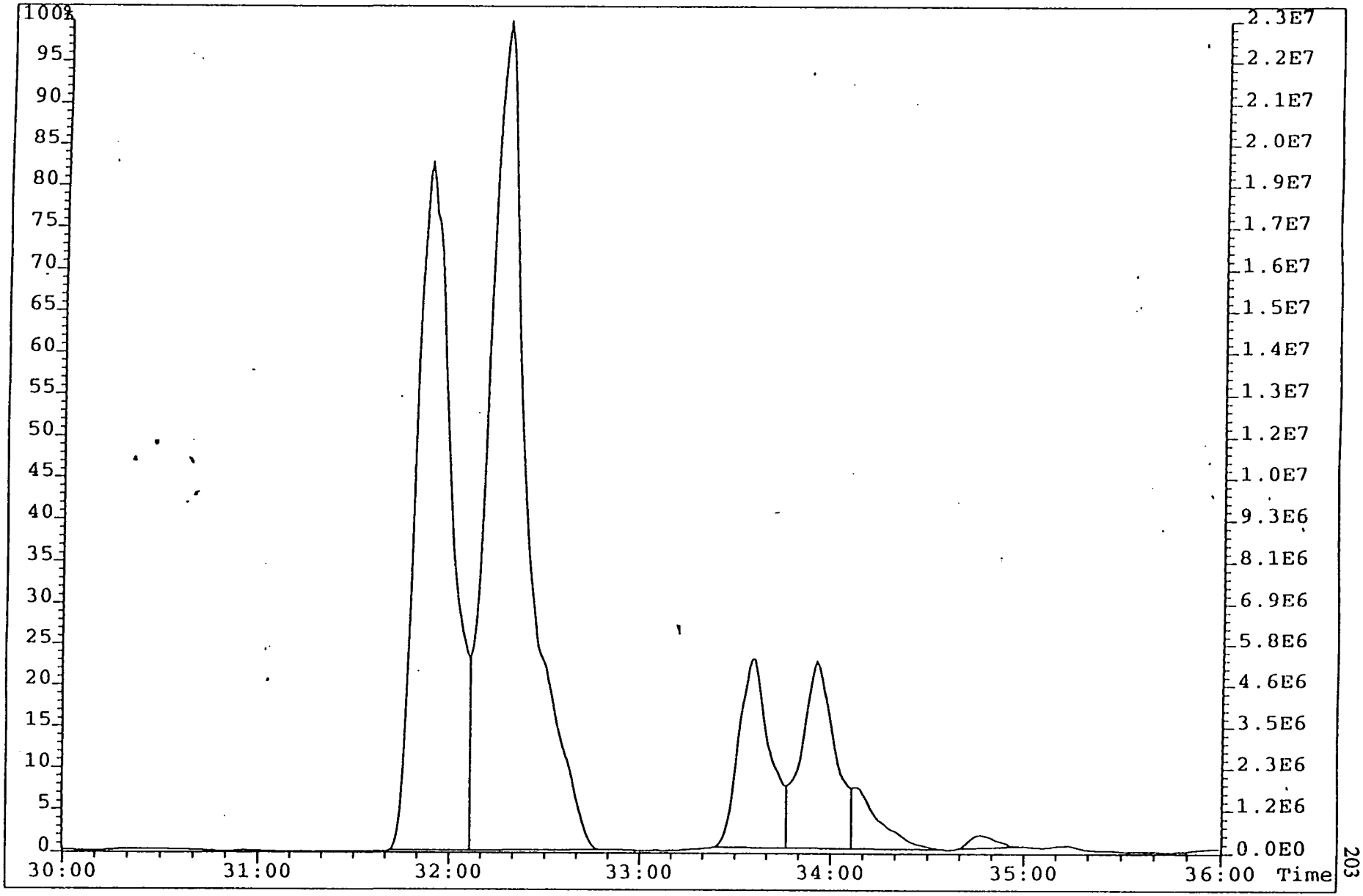

Figure 4.63 b. GCMS chromatogram (m/z 192) of the aromatic fraction of oil A3.

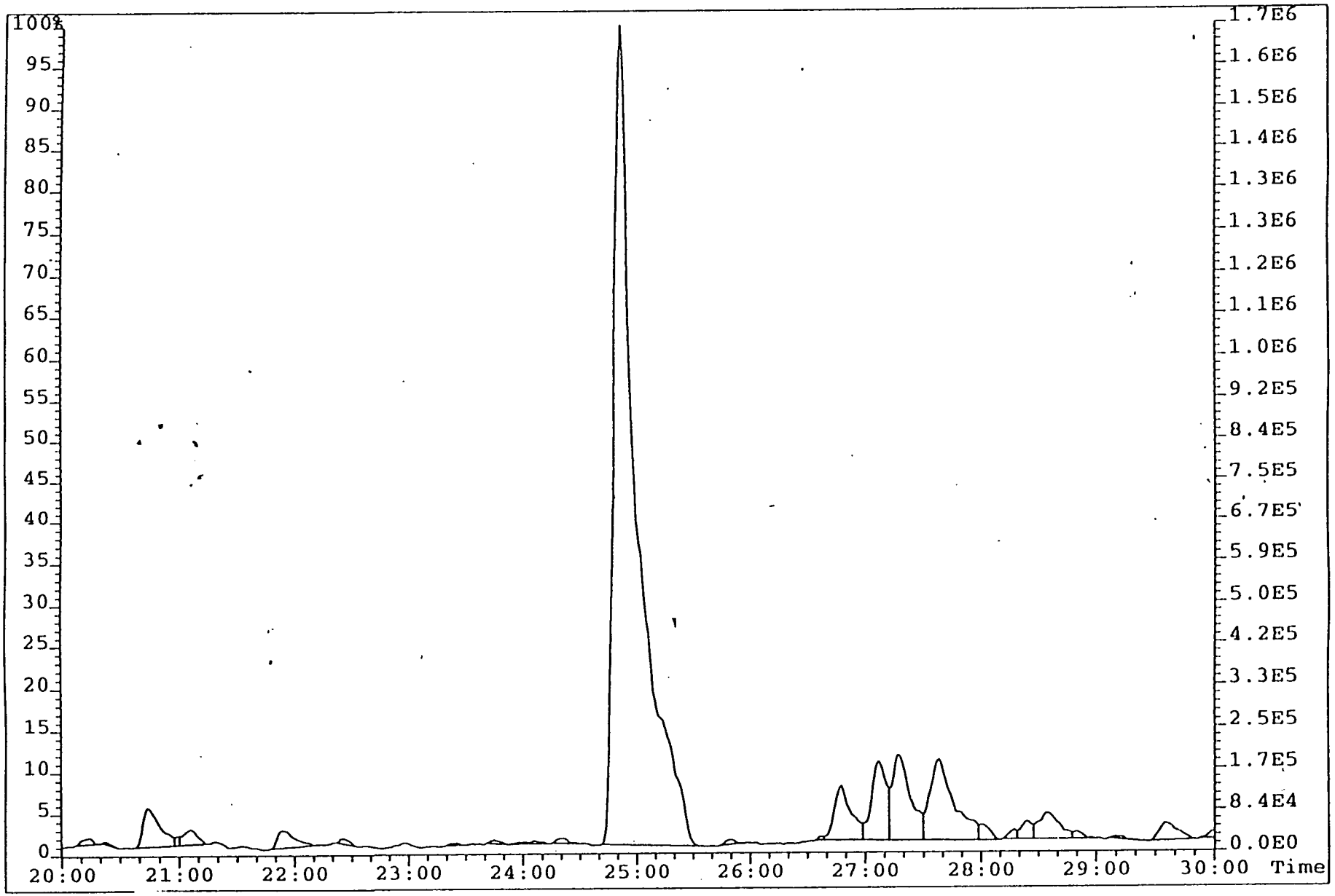

Figure 4.64 a. GCMS chromatogram (m/z 178) of the aromatic fraction of oil B1.

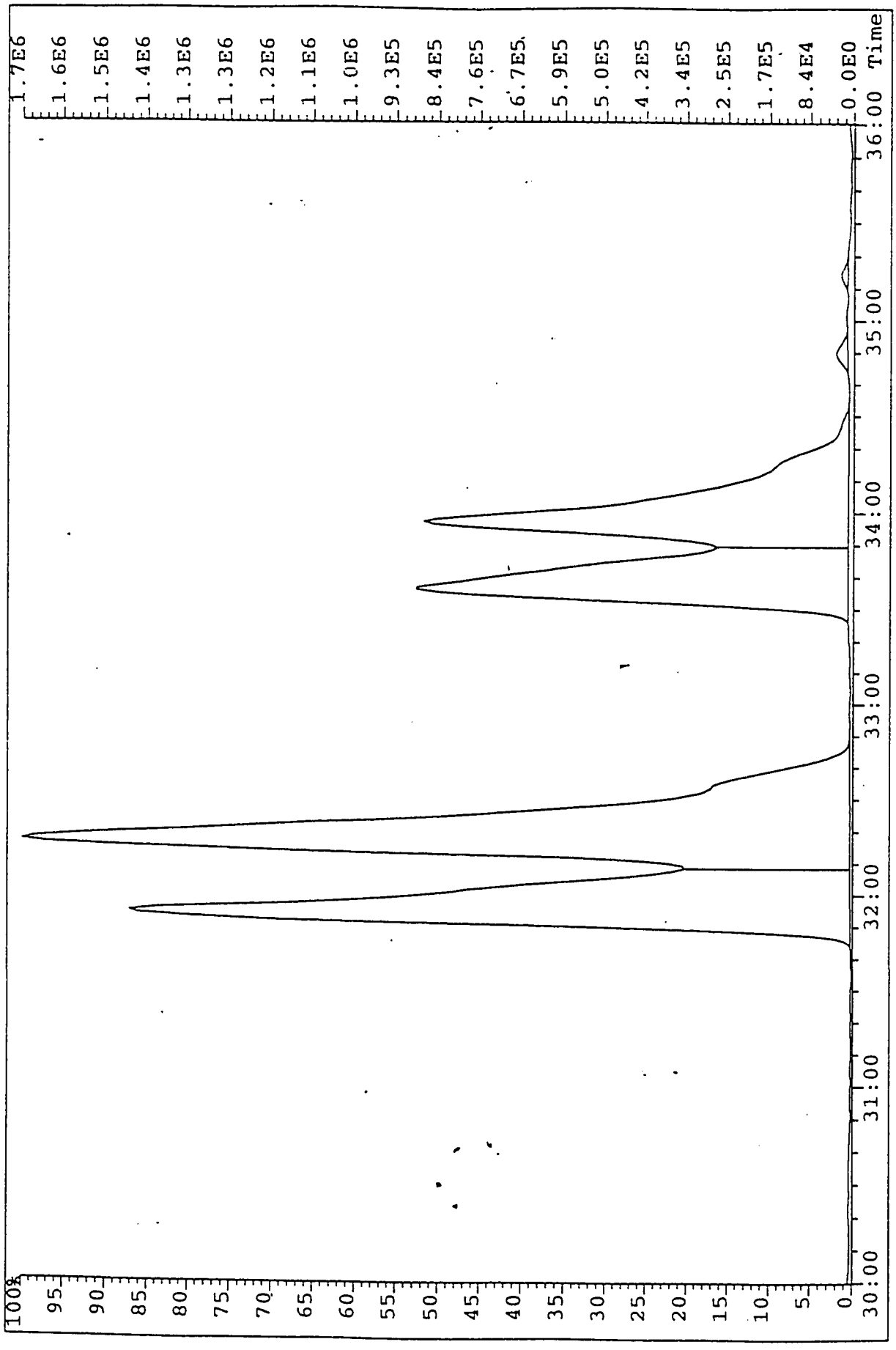

Figure 4.64 b. GCMS chromatogram (m/z 192) of the aromatic fraction of oil B1.

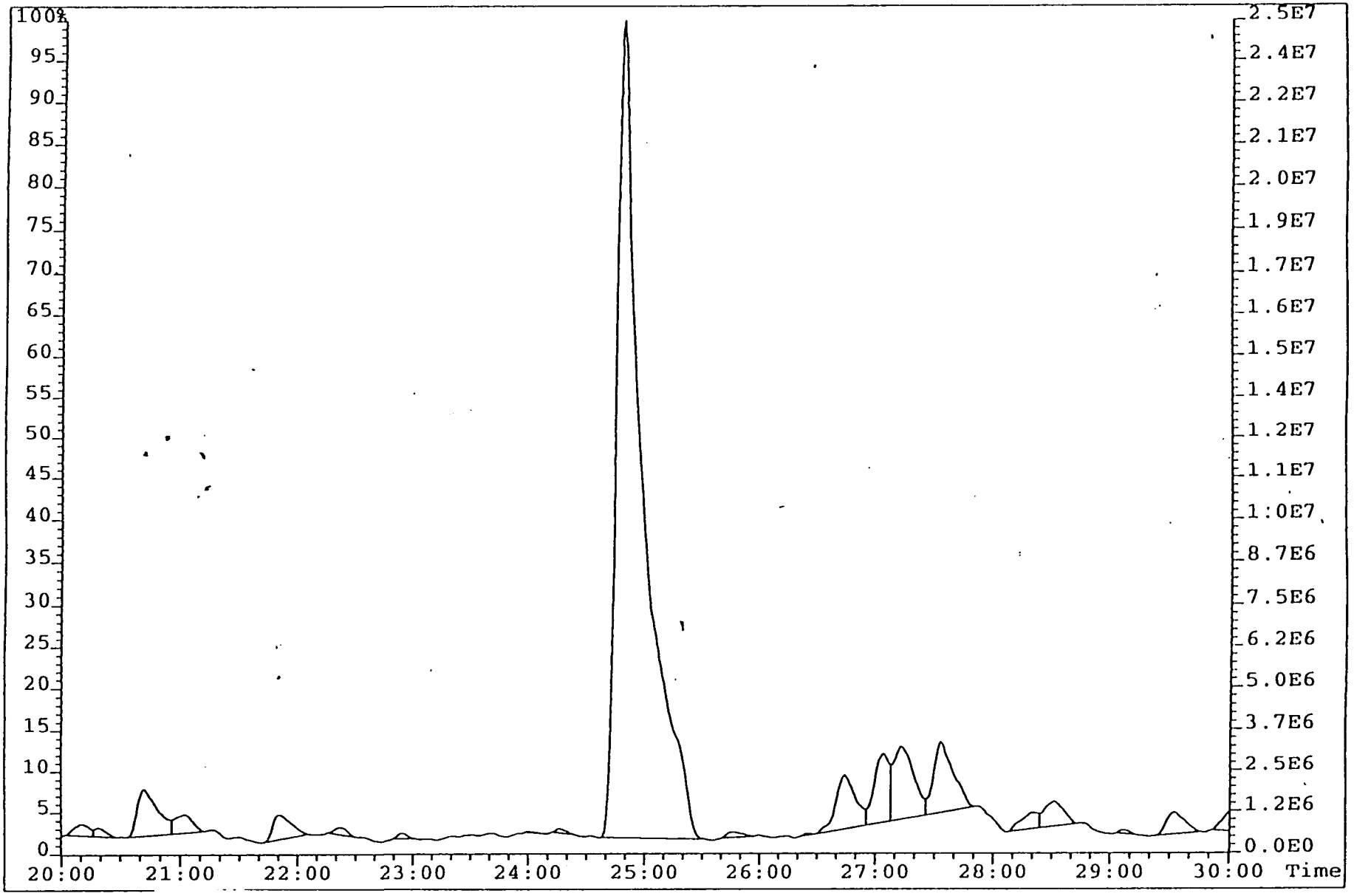

Figure 4.65 a. GCMS chromatogram (m/z 178) of the aromatic fraction of oil B2.

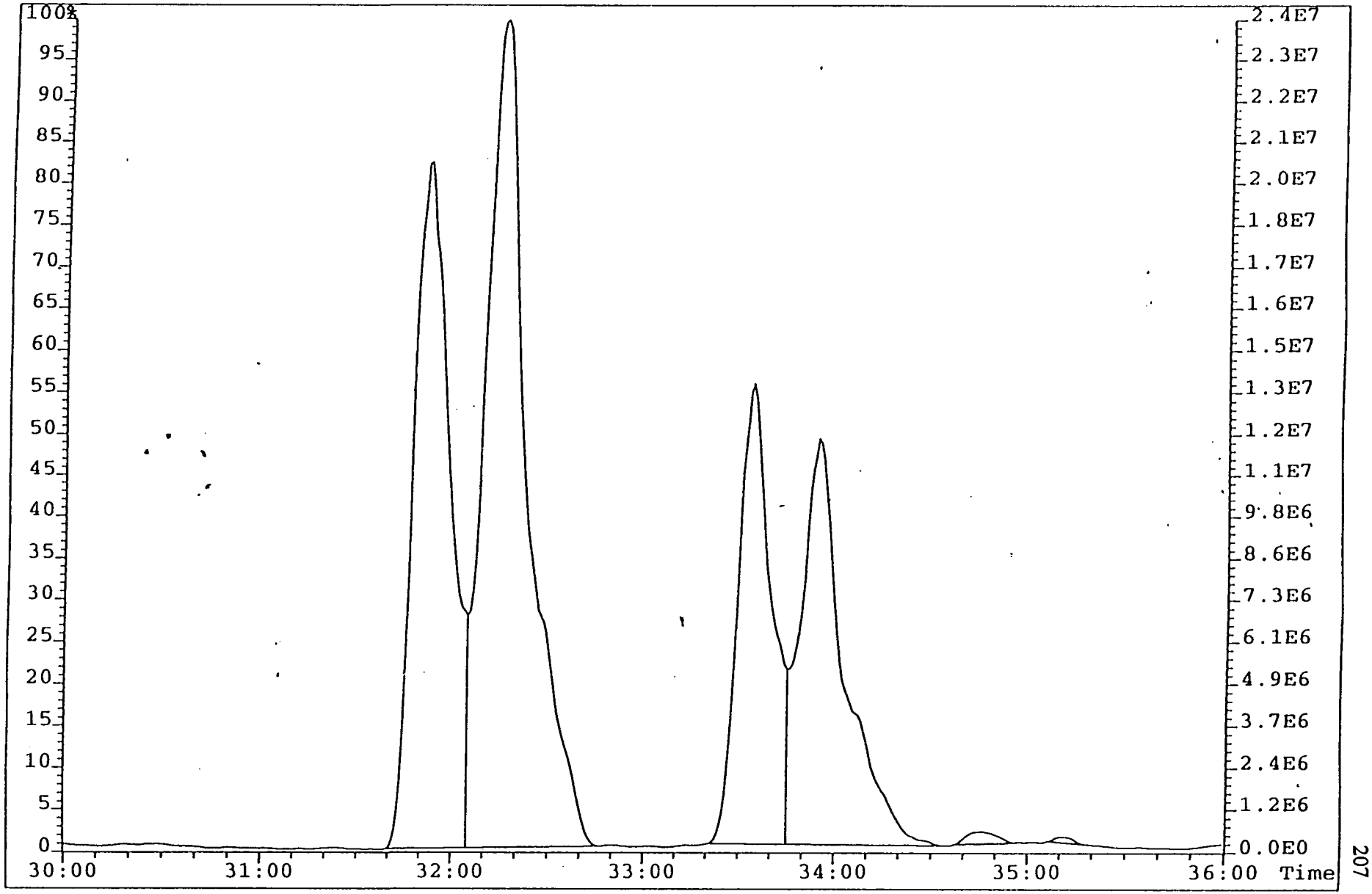

Figure 4.65 b. GCMS chromatogram (m/z 192) of the aromatic fraction of oil B2.

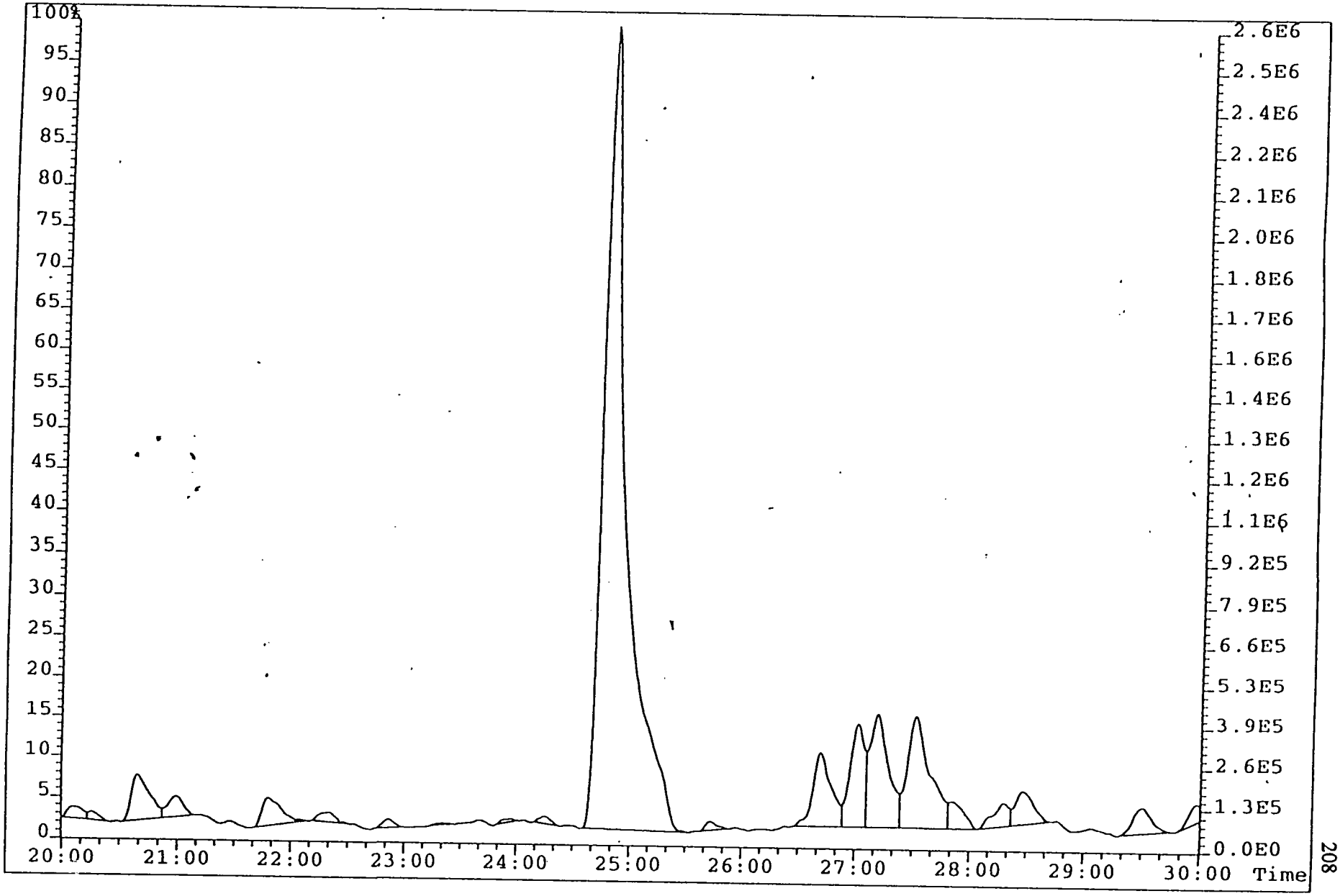

Figure 4.66 a. GCMS chromatogram (m/z 178) of the aromatic fraction of oil B3.

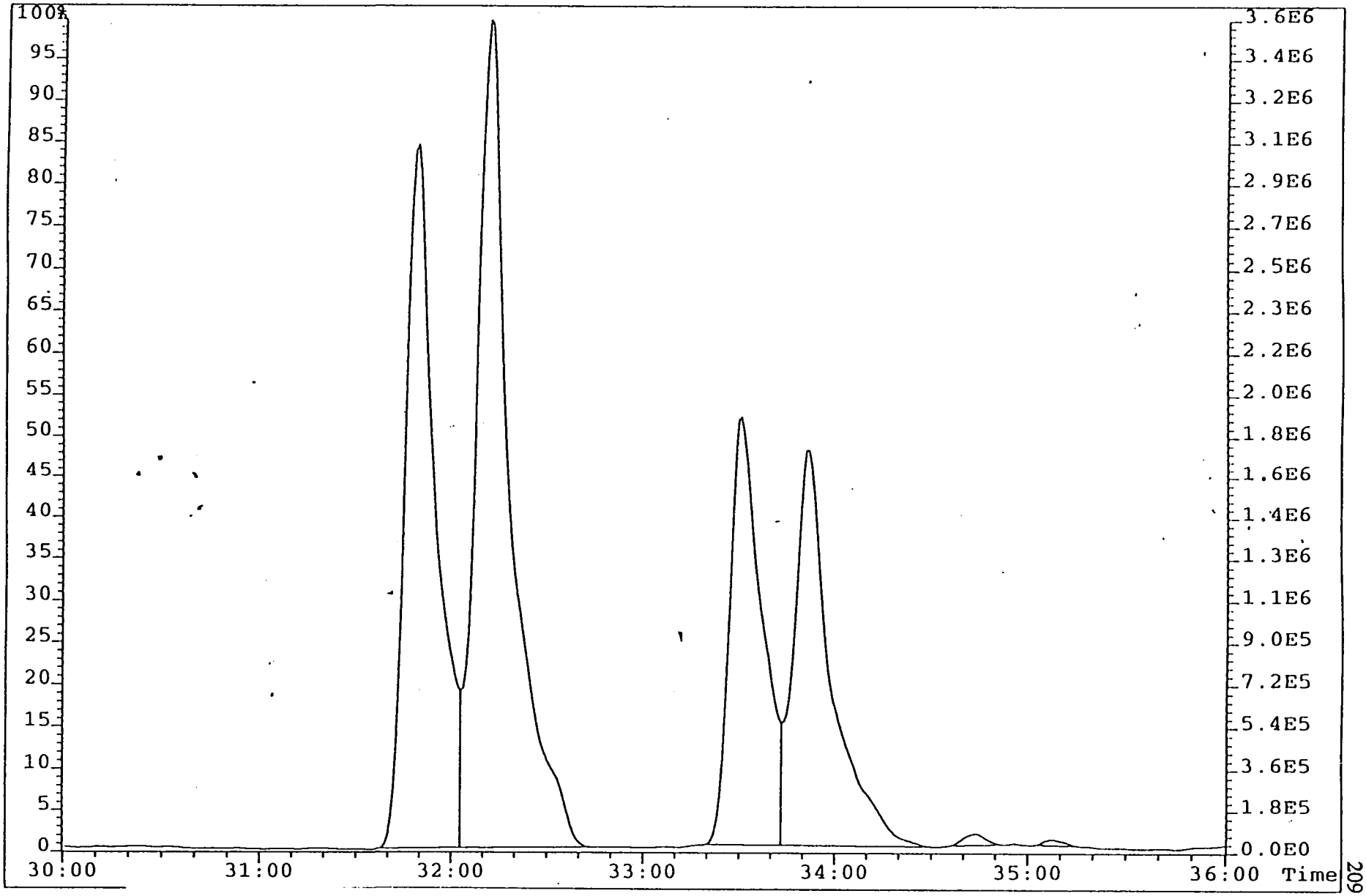

Figure 4.66 b. GCMS chromatogram (m/z 192) of the aromatic fraction of oil B3.

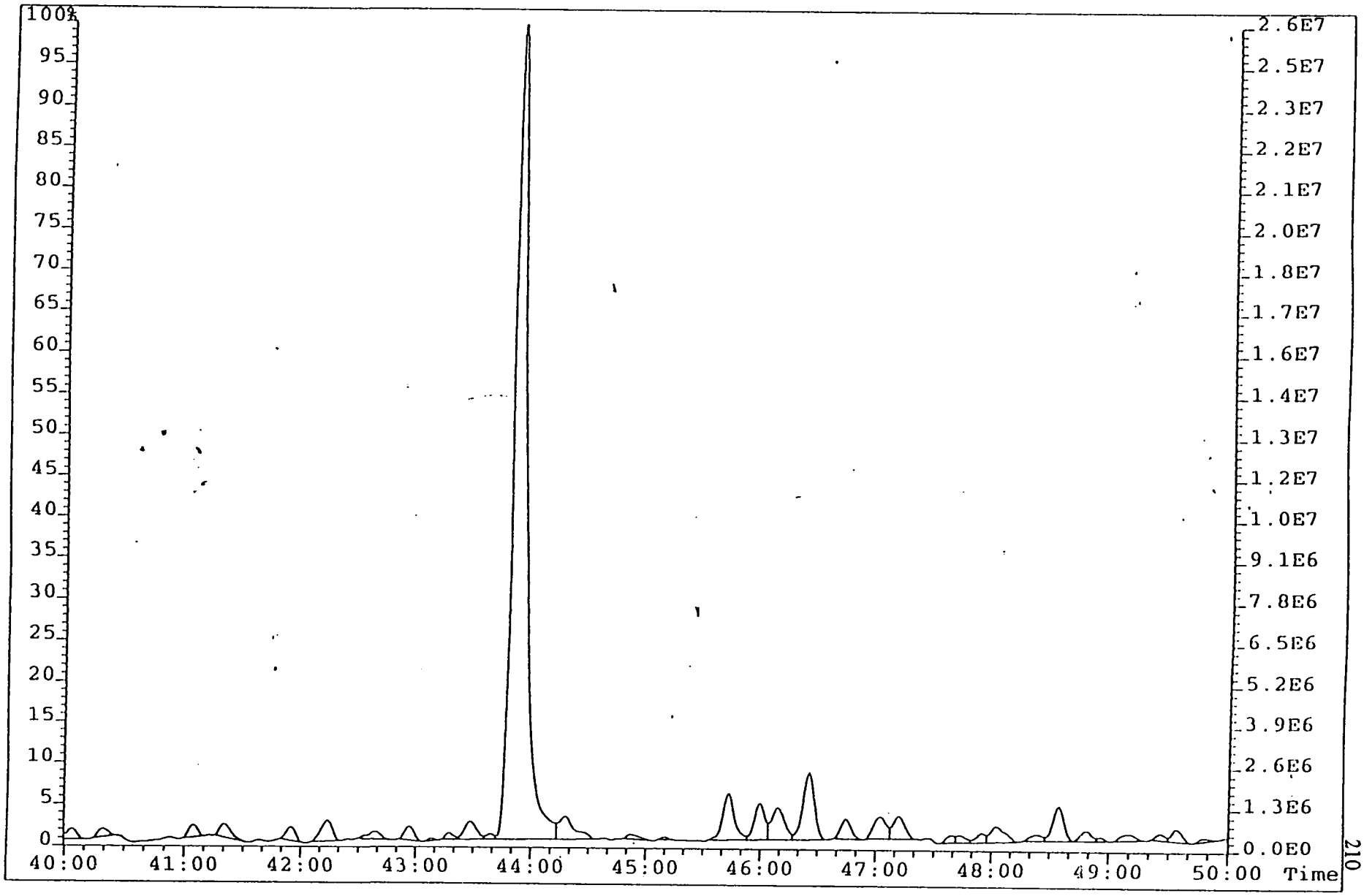

Figure 4.67 a. GCMS chromatogram (m/z 178) of the aromatic fraction of oil C1.

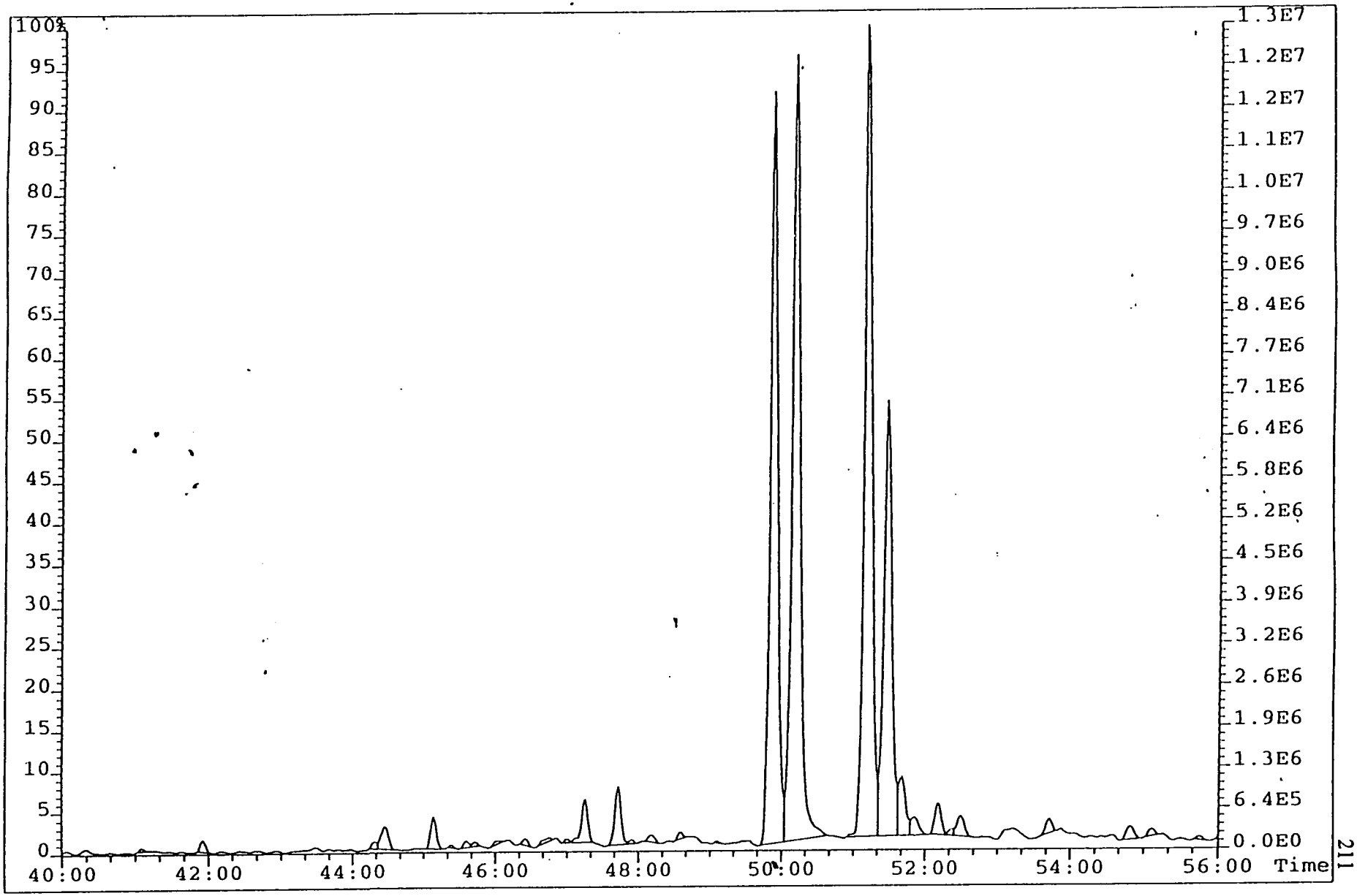

Figure 4.67 b. GCMS chromatogram (m/z 192) of the aromatic fraction of oil C1.

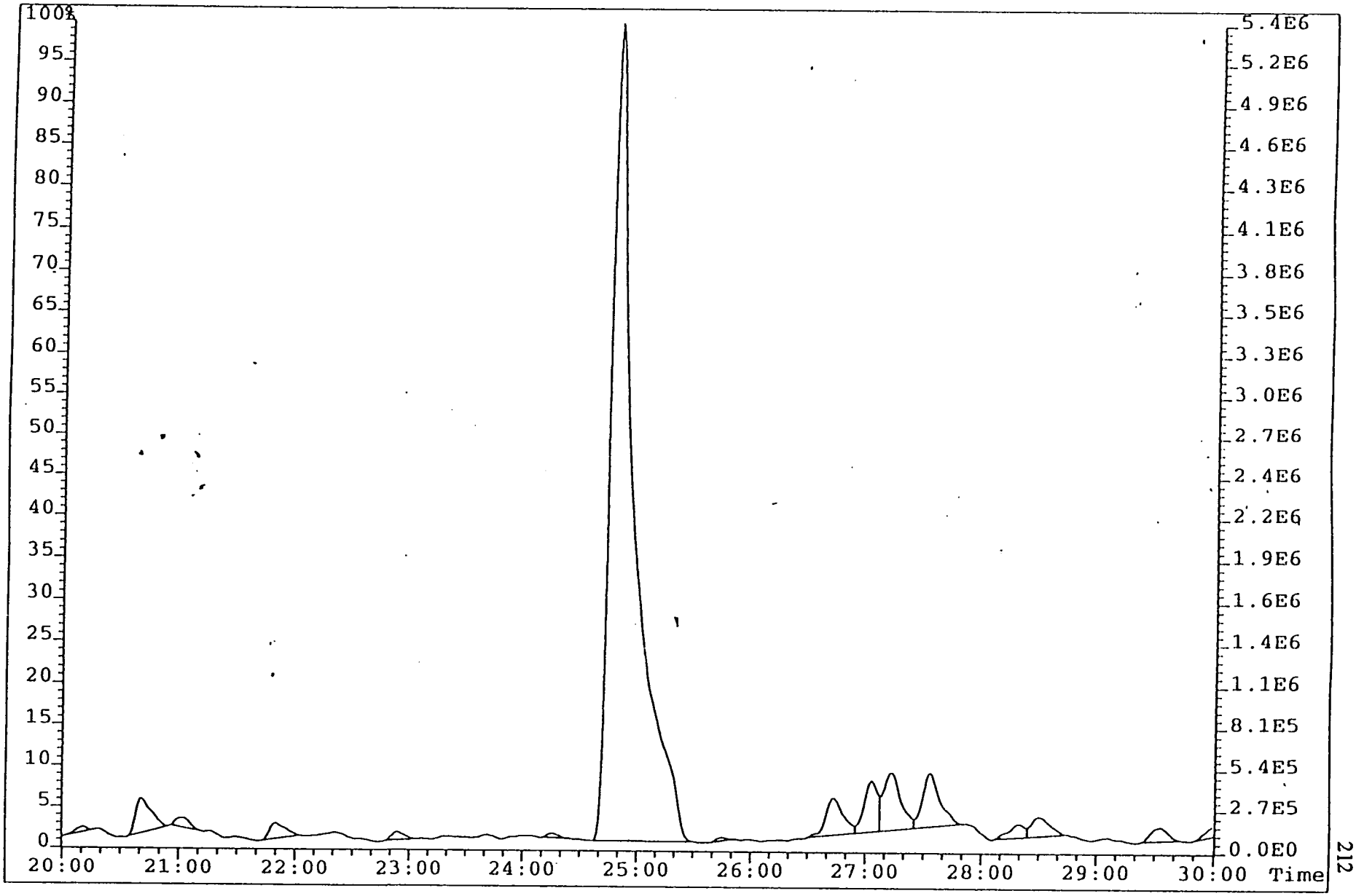

Figure 4.68 a. GCMS chromatogram (m/z 178) of the aromatic fraction of oil C2.

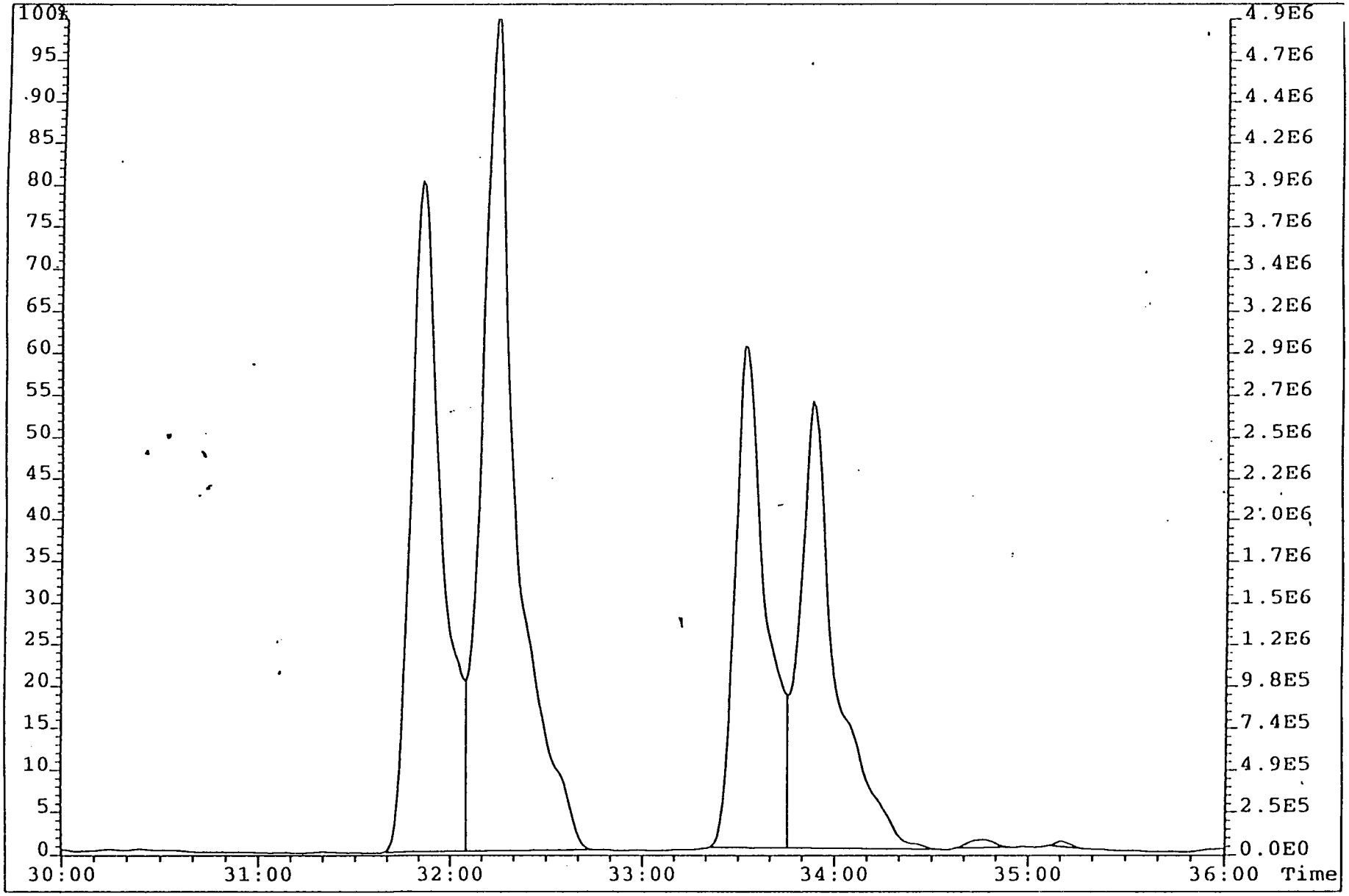

Figure 4.68 b. GCMS chromatogram (m/z 192) of the aromatic fraction of oil C2.

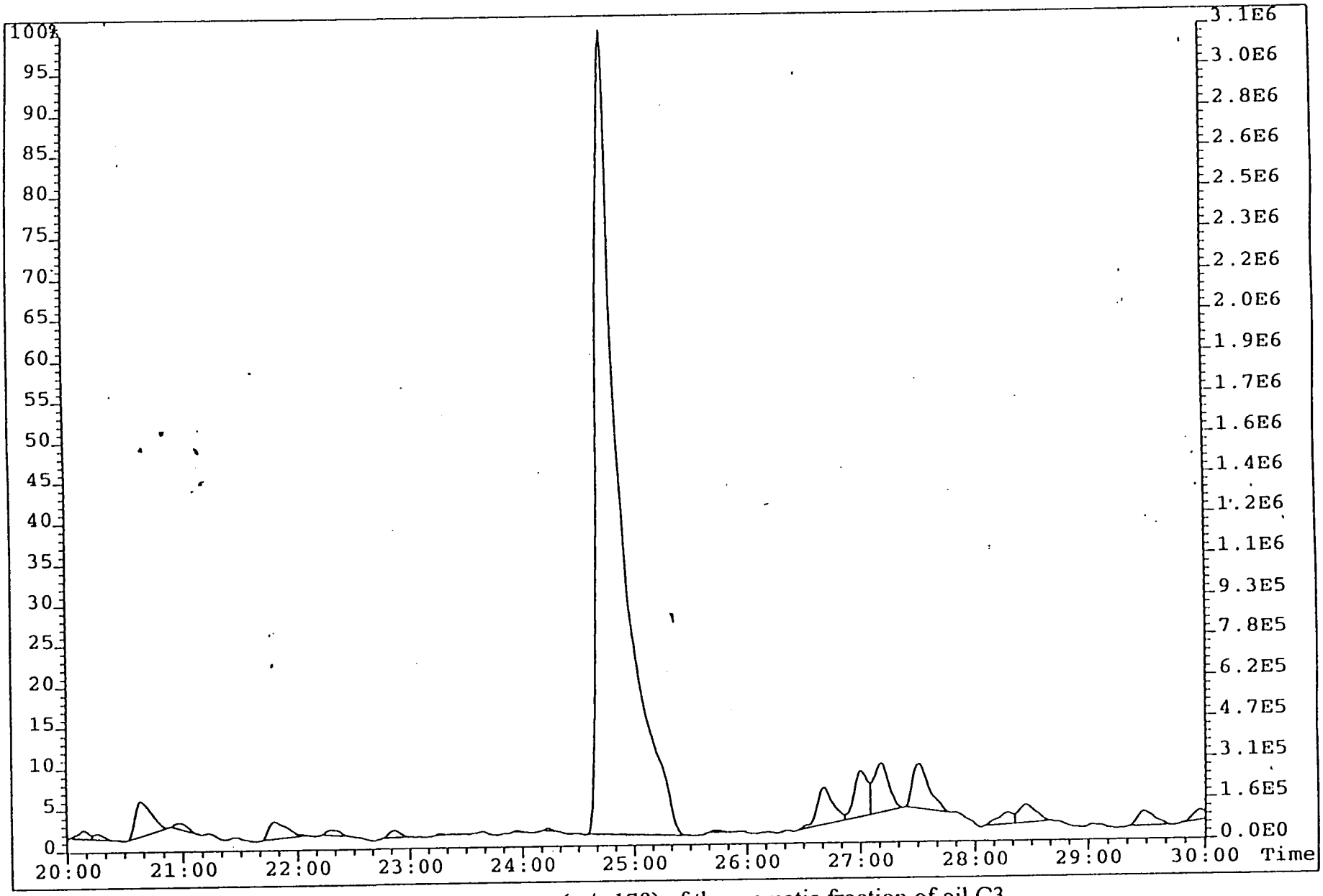

Figure 4.69 a. GCMS chromatogram (m/z 178) of the aromatic fraction of oil C3.

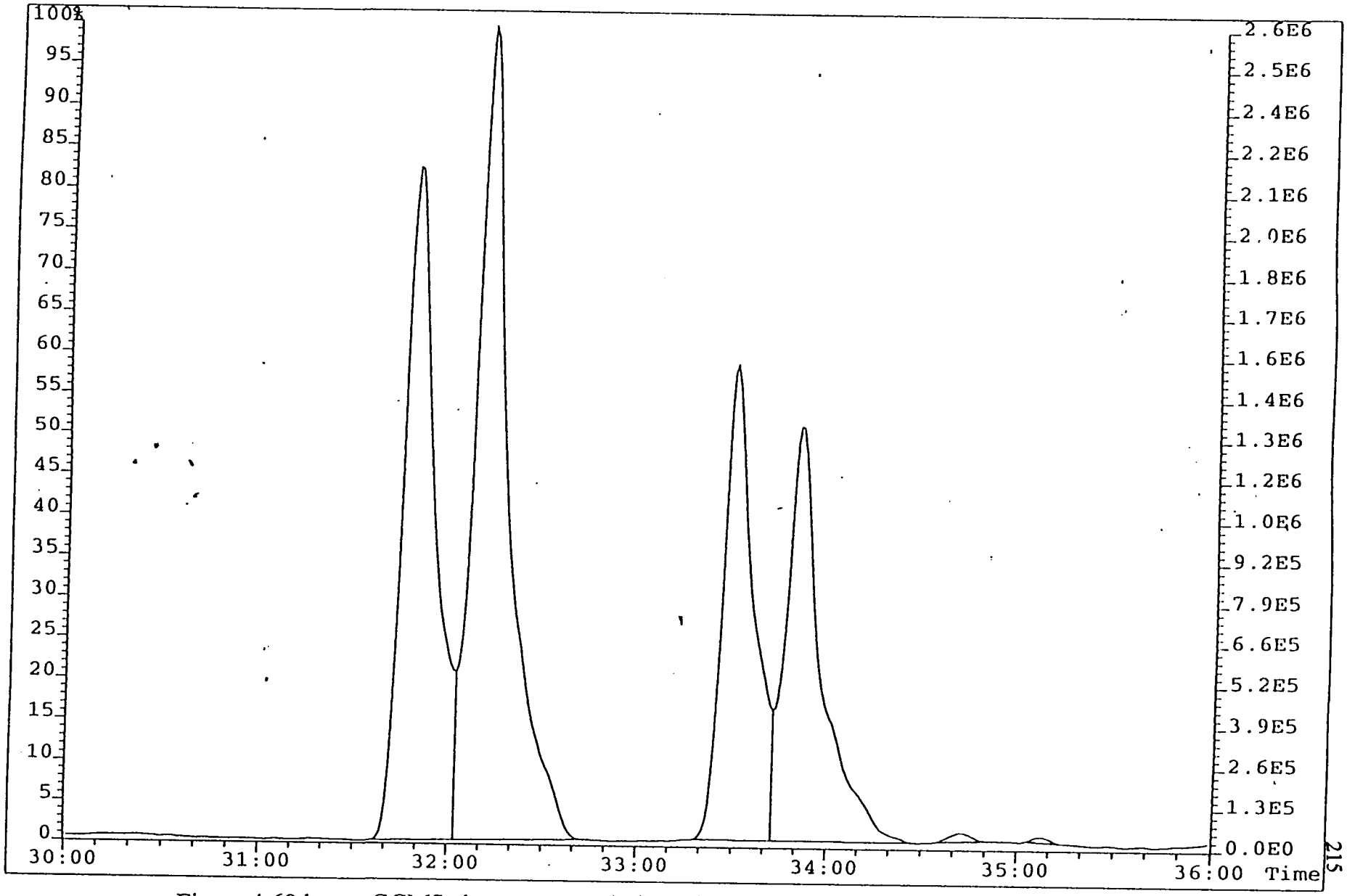

Figure 4.69 b. GCMS chromatogram (m/z 192) of the aromatic fraction of oil C3.

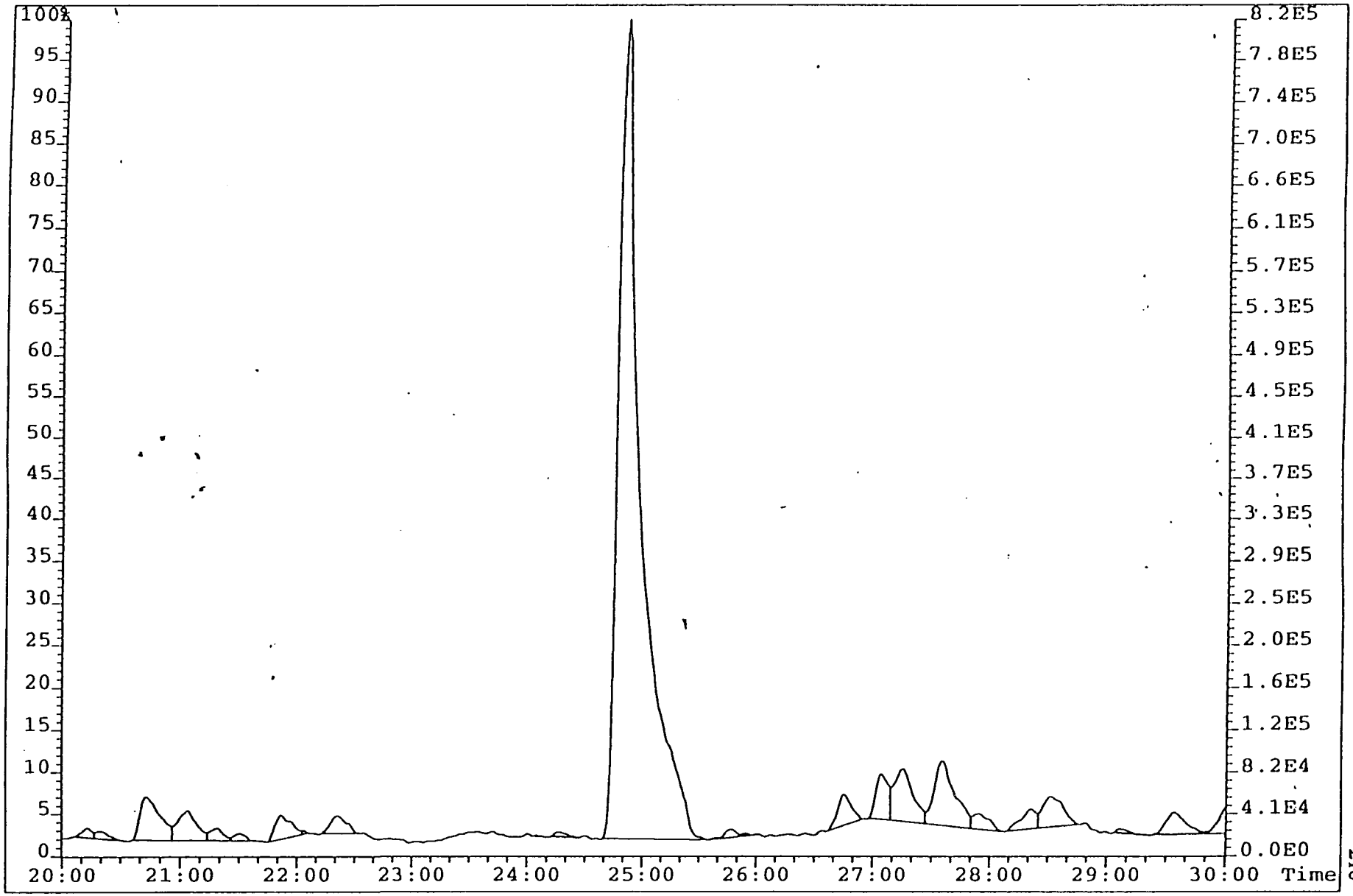

Figure 4.70 a. GCMS chromatogram (m/z 178) of the aromatic fraction of oil D1.

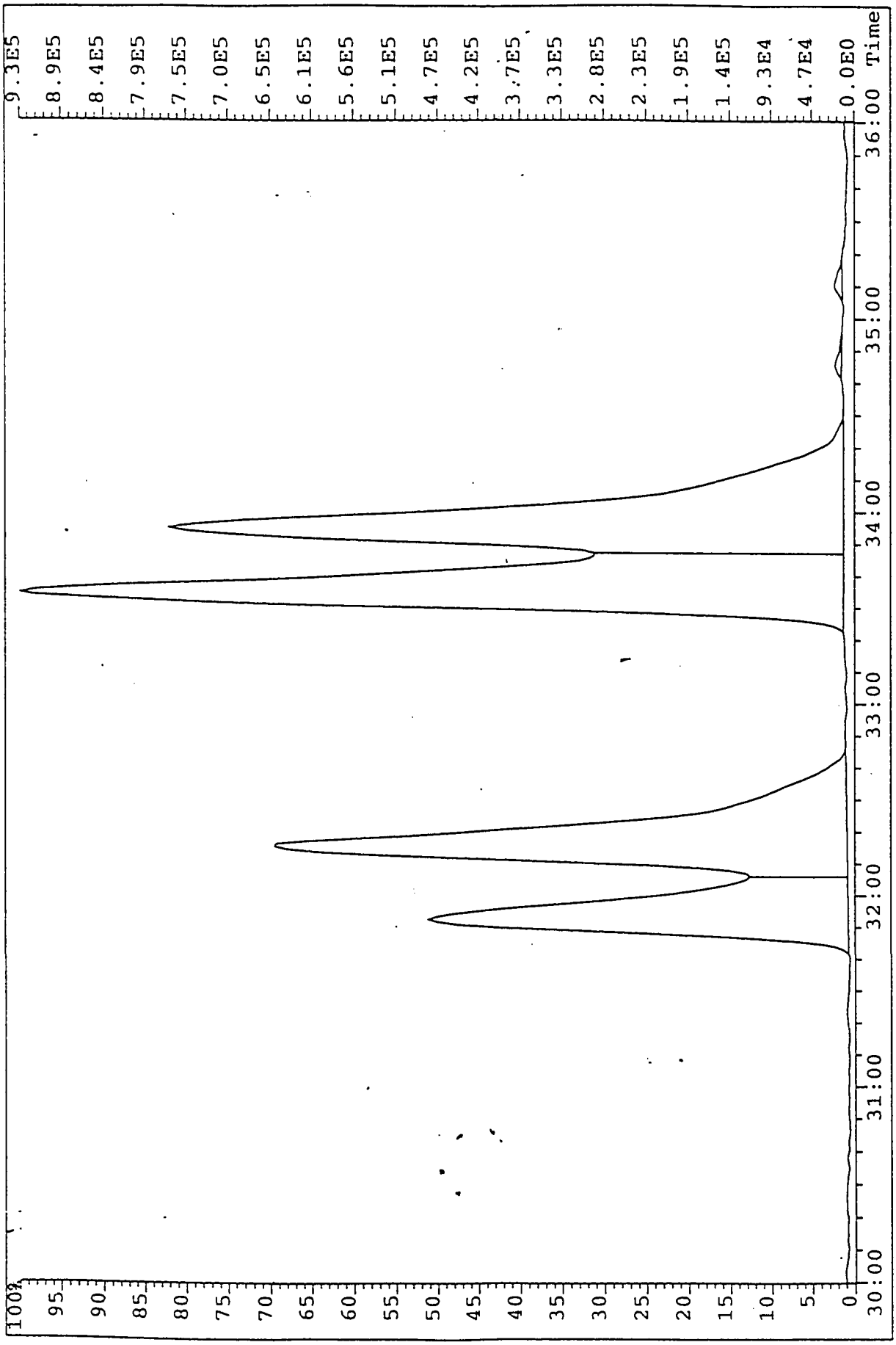

Figure 4.70 b. GCMS chromatogram (m/z 192) of the aromatic fraction of oil D1.

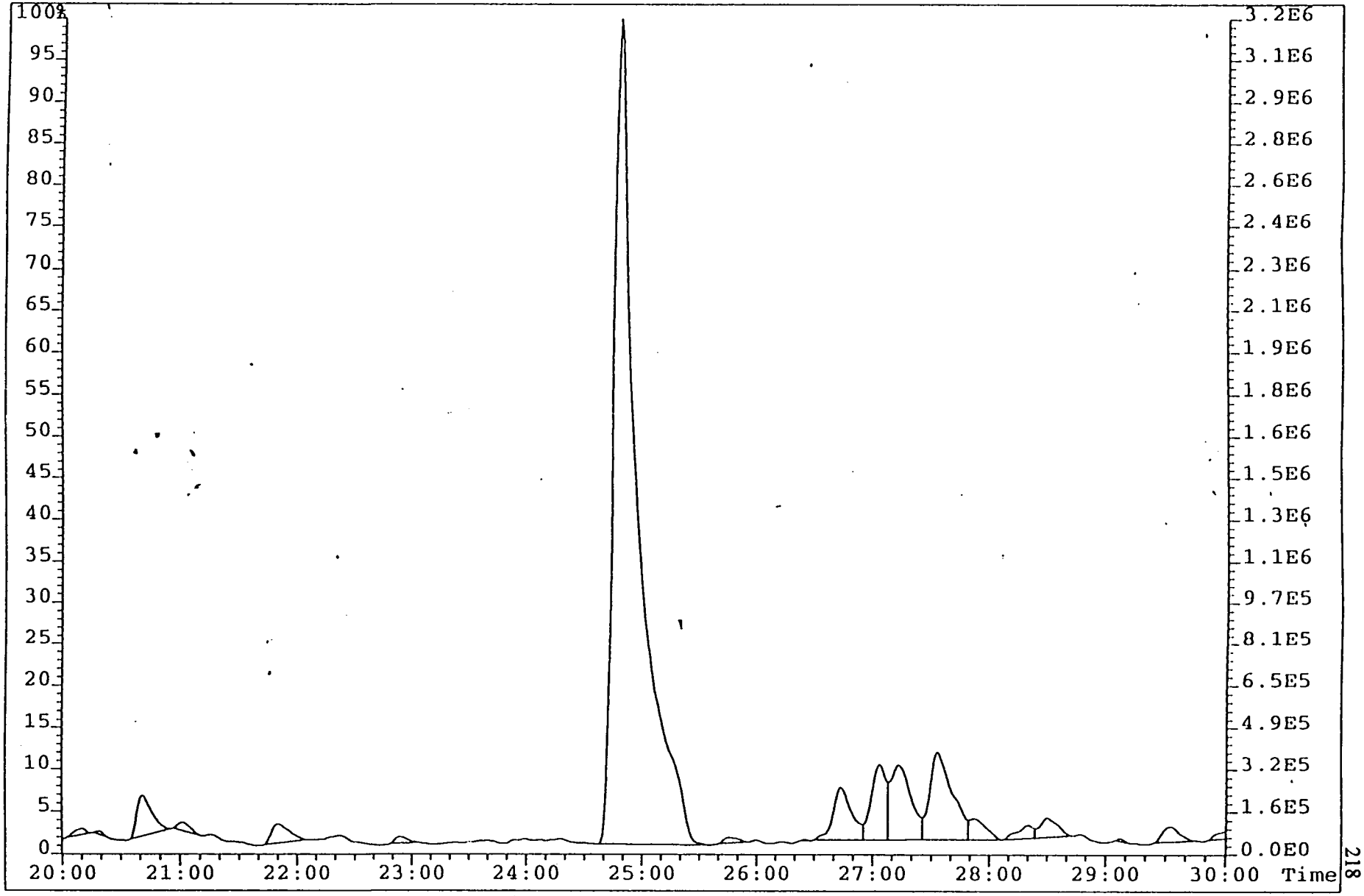

Figure 4.71 a. GCMS chromatogram (m/z 178) of the aromatic fraction of oil E1.

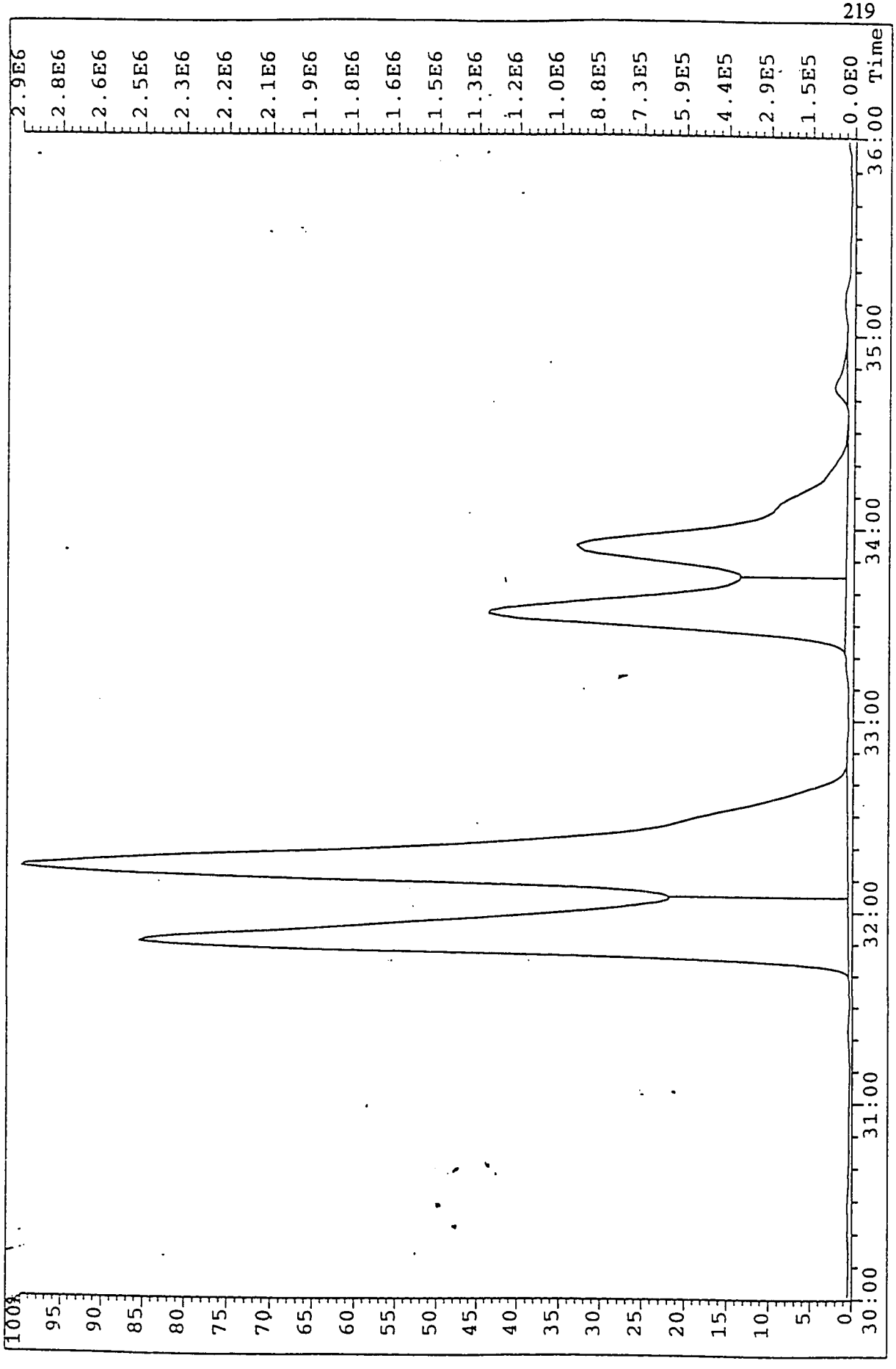

Figure 4.71 b. GCMS chromatogram (m/z 192) of the aromatic fraction of oil E1.

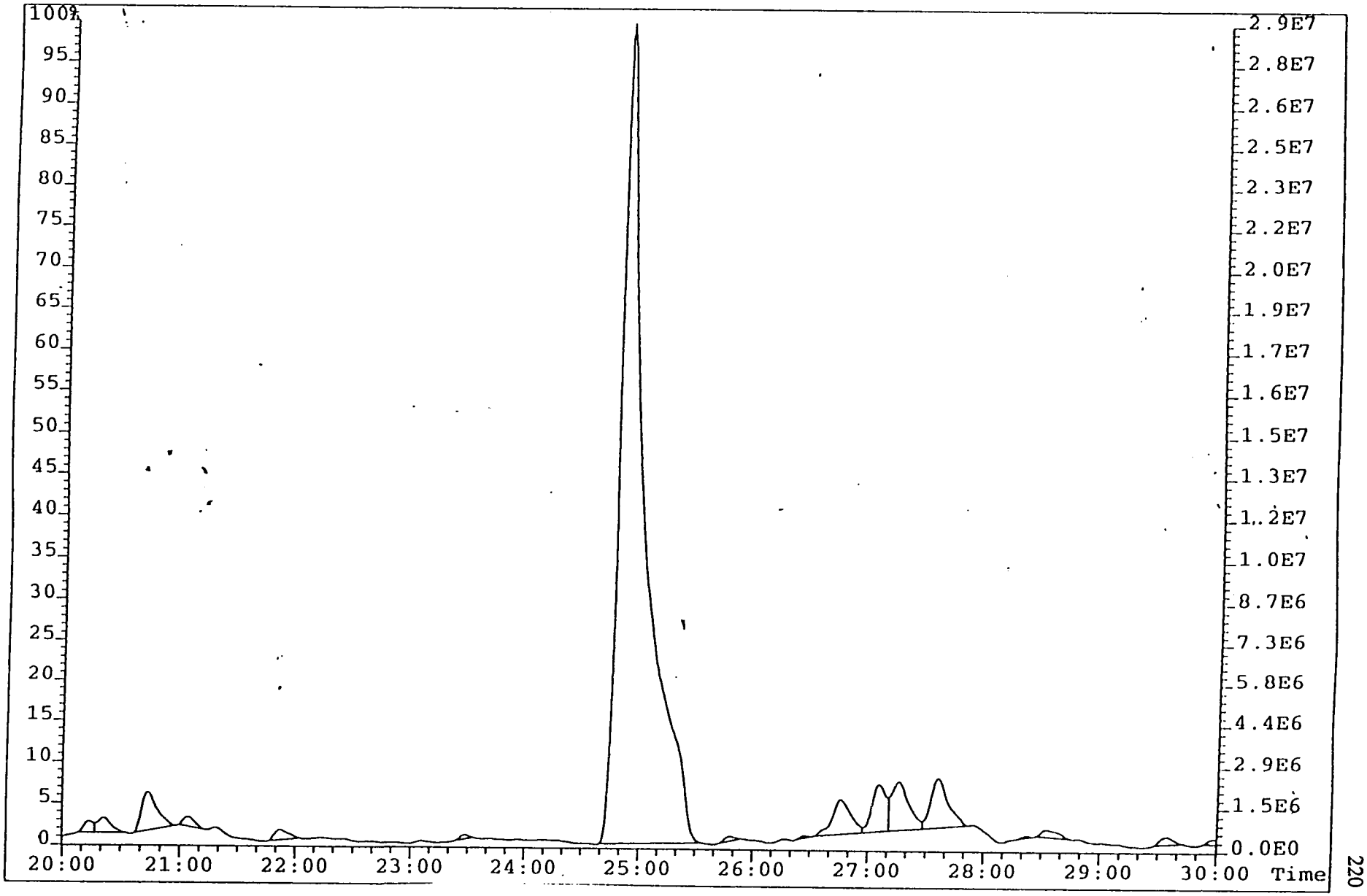

Figure 4.72 a. GCMS chromatogram (m/z 178) of the aromatic fraction of oil F1.

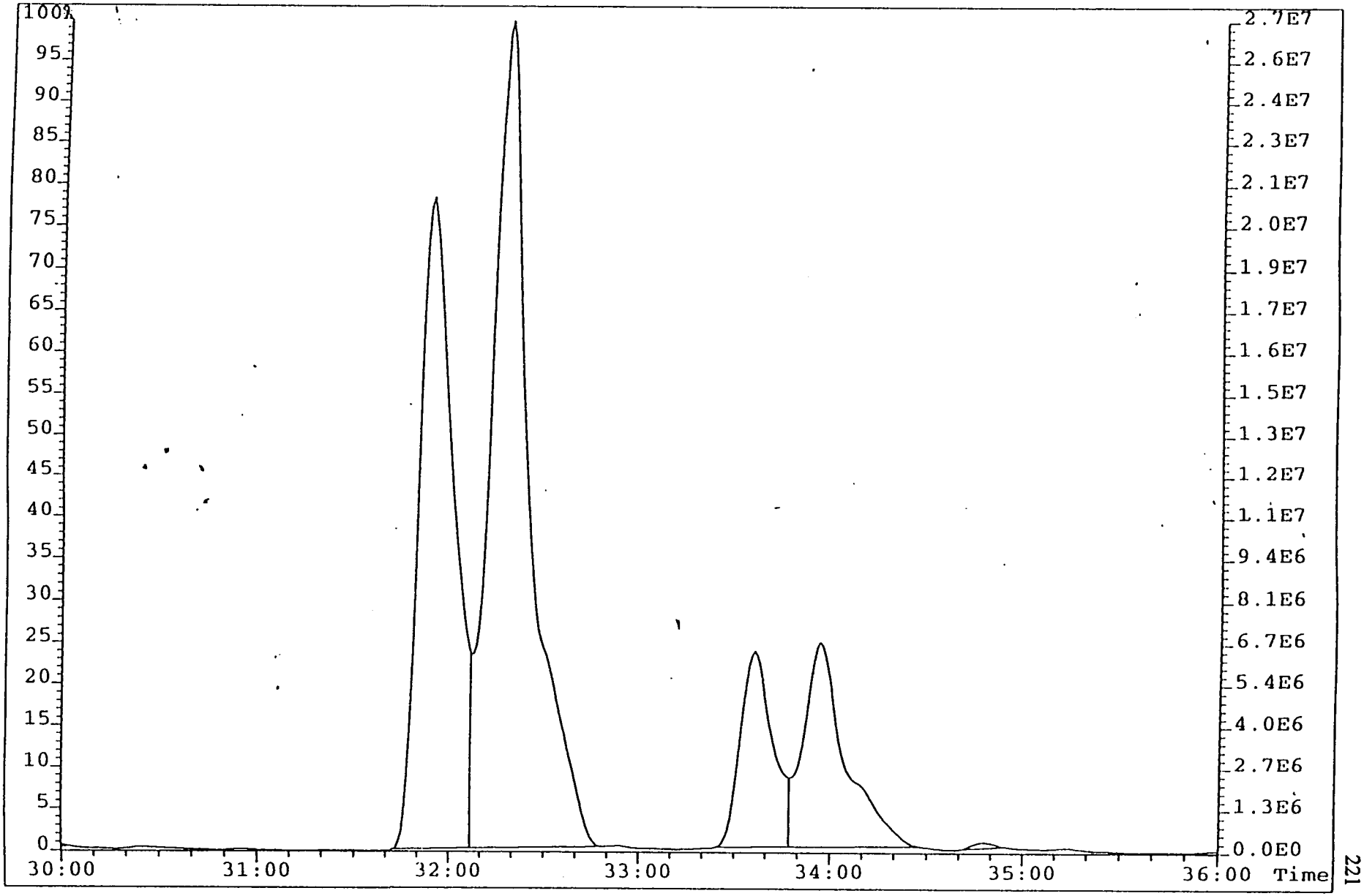

Figure 4.72 b. GCMS chromatogram (m/z 192) of the aromatic fraction of oil F1.

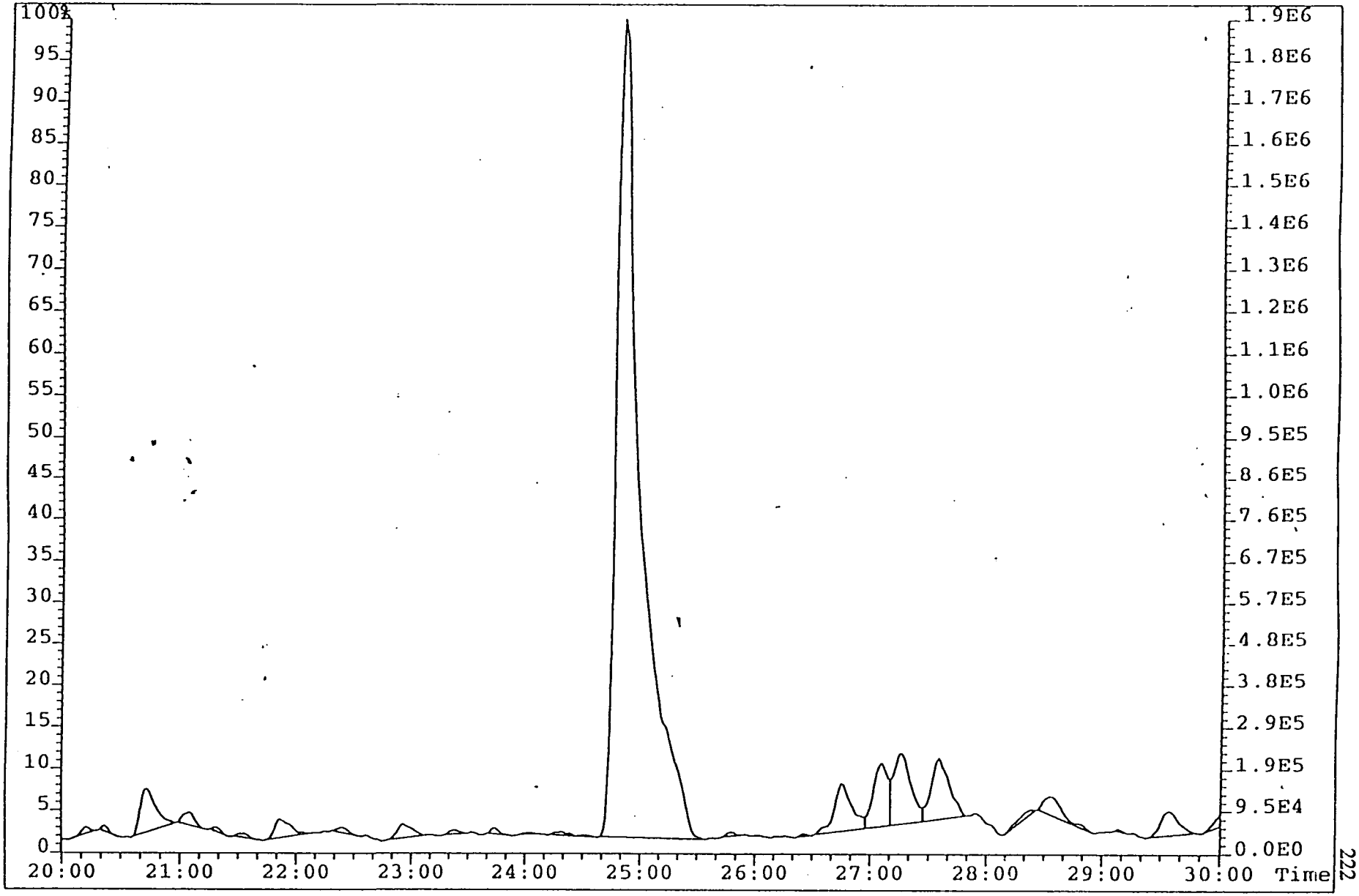

Figure 4.73 a. GCMS chromatogram (m/z 178) of the aromatic fraction of oil G1.

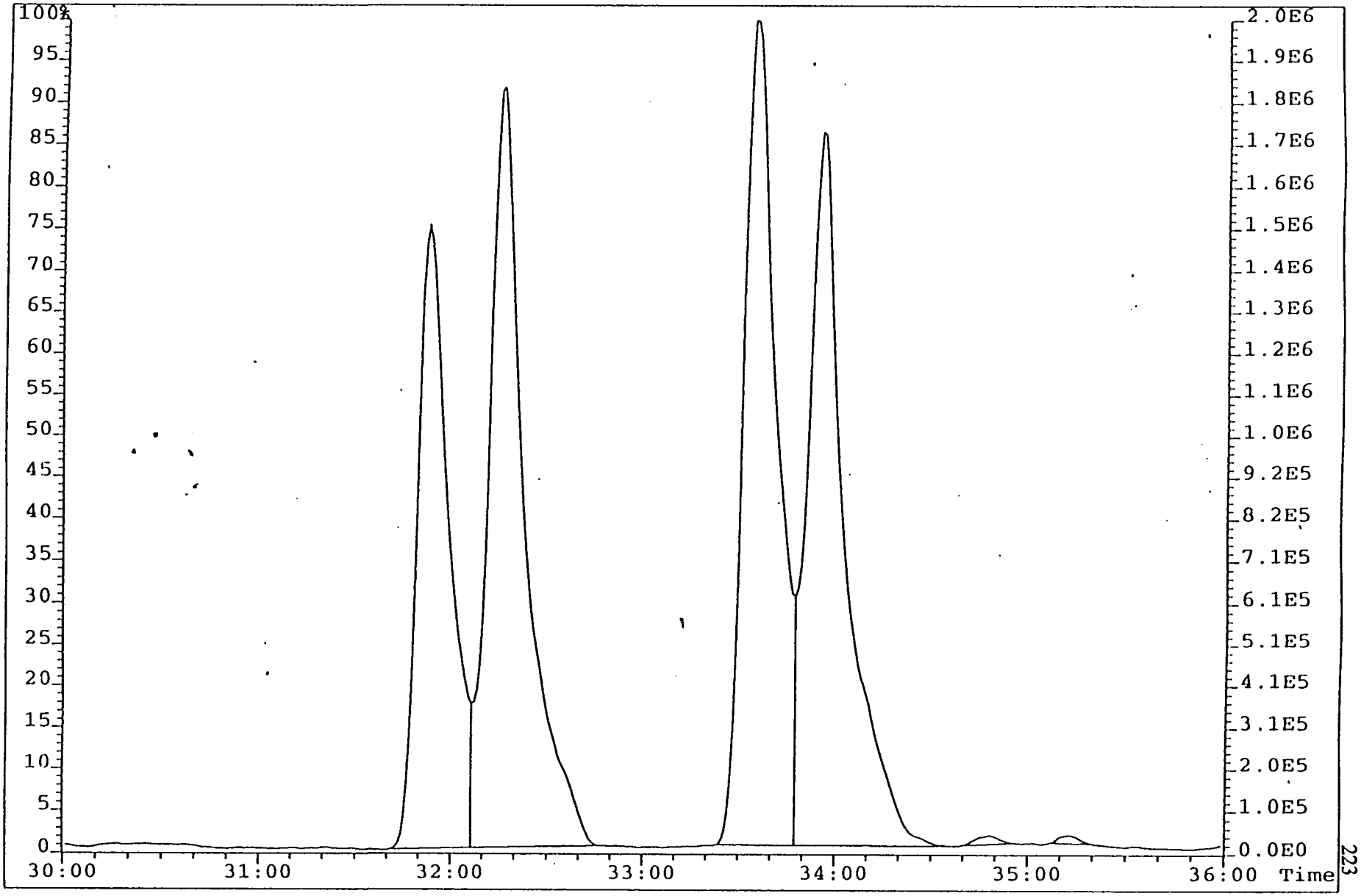

Figure 4.73 b. GCMS chromatogram (m/z 192) of the aromatic fraction of oil G1.

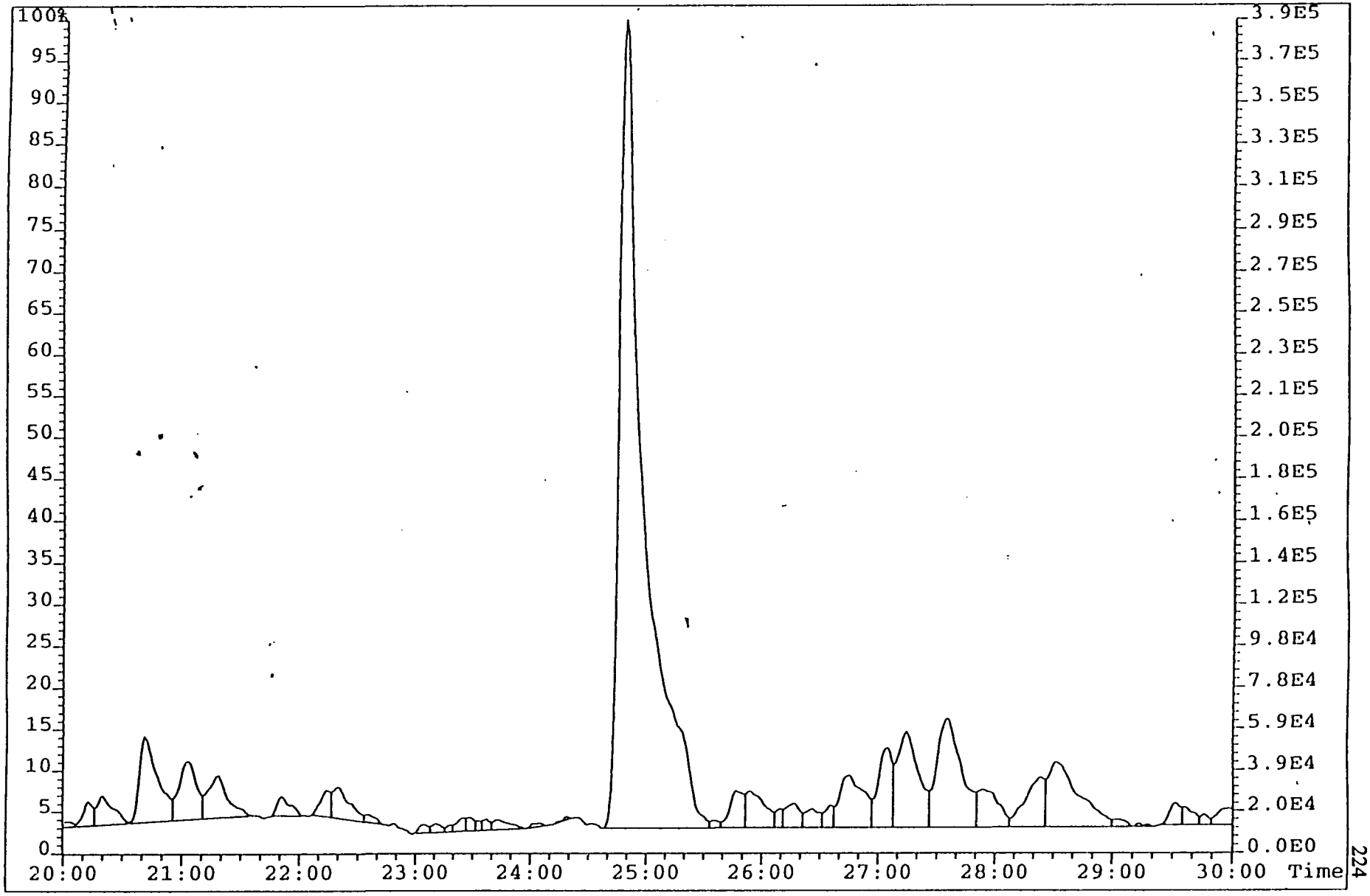

Figure 4.74 a. GCMS chromatogram (m/z 178) of the aromatic fraction of oil H1.

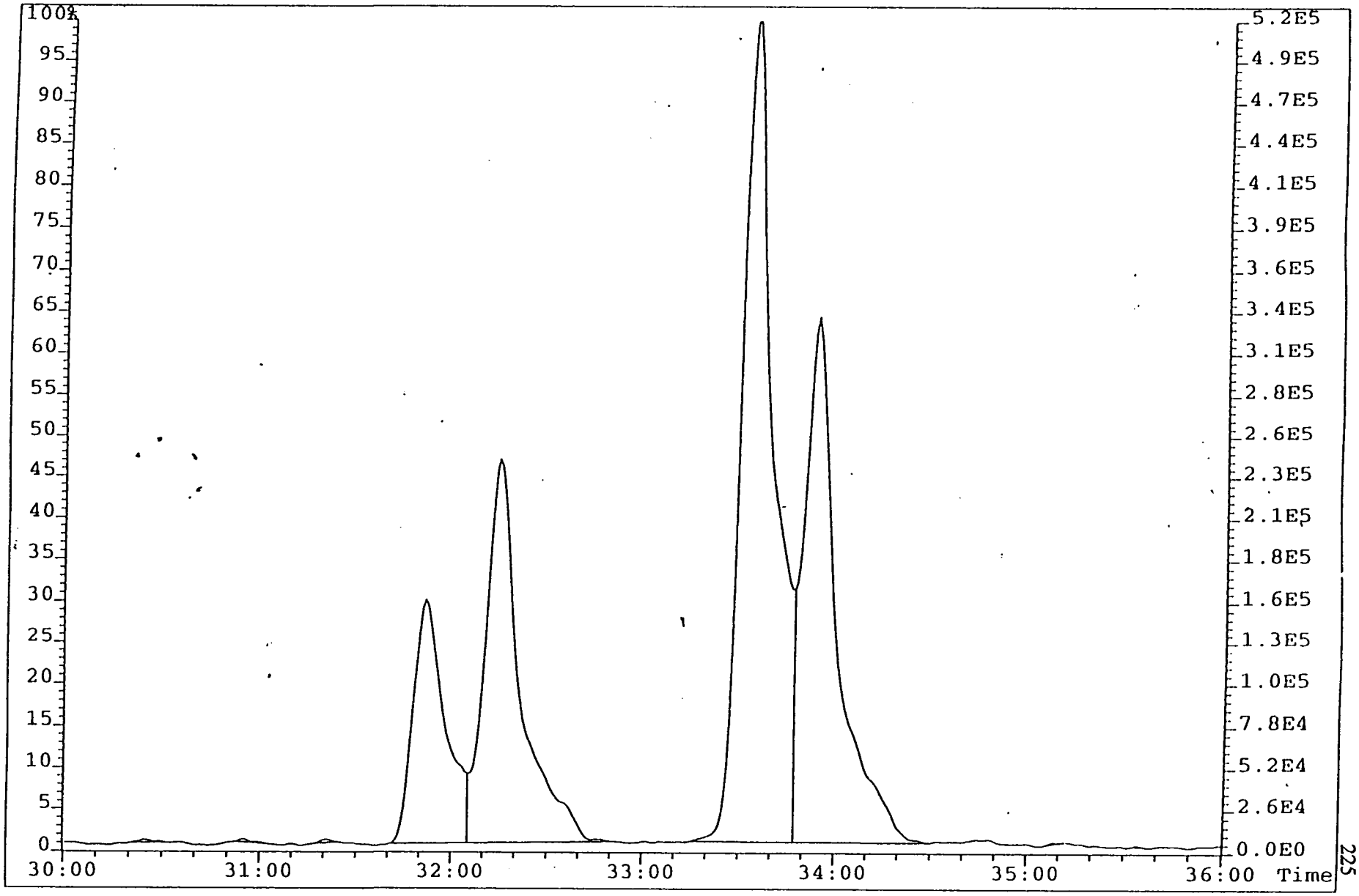

Figure 4.74 b. GCMS chromatogram (m/z 192) of the aromatic fraction of oil H1.

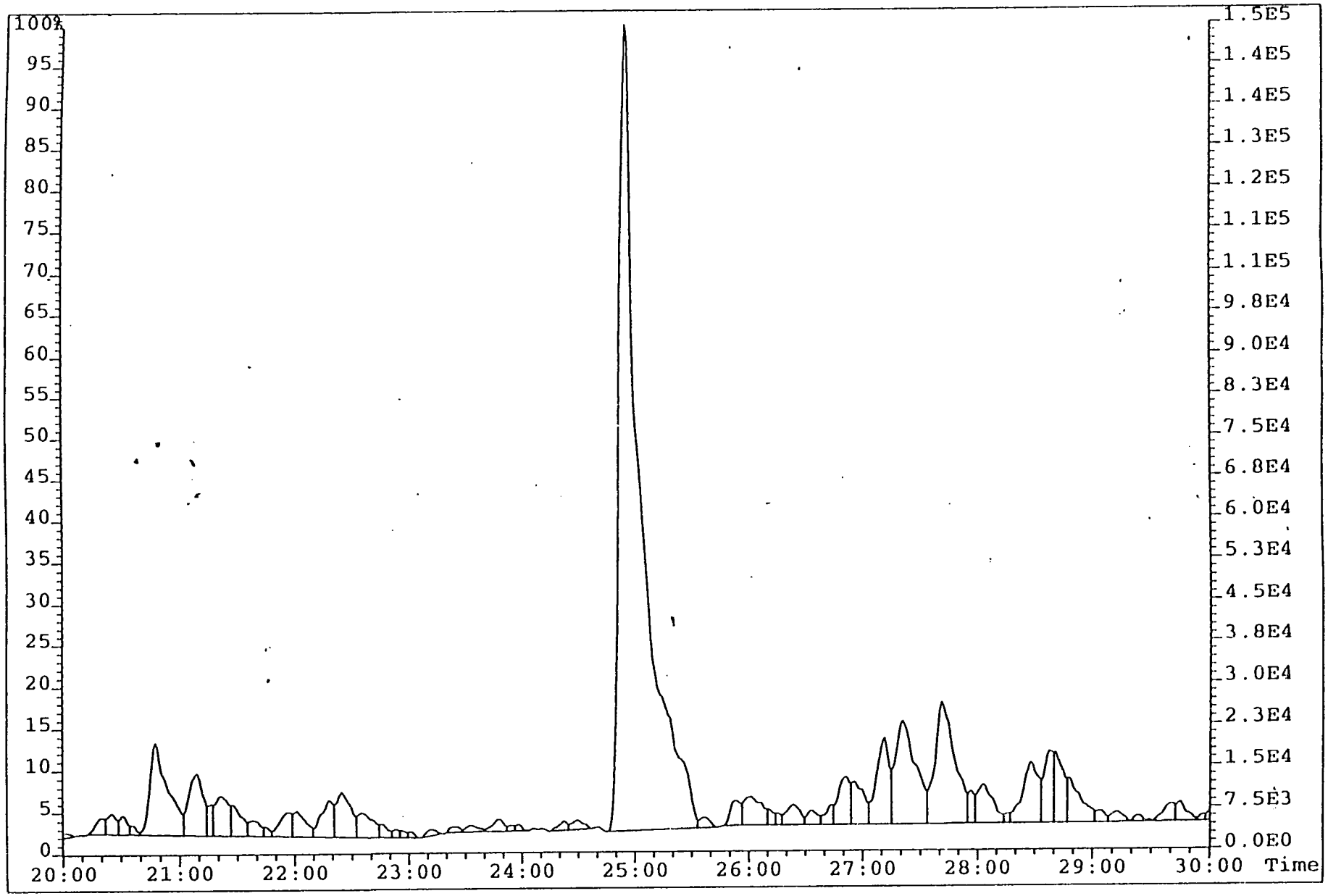

Figure 4.75 a. GCMS chromatogram (m/z 178) of the aromatic fraction of oil H2.

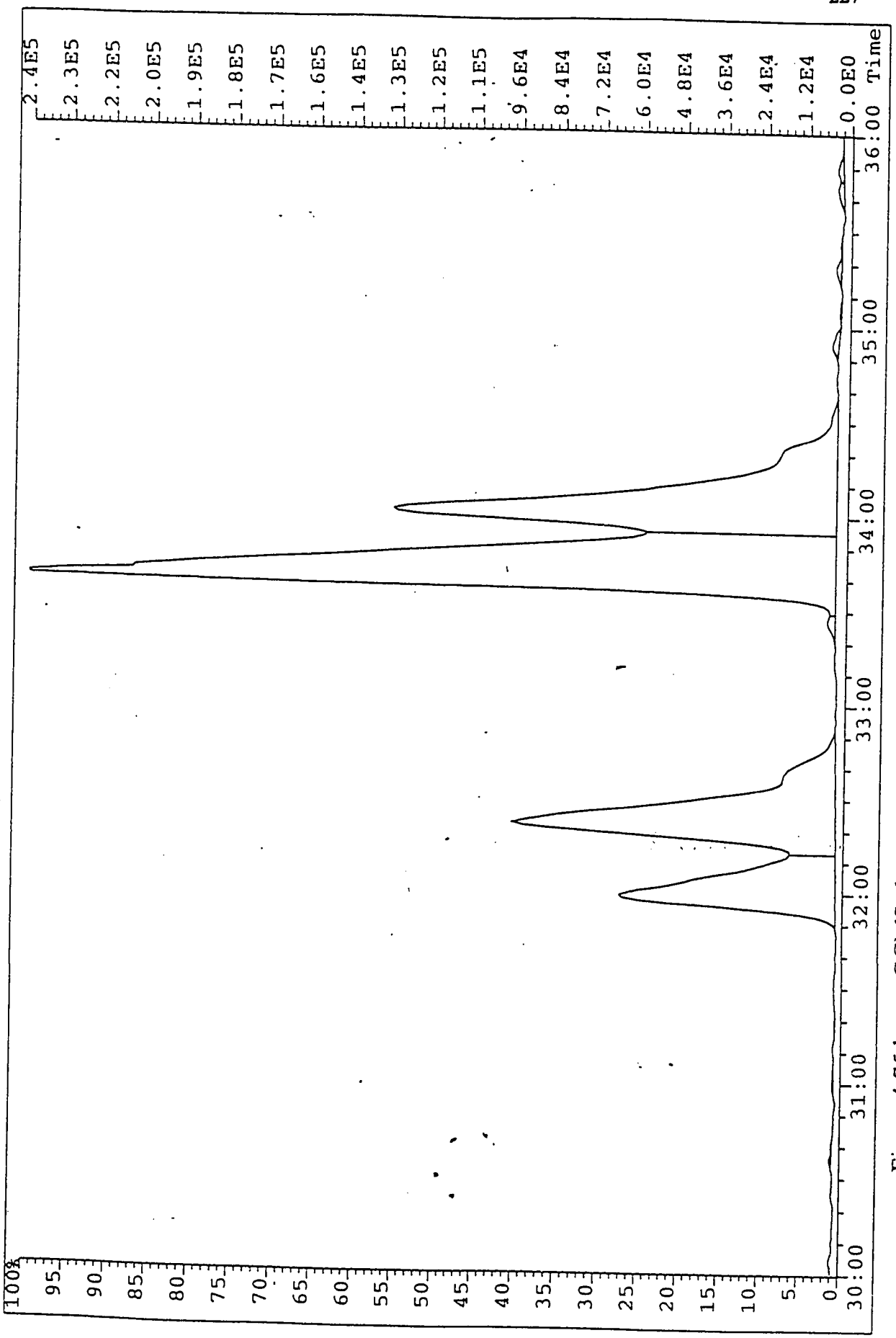

Figure 4.75 b. GCMS chromatogram (m/z 192) of the aromatic fraction of oil H2.